

It's all about perception

Nod factor perception inside nodules of
Medicago truncatula

Sjef Moling

It's all about perception

*Nod factor perception inside nodules of Medicago
truncatula*

Sjef G.J.A. Moling

Thesis committee

Promotor

Prof. Dr A.H.J. Bisseling
Professor of Molecular Biology (Development Biology of Plants)
Wageningen University

Co-promotor

Dr E.H.M. Limpens
Assistant professor, Laboratory of Molecular Biology
Wageningen University

Other members

Prof. Dr H. van Amerongen, Wageningen University
Dr M.J. Ketelaar, Wageningen University
Dr S. Goormachtig, Ghent University, Belgium
Dr A. Goverse, Wageningen University

This research was conducted under the auspices of the Graduate School of Experimental Plant Sciences

It's all about perception

*Nod factor perception inside nodules of Medicago
truncatula*

Sjef G.J.A. Moling

Thesis

submitted in fulfilment of the requirements for the degree of doctor
at Wageningen University
by the authority of the Rector Magnificus
Prof. Dr M.J. Kropff,
in the presence of the
Thesis Committee appointed by the Academic Board
to be defended in public
on Monday 25 August 2014
at 1.30 p.m. in the Aula.

Sjef G.J.A. Moling
It's all about perception
Nod factor perception inside nodules of *Medicago truncatula*
190 pages.

PhD thesis, Wageningen University, Wageningen, NL (2014)
With references, with summaries in Dutch and English

ISBN 978-94-6257-039-9

THESIS CONTENT

Thesis content	5
Outline of the thesis.....	7
Chapter 1. General introduction	11
Chapter 2. A fate map of Medicago root nodules.....	23
Chapter 3. Nod factor receptors are essential for intracellular infection of Medicago nodule cells	51
Chapter 4. The Nod factor receptors LYK3 and NFP form heteromers in Medicago nodules	75
Chapter 5. Interactors of the Nod factor receptor LYK3	91
Chapter 6. Laser capture microdissection to study spatial differences in gene expression of the Nod factor signaling cascade	113
Chapter 7. General discussion	143
References	157
Summary	173
Samenvatting	177
Acknowledgements	181
Curriculum vitae.....	183
Publications	185
Education Statement of the Graduate School Experimental Plant Sciences.....	187



OUTLINE OF THE THESIS

It's all about perception. Nod factor perception to be more precise. In this thesis I'll present the results of my PhD research on Nod factor perception inside nodules of *Medicago truncatula*. Legumes, of which *Medicago* is a model species, are unique in their ability to establish a mutualistic symbiotic interaction with nitrogen fixing bacteria (rhizobia). This interaction provides the plant with a source of nitrogen in an environment where nitrogen sources are low. The bacterial symbiont gets carbohydrates in return. This symbiosis is strictly controlled by the plant and the most important components of the signaling cascade were identified in the past decade. All these genes contribute to the offset of symbiosis in the root epidermis and the initiation of the symbiotic interaction. This interaction results in the formation of a new organ: the root nodule. In this nodule the bacteria finally infect the host cells, differentiate and develop into nitrogen fixing symbiosomes. In Chapter 1 we give an overview of the evolution of symbiosis. We'll zoom into the cell biological features a plant has to develop in order to be able to establish a symbiotic interaction.

The formation of a nodule starts shortly after perception of the bacterial signal molecule (the Nod factor). In Chapter 2 we asked ourselves the question how this nodule is formed. A series of divisions in the root cortex and endodermis leads to the formation of a nodule, but in which way do all these cell layers contribute to the nodule? The research presented in Chapter 2 results in a nodule fate map map describing all these contributions.

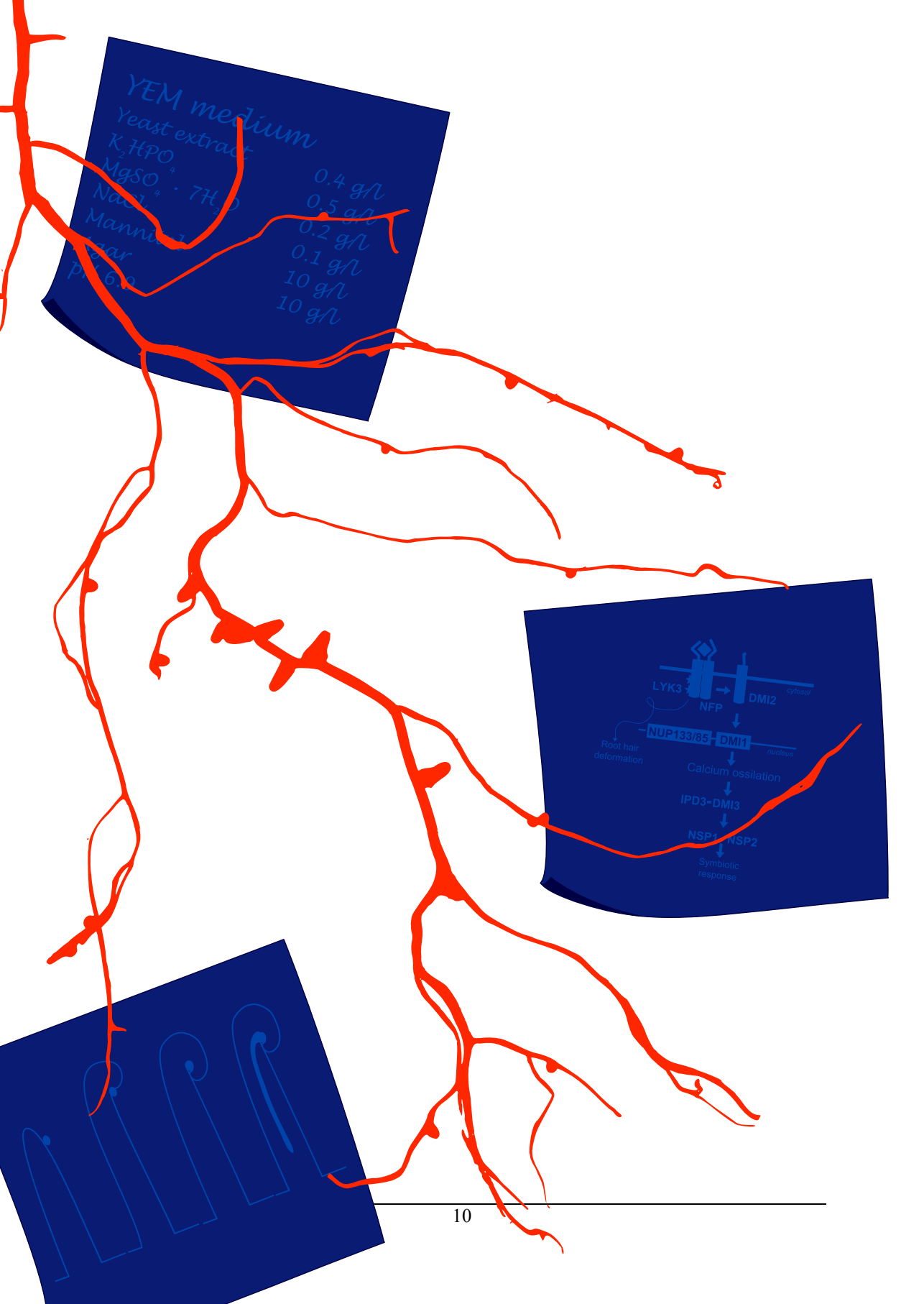
If the nodule is finally made, the bacteria need to infect or (from a plant point of view) be released. In Chapter 3 we will discuss the role of the Nod factor receptors on bacterial release inside the nodule. We know that these receptors are the key regulators of symbiosis in early stages, but what is their function in the nodule? There is some evidence that at least downstream targets of the Nod factor receptors are essential for bacterial release. We made use of fluorescent tagged versions of the receptor to study their behaviour in nodules. Furthermore, we removed the receptors specifically inside the nodule. This strategy allows the early steps in the root epidermis to take place and thus the initiation of a nodule. Finally, we were interested in the question why these receptors are so hard to visualize. They seem strictly controlled and we wanted to know why. To do so, we ectopically expressed the receptors to see what the effect was on the development of nodules.

Since we were able to localize the Nod factor receptors in Chapter 3, we made use of this knowledge to study the formation of receptor complexes in Chapter 4. Already at the time of their discovery the Nod factor receptors were thought to form heteromeric complexes. Recent studies have shown that these complexes are formed when the receptors are expressed in a heterologous system. Remarkable, upon co-expression in heterologous

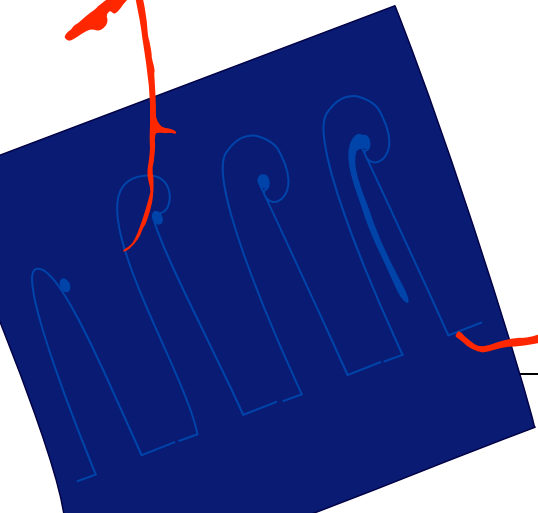
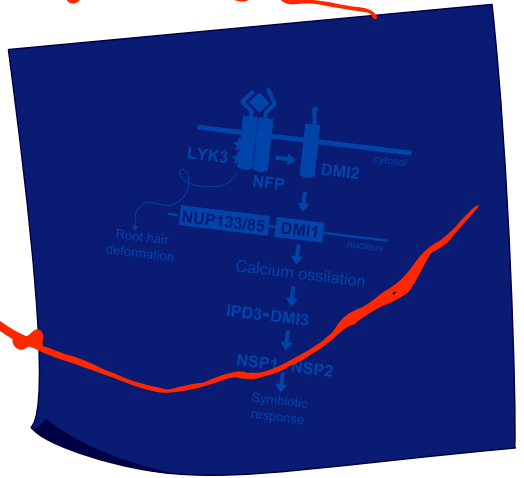
systems cell death is induced. Complex formation in the symbiotic context has not been shown, and cell death is not observed nor expected in this context. We co-expressed the fluorescent tagged receptors in nodules of *Medicago* and used FRET based techniques to study complex formation. With FRET, elicitation of one of the receptors (the donor) results in excitation of the other (the receptor). This transfer of energy only occurs when the two are in close proximity and thus likely are in a complex.

These receptor complexes are known to contain a broad range of other components and the composition often changes depending on the biological environment. To get a list of possible other proteins present in the Nod factor signaling complex we used immunoprecipitation in Chapter 5. For this immunoprecipitation we expressed one of the receptors tagged with GFP in *Medicago*. By using an antibody against the GFP tag we were able to precipitate the receptor and several proteins that might be in a complex with it. Subsequently, we used mass spectrometry to identify these proteins. Next to this list of possible interactor we wanted to know if two proteins known to co-localize or interact accumulate at the same place as the receptor. This because we were not able to identify those proteins in the immunoprecipitation.

Because expression at the same place in the nodule is essential for interaction we studied in Chapter 6 how the known Nod factor signaling genes are differentially expressed in the different zones of the nodule. We used laser capture micro dissection to isolate the different zones of the nodule, isolated the transcripts and hybridized these transcripts on a microarray to detect the expression of the *Medicago* genome in the nodule zones. This experiment provides the community with a digital *in situ* hybridization experiment for *Medicago* nodules. Finally, in Chapter 7 I'll discuss the results presented in this thesis in light of the available literature and discuss why it's all about perception.



YEM medium
Yeast extract
 K_2HPO_4 0.4 g/l
 $MgSO_4 \cdot 7H_2O$ 0.5 g/l
 $NaCl$ 0.2 g/l
Mannitol 0.1 g/l
Glycerol 10 g/l
pH 6.0 10 g/l



Chapter 1.

GENERAL INTRODUCTION

Sjef Moling¹ and Ton Bisseling^{1,2}

¹*Laboratory of Molecular Biology; Wageningen University; Wageningen, The Netherlands*

²*College of Science; King Saud University; Riyadh, Saudi Arabia*

Published in *Biological Nitrogen Fixation*, Bruijn, F. de (Ed.), in press

ABSTRACT

All plants need nitrogen for their growth. Legumes have the unique ability to compensate for low fixed nitrogen in the soil by establishing an interaction with nitrogen fixing bacteria collectively named rhizobium. In this interaction, the plant forms a new organ in which the bacteria are hosted, the root nodule. The rhizobia are hosted intracellular, in these nodules, and are surrounded by a plant membrane. This membrane is the interface which allows exchange of nutrients between the two symbionts. We will focus on the formation of this new organ and the evolution of the symbiotic interface.

INTRODUCTION AND DISCUSSION.

Nodule formation in a nutshell

The formation of the root nodule is initiated at the epidermis of plant roots where signals of the bacteria are perceived. In response to the signal, among others, root hairs redirect their growth towards the bacterium. In this way a curl is formed around the dividing bacteria which become entrapped in a pocket inside the curl. After completion of the curl an infection thread is initiated starting from this pocket. This infection thread is a tubular invagination of the plant plasma membrane, filled with rhizobia, that grows inside the root hair towards the root cortex. While the infection thread grows inwards, cells of the cortex start to divide to form the nodule primordium from which the nodule develops [Ferguson et al., 2010; Hirsch, 1992; Luyten and Vanderleyden, 2000].

Signalling in symbiosis

To establish a symbiotic interaction the two partners need to exchange signals as a biochemical handshake. For the rhizobium–legume symbiosis the signalling is mainly studied during early steps in the epidermis. The signal that sets the nodulation process in motion is the Nod factor. This is a decorated lipochito-oligosaccharide (LCO) that is perceived by two Nod factor receptors. These are the LysM receptor kinases LYK3/NFR1 and NFP/NFR5 in *Medicago truncatula* and *Lotus japonicus*, respectively [Arrighi et al., 2006; Limpens et al., 2003; Radutoiu et al., 2003; Smit et al., 2007]. The receptors activate the so called common signalling pathway. This pathway is, as its name suggests, not unique to the rhizobium–legume symbiosis but also used in the mycorrhizal symbiosis [Catoira et al., 2000; Geurts and Bisseling, 2002; Hocher et al., 2011]. The common signalling pathway starts with the LRR-type receptor DMI2 [Limpens et al., 2005] and the putative cation channel DMI1 [Ane et al., 2004]. Downstream of DMI1 and DMI2 act two nucleoporins: NUP133 and NUP85 [Kanamori et al., 2006; Saito et al., 2007]. All these components are essential for the induction of nuclear calcium oscillations [Peiter et al.,

2007; Wais et al., 2000]. These oscillations are interpreted by the calcium and calmodulin-dependant kinase CCamK/DMI3 [Levy et al., 2004; Mitra et al., 2004; Oldroyd and Downie, 2004]. CCamK and its interactor Cyclops/IPD3 are the last components of the common (see below) signalling pathway [Limpens et al.; Messinese et al., 2007; Yano et al., 2008] and activate transcription factors that regulate a wide range of genes which initiate the formation of a nodule and ultimately the formation of the symbiotic interface.

The indeterminate nodule

In legumes two types of nodules can be distinguished: determinate and indeterminate nodules. Determinate nodules are formed on for instance the model legume *Lotus japonicus* and soybean. In these nodules the meristem is transiently present and as a result the formation of infected cells, and so the symbiotic interfaces, are formed more or less simultaneously [Ferguson et al., 2010]. Therefore the subsequent developmental stages of symbiotic interface formation are rather difficult to study in determinate nodules.

Indeterminate nodules are formed among others on the model organism *Medicago truncatula*, pea, alfalfa, clover, and vetch. These indeterminate nodules contain a nodule meristem at their apex that continuously adds new cells to the nodule. Therefore in these nodules a series of subsequent developmental stages are present along their longitudinal axis. This facilitates research on the development of the symbiotic interface. The indeterminate nodule has four developmental zones: the meristem, the infection zone, the fixation zone and the senescent zone. The meristem continuously provides the nodule with new cells. In the infection zone the cells derived from the meristem are continuously infected by rhizobia which are released from an infection thread that penetrates these cells. In indeterminate nodules, in general, individual bacteria are surrounded by a host derived membrane. The bacterium with the plant derived membrane is called symbiosome (Figure 1.1a). The symbiosomes continue to divide and develop into a mature state where they fix atmospheric nitrogen into ammonia in return for carbohydrates. This zone, where the rhizobia fix nitrogen and the symbiotic interface is completed, is called the fixation zone. Finally, in the senescent zone symbiosis is terminated by the plant by fusion of symbiosomes with lytic vacuoles [D'Haeze and Holsters, 2002; Downie, 2007; Esseling et al., 2003; Ferguson et al., 2010; Hirsch, 1992; Jones et al., 2007; Murray, 2011].

Signalling inside the nodule

Inside nodules recognition of the rhizobial Nod factor might be essential for the formation of the symbiotic interface, although this has not yet been demonstrated. In nodules the Nod factor receptors and other components of the signalling cascade are expressed at the apex [Limpens et al., 2005]. However, attempts to visualise the Nod factor receptors in nodules failed [Haney et al., 2011; Madsen et al., 2011]. Further a functional analysis of the Nod

factor receptors in nodules is not available. However, some components of the Nod factor signalling cascade have been shown to control bacterial release from infection threads, and so the formation of the symbiotic interface. Knock down of DMI2 or IPD3 (the interactor of DMI3) blocks the formation of the symbiotic interface [Limpens et al., 2005; Limpens et al., 2011]. When the *Medicago* DMI3 mutant is complemented with the DMI3 homologue from rice a nodule is formed, but release of the bacteria is blocked [Chen et al., 2007]. This suggests that DMI3 is also an essential component for the release of rhizobia. How the signalling cascade is activated remains to be demonstrated, but Nod factors might play a role. The rhizobial genes essential for the production of Nod factors are active in the infection zone of root nodules [Schlaman et al., 1991; Sharma and Signer, 1990]. Further, rhizobia unable to produce Nod factors inside the nodules are not released [Marie et al., 1994]. Whether and how Nod factors are perceived in root nodules and whether this results in the activation of Nod factor signalling cascade remains to be demonstrated. Rhizobia are checked for their Nod factor profile/ signature by the entry receptor in curled root hairs [Ardourel et al., 1994; Catoira et al., 2001; Smit et al., 2007]. Nevertheless a final Nod factor structure checkpoint would contribute to the maintenance of the symbiotic nature of the interaction.

Rhizobium symbiosis in Parasponia

Insight in the evolution of the legume-rhizobium symbiosis can be obtained by a comparison with other (non -) legume endosymbioses. First we make a comparison with the rhizobium- *Parasponia* symbiosis. The symbiosis with rhizobia is almost completely restricted to legumes. The only exceptions are tropical trees belonging to the genus *Parasponia* that also can form an interaction with rhizobia. *Parasponia* is part of the *Celtidaceae* and so only remotely related to legumes. Therefore this symbiosis evolved independently. *Parasponia*, like the legumes, forms a nodule to house the bacteria. These *Parasponia* nodules are modified lateral roots. This nodule has a central vascular bundle, no root cap and the bacteria are hosted in the expanded cortex.

The infection thread penetrates nodule cells, but rhizobia are not released from the infection thread. Instead, fixation threads are formed which form a continuum with the infection thread. Like infection threads the fixation threads are bound by a cell wall albeit it is markedly thinner than the wall of an infection thread (Figure 1.1b). So a clear difference between fixation threads and symbiosomes is the presence of this thin cell wall, which is absent in symbiosomes [Webster et al., 1995]. The rhizobia fix nitrogen in the fixation threads and must get carbohydrates in return. This symbiotic interface of *Parasponia* is similar to the symbiotic interface formed in primitive legumes like *Andira spp.* and many species belonging to the *Fabaceae* subfamily *Caesalpinoideae* [Defaria et al., 1989].

Research on *Parasponia* has been recently revitalized and can now make use of the achievements obtained with model legume systems. It has not yet been studied whether the

common signalling pathway is involved in *Parasponia*. However, studies on one of the Nod factor receptors provided insight in the evolution of these receptors. To prove that also in *Parasponia* the Nod factor is the signal that starts symbiosis Op den Camp et al. [2011] knocked down the *Parasponia* homologue of the Nod factor receptor NFP. This led to a marked (90%) reduction of nodule number. So although evolved independently the same signal molecule is recruited to induce this non-legume nodule symbiosis. This points to an important constraint in nodule evolution. This experiment revealed an important role of Nod factor perception. In the nodules that are formed the knock down of NFP specifically blocked the formation of fixation threads. So it proved that Nod factors need to be perceived to form a symbiotic interface in *Parasponia* and this strongly suggests that this is also the case in legumes which is well in line with the important role of the common signalling pathway in the formation of the interface.

Parasponia acquired nodulation rather recently. This makes *Parasponia* and the closely related non-nodulating *Trema* an ideal biological system to study the evolutionary origin of nodulation as the amount of evolutionary noise is lower than in legumes.

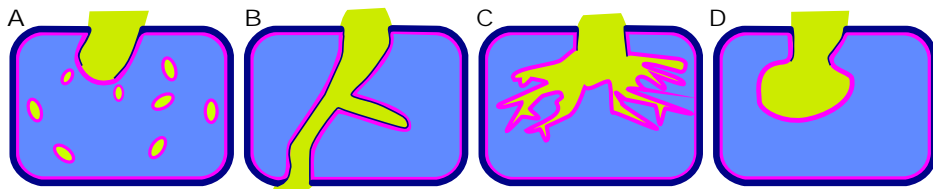


Figure 1.1 : Symbiotic interfaces are formed in several symbiotic interactions. (a) In legumes the symbiosis with rhizobia leads to the formation of intracellular symbiosomes. (b) Formation of fixation threads in *Parasponia* in symbiosis with rhizobia. (c) Formation of arbuscules in symbiosis with arbuscular micorhizal fungi. (d) In pathogenic biotrophic fungi interaction leads to the formation of haustoria.

Actinorhizal N-fixing symbiosis

Another N fixing nodule symbiosis is the interaction of actinorhizal plants (for example alder, *Casuarina sp.*, bayberry and sweet fern) and (gram positive) actinobacteria of the genus *Frankia*. The root nodule that is formed is a modified lateral root like the *Parasponia* nodules. In these nodules the bacteria are also hosted intracellular. The hyphae of *Frankia* enter the plant by an infection thread like structure. Inside the nodule these hyphae branch extensively to fill the entire nodule. Like in *Parasponia* the bacteria are not released from the thread: a vegetative hyphae surrounded by a plant membrane is formed (Figure 1.1b). The membrane surrounding the hyphae is the symbiotic interface. From the tip of these vegetative hyphae symbiotic vesicles are formed in which nitrogen fixation takes place [Berg et al., 1999; Pawlowski and Demchenko, 2012; Wall, 2000].

A knock down of the SymRK homolog, a component in this common signalling pathway, blocks the formation of vegetative hyphae in *Casuarina*. Although other components of the

common signalling pathway have not been tested, this suggests that the common signalling pathway is essential for the formation of the symbiotic interface in *Casuarina* [Gherbi et al., 2008; Markmann et al., 2008]. The nature of the signal molecule initiating *Frankia* symbiosis is unknown. However, the fact that the common signalling pathway seems involved suggests a shared evolutionary origin with the rhizobium symbiosis. We will now focus on the oldest endosymbiosis that is maintained in higher plants: the interaction with arbuscular mycorrhizal fungi.

Arbuscular mycorrhizal Symbiosis

Compared to the rhizobium–legume as well as the actinorhizal symbiosis the arbuscular mycorrhizal (AM) symbiosis has a much broader host range. Approximately 80% of all land plants can interact with AM fungi. The rhizobial and actinorhizal symbioses are also much younger (~60-80 million years) compared to the AM symbiosis (475 million years). The symbiosis with AM fungi provides the plant with an improved uptake of for example water, phosphate and nitrogen. It is thought that this symbiosis was important for the colonization of land by plants [Hata et al., 2010]. The AM symbiosis starts off with the germination of a fungal spore. Upon contact with the plant epidermis a hyphopodium is formed to allow the fungus to penetrate the root. When the fungus reaches the root cortex it spreads longitudinally. The fungus forms a trunk that penetrates the plant cell. This trunk is still surrounded by a cell wall. From the trunk arbuscules are formed; highly branched intracellular hyphae that are surrounded by a host membrane and lacking a cell wall. This periarbuscular membrane is the symbiotic interface (Figure 1.1c) [Genre et al., 2005; Hata et al., 2010; Ivanov et al., 2010]. So in this way AM fungi, rhizobia, and *Frankia* are hosted in a similar intracellular manner.

Like rhizobia, the mycorrhizal fungi produce signal molecules that induce symbiosis (Myc factors). One of these Myc factors has a remarkably similar structure as the rhizobial Nod factor: both are lipochito-oligosaccharides (LCOs) [Maillet et al., 2011]. Further, chitin tetramers and pentamers are produced by AM fungi. These are shorter than the chitin fragments inducing defence responses and do not trigger defence responses [Genre et al., 2013]. For defence responses chitin octamers are needed to facilitate receptor dimerization [Liu et al., 2012]. The tetramers and pentamers are not able to facilitate receptor dimerization. Interestingly the Nod factor and LCOs have a backbone of four chitin residues. The short chain oligomers can, like LCOs, induce nuclear calcium spiking in *Medicago* via the common signalling pathway. Which receptors recognize these AM fungal LCOs and chitin oligomers in legumes is not known. In contrast to *Parasponia* [Op den Camp et al., 2011], legume Nod factor receptors are not needed to establish a symbiosis with AM fungi [Radutoiu et al., 2003].

The legume Nod factor receptors belong to gene families where for example NFP is often a single copy “family” in non-legumes. Therefore it seems probable that at least the fungal

LCOs are perceived by receptors that are closely related to Nod factor receptors. In legumes, these have probably diverged by gene duplication and neofunctionalization [Zhang et al., 2007]. So most likely both the Nod factor, its receptor and the common signalling pathway have an evolutionary origin in the mycorrhizal symbiosis.

In both the rhizobium nodule and the AM fungal symbiosis a cell wall free symbiotic interface is formed. In the rhizobium symbiosis this is the membrane around the symbiosome, in the AM symbiosis the periarbuscular membrane. Ivanov et al. [2012] identified in *Medicago* a specific exocytotic pathway that is required for the formation of the symbiotic interface by studying the role of VAMPs. VAMPs (vesicle associated membrane proteins) are essential for exocytosis. VAMPs belong to the SNARE proteins. These proteins guide the fusion of vesicles with the appropriate target membrane. Only if the SNARE proteins on both target and vesicle membrane match, fusion occurs. Knockdown of two closely related VAMP72 proteins in *Medicago* inhibits the formation of a cell wall free interface in both the rhizobium and AM symbiosis. Further growth of the root, nodule formation and infection thread/ trunk formation are not affected. So the exocytotic pathway in which these VAMP72 SNAREs participate is essential for the formation of the symbiotic interface but not for other exocytosis dependant processes.

So the comparison of the mechanism controlling symbiotic interface formation in AM and rhizobium symbiosis strongly suggest that the signalling as well as cellular processes controlling symbiotic interface formation in the ancient AM symbiosis have been recruited by the rhizobium nodule symbiosis. Some elements of the common signalling pathway are essential for the formation of the symbiotic interface in the *Frankia* nodule symbiosis. Therefore we hypothesise that also in this symbiosis both signalling and cellular processes have been co-opted from the AM symbiosis.

Interactions with (biotrophic) pathogens

In addition to endosymbiotic interactions, also in interactions with biotrophic fungi an interface needs to be created. These are formed around the intracellular feeding structures developed by the fungus to feed on the plant (Figure 1.1d). In these biotrophic interactions the fungal hyphae first enters the plant intercellular. Inside the root the hyphae branch and penetrate host cells to form haustoria. These haustoria lack a cell wall and are surrounded by an extrahaustorial membrane; a host membrane that is connected to the plasma membrane. However, a cell wall is lacking [Ivanov et al., 2010]. So this interface is similar to the symbiotic interface of AM fungi, *Frankia* and rhizobium in *Parasponia* and primitive legumes. This raises the question whether the biotrophic pathogenic and symbiotic interactions of fungi and plants are evolutionary related, and if so which is the oldest. Some studies showed that the common signalling pathway is not required for haustorium formation. However, this is especially involved in pathogens that interact with leaves [Mellersh and Parniske, 2006]. For the genes encoding components of the common

signalling pathway it is known that they are hardly expressed in the shoot [Benedito et al., 2008]. Therefore it is not so strange that they are not involved in the interaction with pathogens in leaves. It remains to be studied whether root biotrophs use the common signalling pathway and which exocytotic pathway is involved.

In biotrophic interactions plants form an interface and are “forced” to support the pathogen. However, a more general response to pathogens is defense. Plants recognize the pathogens by so called PAMPs (Pathogen Associated Molecular Patterns). One of the PAMPs plants can recognize is chitin. This chitin forms the backbone of both the Nod factor and the Myc factors (LCOs and short chitin oligomers). The similarities in the structure of these signaling molecules indicate that the perception of chitin is also similar to the perception of Nod and Myc factors. Therefore the recognition of these symbiotic signals may originate from pathogenic interactions or vice versa as well.

In rice chitin oligomers are recognized by two receptors: CEBIP and CERK1. CEBIP has several extracellular LysM domains, but lacks an active kinase. CERK1 is a LysM receptor like kinase. This is very similar to the Nod factor receptors (Figure 1.2) [Gough and Cullimore, 2011; Nakagawa et al., 2011]. When the extracellular part of the Nod factor receptor is combined with the intracellular part of CERK1 this chimeric receptor is able to function as a Nod factor receptor. This shows that the intracellular part of the receptor hardly changed.

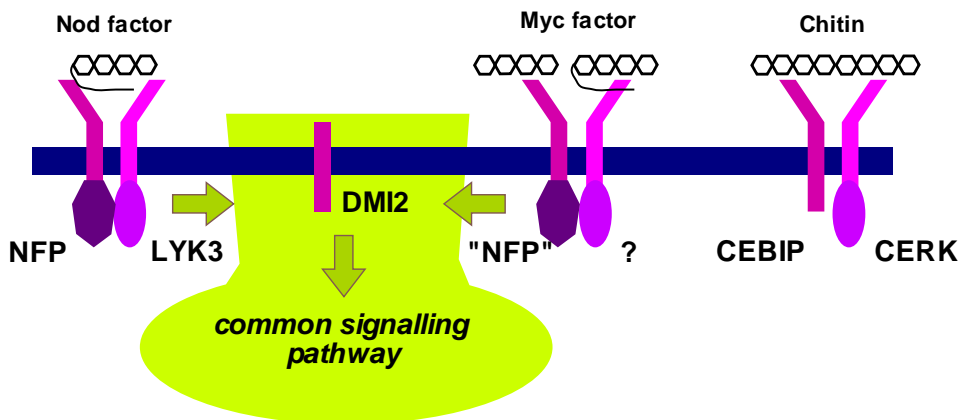


Figure 1.2: Perception of symbiotic and pathogenic signals is similar. Two LysM type receptors perceive the signal of which one has no (active) kinase. The signal is a chitin derived molecule. For the perception of the Myc factor in legumes NFP is not needed, but in the non-legume Parasponia it is essential. Likely, in legumes another receptor performs this function.

Furthermore, it is shown that in Lotus the Nod factor not only induces symbiosis, but also activates defence-related genes [Nakagawa et al., 2011]. When the receptors are expressed in Nicotianum leaves they cause cell death in the absence of Nod factors [Madsen et al.,

2011; Pietraszewska-Bogiel et al., 2013]. These studies underline the close relationship of these pathogenic and symbiotic receptors.

In *Parasponia* it is shown that the kinase death NFP receptor is required for Nod factor, as well as mycorrhizal responses. However, whether a second LysM domain receptor like kinase is involved in the AM symbiosis is not known. Information about the LysM domain receptors involved in the AM symbiosis will be important to resolve the evolutionary relationship of these symbiotic and pathogenic receptors.

The evolution of the rhizobium nodule symbiosis

Studies that are described above strongly indicate that the rhizobium nodule symbiosis evolved from the more ancient AM symbiosis. In both cases a symbiotic interface forms the heart of the symbiosis as it allows an intracellular hosting of the microsymbiont and a well-controlled exchange of nutrients. The cellular mechanism by which the interface is formed involves the same exocytotic pathway [Ivanov et al., 2012]. Also the signalling mechanism by which responses are induced in these two endosymbioses is in part still identical (the common symbiotic pathway). Some elements, for example the LCO (Nod factor) receptors have probably diverged due to gene duplication and neofunctionalization. This hypothesis is especially based on studies in *Parasponia* which revealed that the same receptor is essential in both interactions and identification of the structure of LCOs made by AM fungi. The latter revealed that AM LCOs have a very similar structure as basal Nod factors. However, as rhizobia can produce decorated LCOs that play an important role in host specificity, co-evolution of receptors and Nod factor structure should have taken place.

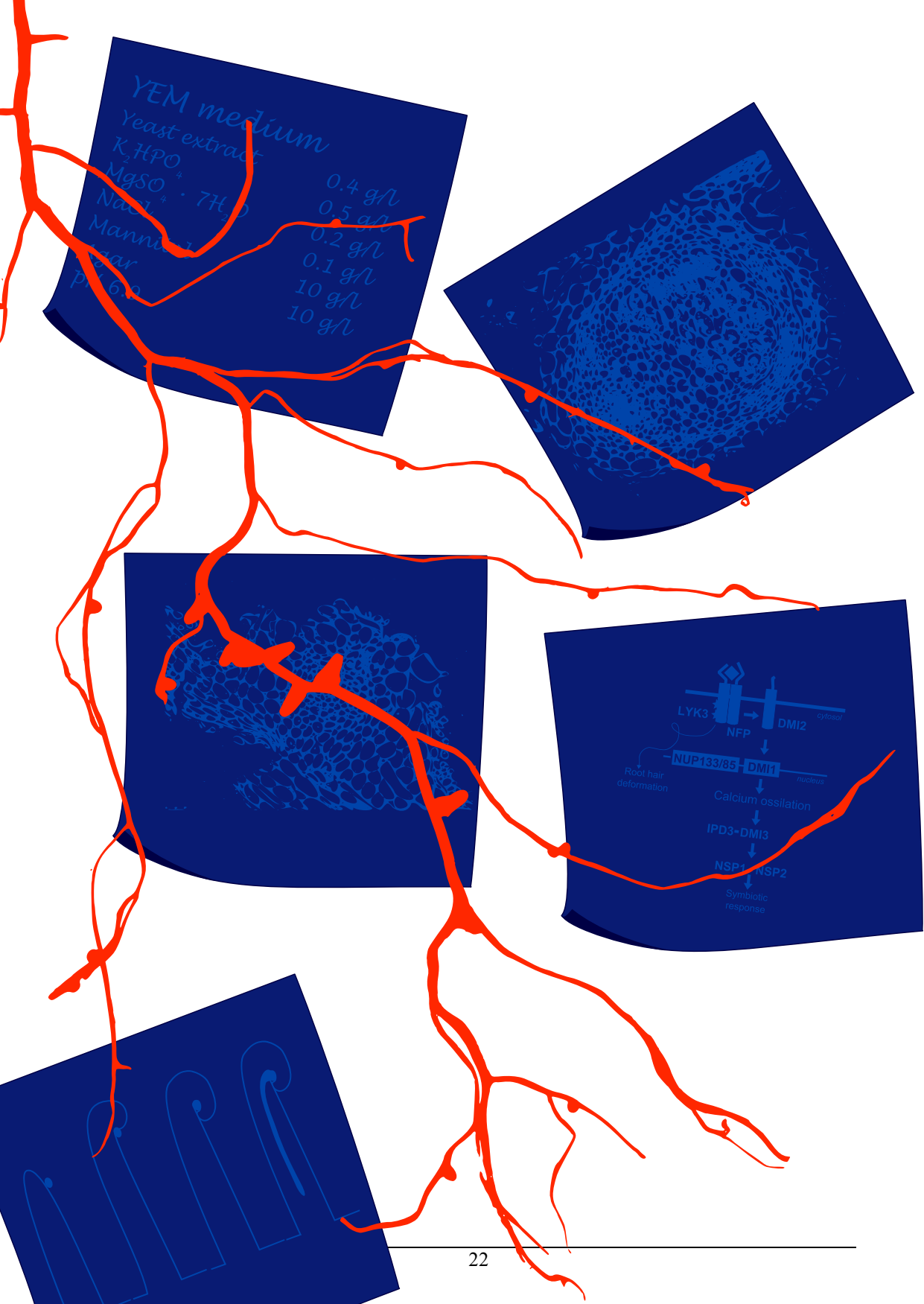
The rhizobium-*Parasponia* symbiosis evolved independently from the legume-rhizobium symbiosis. The fact that both are based on Nod factor induced signalling points to an important evolutionary constraint, namely that the AM mechanisms form the foundation for the evolution of the rhizobium symbiosis. Phylogenetic data suggest that in the Fabaceae the symbiosis has evolved up to six times. It will be interesting to determine whether in all cases the AM machinery was the evolutionary driving force [Doyle, 2011; Geurts et al., 2012; Streng et al., 2011]. Further support for the importance of the AM symbiosis for the evolution of N fixing nodule symbiosis comes from the actinorhizal-Frankia symbiosis. This interaction has been shown to depend on the homologue of SymRK from the common signalling pathway. Therefore we propose that also this endosymbiosis evolved from the AM symbiosis.

The AM symbiosis is maintained in the vast majority of land plants. Therefore the observation that this symbiosis forms the evolutionary blueprint for the N-fixing endosymbioses shows that these novel symbioses evolved by co-opting rather common mechanisms. These N-fixing nodule symbiosis further evolved by recruiting other common processes. Examples are the cell cycle machinery that is modified to support infection

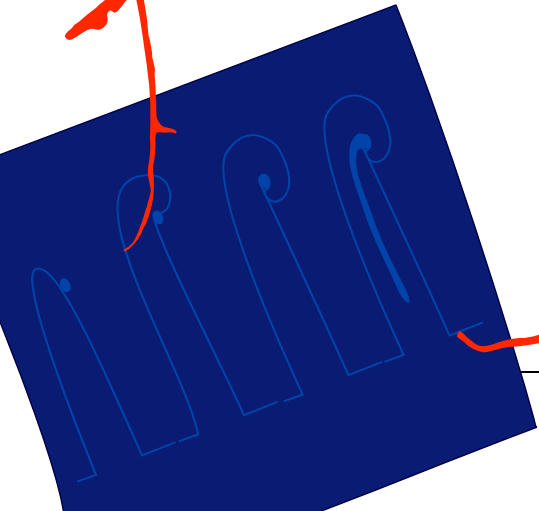
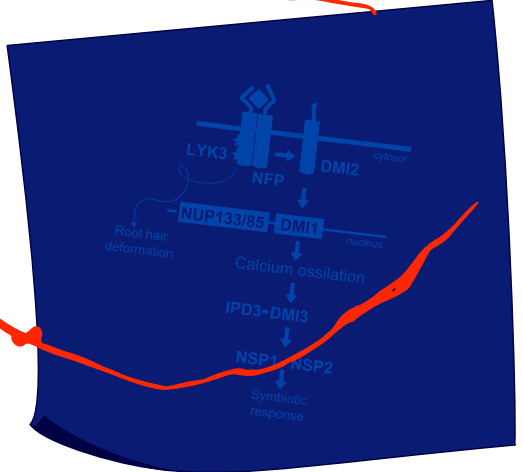
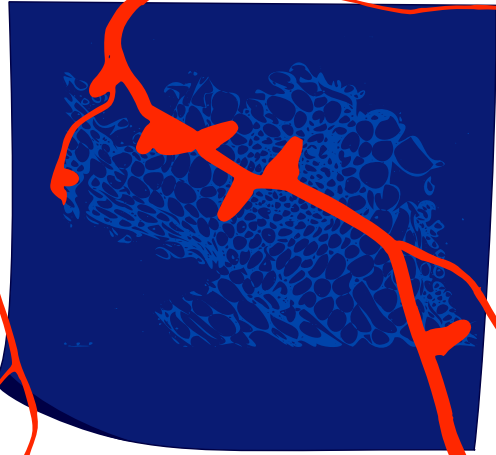
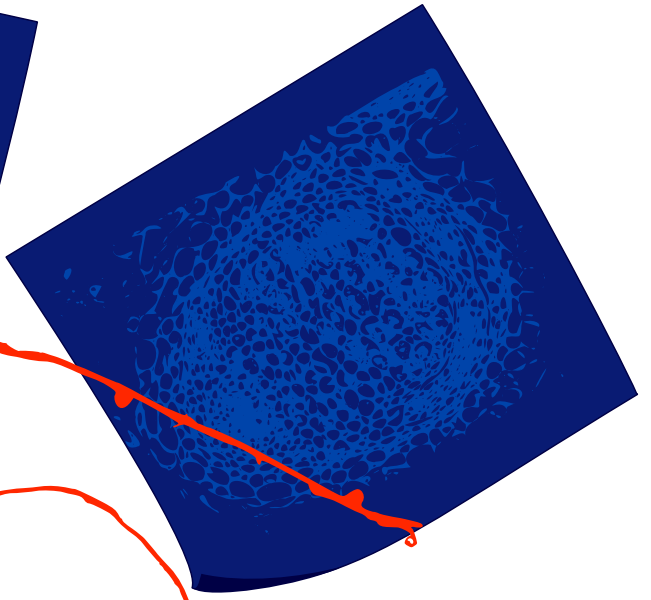
thread growth [Yang et al., 1994] and recruitment of the transcriptional regulators of strigolactone biosynthesis as key regulator of nodule symbiosis [Liu et al., 2011].

The co-option of common processes during nodule evolution seems to contrast with earlier studies on molecular mechanisms controlling root nodule formation. Before the development of model legume systems that allowed the cloning of mutated genes, studies where especially focussed on genes specifically expressed in root nodules (nodulins) [Bisseling et al., 1983; Legocki and Verma, 1980]. These studies were in part driven by the idea that the evolution of nodule symbiosis had created novel genes. However, further studies on nodulin genes revealed that they are often expressed in other organs, albeit at a low level. Further, several nodulins are the result of gene duplication by which nodule specific variants could evolve. Examples are Flotillins [Haney and Long, 2010] and Remorins [Lefebvre et al., 2010; Toth et al., 2012]. The importance of gene duplication in the refinement of the nodule symbiosis is also shown by the analysis of the Medicago genome [Young et al., 2011]. This revealed that a whole genome duplication most likely contributed to the evolution of nodulation. Of the whole genome duplication a certain percentage of the genes are maintained. From these maintained genes only a subset is expressed during nodulation. The notion that nodulins are late additions in nodule evolution is supported by the fact that many of these genes are specific to the rhizobium-legume symbiosis and not shared with the AM symbiosis [Deguchi et al., 2007; Manthey et al., 2004].

Although there are many similarities between the rhizobium and AM symbiosis there must be some striking differences, otherwise all plants would be able to establish a rhizobium symbiosis. A major difference between the two symbioses is the fact that rhizobia never establish a symbiotic interface in existing/ normal root cells, where AM fungi always do. AM fungi form arbuscules in root cortical cells, whereas rhizobia always form an interface in newly formed cells, mostly in root nodules. Even a basal legume like *Gleditsia triacanthos* that does not form root nodules does induce cell divisions in the root cortex to create an environment in which the bacteria can be hosted intracellular [Fehér and Bokor, 1926]. We hypothesize that in normal root cells the turgor pressure is too high to allow release of symbiosomes from an infection thread. In contrast a fungus can create force to enter a plant cell against the turgor of the host cell allowing intracellular growth [Howard et al., 1991]. Therefore, we hypothesize that a major step in the evolution of the rhizobium symbiosis is the formation of a cell type, probably with a temporal reduced turgor pressure, that allows the formation of a symbiotic interface by bacteria.



YEM medium
Yeast extract 0.4 g/l
 K_2HPO_4 0.5 g/l
 $MgSO_4 \cdot 7H_2O$ 0.2 g/l
 $NaCl$ 0.1 g/l
Mannitol 10 g/l
agar 10 g/l
pH 6.0



Chapter 2.

A FATE MAP OF MEDICAGO ROOT NODULES

Ting Ting Xiao¹, Stefan Schilderink¹, Sjeff Moling¹, Eva E. Deinum^{1,2}, Eva Kondorosi³,
Henk Franssen¹, Olga Kulikova¹, Andreas Niebel^{4,5} and Ton Bisseling^{1,6}

¹ *Department of Plant Sciences, Laboratory of Molecular Biology, Wageningen University, Wageningen, The Netherlands.*

² *Department of Systems Biophysics, FOM institute AMOLF, Amsterdam, The Netherlands.*

³ *Institute of Biochemistry, Biological Research Centre, Hungarian Academy of Sciences, Szeged, Hungary.*

⁴ *INRA, Laboratoire des Interactions Plantes-Microorganismes (LIPM), Castanet-Tolosan, France.*

⁵ *CNRS, Laboratoire des Interactions Plantes-Microorganismes (LIPM), Castanet-Tolosan, France.*

⁶ *College of Science, King Saud University, Riyadh, Saudi Arabia.*

Submitted for publication

ABSTRACT

Legume root nodules are induced by N fixing rhizobium bacteria which are hosted in an intracellular manner. The model legume *Medicago truncatula* forms indeterminate nodules with a meristem at their apex. This organ grows by the activity of this meristem that adds cells to the different nodule tissues. These nodules are formed by reprogramming differentiated root cells. In *Medicago sativa* it has been shown that the nodule meristem is derived from the root middle cortex. During nodule initiation also inner cortical cells and pericycle cells are mitotically activated. However, whether and how these cells contribute to the mature nodule has not been studied. Here we produce a nodule fate map precisely describing the origin of the different nodule tissues based on sequential longitudinal sections and the use of marker genes allowing to distinguish between cells originating from different root tissues. We show that nodule meristem originates exclusively from the third cortical layer while several cell layers of the basis of the nodule are directly formed from cells of the inner cortical layers and root endodermis and pericycle. The latter 2 differentiate into the uninfected tissues that are located at the basis of the mature nodule whereas the cells derived of the inner cortical cell layers form about 8 cell layers of infected cells. This nodule fate map has then been used to re-analyse several mutant nodule phenotypes. This showed for example that intracellular release of rhizobia in primordium cells and meristem daughter cells are regulated in a different manner.

INTRODUCTION

The symbiosis of rhizobium and legumes results in the formation of N-fixing root nodules, which can have a determinate or indeterminate growth. Determinate nodules lose their meristem at an early stage of development. In contrast, indeterminate legume nodules have a persistent meristem at their apexes by which they add cells to the different nodule tissues throughout their lifetime [Hadri *et al.*, 1998]. The model legume *Medicago truncatula* (Medicago) forms indeterminate nodules, so their nodule tissues are of graded age with the youngest cells near the meristem. The central tissue of the nodule is composed of 2 cell types, the infected cells that harbour the rhizobia, interspersed with a specialized uninfected cells. This central tissue is surrounded by 3 uninfected peripheral tissues, the nodule parenchyma, endodermis and cortex [Bond, 1948; Brewin, 1991; van de Wiel *et al.*, 1990]. Uninfected tissues are also present at the basal part of the nodule (See Figure 2.11a).

In general it is assumed that in indeterminate nodules the cells along the complete apical-basal axis are derived from the apical meristem. However, this assumption creates some paradoxes. For example, how can the uninfected tissues at the basal part of the nodule be formed from the meristem and not be infected by rhizobium, whereas the layers that are subsequently formed do become infected? Further, the *nf-ya1* mutant forms nodules lacking

a meristem or have a meristem that gives rise to daughter cells in which intracellular infection is blocked. However, several cell layers with fully infected cells are present at the basis of these nodules [Combier *et al.*, 2006; Laporte *et al.*, 2014]. Assuming that all these cells are indeed derived from the meristem, it raises the question why daughter cells lose the ability to become intracellularly infected.

Root nodule formation is initiated by mitotic activation of root cells. The most detailed analysis of which root tissue cells are activated has been performed on *Medicago sativa* [Timmers *et al.*, 1999]. This study showed that inner and middle cortical cells as well as pericycle cells become mitotically active upon rhizobial inoculation. Further, it was shown that the cells of the middle cortex form the nodule meristem. However, whether cells derived from the inner cortex and pericycle contribute to the mature nodule has not been studied. Based on the mutant nodule phenotype of *nf-ya1-1*, we hypothesize that cells derived from inner cortex form several cell layers of infected cells at the basis of the nodule and intracellular infection of these cells is less strictly controlled than infection of cells derived from nodule meristem. To test this hypothesis, we selected *Medicago* (*M. truncatula* A17) to generate a detailed nodule fate map.

The infection process in *Medicago* starts with the formation of an infection thread in a root hair. This is a tube-like structure resulting from an invagination of the host's plasma membrane at the distal end of a root hair. The infection thread then grows to the base of the infected root hair cell. Subsequently, infection threads traverse outer cortical cells allowing the rhizobia to reach the dividing cortical cells. When a meristem is formed, the infection threads start to penetrate host cells derived from the meristem and rhizobia are internalised. During this release from infection threads, rhizobia become surrounded by host membrane, a process controlled by a specific exocytotic pathway [Ivanov *et al.*, 2012], leading to the formation of nitrogen-fixing symbiosomes [Brewin, 2004; Roth and Stacey, 1989]. Symbiosomes then divide, differentiate and ultimately fill the infected cells.

Nodule formation as well as the infection process is controlled by specific lipochito-oligosaccharides, Nod factors, which are secreted by the rhizobia [Lerouge *et al.*, 1990]. Nod factors mitotically activate root cells and such a cluster of dividing cells is often named nodule primordium [Bond, 1948; Brewin, 1991; Dudley *et al.*, 1987; Lancelle and Torrey, 1985; Libbenga and Harkes, 1973; Nap and Bisseling, 1990; Nutman, 1948; Timmers *et al.*, 1999; Yang *et al.*, 1994]. However, the difference between a primordium and a young nodule is not well defined.

Our fate map studies confirmed that in *Medicago*, like in *M. sativa*, the inner and middle cortical and pericycle cells are mitotically activated upon rhizobium infection and the nodule meristem is derived from the middle cortex [Timmers *et al.*, 1999]. We have in addition established, that the first and second cortical layers only have a limited role in nodule ontogeny, that the third cortical layer gives rise to the nodule meristem and about 8 cell layers with fully infected cells at the basis of the central tissue are derived from the

inner cortex (4th and 5th cortical layer). Furthermore, cell divisions are also induced in the root endodermis and the endodermis/pericycle derived cells form the uninfected cell layers at the basis of the nodule.

Using this nodule fate map we re-analysed several *Medicago* mutants and could describe more accurately the nodule developmental steps that are affected.

RESULTS AND DISCUSSION

Pericycle, endodermis and cortical layers contribute to the *Medicago* nodule primordium

Medicago roots have in general 5 cortical cell layers, although also roots with 4 and 6 layers do occur. We will name the outermost layer C1 and the inner most C5. The inner most cortical cells are about 15 µm thick, whereas the cells of the other 4 cortical layers are about twice as thick (30 µm). The epidermis, endodermis and pericycle each contain a single cell layer (Figure 2.1a).

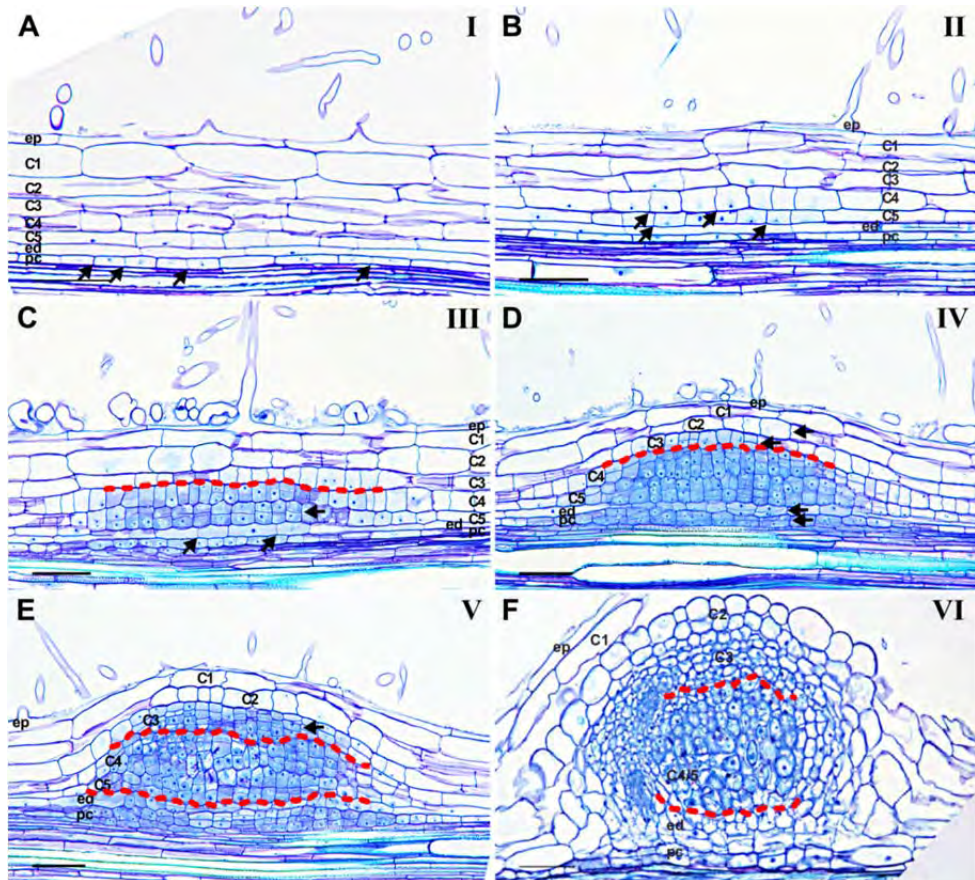


Figure 2.1: *Medicago* nodule primordia at subsequent stages of development. Longitudinal sections of *Medicago* root segments. (A) Stage I: Anticlinal cell divisions are induced in the pericycle (arrows) and that occasionally occur in C5 and C4. (B) Stage II: Cell divisions (anticlinal) extend to C5 and C4 (arrows); anticlinal divisions occasionally occur in C3. The higher frequency of divisions in the inner layers reflects that the divisions start from there. (C) Stage III: Anticlinal divisions occur in C3 (arrow) and endodermis (arrows); periclinal divisions are induced in C4 and C5 derived cells (arrow); anticlinal cell divisions occasionally occur in C2. (D) Stage IV: Periclinal cell divisions are induced in C3 (arrow), endodermis (arrow) and pericycle (arrow); C4 and C5 cell division continue; anticlinal cell divisions occur in C2 (arrow). (E) Stage V: C3 derived cells form multiple cell layers (arrow); C4/5 have form about 8 cell layers; pericycle and endodermis contribute about 6 cell layers to the basal part of the primordium; C2 and C1 have divided a few times anticlinally. (F) Stage VI: vascular bundles are formed at the periphery of the primordia; meristem starts functioning. From this moment on a nodule primordium become a nodule. In D, E and F a red line indicates the border between cells derived from C3 and C4/5 and endodermis, respectively. Epidermis (ep), Cortical cell layers 1st (C1), 2nd (C2), 3rd (C3), 4th (C4), 5th (C5), Endodermis (ed), Pericycle (pc). Bars, 75 µm.

To determine which cell layers of the root contribute to the formation of a nodule primordium, *Medicago* seedlings were inoculated with *Sinorhizobium meliloti* 2011 and root segments were collected at different time points within 1-5 days after inoculation. These were fixed and embedded in Technovit 7100. Longitudinal sections of about 50 root segments were made and analyzed by light microscopy. Based on these analyses we divided nodule development in 6 stages (Figure 2.1). At stage I, anticlinal divisions are

induced in the pericycle (Figure 2.1a). This is rapidly followed by anticlinal divisions first in C5 and slightly later in C4 (stage II) (Figure 2.1b). During stage III, periclinal divisions are induced in C5 and C4 and anticlinal divisions occur in C3 and endodermis (Figure 2.1c). At stage IV, periclinal divisions occur in C3, pericycle and endodermis, cell divisions continued in C5 and C4 and some anticlinal divisions are induced in C2 (Figure 2.1d). At stage V, C3 derived cells have formed a multi layered (future) meristem, C4 and C5 have formed about 8 cell layers and the endodermis and pericycle 6-8 cell layers. At this stage of nodule development mitotic activity in the non-meristematic cells stops (Figure 2.1e). At stage VI, vascular bundles are established at the periphery and the meristem starts to add cells to the nodule tissues (Figure 2.1f). Therefore at stage VI the nodule primordium has become a root nodule. We propose to name the clusters of dividing cells a nodule primordium up to stage V and nodule from stage VI on. Previously, it was proposed to call the clusters of dividing cells at stage I and II an initial primordium [Timmers *et al.*, 1999]. However, as these cells become part of the mature nodule (see below) there is no reason to distinguish these stages from stage II-V primordia.

To obtain better insight in the timing of the different stages of nodule primordium formation, we also spot inoculated *Medicago* roots with *Sinorhizobium meliloti*. Stage I starts at about 24 hours post inoculation (hpi); stage II 27-33 hpi; stage III from 33-35 hpi; stage IV from 42-48 hpi; stage V from 65-70 hpi and stage VI after 80 hpi.

Medicago lateral root formation also starts with divisions in the pericycle, endodermis and cortex cells [Herrbach *et al.*, 2014; Op den Camp *et al.*, 2011], which is very similar to nodule primordium initiation. To distinguish a young lateral root primordium from an early stage (I-III) nodule primordium, we made use of transgenic *Medicago* roots expressing MtENOD40::GUS. This reporter is strongly induced in rhizobium activated pericycle and cortical cells and markedly less and restricted in pericycle cells of the lateral root primordia (Figure 2.2).

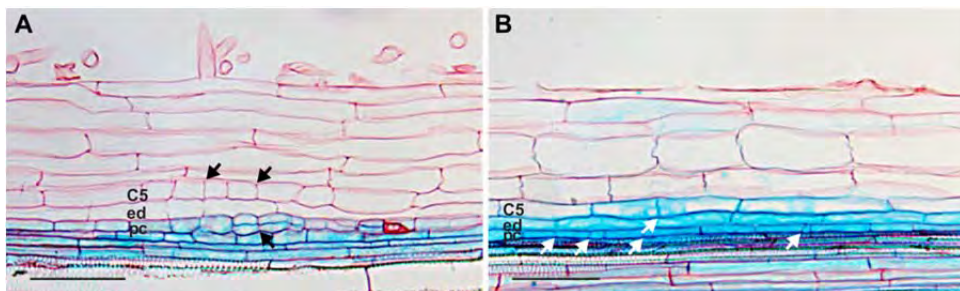


Figure 2.2: MtENOD40::GUS is a marker to distinguish between early root primordium and nodule primordium. The root (A) and nodule (B) primordia are initiated on the same MtENOD40::GUS transgenic root. In both primordia C5 and pericycle cells have divided (black and white arrows), MtENOD40 is markedly higher expressed in the nodule primordium (B).

We showed that in *Medicago* the mitotic activation of root cells by rhizobium starts in the pericycle and extends outwards to the cortical cell layers. The middle cortical cell layer (C3) ultimately forms the nodule meristem. This is similar to nodule primordium initiation in *M. sativa* [Timmers *et al.*, 1999]. In addition, we showed that the endodermis also divides and together with pericycle and inner cortex cell layers (C4 and C5) contribute about 16 cell layers to the nodule primordium. Based on these observations we addressed the following 2 questions: How can perception of the rhizobial signal at the root surface lead to a wave of cell division that starts in the most inner layers? And do the primordium cell layers that originate from pericycle up to C4 contribute to mature nodule tissues?

How can perception of Nod factors at the epidermis lead to a wave of cell division that starts in the inner most layer?

When pericycle cells are mitotically activated by Nod factors secreted by rhizobia the bacteria are still present at or in the epidermis. As Nod factors are rather immobile signal molecules [Goedhart *et al.*, 2000], perception of Nod factors at the epidermis most likely triggers mitotic activity in inner root cell layers. So how could an exogenously applied signal lead to cell division starting in the cell layer that is most remote, while the cells closest to the signal respond last? Previously, we made a theoretical model to investigate how Nod factors can induce cortical cell divisions [Deinum *et al.*, 2012]. It is known that Nod factor perception leads to cytokinin signaling, while cortical cell division is associated with increased auxin. Cytokinin is known to affect negatively the accumulation of auxin efflux carriers (PIN) in the plasma membrane [Dello Ioio *et al.*, 2008; Marhavý *et al.*, 2011]. Therefore we simulated that Nod factor signaling induces the decrease of the level of PIN protein in all cortical cell layers of the region responding to Nod factors. This block of cortical cells was named “controlled area”. This resulted, in the model, in a local increase of auxin in the cortex which coincided with the site where cortical cell divisions are induced. Here we included the pericycle and endodermis into the “controlled area” (Figure 2.3a) and further we focused on the early dynamics of the resulting auxin accumulation in relation to the patterns of cell division we have observed.

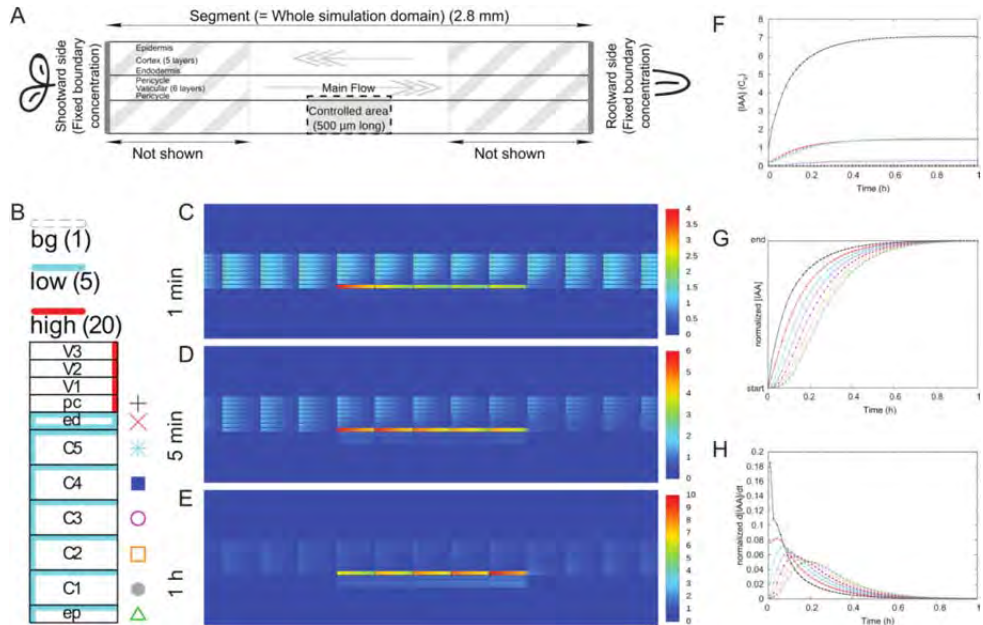


Figure 2.3: Auxin accumulation following a local reduction of the effective efflux permeability starts from the inner root layers. Simulations are based on a root segment representing the susceptible zone of *Medicago* roots (A) [Deinum et al., 2012]. At $T = 0$ s, the efflux is reduced in a block of cells that is 5 cells long and comprises all cell files from epidermis to pericycle. This we call the “controlled area”. The PIN distribution (B) of this root segment is such that the main auxin flux in the vascular tissue is rootward and reversed in the cortex. The starting concentration of PINs in each membrane segment is one of three levels: “high” (red, $P_{eff} = 20 \mu\text{m/s}$), “low” (cyan, $P_{eff} = 5 \mu\text{m/s}$), or “bg” (white, $P_{eff} = 1 \mu\text{m/s}$) [Deinum et al., 2012; Laskowski et al., 2008]. (C-E) Concentration heat maps of the middle part of the root segment including the controlled area at $T = 1$ min (C), $T = 5$ min (D) and $T = 1$ h (E). (F) The concentration in the middle row of cells is tracked for all cell files in the controlled area with symbols and colours as indicated in B. The concentration in the pericycle remains highest, followed by endodermis and inner cortex (C5). (G) When rescaling the concentration in each file from its starting level to the level reached at the end of the simulation ($T = 1$ h), it becomes clear that the concentration in the pericycle increased first, followed by the other layers in an interior to exterior order. The moment of fastest concentration increase, the peaks of the curves in H (time derivative of G, expressed in rescaled concentration units per minute), showed the same relative order.

Start from pericycle, vasculature cell layer 1st (V1); 2nd (V2); 3rd (V3). For our current simulations we used a PIN layout that gave rise to auxin accumulation patterns matching experimental observations (Figure 2.3b) as our starting point. This layout, and all variants that we have used, produce a root-ward auxin flux in the stele/vascular tissue and a shoot-ward and inward flux in the cortex.

The reduction of membrane PINs resulted in an increase of the auxin concentration in all cell layers. However, only in the pericycle, endodermis and inner cortical layers the auxin concentration in the controlled area reached a level similar to or higher than the vascular starting level. Furthermore, in the outer layers the absolute increase was very small compared to this (Figure 2.3c-f). The auxin sensing system of TIR1-SCF controlled

ubiquitination of Aux/IAA proteins can detect changes in auxin concentration [Middleton *et al.*, 2010]. We therefore plotted the concentration increase in each layer normalized by the concentrations at the beginning and the end of the simulation (Figure 2.3g) and the time derivative of these curves (Figure 2.3h). This shows that the auxin concentration increased first and fastest in the pericycle, followed by the endodermis and C5 and then by other layers in an outward fashion. The time derivatives (Figure 2.3h) clearly show that the pericycle was also the first layer where the increase of concentration started slowing down; the peaks of these curves occurred in an interior to exterior order.

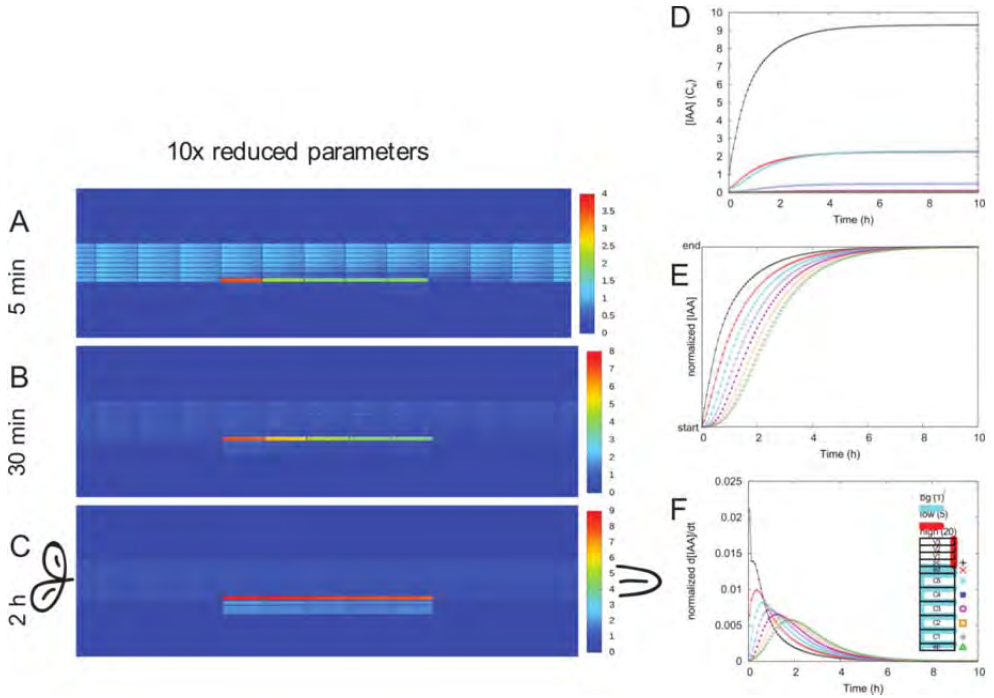
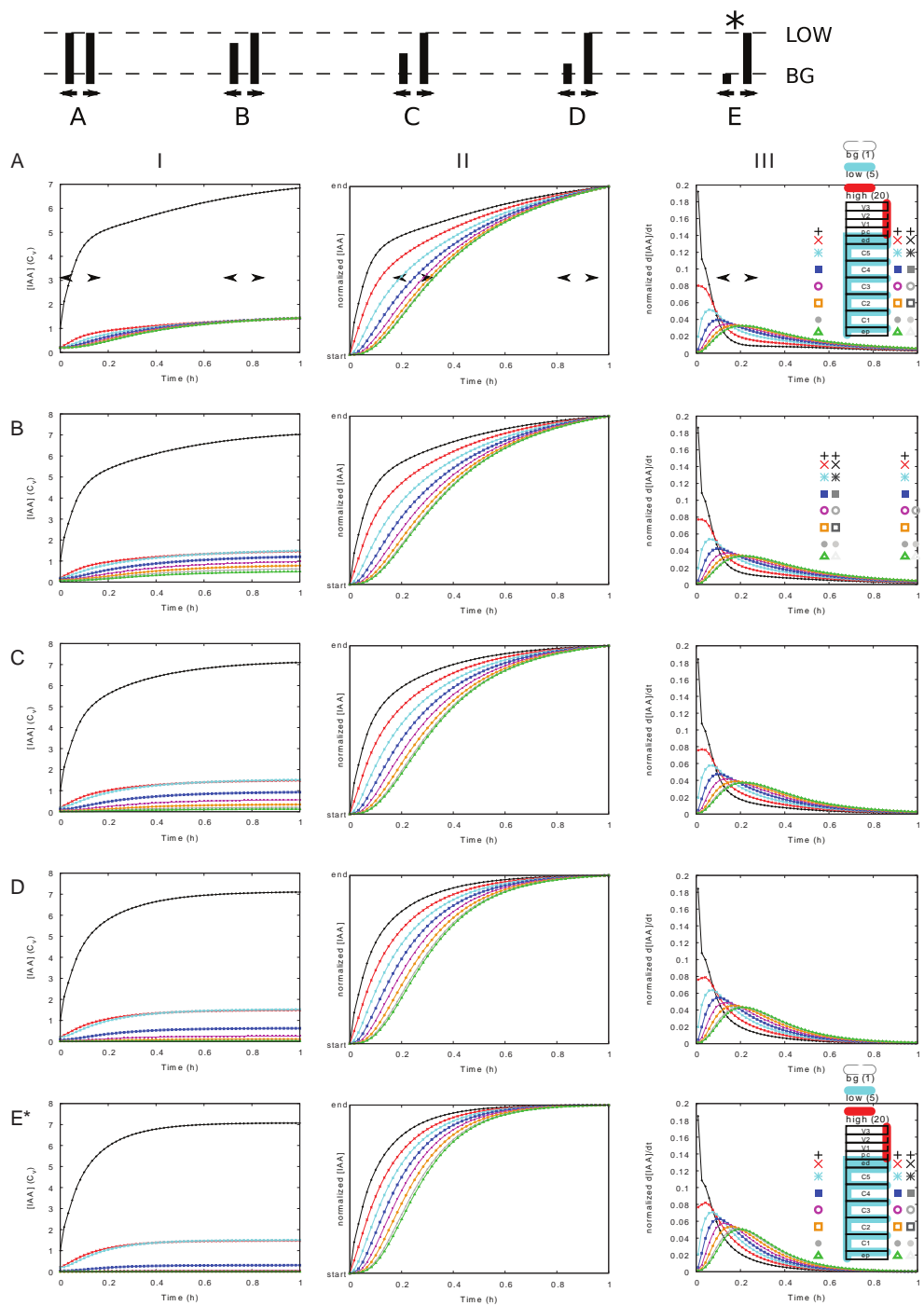


Figure 2.4: Also with slowed down auxin dynamics, auxin accumulation following a local 10x reduction of the effective efflux permeability starts from the inner root layers. The starting concentration of PINs in each membrane segment is one of three levels: “high” (red, $P_{eff} = 2 \mu m/s$), “low” (cyan, $P_{eff} = 0.5 \mu m/s$), or “bg” (white, $P_{eff} = 0.1 \mu m/s$) [Deinum *et al.*, 2012]. (A-C) Concentration heat maps of the part of the root segment including the controlled area at $T = 5$ min (A), $T = 30$ min (B) and $T = 2$ h (C). (D) The concentration in the middle row of cells is tracked for all cell files in the controlled area. The concentration in the pericycle remains highest, followed by endodermis and inner cortex (C5). (E) When rescaling the concentration in each file from its starting level to the level reached at the end of the simulation ($T = 20$ h), it becomes clear that the concentration in the pericycle increased first, followed by the other layers in an interior to exterior order. The moment of fastest concentration increase, the peaks of the curves in F (time derivative of E, expressed in rescaled concentration units per minute), showed the same relative order.



To investigate the robustness of our simulation results we performed two controls. First, we repeated the simulation with 10 fold altered influx and efflux values (Figure 2.4). This slowed down the dynamics of auxin accumulation by a corresponding degree, but conserved the order and relative magnitudes of changes. Second, we varied the inward: outward ratio of the cortical PINs (Figure 2.5). A decrease of this ratio from our default (departing from Figure 2.5e) resulted in a flatter auxin gradient over the cortex, but conserved the relative order of auxin increase. Taken together these results show that auxin accumulation from the inner layers is a robust feature of this system.

If we use auxin as a proxy for the induction of cell divisions, these results show that the divisions would start from the interior layers and proceed outward. This would happen both, when absolute auxin concentration controls divisions and when the change in auxin concentration does it. In reality it is likely that both play a role and the low absolute increase we found in the outermost layers could explain that no divisions were induced in C1.

Do primordium cells derived from C4/5 become part of the mature nodule?

In a nodule primordium, about 16 cell layers are derived from pericycle, endodermis, C4 and C5 and not from the nodule meristem. We studied whether and how these layers become part of a nodule. First we determined whether rhizobia can infect these cells. Serial sections of 30 primordia at stage III-IV were analyzed. In 5 primordia (stage III), the infection thread was still in C1 or C2 and in 10 (stage III) primordia, the infection thread had just reached C3 (Figure 2.6a). In 15 primordia, the infection thread was present in cells derived from C4 and C5 (Figure 2.6b). In 10 of these latter primordia, C3 cells had divided several times including both anticlinal and periclinal divisions (stage IV). Therefore it is likely that cells derived from C3 can still be penetrated by an infection thread after the first anticlinal divisions (stage III). As nodule meristematic cells are not penetrated by infection

← Figure 2.5: Auxin accumulation always starts from the interior layers, regardless of inward: outward PIN bias in the cortex. The amount of PIN (P_{eff}) before efflux reduction in the abaxial membrane of the cortical cells decreases from A, with $P_{eff} = 5 \mu\text{m/s}$ ("low") for abaxial and adaxial cell faces, to E, with $P_{eff} = 1 \mu\text{m/s}$ ("bg") for the abaxial cell face. This is illustrated in the cartoon on top. The root from figure 3, E in this figure, is marked with an asterisk (*). The full PIN distribution pattern is illustrated for A and E similar to figure 3-B. This also shows the markers for the different cell layers. I: Concentration in the controlled area from the moment of efflux reduction (c.f. figure 3-F). II: Concentration, rescaled from the initial value to the concentration at the end of the simulation ($T = 1\text{h}$; c.f. figure 3-G). III: Concentration change. This is the time derivative of II, expressed in rescaled concentration units per minute (c.f. figure 3-H). In all cases (A-E) the same relative order occurs: the first, strongest and fastest increase occurs in the pericycle, followed by endodermis, C5, etc. towards outer layers. The stronger the inward bias of the cortical PINs, the lower the steady state concentrations reached in the exterior root layers epidermis and outer cortex. It is likely that with a strong inward bias, i.e., towards the bottom of the figure, the maximum concentration reached in the outer cortex is insufficient to trigger a cell division response.

threads it is probable that infection thread have to reach C4 and C5 derived cells before stage IV, i.e. before periclinal divisions are initiated in the C3 layer.

To determine the timing of the infection of the primordium more precisely, spot inoculated *Medicago* roots were analyzed. At 42-48 hpi, the infection thread had reached C4/5 derived cells (stage IV). Around 80 hpi (stage VI) bacterial release had taken place in cells derived from C4/5 (Figure 2.6c-d). This means that release occurs about 24 hrs after the infection thread reached the primordium cells.

C4/5 derived cells that are infected by rhizobia develop into large infected cells. So, in a mature nodule about 8 cell layers of the central tissue directly developed from C4/5 derived cells and not from the meristem (C3).

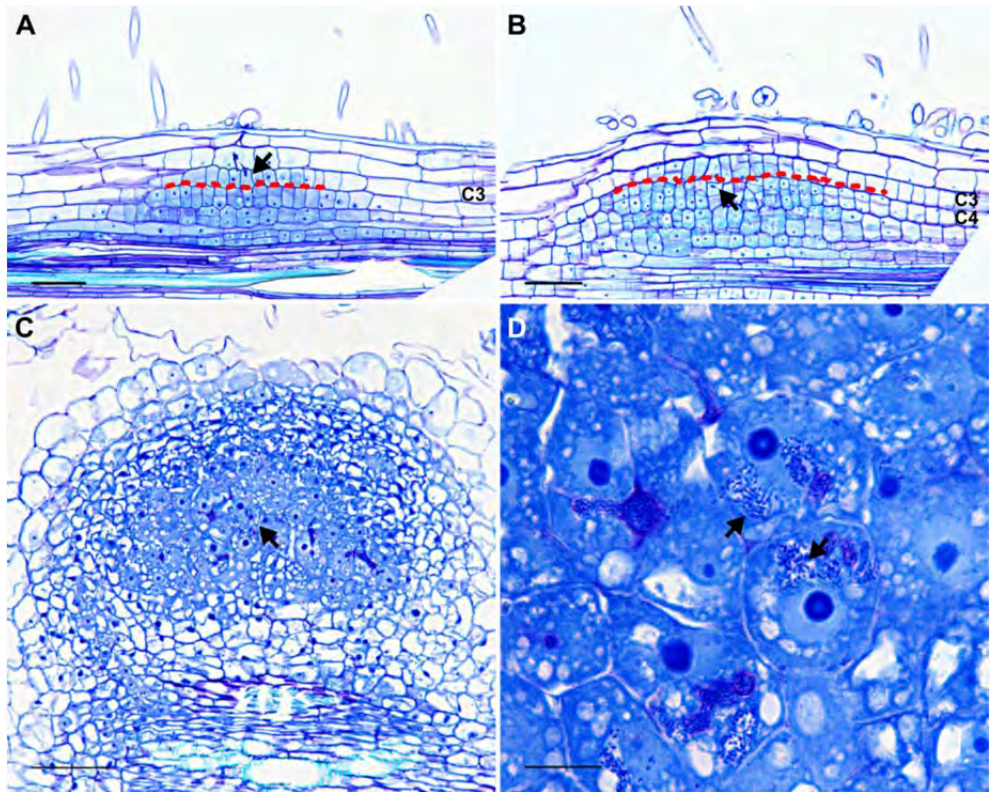


Figure 2.6: Infection threads reach C4/5 derived cells before stage IV. (A) At stage III of primordium development, anticlinal divisions are induced in C3 and the tip of the infection thread (arrow) reached C3. (B) At stage IV, the tip of the infection thread has reached the cells derived from C4/5 (arrow). (C) At stage VI (80 hpi), rhizobia are released in C4/5 derived cells. (D) Magnification of C shows the released rhizobia (arrows). In A and B a red line indicates the border between cells derived from C3 and C4. Bars, 75 µm in A-C; 10 µm in D.

Do primordium cells derived from pericycle/endodermis become part of the mature nodule?

The analysis of nodule primordia showed that C4 and C5 derived cells can be infected by rhizobia. However, whether endodermis and pericycle derived cells may also become infected cannot be excluded. In order to trace primordium cells derived from endodermis and pericycle more precisely, we made use of CASP1, an Arabidopsis gene that is specifically expressed in the root endodermis. It encodes a transmembrane protein that is involved in the formation of casparian strips (Roppolo *et al.*, 2011). To determine whether this gene can be used as an endodermis marker in *Medicago*, we transformed *Medicago* roots with AtCASP1::GUS [Vermeer *et al.*, 2014] and showed that this construct is specifically expressed in the endodermis (Figure 2.7a).

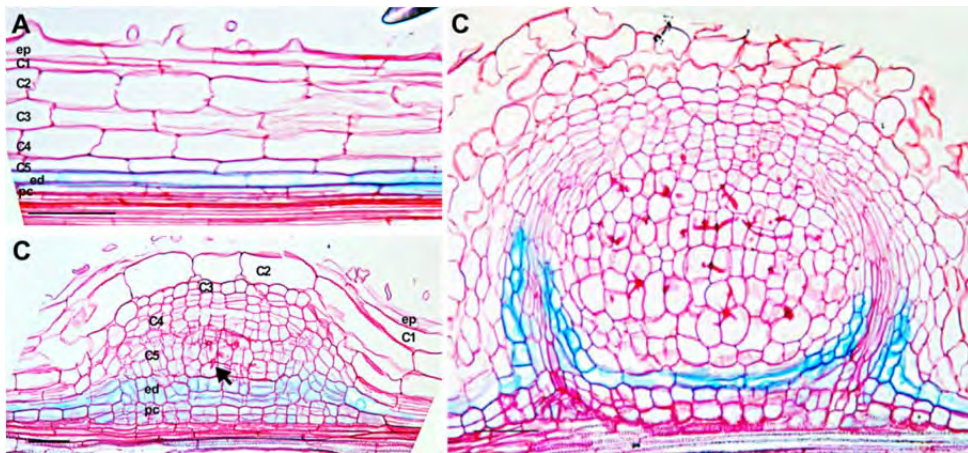


Figure 2.7: Endodermis and pericycle derived cells of the primordium are not infected. AtCASP1::GUS (A) is specifically expressed in the *Medicago* root endodermis. AtCASP1::GUS (B) remains in endodermis derived cells at stage IV. Infection threads (arrow) never reach endodermis and pericycle derived cells. (C) At stage VI, AtCASP1::GUS expression is restricted to a single cell layer surrounding the nodular vascular bundle (endodermis). Bars, 75 μ m.

In general, it is assumed that root cells that are mitotically activated are completely de-differentiated. Therefore we expected that AtCASP1::GUS would be repressed when cell divisions are induced in the endodermis. However, when the endodermis had undergone several periclinal as well as anticlinal divisions all endodermis derived cells displayed GUS activity. Therefore we were able to trace endodermal cells during the formation of a nodule primordium and could distinguish them from cortex and pericycle derived cells (Figure 2.7b). The intensity of the signal in the endodermis derived cells is (at least) as high as in the endodermis before division. So it is not simply a dilution of GUS present in the root endodermis before cell divisions are induced and the AtCASP1 promoter must have remained active during endodermal cell divisions. Analyses of serial sections of 30 stage IV-V primordia showed that infection threads do not penetrate endodermis and pericycle

derived cells in contrast to C4 and C5 derived cells. So the origin of the primordial cells appears to determine whether they can be penetrated by an infection thread or not.

At stage VI of development the expression of AtCASP1::GUS is repressed in most of the endodermis derived cells and becomes restricted to a single cell layer and vascular endodermis when vascular bundles start to be formed at the periphery (Figure 2.7c).

The maintenance of endodermal specific gene expression in nodule primordium is also illustrated by the expression of Scarecrow (SCR). Arabidopsis SCR is a GRAS type transcription factor that is specifically expressed in the root endodermis and is essential for the formation of this tissue [Di Laurenzio *et al.*, 1996]. AtSCR::GUS is also specifically expressed in the endodermis of transgenic Medicago roots (Figure 2.8a). Like AtCASP1, it remains active in divided endodermal cells in a nodule primordium up to the stage when vascular bundles start to be formed (Figure 2.8b). It is also activated in cells around the vasculature (Figure 2.8c).

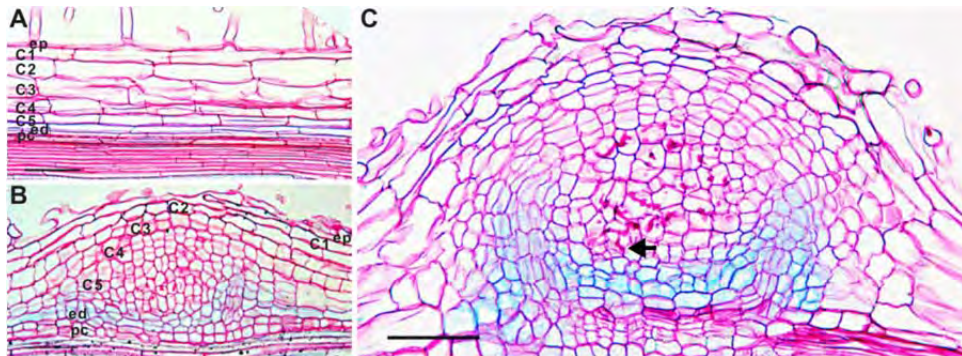


Figure 2.8: AtSCR::GUS is expressed in endodermis (A) and cells derived from endodermis (B) and these cells are not infected by rhizobium (B-C). Infection threads are indicated by arrows. Bars, 75 μ m..

So, AtCASP1 and AtSCR promoters that are specifically expressed in the root endodermis remain active when cell division is induced. Therefore we studied whether casparian strips, the hallmark of endodermal cells, are formed in the dividing endodermis cells (Figure 2.9). Casparian strips are present in the Medicago root endodermis (Figure 2.9a), but upon the first divisions induced by rhizobium, these are lost (Figure 2.9b). They are again formed in the single cell layer at the basis of the nodule, where expression of AtCASP1::GUS is maintained (Figure 2.9c). AtCASP1::GUS is also expressed in the endodermis around the nodule vascular bundles, and there casparian strips are present (Figure 2.9d). In contrast, AtCASP1::GUS is not expressed in the nodule endodermis and casparian strips are not formed (Figure 2.9d). So a “real” endodermis is only formed at the basis of the nodule and around nodule vascular bundles. The fact that the casparian strips are (have to be?) removed before cell division is induced could be a reason why induction of mitotic activity in this tissue is slightly delayed compare to C4 and 5 cells.

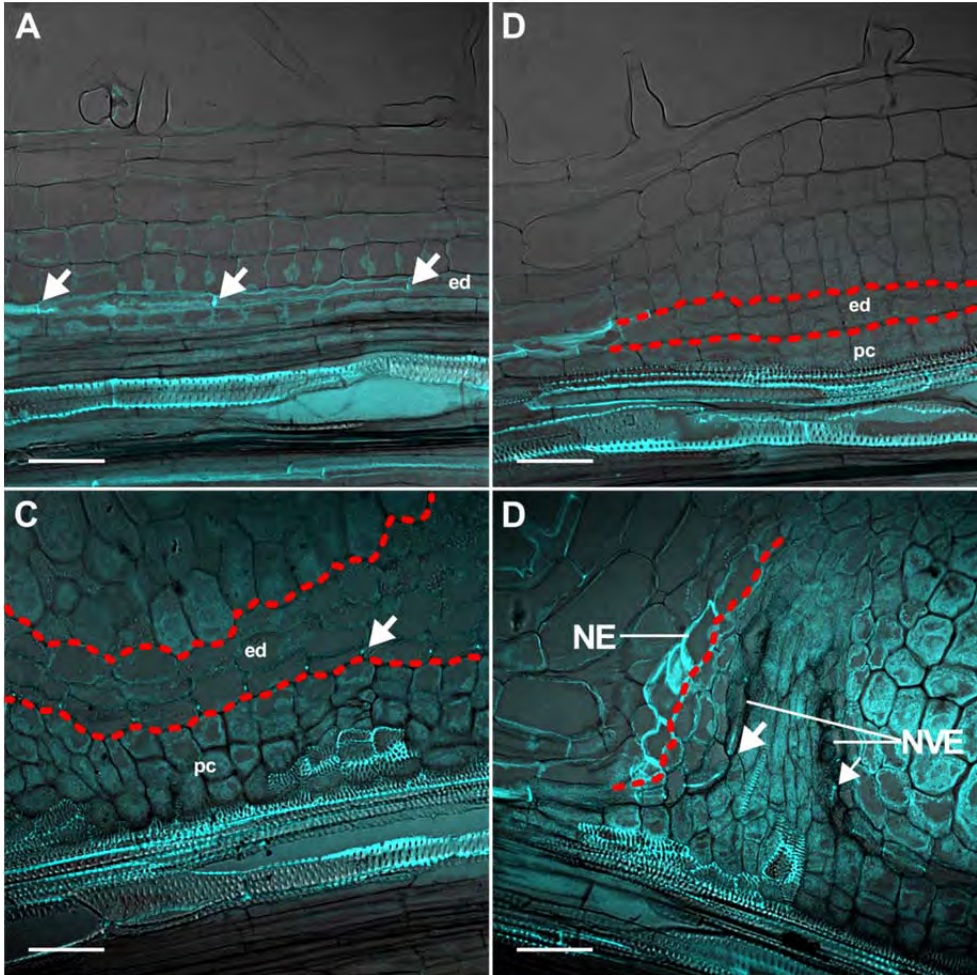


Figure 2.9: Casparian strips disappear in the dividing endodermis of nodule primordium. (A) Casparian strips (arrows) in the root endodermis. (B) Casparian strips are absent in dividing endodermal cells. (C) At stage VI, casparian strips (arrow) are formed in the single cell layer at the basis of which *AtCASPI* are expressed. (D) Casparian strips (arrows) are formed in the endodermis of nodule vascular bundles but not in the nodule endodermis. In B and C red lines indicate the border between cells derived from endodermis and C5 or pericycle, respectively; in D a red line indicates the border between nodule endodermis and nodule parenchyma. Casparian strips are detected as autofluorescence under UV light. Nodule vascular endodermis (NVE), Nodule endodermis (NE). Bars, 50 μ m.

These results show that primordium cells derived from pericycle and endodermis, in contrast to those with a cortical origin, cannot be infected by rhizobia. As the endodermis derived primordium cells maintain expression of endodermal genes, it is most likely that these cells do not completely de-differentiate but switch from one differentiated cell type into another, a process named trans-differentiation [Sugimoto *et al.*, 2011]. By which mechanism infection in these endodermis derived cells is prohibited is unclear. We hypothesise that the (partial) maintenance of the endodermal fate can contribute to this.

In nodules the pericycle and endodermis derived cells form the peripheral tissues at the basis of the nodule. These are the nodule parenchyma and a few cell layers that are adjacent to the root vascular bundle. In between these two tissues an endodermis containing casparian strips is present. At the periphery of the primordium, pericycle and endodermis derived cells locally differentiate into vascular tissue.

Markers to distinguish C4/5 derived cells and meristem

We searched for molecular markers enabling us to distinguish between C4/5 derived cells and (future) meristem cells. Infected cells in the infection zone of a mature nodule undergo endoreduplication. Therefore, we expected that C4 and C5 derived cells enter endoreduplication when they stop dividing (stage V). In this case markers for mitosis and endoreduplication could be used to distinguish these cells from (future) meristem cells. To identify mitotically active and endoreduplicating cells we used Medicago lines containing a Arabidopsis Cyclin B1 reporter (AtCyclB1.1::GUS) which is active during mitotic divisions and MtCCS52A::GUS which is expressed in endoreduplicating cells [Vinardell *et al.*, 2003]. Both lines were inoculated with *S. meliloti* and roots were harvested at 48 and 72 hpi. At stage IV the AtCyclB1.1 promoter is active in “a salt and pepper” pattern in the complete primordium, confirming that C4 and 5 derived cells continue to divide when they are penetrated by an infection thread (Figure 2.10a). At stage V, cell divisions continued in cells derived from C3 and had stopped in those derived from C4/5. Indeed, the AtCyclB1.1 promoter remained active in C3 derived cells and was switched off in C4/5 derived cells at stage V and later stages (Figure 2.10b). The endoreduplication reporter had an expression pattern that is complementary to that of AtCyclB1 at stage VI; when the latter is switched off in the C4/5 derived cells, MtCCS52A::GUS is switched on in these cells (Figure 2.10c). This endoreduplication reporter is not expressed in nodule primordia before stage V.

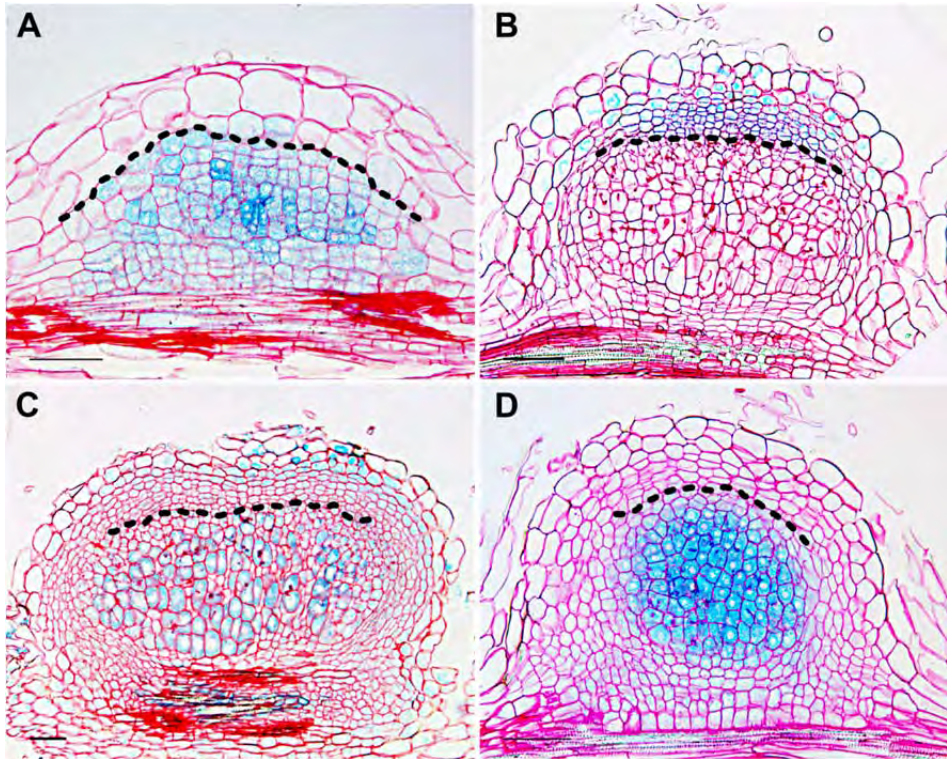


Figure 2.10: Molecular markers to distinguish C4/5 derived cells from the nodule meristem (C3). Before stage V, C4 and C5 are still mitotically active. (A) At stage IV, *AtCyclB1.1::GUS* is expressed in C4/5 derived cells. (B) At stage VI, *AtCyclB1.1::GUS* is expressed in C3 derived cells, but not in C4/5 derived cells. (C) At stage VI, the cell endoreduplication marker *MtCCS52A::GUS* is expressed in C4/5 derived cells and some C1/2 and epidermis derived cells, but not in C3 derived cells. (D) In transition from stage V to VI, *MtSYMREM1::GUS* is detected in C4/5 derived cells. A black line indicates the border between cells derived from C3 and C4. Bars, 75 μ m.

We also tested whether the nodule specific remorin (*MtSYMREM1*) that is involved in bacterial release [Lefebvre *et al.*, 2010] can be an extra marker. *Medicago MtSYMREM1::GUS* transgenic roots inoculated with *S. meliloti* showed that this marker is first induced in C4/5 derived cells in between stage V and VI, and it is not active in cells derived from C3 (Figure 2.10d).

We thus have identified three markers allow to distinguish between C4/5 and C3 derived cells during nodule developmental stage V and VI.

Analyses of symbiotic mutants

To illustrate the value of our *Medicago* nodule fate map for understanding the nodule development we have re-analyzed four previously characterized mutants with greater accuracy, namely *nf-ya1* [Combiér *et al.*, 2006; Laporte *et al.*, 2014], *sickle* [Penmetsa and

Cook, 1997], *lin* [Guan et al., 2013; Kiss et al., 2009; Kuppusamy et al., 2004] and *ipd3* [Ovchinnikova et al., 2012; Singh et al., 2014], respectively.

nf-ya1

nf-ya1-1 [Combier et al., 2006; Laporte et al., 2014] forms nodules of variable size, but all are markedly smaller than wild type nodules. The largest *nf-ya1-1* nodules (Figure 2.11b) have about 8 cell layers with well infected cells at their proximal part. In these cells development of rhizobium into N fixing symbiosomes is like in wild type, as described in Laporte et al. [2014]. These nodules have a relatively small meristem and in cells derived from it infection threads are present, but release is blocked. This phenotype suggests that during primordium formation, cell divisions in C4 and C5 have occurred and rhizobia, like in wt nodules, are released in these cells. However, the formation of a wt-sized meristem that can produce daughter cells competent for bacterial release requires NF-YA1. In addition to these relatively large *nf-ya1-1* nodules also smaller nodules are formed. These can have only a few layers with fully infected cells (Figure 2.11c), a nodule meristem is absent and the nodule is completely surrounded by the nodule endodermis. In these cases, divisions in C4 and C5 have most likely occurred to a certain extend and these cells differentiate into wt-like infected cells. However, the formation of a meristem (from C3) appears to be blocked.

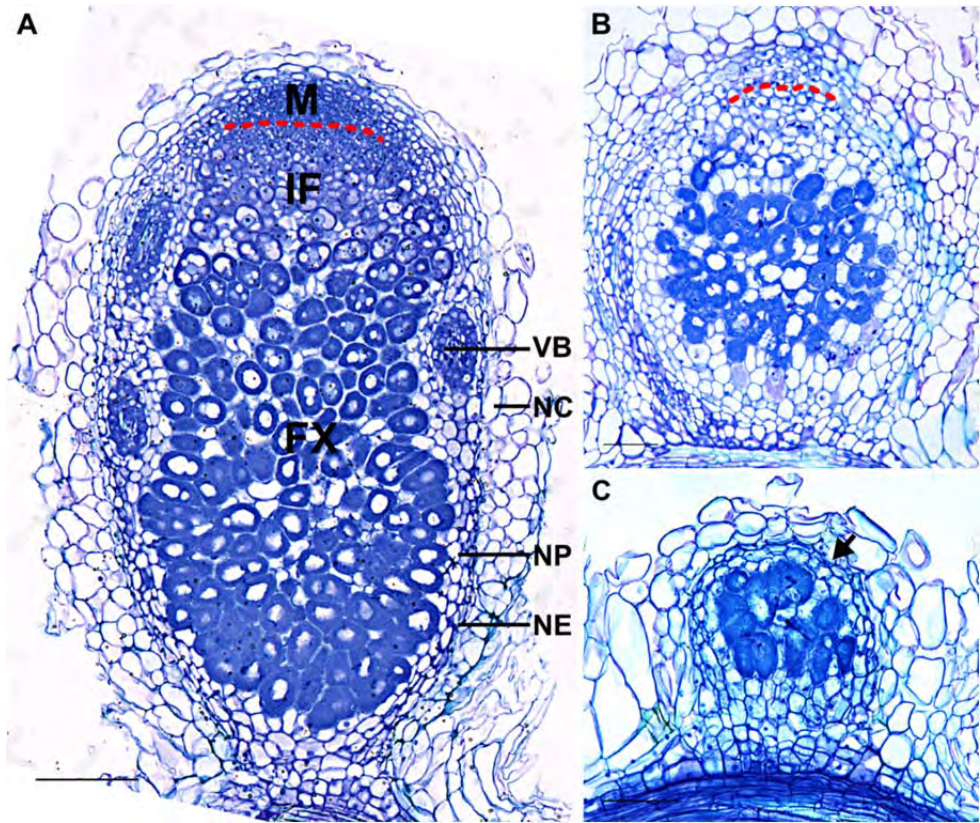


Figure 2.11: Mutant *nf-ya1-1* forms nodules with a small nodule meristem or no nodule meristem. Two weeks old wt (A) and *nf-ya1-1* (B-C) nodules have a central part well infected by rhizobia. (B) A relatively large *nf-ya1-1* nodule has a small nodule meristem. (C) A small *nf-ya1-1* nodule does not have a nodule meristem and develops closed nodule endodermis (arrow). Meristem (M), Infection zone (IF), Fixation zone (FX), Vascular bundle (VB), Nodule parenchyma (NP), Nodule cortex (NC). In A and B a red line indicates the border between nodule meristem and infection zone. Bars, 75 μ m.

To test these hypotheses we studied nodule primordia of the *nf-ya1-1* mutant. Roots were sectioned at 1-5 dpi. This showed that primordia are rather diverse which is well in line with the diverse nodule phenotypes. The largest primordia are composed of cells derived from pericycle up to C3 (Figure 2.12a). Cells derived from C4/5 are infected and contain released bacteria which in wt is a hall mark of stage VI (Fig. 9B) and several of these infected cells have already enlarged (Figure 2.12a). In such primordia, some periclinal divisions have occurred in C3 derived cells, but markedly less than in wt stage VI (Figure 2.1f). It seems that such primordia can develop into the relatively large *nf-ya1-1* nodules with a small meristem and hampered bacterial release in its daughter cells. In addition, markedly smaller primordia are formed, where cell divisions have occurred in C4 and C5, albeit with a lower frequency. Further, only a few anticlinal and no periclinal divisions or bacteria release have occurred in C3 (Figure 2.12c). Probably, such primordia develop into the small nodules that lack a meristem.

Using our fate map we have thus been able not only to confirm and to describe more thoroughly that meristem formation is hampered in the *nf-ya1-1* mutant but we have also shown the well infected cells inside mutant nodules are derived from C4 and C5. Further the cells that are derived from the (small) nodule meristem cells cannot differentiate into cells competent for bacterial release. The latter implies that release of rhizobia in primordia cells derived from C4/5 is not affected in the *nf-ya1-1* mutant, whereas in daughter cells derived from the meristem release requires NF-YA1. Our data also suggest that NF-YA1 is required for proper nodule meristem formation but not for nodule primordium development.

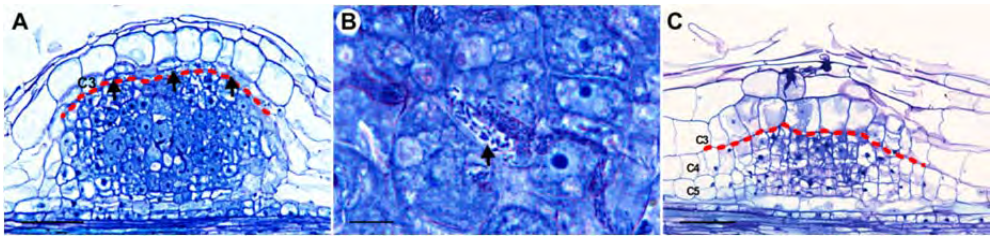


Figure 2.12: Reduced cell division in C3 of *nf-ya1-1* nodule primordia. (A) Relatively large *nf-ya1-1* nodule primordium with bacteria release in C4/5 derived cells; the number of C3 derived cells is less than in wt at stage III or VI (arrows). (B) Bacteria are released from infection threads (arrow) (magnification of the primordium A). (C) A *nf-ya1-1* nodule primordium with about 8 cell layers derived from C4/5 and no periclinal division in C3. In A and C a red line indicates the border between cells derived from C3 and C4. Bars, 75 μ m in A and C; 10 μ m in B.

sickle

The *sickle* mutant makes markedly more root nodules than wt as it is mutated in an ethylene signalling gene. The nodule histology of this mutant is in general considered to be wt-like [Penmettsa and Cook, 1997]. We sectioned about 50 *sickle* nodules that are formed at the “sickle” shaped zone [Penmettsa and Cook, 1997]. The vast majority has about 8 (or less) layers with well infected cells. These nodules have no or only a small meristem (Figure 2.13a). The reduced meristem formation might be a direct effect of the defect in ethylene signalling. However, it could also be indirect due to autoregulatory feedback created by the formation of a high number of primordia. Beside this, *sickle* also forms nodules morphologically like wt (Figure 2.13b), however, the nodule size is much smaller compared to wt (Figure 2.13c).

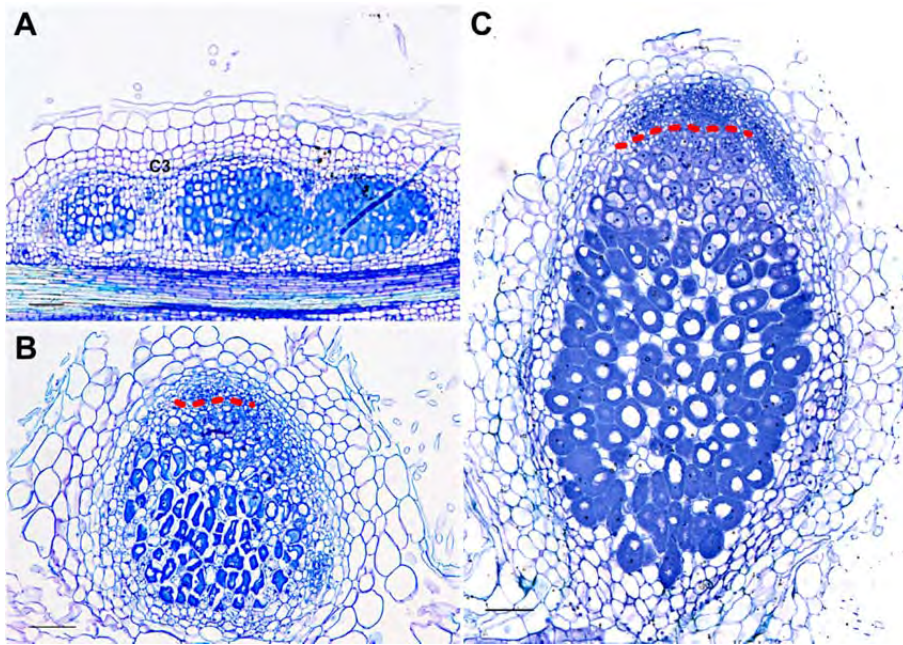


Figure 2.13: Meristem formation is hampered in some sickle nodules. Two weeks old sickle (A-B) and wt (C) nodules. (A) sickle nodules that are “fused” have no meristem and are surrounded by an endodermis. (B) A sickle nodule is smaller than (C) wt nodule. In A and C a red line indicates the border between nodule meristem and infection zone. Bars, 75 μ m.

This mutant was previously used by Timmers *et al.* [1999] to study the timing of meristem formation and infection thread growth. However, as the sickle mutant can be disturbed in nodule meristem formation these studies might not provide reliable insight in the timing of these processes in wild type nodules.

lin

Some Medicago mutants form nodule-like structures with a central vascular bundle, whereas wild type nodules have peripheral vascular bundles. An example is *lin*, which is essential for infection [Guan *et al.*, 2013; Kiss *et al.*, 2009; Kuppasamy *et al.*, 2004], it codes for a E3 ubiquitin ligase that contains a U-Box and WD40 repeat domains. *lin-1* [Kuppasamy *et al.*, 2004] forms non-infected nodules without a nodule meristem and with central vascular bundles (Figure 2.14a). The infection threads in these nodules are arrested in the epidermis. We hypothesize that these central vascular bundles can be formed due to a reduced cortical divisions combined with extended mitotic activity in pericycle and endodermis.

We tested whether such a disturbed “balance” occurs in *lin-1* primordia by using the endodermis marker (AtCASP::GUS). In several primordia, cortical divisions (C4/5) are at stage III-IV, while pericycle and endodermis divisions are at stage V or have divided even more frequently (Figure 2.14b). In addition to that, C3 divisions are in between stage II-IV

and never go further than stage IV. This indicates that the higher mitotic activity of pericycle and endodermis probably leads to the formation of central vascular bundles (Figure 2.14c). The phenotype of the *lin-1* mutant suggests that the expression of this gene is important to block the formation of vascular tissue from the pericycle derived cells.

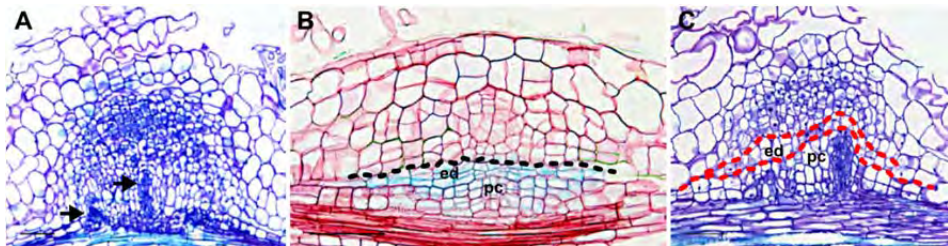


Figure 2.14: Extensive cell divisions in root pericycle and endodermis during *lin1-1* nodule primordium development correlates with formation of central vascular bundle. Two weeks old *lin1-1* nodule (A), which have a few central vascular bundles (arrows) and does not have a meristem. (B) In *AtCASPI::GUS* expressing *lin1-1* roots, a nodule primordium has more endodermis and pericycle divisions than the wt stage V primordium. The number of C3 and C4/5 derived cells are less or comparable to wt cell numbers at stage IV. (C) Central vascular bundles of *lin1-1* nodules are derived from pericycle. In B and C the lines confine cells derived from endodermis. Bars, 75 μ m.

ipd3

IPD3 is a transcriptional regulator that interacts with the kinase CCaMK that is essential for symbiosome formation [Ovchinnikova *et al.*, 2012; Singh *et al.*, 2014]. The *Medicago ipd3* (*Mtsym1-1/TE7*) mutant [Ovchinnikova *et al.*, 2012] forms nodules with a meristem and numerous infection threads (Figure 2.15a) from which rhizobia are not released, as well as very small nodules lacking infection threads (Figure 2.15b). We hypothesize that these non-infected small nodules could be the result of delayed infection thread growth that fail to penetrate C3 cells at the right time.

To test our hypothesis, serial sections of roots (1-5 dpi) were made. Two types of primordia were detected. One type is similar to wt (Figure 2.15c), C4 and C5 have formed about 8 cell layers and these cells contain infection threads. So, the infection threads have successfully passed C3. These primordia probably develop into nodules containing numerous infection threads (Figure 2.15a). The other type of primordium is composed of cells derived from C5, C4 and C3. C3 has already divided several times whereas the infection thread has just reached the outer cortex (Figure 2.15d). These primordia probably result in a small non-infected nodule (Figure 2.15b) and this is consistent with the condition that infection threads no longer can traverse the meristem when periclinal divisions have been induced in most C3 derived cells (stage IV).

A mutation that delays infection thread growth can thus result in a block of infection threads in the outer cortical cell layers although a primordium has been formed in the inner cortex. To be successful, infection threads have to reach C4 and C5 derived cells before

stage IV. In other words, a few hours difference in reaching or passing C3 can cause a major difference in nodule development.

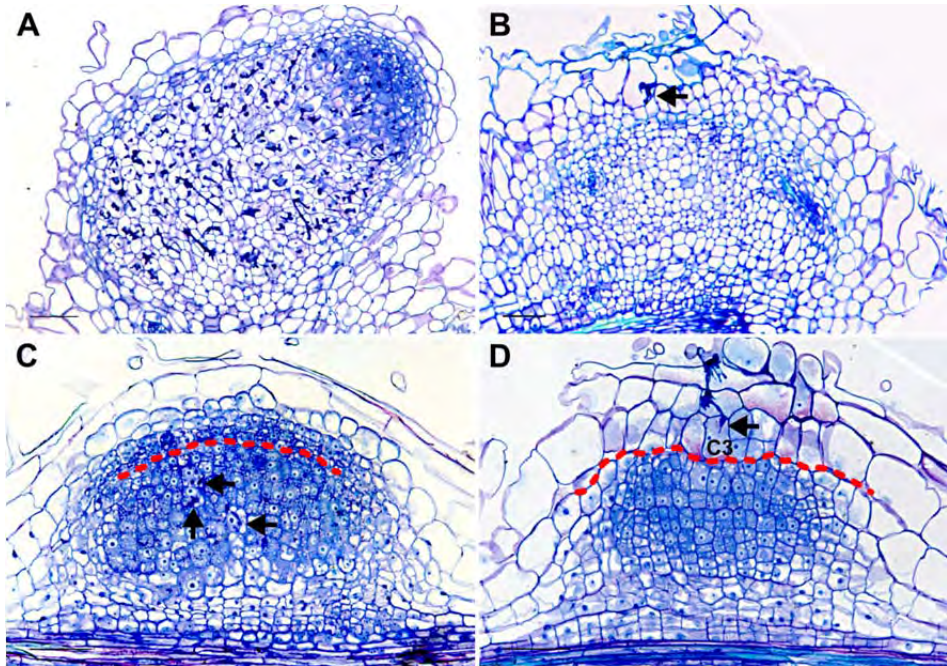


Figure 2.15: Infection thread failed to pass the future nodule meristem cells (C3) before stage IV in ipd3 mutant. Two types of three weeks old ipd3 nodules (A-B). (A) A large infected ipd3 nodule and (B) small non-infected nodule with infection thread (arrow) arrested in outer cortex layers. (C-D) Nodule primordia (C) with infection threads (arrows) successfully reached cells derived from C4/5 and (D) with infection thread (arrow) failed to pass through C3 at stage IV. In C and D a red line indicates the border between cells derived from C3 and C4. Bars, 75 μ m.

CONCLUSION

In this study we produced a fate map for *Medicago* root nodules. This fate map is summarized in the cartoon shown in Figure 2.16. In a mature nodule, about 8 cell layers of the basal part of the nodule central tissue are derived directly from the nodule primordium (C4/5 derived) and not from the meristem. The uninfected basal tissues are developed from primordium cells, which are derived from endodermis and pericycle. The nodule meristem is derived from a single central cortical layer (C3) and when the meristem becomes functional at stage VI, it continuously adds cells to the different nodule tissues.

Our nodule fate map underlines the impact of the multistep nature of nodule formation as well as the involvement of different root tissues in nodule formation. Similar processes can occur at different time points and in different cell types. A clear example is the release of rhizobia from infection threads in nodule primordium cells and in daughter cells of the meristem, respectively. In the latter case, NF-YA1 appeared to be essential for release,

whereas release is not affected in primordium cells of the *nf-ya1-1* mutant. This shows that similar processes can be controlled by different mechanisms (or with different stringency) during subsequent steps of nodule development. Our re-analysis of nodule mutant phenotypes also underlines that a nodule fate map is essential to identify the step(s) in nodule formation that are affected in mutants.

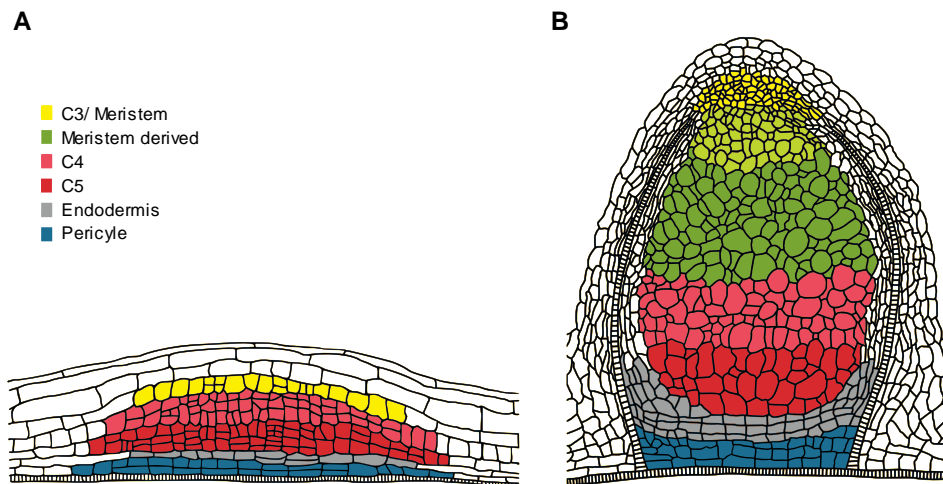


Figure 2.16: Root nodule fate map, (A) nodule primordium and (B) nodule. The origins of cells in primordium and nodule are indicated by the same colour. The origin of nodule cortex, vascular bundles and nodule parenchyma are not shown.

MATERIAL AND METHOD

Plant material and bacterial strains

M. truncatula accession Jemalong A17 plants were used to study nodule primordium formation. This accession is also used to generate *Agrobacterium rhizogenes* (strain MSU440) mediated transgenic roots as previously described by Limpens *et al.* [2004]. *M. truncatula* accession R108 seedlings were used to make the stable AtCyclB1.1::GUS [Burssens *et al.*, 2000] transgenic line by using *Agrobacterium tumefaciens* (strain AGL1) and followed the protocol described by [Chabaud *et al.*, 2003]. MtCCS52A::GUS is also introduced in R108 [Vinardell *et al.*, 2003]. The symbiotic mutants re-analyzed in this study were described previously, namely *nf-ya1-1* in Laporte *et al.* [2014], *sickle* in Penmetsa and Cook [1997], *lin1-1* in Kuppusamy *et al.* [2004] and *ipd3* in Ovchinnikova *et al.* [2012]. The surface-sterilization, germination of *Medicago* seeds were performed as previously described by Limpens *et al.* [2004]. Roots of A17 were inoculated with *Sinorhizobium meliloti* strain 2011 and R108 with *S. meliloti* Rm41.

Constructs

The AtCASP1::GUS construct is described in [Roppolo *et al.*, 2011]. For MtENOD40::GUS and AtSCR::GUS constructs, DNA fragments of putative promoters were amplified from *M. truncatula* and *A. thaliana* genomic DNA respectively using primer combinations listed in Table 2.1 and Phusion™ High-Fidelity DNA Polymerase (Finnzymes). Then, the Gateway® technology (Invitrogen) was used to create genetic promoter-GUS constructs [Karimi *et al.*, 2002]. For MtENOD40::GUS, the pENTR™/D-TOPO® Cloning Kits (Invitrogen) was used to create entry clones. The entry vector was recombined into Gateway®-compatible binary vector pKGW-RR, that contains GUS reporter gene and AtUBQ10::DsRED1 as a selection marker [Limpens *et al.*, 2004], by using Gateway® LR Clonase® II enzyme mix (Invitrogen). For AtSCR::GUS, the AtSCR DNA fragment was introduced into Gateway® donor vector pENTR4-1, GUS reporter gene into pENTR1-2 and 35S CaMV terminator into pENTR2-3, using Gateway® BP Clonase® II enzyme mix. These entry vectors were recombined into Gateway®-compatible binary vector pKGW-RR-MGW, that contains AtUBQ10::DsRED1 as a selection marker using Gateway® LR Clonase® II Plus enzyme mix (Invitrogen).

Table 2.1: List of primers used for MtENOD40 and AtSCR promoter amplification.

Gene name	Gene locus	Primer name	Primer sequence (5'-3')
MtENOD40	AJ388939.1	pMtENOD40-F	CACCTAAATTGTCAGTCTCGTAA AATAGC
		pMtENOD40-R	TCTCTGATCATTGTTTTAAATAC TTG
AtSCARECROW	At3g54210	pAtSCR-F	GAACACGTCGTCGCGTGTCTC
		pAtSCR-R	GTAAGAAAAGGGTTAAATCCAAA ATCG

Histochemical β -glucuronidase (GUS) staining

Transgenic plant material (nodules and part of roots) containing GUS constructs were incubated in GUS buffer (3% sucrose, 2 mM K₃Fe(CN)₆, 2 mM K₄Fe(CN)₆, 10 mM EDTA, and 1 mg/ml X-Gluc salt in 100 mM phosphate buffer solution, pH 7.0) under vacuum for 30 min and then at 37°C for 3 to 24h [Jefferson *et al.*, 1987].

Tissue embedding, sectioning and section staining

Root segments and nodules were fixed at 4°C overnight with 4% paraformaldehyde (w/v), 3% glutaraldehyde (v/v) in 0.1M potassium phosphate buffer (pH7.2). The fixed material was dehydrated in an ethanol series and subsequently embedded in Technovit 7100 (Heraeus Kulzer) according to the manufacturer's protocol. Five μ m thin longitudinal

sections were made by using a RJ2035 microtome (Leica Microsystems, Rijswijk, The Netherlands), stained 5 min in 0.05% toluidine blue O. For GUS stained plant material 9-10 μm thick longitudinal sections were stained for 15 min in 0.1% ruthenium red. Sections were analysed by using a DM5500B microscope equipped with a DFC425C camera (Leica Microsystems, Wetzlar, Germany).

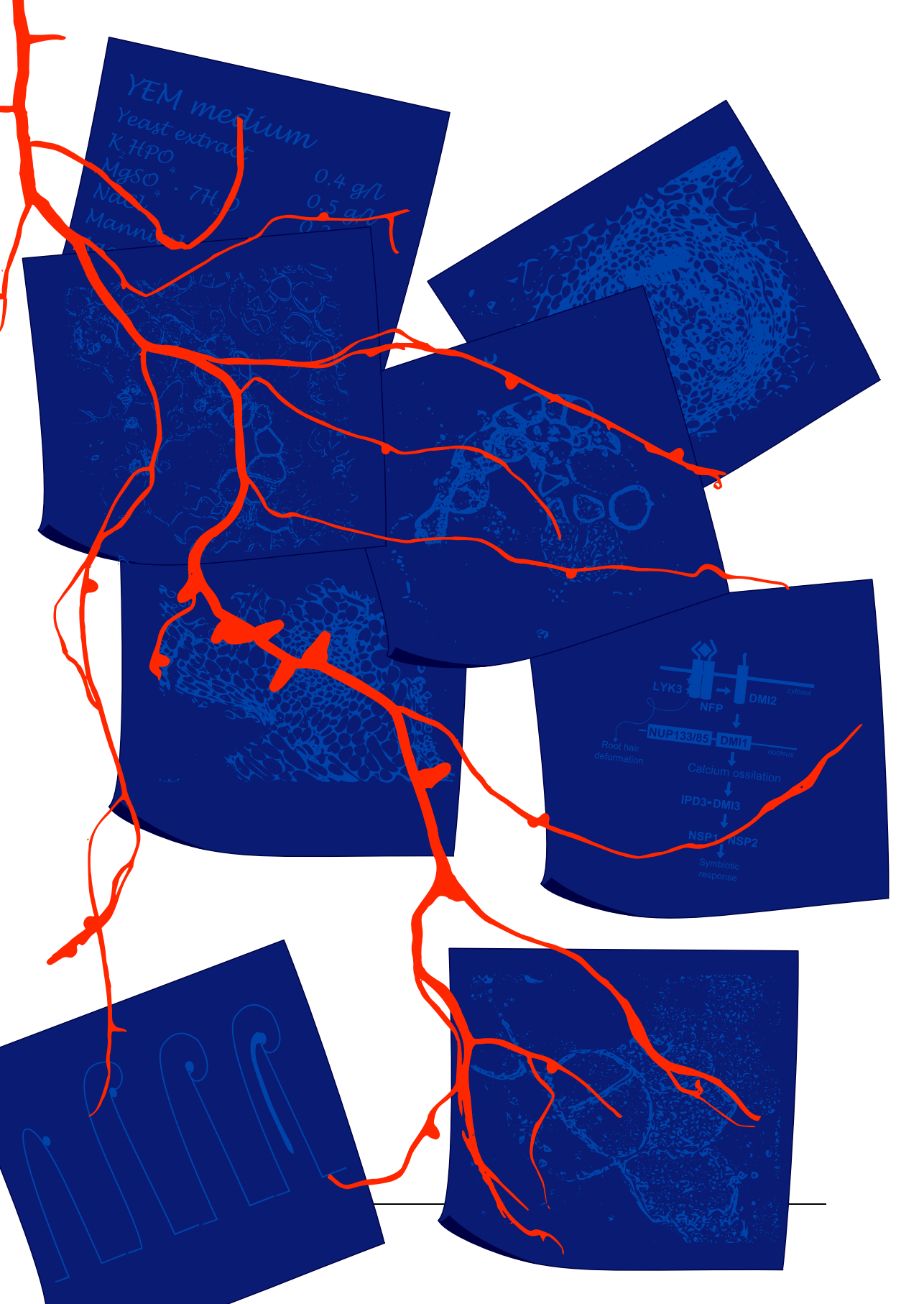
Simulation methods

We used our previously described simulation platform [Deinum *et al.*, 2012] with small adaptations: the controlled area, the region where parameters are changed in a hypothetical response to some signal was extended to include the pericycle and endodermis. Because we focus on early events we used an integration time step of 0.1 second.

As in Deinum *et al.* [2012], root segments are 28 cells long. Individual cells are 100 μm long and 20 μm (cortex) or 10 μm (all others) wide. We used an auxin diffusion constant of 300 $\mu\text{m}^2 \text{ s}^{-1}$ in the cytoplasm and 44 $\mu\text{m}^2 \text{ s}^{-1}$ in the apoplast. Auxin transport is modeled using effective influx and efflux permeabilities, P_{inf} and P_{eff} , respectively, with a homogeneous effective influx permeability of 20 $\mu\text{m} \text{ s}^{-1}$ and effective efflux permeabilities per cell face as indicated in Figure 2.3b as default starting values. For further details and references, see Deinum *et al.* [2012].

ACKNOWLEDGEMENTS

We thank Niko Geldner for providing the AtCASP promoter GUS fusion vector; Dirk Inzé for the AtCyclB1.1 promoter GUS fusion vector; Thomas Ott for the MtSYMREM promoter GUS fusion vector.



YEM medium

Yeast extract

K_2HPO_4

$MgSO_4 \cdot 7H_2O$

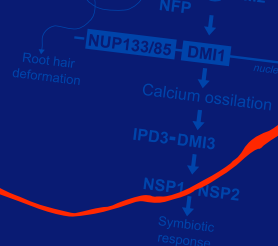
$NaCl$

Mannitol

0.4 g/l

0.5 g/l

0.5 g/l



Chapter 3.

NOD FACTOR RECEPTORS ARE ESSENTIAL FOR INTRACELLULAR INFECTION OF MEDICAGO NODULE CELLS

Sjef Moling¹, Erik Limpens¹ and Ton Bisseling^{1,2}

¹Laboratory of Molecular Biology; Wageningen University; Wageningen, The Netherlands

²College of Science; King Saud University; Riyadh, Saudi Arabia

Submitted for publication in a modified form

ABSTRACT

In *Medicago* nodules, the Nod factor receptors NFP and LYK3 localize to the plasma membrane in a narrow zone of about two cell layers at the nodule apex. The distal layer of this zone is part of the meristem and the proximal layer is part of the infection zone. In this second layer the receptors can most likely perceive the bacterial Nod factors. There, the Nod factor receptors control the release of the rhizobia from the infection threads and their uptake into the host cells. Our data indicate a strict regulation of NFP and LYK3 at the post-translational level to ensure the restricted accumulation of the two receptors at the plasma membrane, which appears to be required to prevent a defense response.

INTRODUCTION

Legumes have the unique ability to compensate for low levels of nitrogen in the soil by establishing an interaction with rhizobium bacteria. In this interaction the bacteria are hosted intracellular in a newly formed organ, the root nodule, where they reduce atmospheric nitrogen into ammonium [Stewart, 1966]. Nodule formation starts, at the root epidermis, with the perception of specific lipo-chitoooligosaccharides, secreted by the rhizobia. These are named Nod factors and they have a pivotal role in the induction of early responses in the root epidermis and cortex [Lerouge *et al.*, 1990; Spaink *et al.*, 1991; van Brussel *et al.*, 1992]. Nod factors are recognized by specific receptors that activate the symbiotic signaling pathway, which sets in motion root nodule formation [D'Haeze and Holsters, 2002; Truchet *et al.*, 1991]. In the model legume *Medicago truncatula* (*Medicago*), rhizobia also produce Nod factors in root nodules [Schlaman *et al.*, 1991; Sharma and Signer, 1990]. However, it is unclear which process is triggered by Nod factors at this stage of development, and this question will be addressed in this chapter.

Medicago has two Nod factor receptors. These are the LysM receptor like kinases NFP and LYK3, respectively [Arrighi *et al.*, 2006; Limpens *et al.*, 2003; Smit *et al.*, 2007]. NFP and LYK3 have three extracellular LysM domains. Further, LYK3 has an active kinase domain allowing downstream signaling, whereas an active kinase domain is missing in NFP [Arrighi *et al.*, 2006; Limpens *et al.*, 2003]. The two receptors may form a complex, although their functions are slightly different [Arrighi *et al.*, 2006; Catoira *et al.*, 2001; Madsen *et al.*, 2011]. In Chapter 4 we studied this complex by FRET based techniques. NFP as well as LYK3 have a function in early stages of nodule formation, but NFP is already active in earlier responses. For example, both are essential for the induction of root hair curling. Within these curls rhizobia are entrapped and form a micro-colony, followed by the formation of an infection thread. Infection threads are tube-like structures surrounded by a membrane and bound by a cell wall of the host. They grow inward and in this way the rhizobia infect the plant in a host-controlled manner. Concomitantly, cortical cells are mitotically activated and form a nodule primordium that will develop into a nodule. The formation of a nodule primordium also requires both Nod factor receptors,

although LYK3 is not absolutely essential for the induction of cortical cell divisions [Catoira *et al.*, 2001].

After perception of Nod factors by the receptors, the signal is transduced via the symbiotic signaling pathway to the nucleus, where transcription factors are activated. The receptors first activate, (in)directly, the LRR-type receptor SymRK at the plasma membrane [Limpens *et al.*, 2005] and then the putative cation channel DMI1 at the nuclear envelope [Ane *et al.*, 2004]. Two nucleoporins, NUP133 and NUP85, act downstream of DMI1 and SymRK [Kanamori *et al.*, 2006; Saito *et al.*, 2007]. All these components are essential to induce nuclear calcium oscillations [Oldroyd and Downie, 2004; Oldroyd *et al.*, 2011]. This calcium spiking is interpreted by the calcium and calmodulin-dependant kinase DMI3/CCaMK [Levy *et al.*, 2004; Mitra *et al.*, 2004] which subsequently interacts with Cyclops/IPD3 [Horvath *et al.*, 2011; Limpens *et al.*, 2011; Messinese *et al.*, 2007; Yano *et al.*, 2008]. Downstream of CCaMK and Cyclops/IPD3 the transcription factors NSP1 and NSP2 are activated [Kalo *et al.*, 2005; Smit *et al.*, 2005]. This symbiotic signaling pathway is essential for e.g. root hair curling, and infection thread and nodule primordium formation [Murray, 2011].

The infection thread, that is formed in the curled root hair, subsequently grows to the basal layers of the nodule primordium and there rhizobia are released. Simultaneously, a meristem is formed at the apex of the primordium. The infection threads now grow towards this meristem and cells derived from it can be infected. In *Medicago* nodules, the meristem remains active by which they have an indeterminate growth. So throughout the lifespan of a *Medicago* nodule, cells derived from the meristem become infected by rhizobia. In nodules infection starts with rhizobia that propagate in between plant cells. These rhizobia induce invaginations of the plasma membrane by which intracellular infection threads are formed that are bound by a plant cell wall. The rhizobia are released from these intracellular threads at regions that are cell wall free, and therefore are named unwalled droplets [Brewin, 2004; Rae *et al.*, 1992]. During this process they become surrounded by a plant membrane. The host membrane compartments containing rhizobia, are named symbiosomes [Roth and Stacey, 1989]. This host membrane forms the symbiotic interface between rhizobia and the host cell. [Parniske, 2000; Roth and Stacey, 1989; Vasse *et al.*, 1990].

Medicago nodules have an indeterminate growth and as consequence along their longitudinal axis they are of graded age [Vasse *et al.*, 1990]. The meristem is composed of dividing cells, that are not infected by rhizobia and it forms the most distal zone. In the adjacent infection zone, cells become penetrated by an infection thread and upon release of rhizobia symbiosomes are formed that divide and subsequently enlarge. Ultimately, in the fixation zone, infected cells are fully packed with symbiosomes that reduce nitrogen into ammonia and these nodule cells form the fixation zone.

Inside nodules, rhizobia still produce Nod factors [Schlaman *et al.*, 1991; Sharma and Signer, 1990]. This production is strictly regulated as Nod factors are produced by rhizobia in the infection threads, but upon release from these threads the production most likely stops. The latter was shown by the phenotype of the rhizobial *glmS* mutant. GlmS is a glucosamine synthase essential for bacterial growth [Marie *et al.*, 1994]. GlmS has the same biochemical function as NodM. So when the *nod* genes are expressed the *glmS* mutant can grow. In other words, growth arrest of *glmS* indicates that Nod factor production has stopped. The rhizobial *glmS* mutant forms nodules, but upon release from infection threads division/development of symbiosomes is blocked. This strongly indicates that Nod factor production stops after release of rhizobia into the host cells [Marie *et al.*, 1994].

Which processes are triggered by Nod factors in root nodules is not known, but components of the Nod factor signaling cascade are formed in nodules and some of these are essential for release of rhizobia into the host cells. This was shown by a (partial) knock-down of DMI2/SymRK and a loss of function mutation in IPD3 which both cause a block of bacterial release from the infection threads [Limpens *et al.*, 2005; Ovchinnikova *et al.*, 2012]. This showed that these components of the Nod factor signaling cascade are essential inside nodules. However, whether Nod factors are involved and how they are recognized is unclear, as in legume nodules Nod factor receptors could not be visualized using receptor GFP fusions [Madsen *et al.*, 2011]. Even a Medicago LYK3-GFP construct that could be visualized in root hairs did not result in a detectable signal in nodules [Haney *et al.*, 2011; Madsen *et al.*, 2011]. However, *in situ* hybridizations, promoter GUS studies and transcriptome analyses have shown that the Nod factor receptor genes are expressed in Medicago root nodules, although at a low level [Limpens *et al.*, 2005; Limpens *et al.*, 2013; Mbengue *et al.*, 2010]. Therefore we hypothesized that Nod factor receptors are formed in nodules although at a low but sufficient level to trigger intracellular infection of nodule cells.

By using GFP fusions we showed that Nod factor receptors do indeed accumulate at the plasma membrane in the apex of Medicago nodules. This occurs in a strictly controlled manner in about 2 cell layers at the transition of meristem into infection zone. By reverse genetics their function in controlling release of symbiosomes from infection threads was studied.

RESULTS

Nod factor receptors accumulate in the plasma membrane in ~2 cell layers of Medicago nodules

As a first step to determine the function of Nod factor signaling in Medicago nodules, we reexamined whether and where the Nod factor receptors accumulate in nodules. To determine where the selected NFP and LYK3 promoters regions are active in nodules we expressed β -glucuronidase (GUS) driven by the NFP or LYK3 native promoter. As promoter we used, in both cases, approximately 2kb of the region upstream of the start codon of NFP or LYK3, respectively. These constructs were introduced into Medicago roots by *Agrobacterium rhizogenes* mediated transformation. Figure 3.1 shows that both promoter regions are active in the distal part of the nodule including the whole meristem and part of the infection zone. This expression pattern is similar to that previously identified by *in situ* hybridization and promoter GUS studies [Arrighi *et al.*, 2006; Haney *et al.*, 2011; Limpens *et al.*, 2005], which confirms that the selected upstream regions should be sufficient to express receptor GFP constructs at the right place in the nodule.

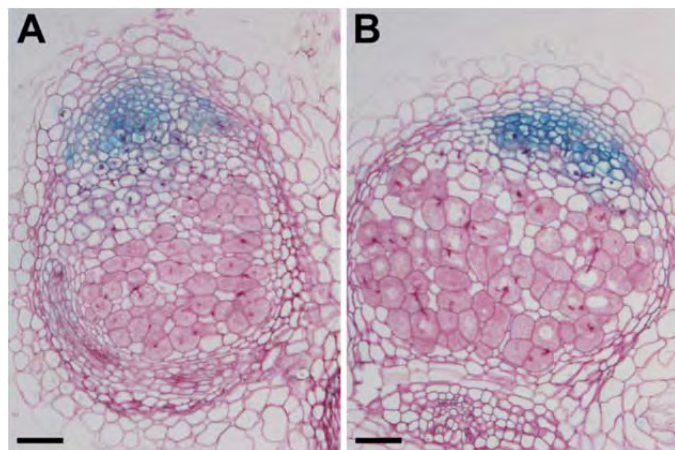
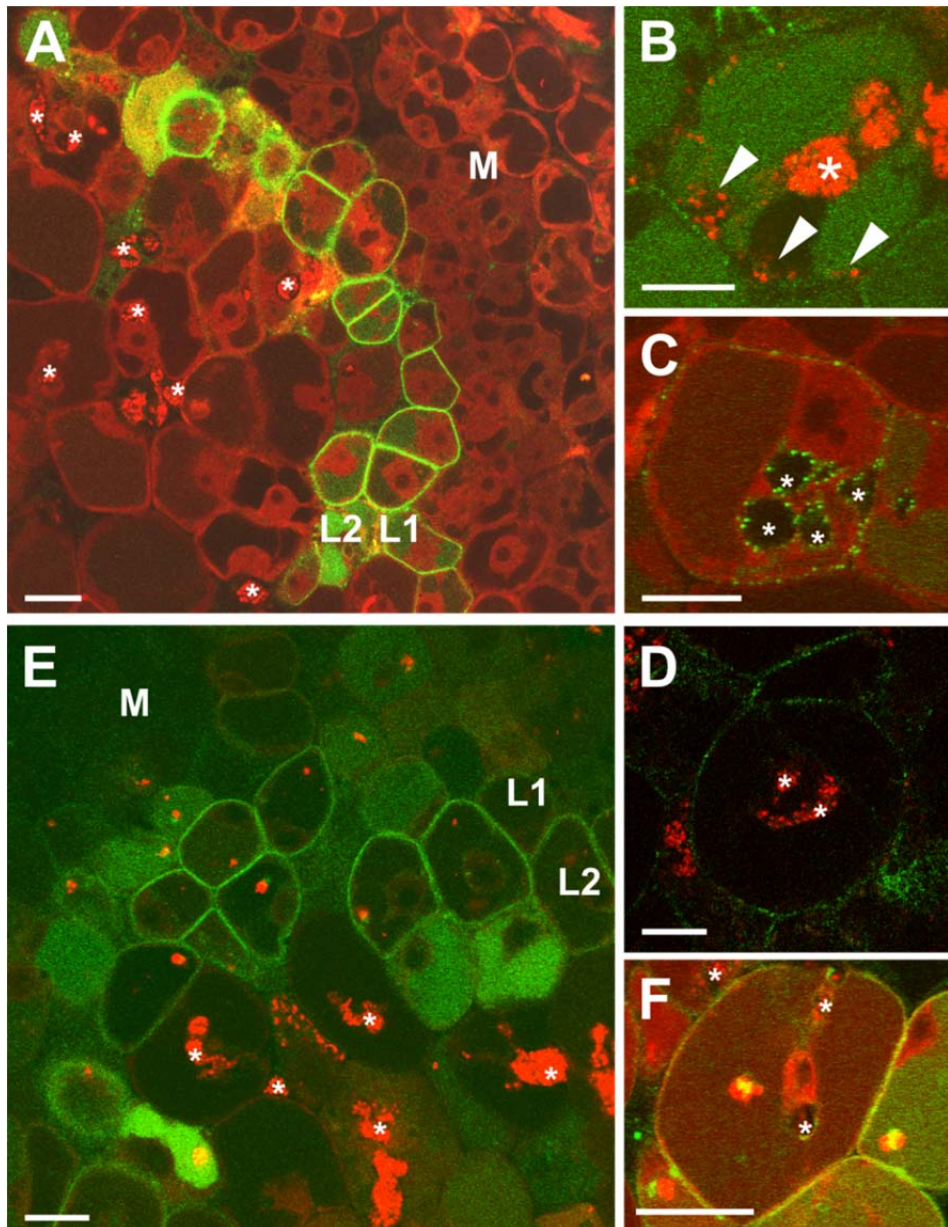


Figure 3.1: Activity of the NFP and LYK3 promoters in Medicago truncatula nodules. (A) Activity of the LYK3 promoter in a nodule. (B) of the NFP promoter in a nodule. Bar indicates 75 μ m

To determine whether NFP and LYK3 accumulate at a level sufficient to visualize them, we made constructs in which we fused GFP to the C-terminus of the receptors. These tagged receptors were put under control of their native promoters. To test whether these fusion constructs are functional, they were introduced by *A. rhizogenes* mediated transformation into the corresponding mutant backgrounds. For NFP-GFP we used the *nfp-2* mutant NFP31 [Arrighi *et al.*, 2006] and for LYK3 – GFP we used the *lyk3-1* mutant B56 [Smit *et*

al., 2007]. The transgenic roots were inoculated with *Sinorhizobium meliloti* expressing RFP. On transgenic roots expressing NFP-GFP or LYK3-GFP, respectively, nodules were formed with a frequency comparable to wild type roots transformed with an empty vector. The cytology of these nodules was also similar to control nodules (data not shown). This shows that the GFP tagged receptors and the regions we selected as promoters are biologically functional.



Subsequently, it was tested whether NFP-GFP and LYK3-GFP could be detected in nodules 10-14 days post inoculation (dpi). As GFP fluorescence markedly decreases during chemical fixation and embedding, hand sections of the transgenic nodules were made and analyzed by confocal microscopy. GFP fluorescence could be detected at the nodule apex (Figure 3.2) and it is absent in nodules of roots transformed with an empty vector. Immunodetection with an anti-GFP antibody confirmed that the observed fluorescence is GFP derived (data not shown). The accumulation of the Nod factor receptors in a very specific nodule region stimulated us to study the role of Nod factor perception in nodules.

Localization of Nod factor receptors

We analyzed 28 nodules expressing LYK3 –GFP and used the median longitudinal plane of the nodule to determine in which cells it accumulates. Fluorescence was detected both at the cell periphery and in vacuoles. As fluorescence at the periphery is associated with the plasma membrane (see below) we considered this to represent the functional receptor and the fluorescence at the vacuole to be the result of degradation. In all nodules, GFP fluorescence at the cell periphery occurs in a narrow zone in the apex of the nodule. This zone consists of about 2 cell layers (average $2.2 \pm 0.7\text{sd}$). In this zone and in additional layers of the infection zone GFP fluorescence was also detected in the vacuoles. The 2 cell layer-wide zone where LYK3 accumulates at the cell periphery, is markedly narrower than the zone in which the promoter is active. This suggests that the accumulation at the plasma membrane is regulated at the post translational level.

The most distal layer where the receptor accumulates (layer L1) has no infection threads and some cells have a morphology that shows that they just ended cytokinesis (Figure 3.2a). Therefore we consider this layer to be the last layer of the meristem. In the more proximal layer where LYK3-GFP accumulates at the plasma membrane (layer L2) the first infection events take place. The layer contains cells that are penetrated by an infection thread (we will refer to these cells as infected cells) and cells that have not yet been penetrated. Therefore we considered this layer to be the first layer of the infection zone. Sometimes a third or fourth layer could be observed. In these cases extra layers of LYK3

← Figure 3.2: localization of the Nod factor receptors in nodules. (A) Overview of a typical nodule expressing LYK3-GFP. In this nodule LYK3 accumulates in two cell layers (L1 and L2) that form the border between meristem (L1) and infection zone (L2). (B) shows a cell in which an infection thread has penetrated and bacteria (in red) are released from the thread. (C) Shows the accumulation of LYK3-GFP on the membrane surrounding an infection thread and the plasma membrane. (D) Shows a cell of the infection zone in which an infection thread penetrated and where LYK3-GFP accumulates only at the plasma membrane. (E) Overview of a typical nodule expressing NFP-GFP. In this nodule NFP accumulates in two cell layers (L1 and L2) (F) Detail of a cell of the infection zone showing NFP-GFP and aggregates of DsRED in the cytoplasm. On the membrane surrounding the infection thread (*) a weak GFP signal can be observed. L1 and L2 indicate the two layers of receptor accumulation. M indicates the position of the nodule meristem, a * marks the infection threads, an arrowhead (v) marks release bacteria. Bar indicates 10 μm .

accumulation were detected either in the meristem or infection zone. In layer L2 the LYK3-GFP does not accumulate in cells in which bacteria are released from the infection thread (Figure 3.2b). We observed that most cells that have been infected in layer L2 do not show LYK3-GFP accumulation (Figure 3.2c,d). We determined whether in the infected cells LYK3 was present at the plasma membrane as well as the membrane surrounding the infection threads. To obtain quantitative data on the subcellular localization of LYK3 we analyzed confocal stacks of cells in the most proximal layer where LYK3 accumulates (eighteen nodules). From these 18 nodules we could only analyze twenty cells in which an infection thread has penetrated and LYK3-GFP could be detected. In all cells LYK3 was present on the plasma membrane (Figure 3.2d). However, only in seven cells LYK3-GFP was present on the plasma membrane as well as on the infection thread membrane (Figure 3.2c). In addition to the fluorescence at the periphery of the cell, fluorescence also occurs in the central vacuole in cells where bacteria have been released (Figure 3.2b). We conclude that LYK3 is most likely present at the plasma membrane and infection thread membrane. Upon release of the bacteria LYK3 is removed from the plasma membrane and targeted to the vacuole for degradation. The removal of LYK3 from the plasma membrane appears to be first completed at the membrane surrounding the infection thread.

The localization of NFP-GFP was studied in a similar manner as LYK3-GFP. We analyzed ten nodules and detected GFP fluorescence at the cell periphery, at the infection threads and in vacuoles. In analogy to LYK3 we expect the accumulation at the cell periphery to be associated with the plasma membrane. Like for LYK3 we observed accumulation of NFP at the plasma membrane only in a zone of approximately two cell layers (average $2.2 \pm 0.57\text{sd}$, Figure 3.2e). In the distal layer where NFP accumulates at the cell periphery (layer L1), based on the morphology, cytokinesis has just ended and infection threads have not entered (Figure 3.2e). Therefore, we considered this layer to be the last layer of the meristem. In the more proximal layer where NFP-GFP accumulates (layer L2) infection threads start to enter (Figure 3.2f). Therefore, this is the first layer of the infection zone. In 21 cells of L2 (10 nodules) we studied the subcellular accumulation of NFP-GFP on the plasma membrane and the infection thread membrane. In the infected cells of layer L2 we could observe NFP-GFP both at the infection thread and at the plasma membrane (Figure 3.2f), whereas LYK3 only accumulated in 35% of the cells at the cell plasma membrane surrounding the infection thread. Occasionally, more than two cell layers in which NFP accumulated at the plasma membrane were present. In younger as well as older adjacent cell layers of L1 and L2 we also observed NFP-GFP accumulation in the vacuoles. In total NFP-GFP accumulates in about six cell layers (average $6.3 \pm 1.3\text{sd}$, Figure 3.2e). The promoter is active in the entire meristem and some layers of the infection zone, whereas the protein accumulates only in the last layer(s) of the meristem and accumulates in the vacuole in the infection zone.

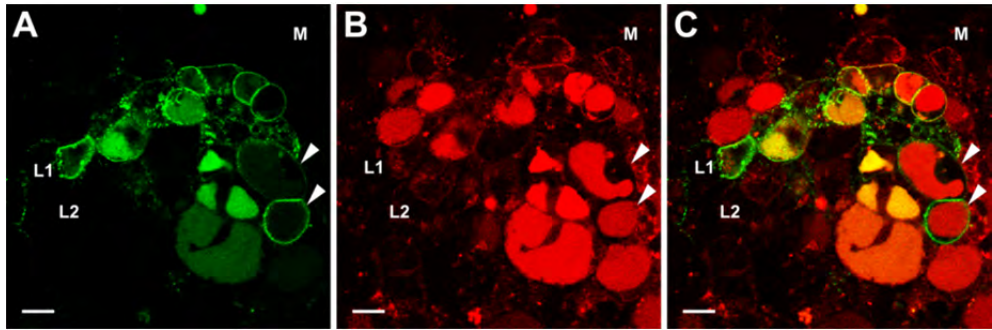


Figure 3.3: co-expression of LYK3-GFP and NFP-RFP under control of their native promoters in a nodule of *Medicago*. (A) LYK3-GFP (B) NFP-mCherry (C) merge. Bar indicates 10 μ m, L1 and L2 indicate the two layer of accumulation, M indicates the position of the meristem, the arrowhead indicated the most proximal cells where LYK3-GFP accumulates.

The cell layers in which NFP and LYK3 accumulate at the cell periphery seem similar (last layer of the meristem and first layer of the infection zone). To confirm this we co-expressed both receptor constructs. First a stable line expressing LYK3-GFP under control of its native promoter was generated. Two individual lines were tested and the localization of LYK3-GFP was similar to that in nodules on the transformed roots described above (Figure 3.3a). In this stable line we introduced NFP-mCherry under control of its native promoter by *A. rhizogenes* root transformation. The receptors indeed do co-localize at the border of the meristem and the infection zone (Layer L1 and L2). Figure 3.3 shows a nodule in which NFP occurs in the meristem at a location more distal than that of LYK3 (arrow). In these nodules NFP-mCherry accumulated in a zone of approximately two cell layers at the periphery of the cells similar to the NFP-GFP localization described above. Next to the co-localization in L1 and L2 we observed accumulation of only one of the receptors in adjacent cells located either in the meristem or infection zone. LYK3 was only observed in the infection zone, where NFP could be observed in both meristem and infection zone. In the infection zone LYK3-GFP accumulated at the cell periphery, NFP-mCherry accumulated already in the vacuole and only at a low level at the periphery (Figure 3.3, arrowhead).

So, both NFP and LYK3 localize at the cell periphery in a zone of two cell layers. This zone is the border between the meristem and the infection zone.

Sub-cellular localization of LYK3-GFP and NFP-GFP

To determine whether LYK3 is localized at the plasma membrane it was immunolocalized by electron microscopy. LYK3-GFP was detected using an anti-GFP antibody and immuno-gold labeling. In the confocal studies we observed LYK3-GFP mainly at the cell periphery and on the membrane surrounding the infection thread. In the cells at the border of the meristem and infection zone we could detect LYK3-GFP at the plasma membrane, in vesicles near this membrane (Figure 3.4a) and in vesicles (Figure 3.4b). It is most likely

that the vast majority of these vesicles are involved in endocytosis leading to degradation of the receptor in the vacuole as we see accumulation of fluorescent tagged protein in the vacuole. We could not detect LYK3-GFP at the membrane surrounding the infection threads. We may have missed LYK3-GFP on infection threads as only one third of the cells in L2 contain LYK3 at the infection threads and in most cases at a lower level than on the plasma membrane (Figure 3.2a).

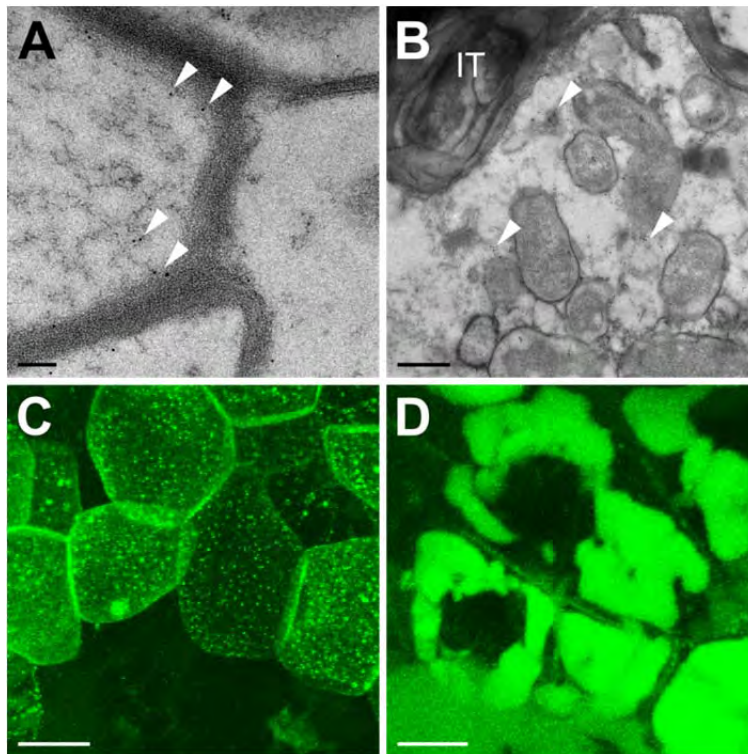


Figure 3.4: sub-cellular localization of LYK3-GFP in nodules 10 days after inoculation. (A) Transmission electron micrograph showing LYK3-GFP labeled with anti-GFP and gold particles (arrow head) at the plasma membrane, bar 100 nm. (B) Detail of an infection thread/ unwallled droplet where bacteria are released showing LYK3-GFP labeled with anti-GFP and gold particles at the infection thread membrane and vesicles (arrow head), IT marks the infection thread, bar 100nm. (C) Projection of a z-stack of cells expressing LYK3-GFP, bar 5 μm. (D) Projection of a z-stack of cells expressing NFP-GFP, bar 5 μm.

To determine whether LYK3-GFP accumulates in puncta, as observed in root hairs [Haney *et al.*, 2011], we made z-stacks by confocal microscopy of nodules formed on *A. rhizogenes* transformed roots expressing LYK3-GFP. The z-stacks were projected on the y-axis and show that LYK3-GFP accumulates in puncta (Figure 3.4c). These puncta have a diameter of up to 500nm. Because of the optical limitations of confocal imaging we cannot conclude if these are vesicles or membrane domains. For NFP-GFP a more uniform labeling of the plasma membrane was observed, but some puncta could be observed as well (Figure 3.4d). The NFP levels were too low to allow immuno-localization by electron microscopy. However, since confocal microscopy showed that NFP and LYK3 co-localized at the

periphery in ~2 cell layer (Figure 3.3) it is probable that also NFP localizes to the plasma membrane.

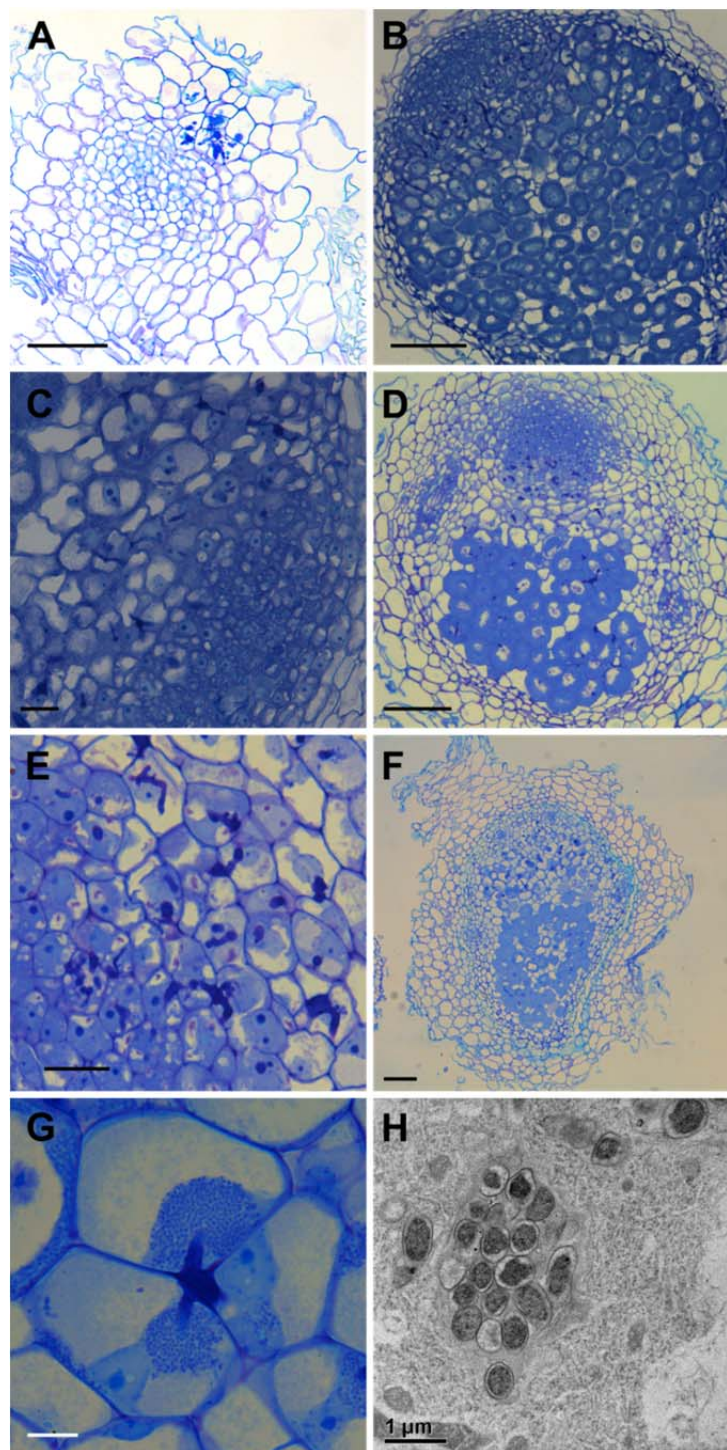
Function of Nod factor perception in nodules

To study the role of Nod factor receptors in root nodules we used an RNAi approach. The challenge was to allow the early symbiotic responses in epidermis and cortex to occur, by which a nodule (primordium) containing infection threads is formed, and specifically reduce the level of the receptors in the nodule. When for instance the epidermis specific *LeExtensin1* promoter was used to complement the B56 *lyk3-1* mutant infection thread growth was blocked in the epidermis or outer cortical cell layers (Figure 3.5a), similar to what was shown for NFP [Rival *et al.*, 2012]. In these cases primordia were formed, but infection threads failed to pass the outer cortical cell layers (Figure 3.5a). Further, a weak allele of *lyk3* (*hcl-4*) indicated that the expression level of *LYK3* had to be reduced to very low levels to obtain a nodule phenotype. *hcl-4* is a splicing mutant which makes about 10% functional *LYK3* mRNA [Smit *et al.*, 2007]. Most of the infections in this mutant get arrested at the curled root hair stage. However, the few infections that pass this stage all form fully infected/functional nodules [Smit *et al.*, 2007]. This suggests either that very low levels of *LYK3* are sufficient for its function in nodules or that there is no nodule phenotype due to functional redundancy [Smit *et al.*, 2007]. We used the *ENOD12* promoter to knock down the receptors in a nodule specific manner [Limpens *et al.*, 2005; Pichon *et al.*, 1992]. This promoter is first activated when cortical cells start to divide and remains active in the meristem and distal part of the infection zone. We expressed a NFP RNAi construct in A17 and the construct for *LYK3*-RNAi in the *hcl-4* mutant background.

We analyzed 10 randomly selected NFP RNAi nodules (Figure 3.5d,e). Of these nodules, 8 are markedly smaller than control nodules (Figure 3.5b,c). The infection zone in these nodules was aberrant. It contained more cell layers and the cells in the central tissue were smaller than in those in control nodules. Infection threads did enter into the cells, but release of the bacteria from the threads was hampered. Although some bacteria were released, they did not develop into mature symbiosomes. In contrast to the block of release in the infection zone a zone of about 8 cell layers at the basal part showed fully infected cells containing symbiosomes that developed as in wild type nodules. Recently we showed (submitted, Chapter 2) that these ~8 basal infected cell layers are directly derived from the primordium and not from the meristem. However, the small cells of the infection zone, where release is blocked, are derived from the meristem. So this results in a chimeric phenotype where in cells derived from the meristem release of rhizobia is blocked, whereas release and subsequent formation/ development of symbiosomes in the primordium cells is similar to the wild type. Because the nodules only contain ~8 infected cell layers, the nodules remain small. The infection zone in the RNAi nodules contained more cell layers suggesting that the meristem is still active in these nodules.

Also 10 LYK3 RNAi nodules were analyzed. The nodules are comparable in size to control nodules and all show impaired release of the bacteria from the infection threads, although the severity of the effect varies. In the infection zone release of the bacteria from the infection threads is affected (Figure 3.5f). Strikingly, the infection threads/ unwallated droplets are much more pronounced and larger compared to control nodules (Figure 3.5f,g). The infection zone is comparable in size to wild type nodules (more than 8 cell layers). This suggests that both in the primordium and in the infection zone bacteria are released. In the infection zone the cells have a normal size, but vacuoles are much larger than in control nodules (Figure 3.5f,g). Because the vacuoles are larger than in control nodules, development of the symbiosomes should be affected as well as there is less space available for the bacteria.

→ Figure 3.5: Phenotypes of knock down of the Nod Factor Receptors in nodules 21 days after inoculation with rhizobia. The nodule apex is located at the top of the images. (A) Nodule expressing LYK3 under control of the epidermis specific EXT1 promoter in which the infection thread could not enter and development stopped. (B,C) control nodule formed on roots transformed with a control (dsRED) construct. (D,E) Nodule expressing a NFP RNAi hairpin in a nodule specific manner (E12:NFPi). In these nodules there are many large infection threads and only in rare situations the bacteria are released. (F,G,H) Nodule expressing a LYK3 RNAi hairpin in a nodule specific manner (E12:LYK3i). These nodules have very large unwallated droplets from which bacteria are eventually released. (H) Shows an electron micrograph of such an unwallated droplet confirming that the plant cell wall is not present (A,B,D,F) Bar indicates 100µm, (C,E,G) bar indicates 10µm, (H) bar indicates 1µm.



Why is NFP and LYK3 accumulation restricted to a very narrow zone?

The accumulation of NFP and LYK3 at the plasma membrane is controlled at the post translational level as it is restricted to a narrow zone of about 2 cell layers, whereas the region where the genes are expressed is markedly broader. To study why the accumulation of the receptors at the plasma membrane is strictly controlled we ectopically expressed both receptors under the control of the Arabidopsis UBIQUITIN3 (Ubq) promoter. This promoter is active in the nodule apex at a markedly higher level compared to the native NFP or LYK3 promoter. We analyzed 12 nodules expressing *Ubq::NFP* 21 days after inoculation. These nodules are all smaller than control nodules. Furthermore, in the infection zone more uninfected cells are present compared to wild type controls (Figure 3.6a,b). Also the infected cells of the infection zone remain small and have a similar size as the uninfected cells, whereas in wild type nodules the infected cells are much bigger than uninfected cells in the infection zone. Additionally, the infected cells showed signs of premature cell death and accumulation of poly-phenolic compounds (observed as yellow/green deposition) (Figure 3.6a,b). The nodules have a relatively large (more than 8 cell layers) fixation zone, so release in both the primordium and in the infection zone has occurred like in control nodules. This suggests that initial development similar to that of control nodules. However, at a relatively young age a systemic “defense response” is induced causing premature death of all infected cells.

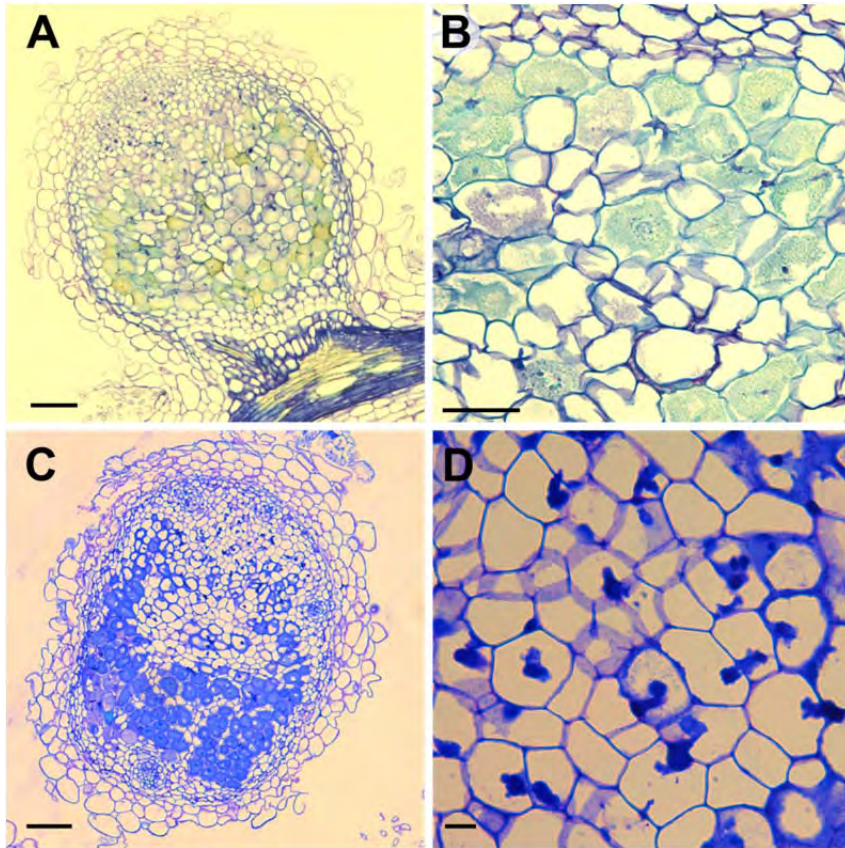


Figure 3.6: Ectopic expression of the Nod factor receptors in nodules 21 days after inoculation with rhizobia. (A,B) Nodule expressing NFP ectopically (Ubq:NFP) showing premature cell death . (c,d) Nodule expressing LYK3 ectopically (Ubq:LYK3) showing no release. (A,C) Bar indicates 100µm, (B) Bar indicates 50µm, (D) bar indicates 10µm .

When LYK3 was ectopically expressed using the Ubq promoter small nodules are formed with infected cells in ~8 cells at base of the nodule. In the apical part of the nodule an enlarged infection zone is formed. Release of the bacteria from the infection threads appears to be severely hampered resulting in infection threads that occupy a large part of the cells (Figure 3.6c,d). Accumulation of polyphenols or premature cell death was not observed, while this was the predominant effect when NFP was ectopically expressed. Although different from the effect of ectopic NFP expression, these experiments do show that LYK3 as well as NFP accumulation needs to be restricted to allow proper symbiosome formation/ maintenance.

DISCUSSION

Here we show that the Medicago Nod factor receptors NFP and LYK3 accumulate in the plasma membrane in a narrow zone of about 2 cell layers at the transition of the nodule meristem to the infection zone. The Nod factor receptors are essential for the release of the bacteria from the infection threads into the cytoplasm of nodule cells derived from the meristem. The accumulation of the receptors is strictly regulated at the post translational level, in order to prevent “defense-like” responses.

NFP and LYK3 accumulate in a narrow zone of two cell layers (L1 and L2) at the nodule apex. Both receptors localize at the plasma membrane in this zone at the border of the meristem and the infection zone. The region where the receptors accumulate at the plasma membrane coincides with the zone where rhizobia still produce Nod factors [Marie *et al.*, 1994; Schlaman *et al.*, 1998]. As Nod factors accumulate in the cell wall and are not translocated to the cytoplasm it is very probable that the receptors at the plasma and infection thread membrane can recognize Nod factors, whereas the vacuolar located proteins will be degraded. The fact that the Nod factor receptors accumulate at the plasma membrane in a very narrow zone implies that this is a very transient and short lasting event. This zone is markedly smaller than the region where the genes are expressed. Therefore it is very likely that the level of active receptors is regulated at a post-translational level. This conclusion is supported by the accumulation of NFP-GFP in vacuoles of meristematic cells that are younger than L1. Previously, it has been suggested that release from infection threads in Sesbania nodules does not require Nod factors. This might mean that Sesbania evolved a Nod factor independent release mechanism. These studies involved the co-inoculation of a nod- rhizobium mutant and an exo mutant. Therefore, it seems equally well possible that the nod- rhizobium accumulated sufficient Nod factors in their outer membrane to trigger release. Others have also proposed that release might occur independent of Nod factors. The always active form of CCaMK/DMI3 is able to initiate nodules independent of rhizobia [Tirichine *et al.*, 2006]. These nodules can be infected by bacteria unable to produce Nod factors. This could of course show that release is independent of Nod factors, but also could show that the only function of Nod factor perception is to activate CCaMK/DMI3. In plants expressing an always active form of this protein, activation of CCaMK/DMI3 by the Nod factor receptors is not needed.

This is to our knowledge the first time that Nod factor receptors have been localized/ visualized in root nodules. We have used the same constructs to study the Nod factor receptors in the root epidermis using confocal and spinning disc confocal microscopy. However, we (data not shown) as well as Anna Pietraszewska-Bogiel (personal communication) were unable to detect the receptors in the root epidermis. This is in contrast to similar studies by Haney *et al.* [2011]. They visualized LYK3 in Medicago root hairs, but could not detect LYK3-GFP in Medicago nodules. Another difference with the study of Haney *et al.* [2011] seems the time period that LYK3 remains at the plasma membrane and infection thread membrane. Haney *et al.* [2011] detected LYK3 at the

infection thread membrane in root hairs, whereas the tip of this infection threads had already reached the cortical layers. Also, GFP fluorescence in the vacuoles was not reported in their study. This suggests that the presence of LYK3 at the infection thread membrane is persistent in root hairs, whereas in nodules it appears to be a very transient process.

NFP and LYK3 are no longer present at the plasma membrane after release of rhizobia from infection threads. Further, in most of the L2 cells LYK3-GFP was only present on the plasma membrane and not on the infection thread membrane. In contrast, NFP was detected at both membranes in most of the L2 cells. We assume that LYK3 is more rapidly removed from the infection thread membrane than NFP. The accumulation of LYK3 at the infection thread membrane could coincide with the accumulation of its interactor SYMREM1 [Lefebvre *et al.*, 2010]. This Symbiotic Remorin was shown to interact with LYK3. The SYMREM1 protein accumulates at the infection thread membrane and on the symbiosome membrane. SYMREM1 may be a scaffold protein that modulates interaction between LYK3 and other proteins or controls the endocytotic removal of the receptor from the membrane. Our data suggest that the interaction between LYK3 and SYMREM1 may be possible inside the nodule, but that it must occur in a spatially and temporally limited window.

We hypothesize that the strict regulation of Nod factor receptors is controlled in the following manner: The receptor genes are expressed in a relatively broad zone at the apex of the nodule. This includes cells of the meristem that are not in contact with Nod factors. Nod factor receptors accumulate at the plasma membrane at low, non-detectable levels, by which the meristem cells are primed to respond to Nod factors. L1 cells are the first cells that are in contact with Nod factor (secreted by rhizobia in between cells). This activates a positive feedback mechanism by which more Nod factor receptors accumulate in the plasma and infection thread membrane. Increased signaling likely triggers the release of the rhizobia from the infection threads, but at the same time triggers a negative feedback mechanism by which the receptors are targeted for degradation in the vacuoles. In this way relatively high levels of active receptors are restricted to only two cell layers. This strict regulation appears essential to avoid a defense response and to allow normal nodule development. Due to this down-regulation of the receptors the release of the bacteria from the infection threads (or the formation of an unwallled infection droplet) can only occur transiently at a peak of Nod factor signaling. Indeed, only several bacteria are released from an unwallled droplet after which release does not happen any longer, and the released bacteria start to populate the infected cells. A post translational mechanism to maintain receptor levels at a low level may also be active in uninoculated roots and can explain why it has been difficult to visualize the receptors. We assume that *Nicotiana* leaves lack this post translational mechanism by which the receptors accumulate and induce a defense response [Madsen *et al.*, 2011; Pietraszewska-Bogiel *et al.*, 2013].

Both Nod factor receptors are important for release of rhizobia into the cytoplasm of cells derived from the meristem.. The involvement of Nod factor signaling in release of rhizobia

is in line with studies in *Parasponia*. Also in this non-legume, which is able to establish a nitrogen-fixing symbiosis with rhizobia, the NFP homologue is essential for the formation of the symbiotic interface [Op den Camp *et al.*, 2011].

After release of rhizobia the infected cells in wild type nodules differentiate and this includes induction of endoreduplication by which the infected cells enlarge. Knock down of NFP leads to the most severe phenotype. Release of rhizobia from infection threads is blocked and the cells containing an infection thread remain small. The latter suggests that they do not enter endoreduplication [Gonzalez-Sama *et al.*, 2006; Vinardell *et al.*, 2003]. Knock out/down of IPD3 and SYMRK results in a similar phenotype. This shows that, most likely upon recognition of Nod factors, the Nod factor receptors activate a signaling pathway that contains components of the common symbiotic signaling pathway (that is activated in the epidermis). The block of cell enlargement by knock down of NFP, IPD3 and SYMRK could mean that Nod factor signaling triggers differentiation / endoreduplication. Alternatively, the released rhizobia may secrete a new signal molecule that induces endoreduplication. However, the hypothesis that Nod factor signaling is sufficient to trigger endoreduplication is supported by spontaneous nodules formed by expressing an always active form of CCaMK [Tirichine *et al.*, 2006]. Such *Medicago* nodules do contain a central tissue with cells that endoreduplicate. Another difference between the RNAi of NFP and that of LYK3 is the size of the cells in the infection zone. The RNAi of NFP results in small nodules with smaller cells in the infection zone, where cells in the LYK3 RNAi nodules are normal in size. One hypothesis can be that NFP controls endoreduplication and when NFP levels are reduced the cells stay small as proper endoreduplication is lacking.

In the root epidermis LYK3 is first essential when root hairs curl and infection threads are formed. In contrast, NFP is already essential for the first Nod factor responses. It has been postulated that at stages preceding curling NFP interacts with another LysM domain receptor kinase [Arrighi *et al.*, 2006; Zhang *et al.*, 2007]. The stronger block in release of the bacteria in the NFP knock-down nodules compared to LYK3 knock-down, suggest that also in the nodule NFP interacts with additional LysM domain receptor kinases to allow release.

In *Medicago*, release of rhizobia as well as subsequent symbiosome development requires the accumulation of specific vesicular SNARE molecules that belong to the VAMP72 family [Ivanov *et al.*, 2012]. This accumulation is most likely regulated at the post-transcriptional level and might be a target of Nod factor signaling. This is consistent with the fact that Nod factor signaling is essential for release as well as symbiosome development [Tirichine *et al.*, 2006]. This hypothesis is also supported by a splicing mutant of the pea homologue of DMI2 [Ovchinnikova, 2012]. This mutant does form nodules, but release of bacteria from the infection threads is seriously hampered. Nod factor signaling in layer L1 and L2 could thus influence the cells derived from these layers for a long period of time.

We observed different effects of receptor knock-down in our RNAi experiments in the nodule primordium cells compared to the cells in the infection zone that are derived from the nodule meristem. There are two explanations for this difference: either the RNAi levels did not yet reach a level below the threshold in the primordium or release is regulated different in the primordium and meristem. The ENOD12 promoter that we used to express the RNAi constructs is only activated upon nodulation and it may take some time before the RNAi machinery is able to reduce the transcript below a certain threshold that has to be met in order to observe phenotypical differences. On the other hand, we know from work in pea that an allele of SymRK does allow release in the primordium, but blocks infection in cells that originate from the nodule meristem [Ovchinnikova, 2012]. This shows that there is a difference in demand for Nod factor signaling between the primordium and the nodule meristem. Release from infection threads in cells derived from the meristem appears to be regulated more stringent compared to the primordium.

The Nod factor receptors co-localize to the plasma membrane in a zone of about 2 cell layers at the border of the meristem and the infection zone. An interaction between the two receptors was proposed. Recently such interaction was shown in *Nicotianum benthamianum* leaves [Madsen *et al.*, 2011; Pietraszewska-Bogiel *et al.*, 2013]. However, this interaction was never demonstrated in a homologous legume system as visualization of both receptors was till now never successful. Our co-localization data show that the prerequisites for interaction are met inside the nodule. The receptors accumulate at the plasma membrane in the same cells. For LYK3 we observed a localization in puncta, whereas NFP shows a more uniform accumulation in the plasma membrane. This suggests that, although they may form a heteromer, NFP is also present outside this complex.

MATERIALS AND METHODS

Constructs, Plant material and transformation

The NFP and LYK3 promoters and the genomic sequence of NFP and LYK3 were amplified from *M. truncatula* genomic DNA using the primers described in Table 4.1 using Phusion High-Fidelity DNA Polymerase (Finnzymes) and cloned into pENTR™/D-TOPO® (Invitrogen) .

Table 3.1: primers used for cloning. The sequence used for cloning into pENTR™/D-TOPO® (CACC) is underlined.

	Foreward	Reverse
pNFP	<u>CACCGTGCCTAGAGTCAACCATTG</u> G	CATGCTCGAGAAGAGAAAAGAGAG TTTCTTATGGCA
pLYK3	<u>TTCACCGGACAGATAGCGCAG</u>	TGTATCAAGAAGAGAGAGAGAAAAG AGAA
NFP	<u>CACCATGTCTGCCTTCTTTCTTCC</u>	ACGAGCTATTACAGAAGTAACAAC A
LYK3	<u>CACCACAATATTGTATTGGTGAGA</u> TCATATAAGA	TCTAGTTGACAACAGATTTATGAG AGA
pNFP: NFP	<u>CACCGTGCCTAGAGTCAACCATTG</u> G	ACGAGCTATTACAGAAGTAACAAC A
pLYK3: LYK3	<u>TTCACCGGACAGATAGCGCAG</u>	TCTAGTTGACAACAGATTTATGAG AGA

The LeEXTENSIN1 promoter [Mirabella *et al.*, 2004] was cloned into pENTR™/D-TOPO® (Invitrogen) and subsequently cloned into pENTR™ p4p1r by NotI/AscI. Next, a GATEWAY® reaction with LR Clonase II(Invitrogen, for a single entry clone) or LR Clonase II plus (Invitrogen, for multiple entry clones) was performed to generate the appropriate binary constructs as described in Table 3.2.

Table 3.2: generation of binary vectors using (multisite) GATEWAY® technology.

Binary vector	pENTR p4p1r	pENTR p1p2	pENTR p2rp3	pDEST
pNFP:GUS RR		pENTR pNFP		pKGWFS7 RR [Karimi <i>et al.</i> , 2002]
pLYK3:GUS RR		pENTR pLYK3		pKGWFS7 RR
pNFP:NFP- GFP	empty	pENTR pNFP:NFP	GFP Stop T35S [Ovchinnikova <i>et al.</i> , 2012]	pKGW-RR-MGW [Ovchinnikova <i>et al.</i> , 2012]

Binary vector	pENTR p4p1r	pENTR p1p2	pENTR p2rp3	pDEST
pNFP:NFP-RFP	empty	pENTR pNFP:NFP	mCherry Stop T35S	pKGW-MGW [Ovchinnikova <i>et al.</i> , 2012]
pLYK3:LYK3-GFP	empty	pENTR pLYK3:LYK3	GFP Stop T35S	pKGW-RR-MGW
pEXT:LYK3	pLeEXT1	pENTR LYK3	GFP Stop T35S	pKGW-RR-MGW
pUbq:NFP		pENTR NFP		pUbq3 pK7WGF2-RR [Limpens <i>et al.</i> , 2009]
pUbq:LYK3		pENTR LYK3		pUbq3 pK7WGF2-RR
pE12:NFP RNAi		pENTR NFP		pE12 pK7GWIWG2(II) [Limpens <i>et al.</i> , 2005]
pE12:LYK3 RNAi		pENTR LYK3		pE12 pK7GWIWG2(II)

The pNFP:GUS RR and pLYK3:GUS RR were used to transform *M. truncatula* A17, pNFP:NFP-GFP to transform *nfp31* and pLYK3:LYK3-GFP to transform B56 by *Agrobacterium rhizogenes*-mediated hairy root transformation [Limpens *et al.*, 2004]. The transgenic plants were inoculated with *S.meliloti*, *S.meliloti* 2011 –GFP [Limpens *et al.*, 2003] or *S.meliloti* 2011 –mRFP [Smit *et al.*, 2005].

To create a stable line *M. truncatula* R108 was transformed by *A.tumefaciens* AGL1 containing pLYK3:LYK3-GFP. Roots from 1 day old seedlings were cut in a agrobacterium suspension (SH-medium [Gamborg *et al.*, 1976] supplemented with 0.5mg/l BAP, 3mM MES, 20mg/l Acetoseringone, 400mg/l L-cysteine, 1mM DTT and 0.02% Silvet) and left to incubate for 30 min. Root fragments were incubated on co-cultivation medium (SH-medium supplemented with 0.5mg/l BAP, 5 mg/l 2,4-Dichlorophenoxyacetic acid, 3mM MES, 20mg/l Acetoseringone) for 2-3 days at 25°C in the dark. Transgenic explants were selected on SHMab (SH-medium supplemented with 0.5 mg/l BAP, 5 mg/l 2,4-Dichlorophenoxyacetic acid, 3mM MES) with 300 mg/l cefotaxime and 50mg/l kanamycin and transferred to fresh plates weakly until a callus was formed. Green calluses were transferred to regeneration medium (SH-medium with 20g/l sucrose supplemented with 0.5 mg/l BAP, 0.1mg/l NAA, 10 mg/l AgNO₃, 3mM MES, 300mg/l xefotaxime and 50mg/l kanamycin) until shoots were formed and subsequently to PDM (SH-medium containing 10 g/l sucrose supplemented with 0.5mg/l Indole-3-butyric acid and 300 mg/l cefotaxime) to form roots.

Histochemical Analysis and Microscopy.

Histochemical β -glucuronidase staining was performed according to the procedure described by [Limpens *et al.*, 2005]. Nodules were fixed overnight in a mixture of 4% paraformaldehyde and 3% glutaraldehyde in 50mM potassium phosphate buffer (pH 7.4) at 4°C. Roots were dehydrated in ethanol and subsequently embedded in Technovit 7100 (Heraeus Kulzer). Thin 7 μ m thick longitudinal sections were cut using a microtome, stained with 0.1% ruthenium red and analyzed with a Leica DM5500B microscope.

For structural analysis nodules were selected based on DsRED1 expression using a Leica MZFLIII binocular fitted with HQ470/40, HQ525/50, HQ553/30, and HQ620/60 optical filters (Leica Microsystems, Rijswijk, The Netherlands). Nodules were fixed, dehydrated and embedded as above. Thin 4 μ m thick longitudinal sections were stained with 0.05% toluidine blue and analyzed.

Fluorescent microscopy.

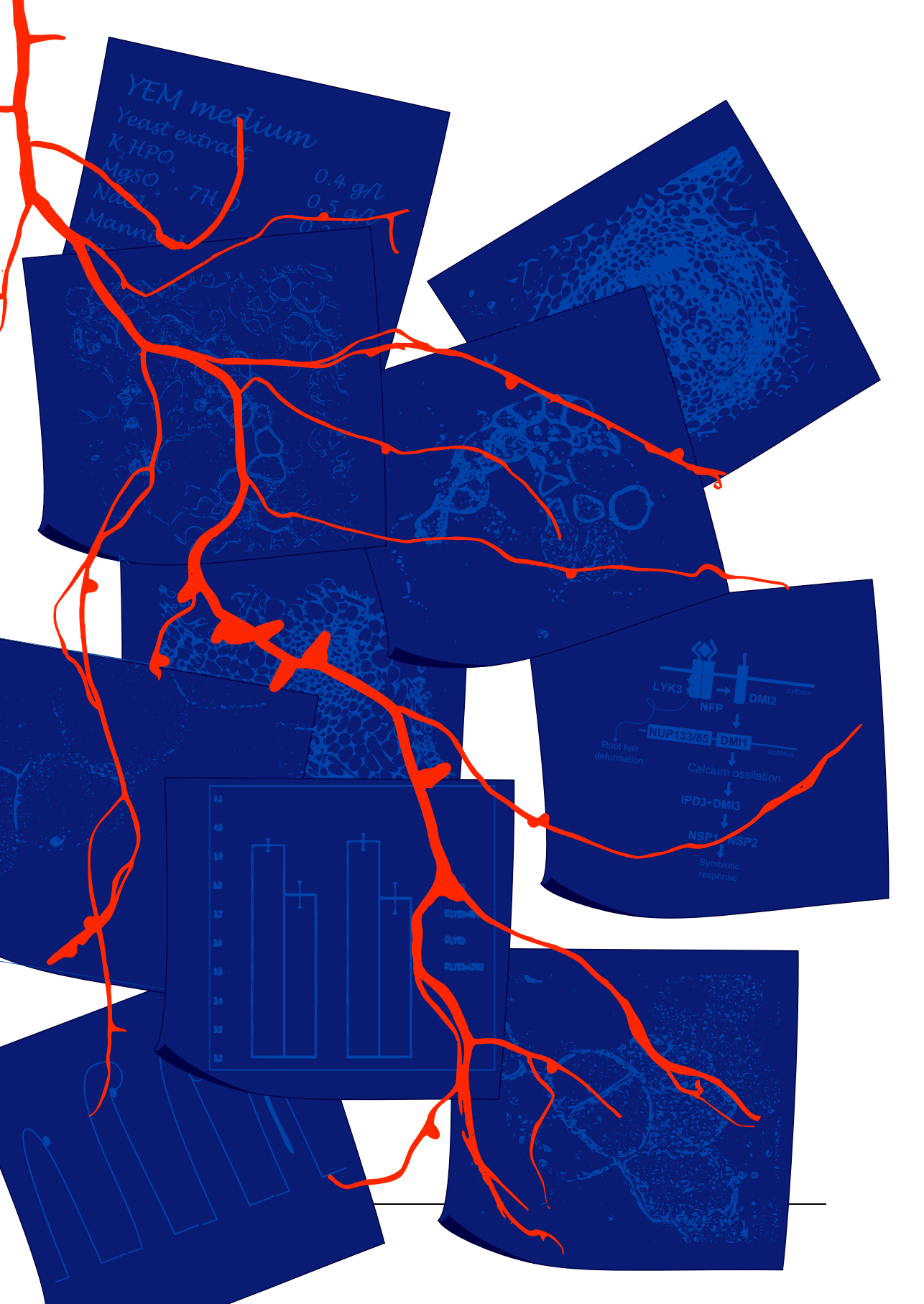
Transgenic roots and nodules were selected based on DsRED1 expression as above. Transgenic nodules were hand sectioned using double-razor blades and mounted on microscope slides in 0.9% NaCl and further analyzed on a Zeiss LSM 510 confocal laser scanning microscope (Carl-Zeiss Axiovert [Oberkochen, Germany] 100 M equipped with a LSM510, an argon laser with a 488-nm laser line, a helium-neon laser with a 543-nm laser line); 488 nm (GFP) and 543 nm (DsRED1/mRFP); GFP emission was selectively detected using a 505- to 530-nm band-pass filter; DsRED1/mRFP emission was detected using a 560- to 615-nm band-pass or 560-nm long-pass filter.

Transmission electron microscopy

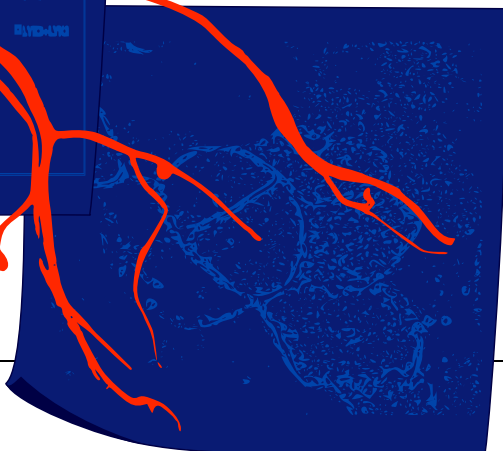
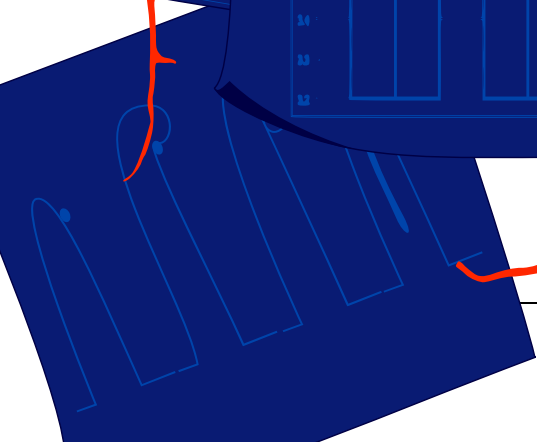
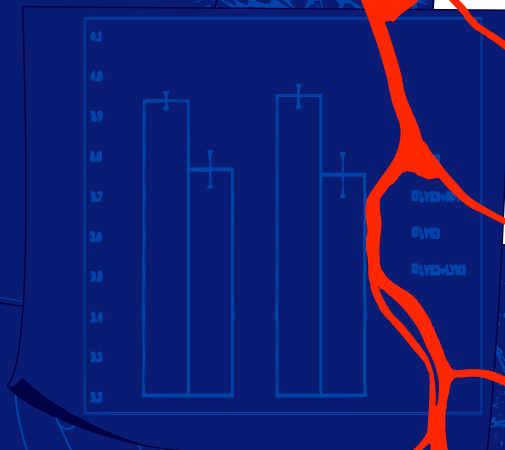
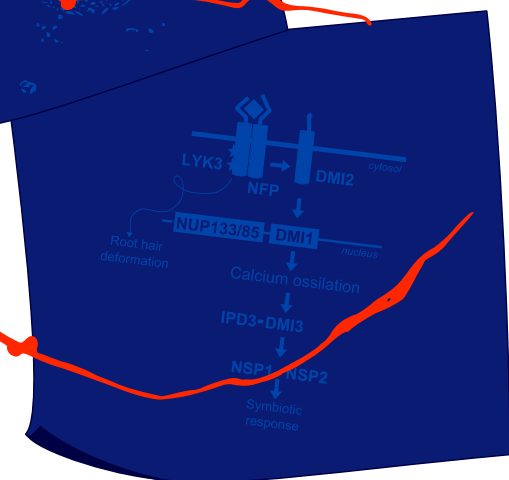
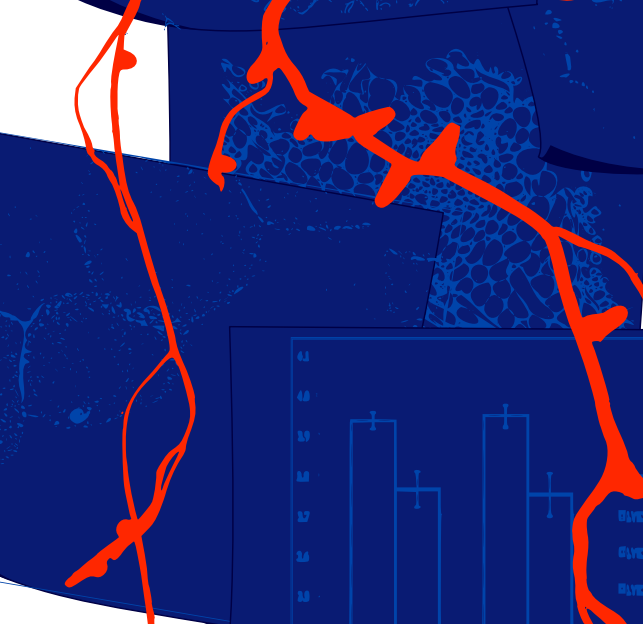
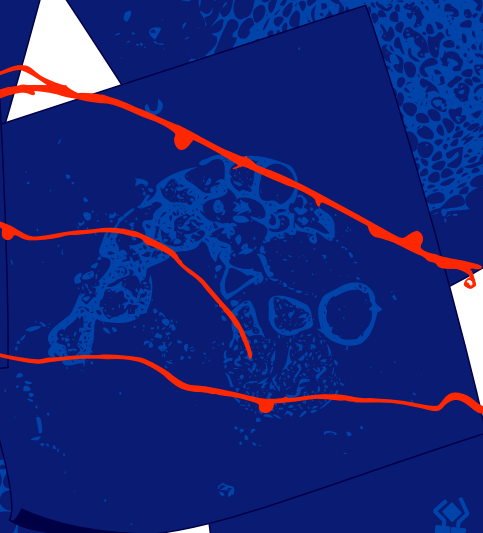
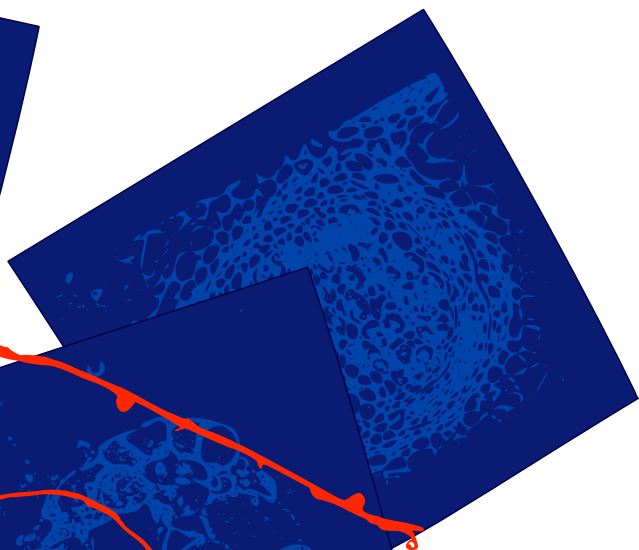
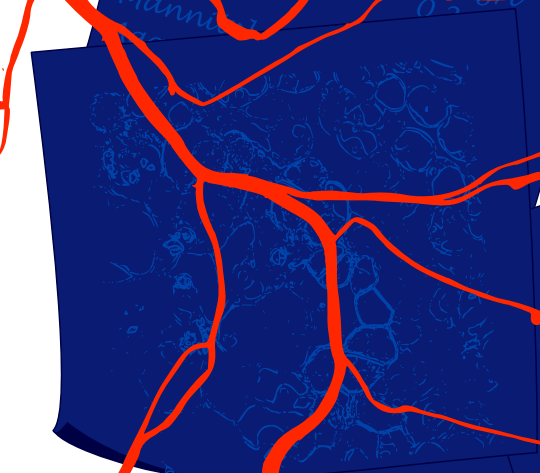
For electron microscopy, nodules were collected 19 days after inoculation and prepared as described previously [Limpens *et al.*, 2009]. Thin sections (60 nm) of the same nodule were cut using a Leica Ultracut microtome (Leica). Nickel grids with the sections were blocked in 2% BSA in PBS and incubated with polyclonal rabbit anti-GFP antibodies (Molecular Probes) in dilution 1:200. Goat anti-rabbit coupled with 15-nm gold (BioCell) (1:50 dilution) were used as secondary antibody. Sections were examined using a JEOL JEM 2100 transmission electron microscope equipped with a Gatan US4000 4K \times 4K camera.

ACKNOWLEDGEMENTS

We thank Elena Fedorova for the help with the electron microscopical analyses.



YEM medium
Yeast extract 0.4 g/l
 K_2HPO_4 0.5 g/l
 $MgSO_4 \cdot 7H_2O$ 0.5 g/l
 $NaCl$ 0.5 g/l
Mannitol 10 g/l



Chapter 4.

THE NOD FACTOR RECEPTORS LYK3 AND NFP FORM HETEROMERS IN MEDICAGO NODULES

Sjef Moling¹, Anna Pietraszewska-Bogiel², Mark Hink², Erik Limpens¹ and Ton Bisseling^{1,3}

¹*Laboratory of Molecular Biology; Wageningen University; Wageningen, The Netherlands*

²*Section of Molecular Cytology, Swammerdam Institute for Life Sciences, University of Amsterdam, Amsterdam, The Netherlands*

³*College of Science; King Saud University; Riyadh, Saudi Arabia*

Submitted for publication in a modified form

ABSTRACT

For the perception of Nod factors in the rhizobium – legume symbiosis two receptor like kinases are essential. An interaction between the two was already postulated at their discovery and recently observed in heterologous systems. Here we show for the first time that the receptors, NFP and LYK3, do form heteromeric complexes inside nodules of *Medicago truncatula*. We used FRET combined with both acceptor photobleaching and fluorescent lifetime imaging to prove the formation of these complexes. Furthermore, we showed that LYK3 is also able to form homomeric complexes.

INTRODUCTION

The symbiosis between legumes and nitrogen fixing bacteria (rhizobia) results in the formation of root nodules in which the bacteria are able to reduce atmospheric nitrogen. The formation of these nodules is in general set in motion by specific lipochito-oligosaccharides secreted by the bacteria. These lipochito-oligosaccharides are named Nod factors. They are acylated chitin oligomers and substitutions can be present at the terminal N-acetyl glucosamine subunits [D'Haese and Holsters, 2002]. Nod factors are recognized by (at least) two receptors [Broghammer *et al.*, 2012; Gough and Cullimore, 2011]. These are receptor-like kinases that have an extracellular region containing several LysM domains [Arrighi *et al.*, 2006; Limpens *et al.*, 2003]. One of these receptors lacks an active kinase domain [Arrighi *et al.*, 2006]. Further, several Nod factor induced responses require both receptors [Arrighi *et al.*, 2006; Limpens *et al.*, 2003; Madsen *et al.*, 2003; Radutoiu *et al.*, 2003; Smit *et al.*, 2007]. Therefore it has been proposed that the receptors form heterodimers [Arrighi *et al.*, 2006; Smit *et al.*, 2007]. Recently, it was shown in *Nicotiana benthamiana* (Nicotiana) that the 2 receptors can interact in this heterologous system [Madsen *et al.*, 2011; Pietraszewska-Bogiel *et al.*, 2013]. However, such interaction remains to be experimentally demonstrated in legumes. Interaction studies in legumes have been hampered because of the general difficulty in visualization of these receptors [Lefebvre *et al.*, 2010; Madsen *et al.*, 2011]. Recently, we showed that in the model legume *Medicago truncatula* (Medicago) both Nod factor receptors accumulate, to detectable levels, in a very narrow zone in root nodules (Chapter 3). This provides now unique opportunities to study the interaction of these receptors in a homologous legume system.

The two Medicago Nod factor receptors are called LYK3 and NFP [Arrighi *et al.*, 2006; Limpens *et al.*, 2003]. LYK3 has an active kinase domain [Limpens *et al.*, 2003; Mbengue *et al.*, 2010] whereas NFP, although essential for nodulation, is a pseudokinase as it lacks the activation loop in the kinase domain [Arrighi *et al.*, 2006; Lefebvre *et al.*, 2012]. The *Lotus japonicus* orthologues of LYK3 and NFP, NFR5 and NFR1, have been shown to interact when co-expressed in Nicotiana [Madsen *et al.*, 2011]. This co-expression causes cell death which is independent of Nod factors. Similarly, when the Medicago receptors are co-expressed in Nicotiana cell death is also induced [Pietraszewska-Bogiel *et al.*, 2013].

This is rather remarkable as in legume roots both receptors are constitutively expressed and Nod factors are essential for their symbiotic activity [Arrighi *et al.*, 2006; Limpens *et al.*, 2003]. Cell death might be avoided in legumes by maintaining the levels of Nod factor receptors at a very low level. We assume/ hypothesize that such a mechanism is absent in *Nicotiana*. The relatively high level of accumulation of the Nod factor receptors and the hypersensitive response are a striking difference with the properties of these receptors in legumes. Therefore it raises the question whether the observed interaction is biologically relevant and not an artifact of the heterologous system.

Medicago nodules have an apical meristem that adds new cells to the nodule tissues. The zone adjacent to the meristem is called infection zone [Vasse *et al.*, 1990]. In the most distal layers of the infection zone rhizobia are released from the infection threads into cytoplasm of nodule cells. Both *Medicago* Nod factor receptors accumulate very transiently at the border between the meristem and the infection zone. In this zone they accumulate at the plasma membrane in a narrow zone of about 2 cell layers (Chapter 3). This zone coincides with the region where rhizobia still produce Nod factors [Marie *et al.*, 1994; Schlaman *et al.*, 1991]. Therefore, the accumulation of Nod factor receptors most likely reflects the period when Nod factors are perceived. The fact that we could not visualize these biological functional receptor constructs in un-inoculated *Medicago* roots is consistent with this hypothesis. As both Nod factor receptors accumulate in a reproducible manner in *Medicago* nodules we decided to study the receptor interaction in this small nodule zone.

We employed Förster Resonance Energy Transfer combined with acceptor photobleaching (FRET-AB)[Ishikawa-Ankerhold *et al.*, 2012] and Fluorescence Lifetime Imaging Microscopy (FRET-FLIM)[Becker, 2012; Ishikawa-Ankerhold *et al.*, 2012] to investigate heteromerization of NFP and LYK3.

RESULTS

Acceptor photobleaching

To study the interaction between NFP and LYK3 we created tagged receptor constructs that can function as donor/acceptor pair in a FRET experiment. Therefore, the NFP and LYK3 genomic sequences were fused to the 5'-terminus of the sequence encoding monomeric cyan fluorescent protein (cerulean, cCFP) or yellow fluorescent protein (Venus) respectively [Goedhart *et al.*, 2012; Kremers *et al.*, 2006]. These construct were put under control of the NFP or LYK3 promoter regions that previously were shown to be biologically functional (Chapter 3). We co-transformed *Medicago* with LYK3-cCFP RR and NFP-Venus RR. To deal with low co-transformation efficiencies we transformed a *lyk3-1 x nfp-1* double mutant. In this case we know that both constructs have been introduced when nodules are formed. In FRET-AB the fluorescent acceptor is bleached and

energy transfer from the donor to the acceptor is no longer possible. This results in an increased intensity of the donor fluorescence. This technique is a relative easy method to investigate a possible interaction between the receptors.

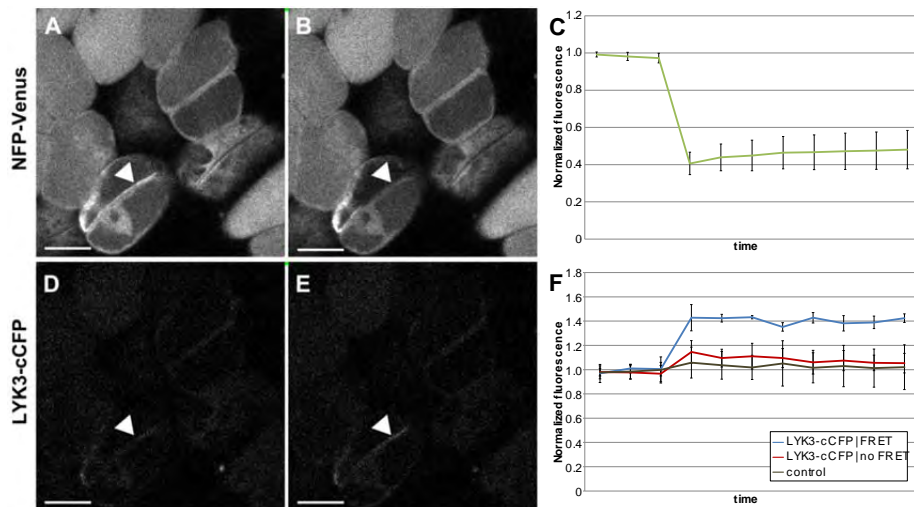


Figure 4.1: acceptor photobleaching of NFP-venus when co-expressed with LYK3-cCFP. (A-C) NFP-Venus signal (A) pre bleach at 0s, (B) post bleach at 38s and (C) plotted as normalized fluorescence as a function of time with standard deviation. (D-F) LYK3-cCFP signal (D) pre bleach at 0s, (E) post bleach at 38s and (F) plotted as normalized fluorescence as a function of time with standard deviation. Two clearly different fractions were observed with either increased fluorescence ($n=4$) or unchanged fluorescence ($n=7$). As a control the cell periphery of an unbleached area of the same cell was used. The bar indicates $10\mu\text{m}$.

With this approach we could detect both fluorescent proteins in the nodule (Figure 4.1 and Figure 4.3). The signal for LYK3-cCFP is clear but very weak. For NFP-Venus a stronger signal was observed. To test if there is a possible interaction between LYK3 and NFP we performed acceptor photobleaching (Figure 4.1). Because of the high laser intensity, the fluorescence detected in the YFP channel decreased with approximately 60%. Simultaneously, the intensity in the CFP (donor fluorophore) channel increased by approximately 57%. This increase was not observed in other areas. Similar, this suggests that there is a physical interaction between LYK3 and NFP. We analysed another 10 nodules by acceptor photobleaching and plotted the normalized fluorescence as a function of the time (Figure 4.1c,f). The first time point was used as a reference sample for normalization. The change in fluorescence in these nodules grouped in two subclasses. In four of these nodules we observed a significant increase ($41 \pm 5.6\%$ standard deviation), where the other seven did not show a significant change in fluorescence intensity. This indicates that NFP and LYK3 may form heteromers inside nodules of *Medicago*.

FRET-FLIM measurements

Because the FRET-AB experiments indicated an interaction of the two receptors we decided to study this interaction more accurately. As we were concerned about possible conversion of YFP fluophores into species emitting in the CFP range, due to the high illumination [Valentin *et al.*, 2005]) using the acceptor photobleaching method, we decided to investigate LYK3 and NFP oligomerization states in Medicago nodules using FRET-FLIM. In order to optimise our FRET-FLIM measurements, we changed the CFP fluorescent protein fused to the receptors from cerulean into Turquoise2 (mTQ2), as the latter displays a monoexponential lifetime decay more suitable for FLIM analysis [Goedhart *et al.*, 2012]. In addition, we removed the *dsRed* reporter gene from the binary constructs in order to minimise the fluorescent species present in the nodule. Because the FRET-FLIM measurement is independent of the intensity of the fluorescent signal, FRET-FLIM allows robust investigation of proximity between molecules. In FRET-FLIM, changes in the donor fluorescence lifetime (τ), i.e. of time the donor stays in the excited state, are monitored. A decrease in lifetime shows the occurrence of FRET because the fluophores are in close proximity (generally not further apart than 10 nm). Such close proximity strongly indicates that there is a physical interaction of the two molecules to which they are fused [Pietraszewska-Bogiel and Gadella, 2011; Vogel *et al.*, 2006].

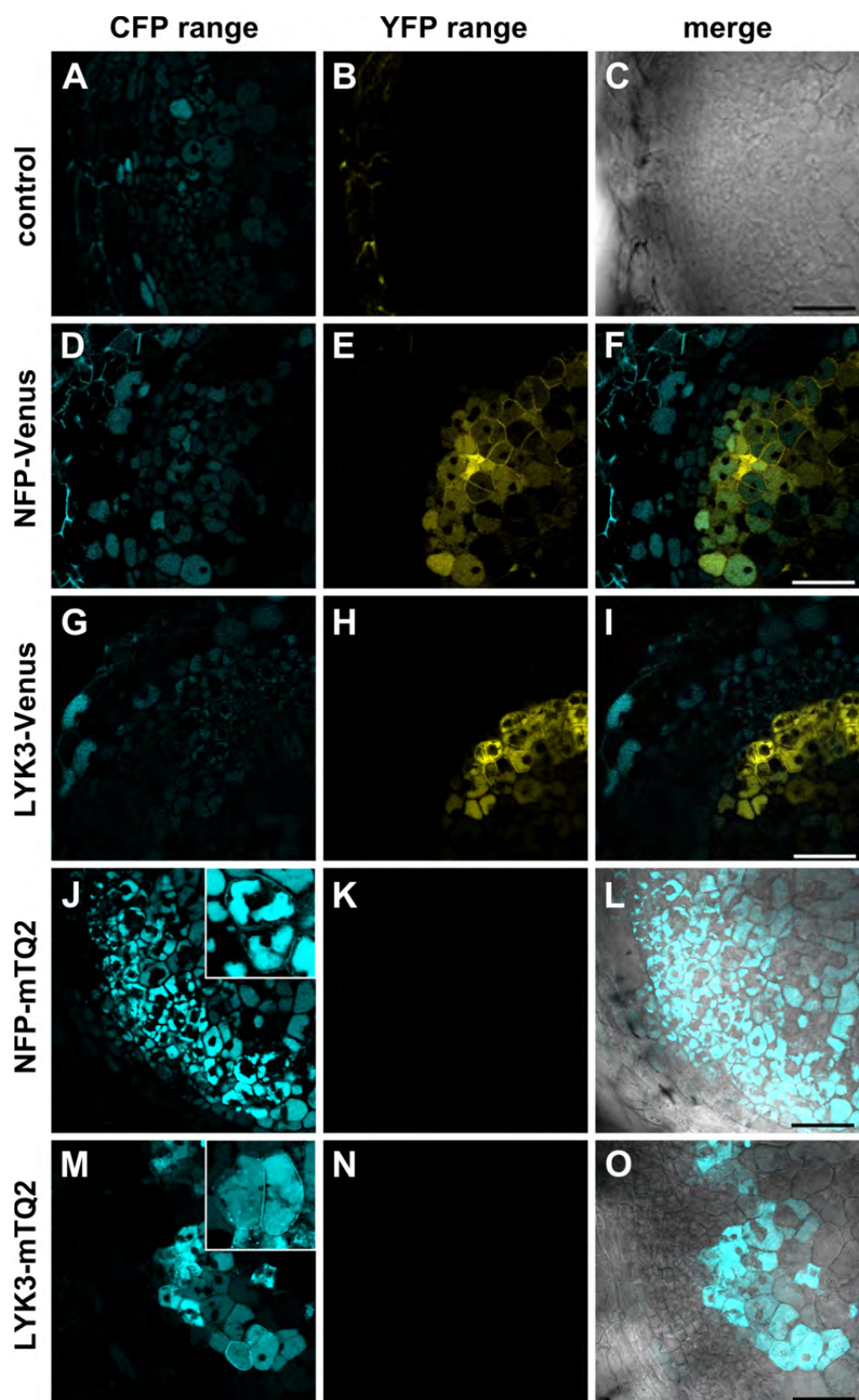
Specific yellow fluorescence was observed in 4 out of 9 nodules produced on either *lyk3-1* mutant complemented with the *pLYK3:LYK3-Venus* construct or on Medicago *lyk3-1* x *nfp-1* double mutant complemented with the *pLYK3:LYK3-Venus* and *pNFP:NFP-mTQ2* constructs. Similar specific yellow fluorescence was observed in 7 out of 14 nodules produced on Medicago *lyk3-1* x *nfp-1* double mutant complemented with the *pNFP:NFP-Venus* and *pLYK3:LYK3-mTQ2* constructs.

Figure 4.2 shows typical nodules expressing NFP or LYK3 as a fusion to either mTQ2 or Venus. Both receptors accumulated in a narrow zone of approximately 2 cell layers at the plasma membrane. This zone is located at the border of meristem and infection zone like we showed in Chapter 3. In addition to the accumulation at the plasma membrane the fluorophores also accumulated in vacuoles (Figure 4.2, Chapter 3). We expect the localization at the plasma membrane to be the active receptor and that accumulation in the vacuoles is due to tight regulation at the post-transcriptional level (degradation).

In contrast, no fluorescence in the YFP range was detected in the apex or central region of the control nodules transformed with an empty vector, although in some control nodules YFP-like autofluorescence could be observed in the cell walls of the outermost cell layer (Figure 4.2b). In addition, control nodules and nodules expressing NFP or LYK3 as a fusion to Venus were used to characterize autofluorescence of nodules in the CFP range (Figure 4.2a-c). We observed CFP-like autofluorescence localized in cell walls of the outermost cell layer (nodule cortex), and (in most nodules) also in vacuoles of several proximal cell layers. However, only in the nodules expressing either NFP-mTQ2 or LYK3-

mTQ2 fusions (in 7 out of 24, and 9 out of 20 nodules, respectively) did we observe a specific CFP signal localized to the plasma membrane in 1-2 cell layers at the border of the meristem and the infection zone (Figure 4.2j-o). As this signal was different from the CFP-like autofluorescence in both subcellular localization and lifetime (see below), we concluded that both mTQ2 and Venus fusions of the receptors could be used to study their oligomerization states in *Medicago* nodules.

→ Figure 4.2: Localization of MtNFP and MtLYK3 fluorescent fusions in *Medicago* nodules. (A-C) control nodules expressing empty vector (D-F) localization of MtNFP-venus and (G-I) MtLYK3-venus fusion protein in nodules approx. 10 days after inoculation with *S. meliloti*. Bar is 50 μ m. (J-L) localization and subcellular localization of MtNFP-mTQ2 and (M-O) MtLYK3-mTQ2 fusion protein in nodules (10 dpi). Bar is 10 μ m. When the receptors are fused to venus there is some autofluorescence observed in the CFP range in the vacuoles in the nodule apex (D and G). This autofluorescence is different in lifetime from the fluorescence of the CFP-fused receptors. No autofluorescence was observed when the receptors are fused to mTQ2 (K and N).



For the FRET-FLIM analysis of the NFP-LYK3 interaction we co-transformed the Medicago *lyk3-1* x *nfp1* double mutant with LYK3-mTQ2 and NFP-Venus. Lifetime of the mTQ2 or of CFP-like autofluorescence present in various regions of 10-12 days old nodules was measured using time-correlated single photon counting (TCSPC). Immediately after acquiring a τ image, two images recording the fluorescence intensity of mTQ2 (termed donor intensity, I_D) and Venus (termed acceptor intensity, I_A) were acquired using direct excitation. In the cell layers at the border of the meristem and the infection zone, the τ , I_D and I_A were measured in the plasma membrane region. Both in the reference and in the FRET samples, fluorescence decay in the plasma membrane regions could be fitted with one component (see below). In contrast, τ measured in the vacuoles or cell walls of the outermost cell layers in control nodules could only be obtained after fitting the fluorescence decay with two components: $\tau_1 = 3.911 \pm 0.043$ ns (mean \pm st. dev.) and $\tau_2 = 1.086 \pm 0.097$ ns ($\tau_{av} = 2.715 \pm 0.141$ ns, $n = 10$) for CFP-like autofluorescence in vacuoles; $\tau_1 = 3.163 \pm 0.159$ ns and $\tau_2 = 0.691 \pm 0.104$ ns ($\tau_{av} = 1.828 \pm 0.256$ ns, $n = 7$) for CFP-like autofluorescence in cell walls. The τ measured in the plasma membrane region of cells expressing *pLYK3::LYK3-mTQ2* or *pNFP::NFP-mTQ2* construct correlated well in value and monoexponentiality with the τ of mTurquoise2 measured *in vitro* (4.3 ns) or as different plasma membrane-localized fusions *in vivo* (4-4.1 ns; Mark Hink, personal communication). This further supports the notion that we observed the specific signal originating from the mTQ2 fusions of the receptors.

The apparent FRET efficiency (E_{app}) is calculated as:

$$E_{app} = 1 - \frac{\tau_{DA}}{\tau_D}$$

where τ_{DA} is the average τ measured in samples containing both donor- and acceptor-fused receptors (so-called FRET samples), and τ_D is the average τ measured in samples containing only the respective donor-fused receptor (the reference samples). Care was taken to compare only the τ_D and τ_{DA} values that were obtained from similarly bright cells (see Pietraszewska-Bogiel *et al.* [submitted] for the discussion on the effect of autofluorescence on the measured τ).

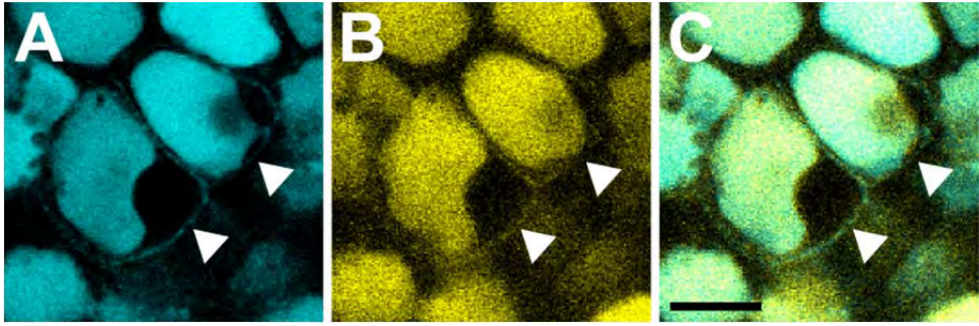


Figure 4.3: co-localization of LYK3-mTQ2 and NFP-venus fusion proteins in nodules approx. 10 days after inoculation with *S. meliloti*. The arrows indicate accumulation at the plasma membrane. Bar is 10 μ m.

Indeed, we did not observe any correlation between lower τ_{DA} values with higher I_A . The only dependence of τ_{DA} on I_A was noted in several cells in *Medicago* nodules co-transformed with *pLYK3::LYK3-mTQ2* and *pNFP::NFP-Venus* constructs, in which only LYK3-mTQ2 fusions and virtually no NFP-Venus fusions were localized to the plasma membrane. The τ_{DA} values measured in these cells were similar to τ_D values, and were therefore regarded as an internal negative control.

The τ_{DA} measured in nodule cells co-expressing LYK3-mTQ2 and NFP-Venus fusions was significantly shorter (on average 3.764 ± 0.078 ns, $n = 14$, mean $I_D = 145$ [arbitrary units.]) than the reference τ_D (on average 3.936 ± 0.056 ns, $n = 28$, mean $I_D = 125$ [a.u.]), yielding an $E_{app} = 4.4 \pm 0.6\%$ (Figure 4.4,b). The E_{app} values calculated for LYK3 and NFP heteromerization were significantly different from the day-to-day error in E_{app} calculations (Figure 4.4b), indicating that we measured significant interactions between these receptors.

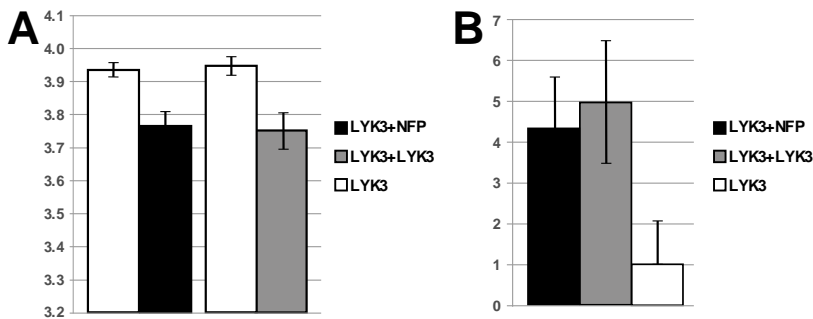


Figure 4.4: Oligomerization of NFP and LYK3 at plasma membrane in *Medicago* nodules. (A) mean τ values measured in nodule cells expressing LYK3-mTQ2 fusions (white columns), co-expressing LYK3-mTQ2 and NFP-Venus fusions (light grey column) or co-expressing LYK3-mTQ2 and LYK3-Venus fusions (dark grey column). Bars present confidence intervals for the mean at $p = 0.05$. (B) mean E_{app} calculated for LYK3 and NFP heteromerization (light grey column), and LYK3 homomerization (dark grey column). Day-to-day error in E_{app} calculations is presented as black column. Bars present confidence intervals for the mean at $p = 0.05$.

Homomerization of LYK3 in Medicago nodules

As many receptors function as homomers [Heldin, 1995] we also determined homomerization and tagged the receptors with both fluorophores. The low expression of NFP under control of its native promoter did not allow us to investigate the formation of NFP homomers. This because there is no way to ensure that roots are transformed with both constructs. Because NFP has no kinase activity, the formation of NFP homomers is seems less relevant compared to the formation of LYK3 homomers. To study the formation of these LYK3 homomers we co-transformed LYK3-mTQ2 and LYK3-Venus into the *lyk3-1* mutant B56 [Smit *et al.*, 2007]. The τ_{DA} measured in nodule cells co-producing LYK3-mTQ2 and LYK3-Venus fusions was significantly shorter (on average 3.752 ± 0.122 ns, $n = 22$, mean $I_D = 259$ [arbitrary units]) than the reference τ_D (on average 3.948 ± 0.066 ns, $n = 24$, mean $I_D = 152$ [a.u.]), yielding an $E_{app} = 5 \pm 0.7\%$ (Figure 4.4a,b). This suggests that a LYK3 homomer is formed inside Medicago nodules.

DISCUSSION

Here, using FRET-AB and FRET-FLIM, we were able to demonstrate specific heteromerization of NFP and LYK3, and homomerization of LYK3 fluorescent protein fusions at the plasma membrane inside Medicago nodules. This agrees with their demonstrated oligomerization upon co-expression in *N. benthamiana* leaf epidermal cells [Pietraszewska-Bogiel, 2013, chapter 3], with the demonstrated oligomerization of their orthologues from *L. japonicus*, LjNFR5 and LjNFR1 [Madsen *et al.*, 2011], and with the demonstrated homomerization of LYK3/NFR1 homolog, OsCERK1 and AtCERK1 [Liu *et al.*, 2012; Shimizu *et al.*, 2010]. As NFP and LYK3 fusions were expressed under the regulation of their respective native promoter, danger of so-called bystander FRET (FRET due to a concentration effect and not due to the specific protein-protein interaction) was small.

We showed that NFP and kinase-active LYK3 heteromerize at the plasma membrane in Medicago nodules. In Nicotiana leaves co-expression of wild type LYK3 and NFP in causes cell death [Pietraszewska-Bogiel *et al.*, 2013]. Therefore the interaction was studied in Nicotiana leaves using NFP and a kinase-inactive mutant of LYK3 (LYK3 G334E encoded by the *lyk3-1* allele). The absence of cell death in nodules, despite the co-accumulation of both receptors, might suggest that interaction between LYK3 and NFP is limited compared to the situation in Nicotiana. Another explanation might be that cells of the legume nodule have a mechanism to repress these responses. This mechanism is not present in Nicotiana. Compared to the situation in Nicotiana, the E_{app} found in our experiments in Medicago nodules is higher ($4.4 \pm 0.6\%$ in Medicago versus $2.5 \pm 0.8\%$ in Nicotiana). This difference could be explained by activity/ lack of activity of the LYK3 kinase. The activity of the kinase could influence complex formation.

Unfortunately, our FRET-FLIM studies did not include cells with LYK3 present on infection thread membranes (seen in only 35% of the nodules described in Chapter 3). Therefore, LYK3 oligomerization status on the IT membranes remains to be analysed. This experiment also requires simultaneous visualization of rhizobia. As we did not observe colocalization of LYK3 and NFP at the plasma membrane in cells containing infection threads (Chapter 3), we hypothesize that LYK3 and NFP heteromerization might occur earlier and be important for the entrance of infection threads into cells derived from the meristem. After signaling the receptors are removed from the membrane and destroyed in the vacuole. It would be interesting to investigate whether a similar LYK3 and NFP heteromerization takes place in the primordium prior the release of rhizobia in cells derived from cortical cell layer 4 and 5 (Chapter 2, Chapter 3).

Next to the formation of heteromers between LYK3 and NFP we observed the formation of LYK3 homomers. The E_{app} calculated for LYK3 homomerization (5%) correlates well with value measured for LYK3 fusions expressed and homomerized at the plasma membrane in *Nicotiana* leaf epidermal cells (6%) [Pietraszewska-Bogiel, 2013, chapter 3]. Di- or oligomerization is often required to stimulate kinase activity (via allostery or intermolecular trans-phosphorylation) of receptor kinases. In *Arabidopsis thaliana*, three receptor kinases: Clavata 1 (AtCLV1), Brassinosteroid Insensitive 1 (AtBRI1), and Flagellin Sensing 2 (AtFLS2), have been demonstrated to homomerize *in planta* [Bleckmann *et al.*, 2010; Guo *et al.*, 2010; Hink *et al.*, 2008; Russinova *et al.*, 2004; Sun *et al.*, 2012]. This homomerization often increases upon ligand stimulation [Wang *et al.*, 2005]. In addition, several plant receptor-like kinases have been shown to heteromerize in a ligand-dependent manner with one or several different members of *Arabidopsis* Somatic Embryogenesis Receptor Kinase (AtSERK) subfamily [Jaillais *et al.*, 2011; Jeong *et al.*, 2010; Karlova *et al.*, 2006; Roux *et al.*, 2011; Schulze *et al.*, 2010; Schwessinger *et al.*, 2011; Wang *et al.*, 2008]. For instance, heteromerization of AtBRI1 and AtBRI1-Associated Kinase 1 (AtBAK1)/AtSERK3 is postulated to result in sequential reciprocal trans-phosphorylation of both proteins, which ultimately increases the kinase activity downstream signaling output of AtBRI1 [Wang *et al.*, 2008].

The observed LYK3 homomerization at the plasma membrane could involve a separate pool of protein or could be realized within higher-order protein complexes that also contain NFP receptors. Therefore, it would be interesting to apply three-color FRET technique [Sun *et al.*, 2010] to investigate the possibility of existing higher order NFP/LYK3 complexes in *Medicago* nodules. In addition, in a situation of pronounced homomerization of LYK3, there will be a significant dilution of FRET signal from the heteromerized LYK3-mTQ2 fusion. Because NFP has no kinase activity, the formation of NFP homomers seems less relevant compared to the formation of LYK3 homomers.

MATERIALS & METHODS

Constructs, Plant material and transformation

The genomic regions containing NFP and LYK3 and their respective promoters were amplified from *M. truncatula* genomic DNA using the primers described in Table 4.1 using Phusion High-Fidelity DNA Polymerase (Finnzymes) and cloned into pENTR™/D-TOPO® (Invitrogen).

Table 4.1: primers used for cloning. The sequence used for cloning into pENTR™/D-TOPO® (CACC) is underlined.

	Foreward	Reverse
pNFP: NFP	<u>CACCGTGCCTAGAGTCAACCATTGG</u>	ACGAGCTATTACAGAAGTAACAACA
pLYK3: LYK3	TTC <u>ACCGGACAGATAGCGCAG</u>	TCTAGTTGACAACAGATTTATGAGAGA

The coding sequence for mTurquoise2 [Goedhart *et al.*, 2012] and venus YFP [Kremers *et al.*, 2006] were cloned into a pENTR-p2rp3-MCS-Stop-T35S [Ovchinnikova *et al.*, 2012] by AscI and KpnI.

Next, a GATEWAY® reaction with LR Clonase II plus (Invitrogen) was performed to generate the appropriate binary constructs as described in Table 3.2.

Table 4.2: generation of binary vectors using multisite GATEWAY® technology.

Binary vector	pENTR p4p1r	pENTR p1p2	pENTR p2rp3	pDEST
pNFP:NFP- venus	empty	pENTR pNFP:NFP	Venus YFP Stop T35S	pKGW-MGW
pNFP:NFP- YFP RR	Empty	pNFP:NFP	Venus YFP Stop	pKGW-MGW RR
pNFP:NFP- mTQ2	empty	pENTR pNFP:NFP	mTQ2 Stop T35S	pKGW-MGW
pLYK3:LYK3- venus	empty	pENTR pLYK3:LYK3	Venus YFP Stop T35S	pKGW-MGW

pLYK3:LYK3- mTQ2	empty	pENTR pLYK3:LYK3	mTQ2 Stop T35S	pKGW-MGW
pLYK3:LYK3- cCFP RR	Empty	pENTR pLYK3:LYK3	cCFP Stop T35S	pLGW-MGW RR

The resulting binary vectors were used to transform *M. truncatula nfp31*, B56 or a *nfp31* x B56 cross by *Agrobacterium rhizogenes*-mediated hairy root transformation [Limpens *et al.*, 2004]. The transgenic plants were inoculated with *S.meliloti*.

Laser-scanning confocal-Setup

Confocal imaging was performed on an inverted Fluoview 1000 laser scanning microscope (Olympus). The excitation light: 440 nm 20 MHz pulsing laser diode (Picoquant), attenuated 10 times by a neutral density filter, and 515nm Argon laser, was guided via a D440/514/594 primary dichroic mirror (Chroma) through a water immersed 60x UPlanS-Apo objective (NA 1.2) into the sample. The emission light was guided via a size-adjustable pinhole, set at 120 µm, through the Olympus detection box to the fibre output channel. The emission light was splitted by the 510 dichroic mirror and guided into photomultiplier tubes (PMTs) where it was filtered by a 455-500 emission filter (Chroma) or 525-550 emission filter (Chroma).

Time-domain FLIM-Setup

Measurements were performed on an inverted Fluoview 1000 laser scanning microscope (Olympus). The excitation light of a 440 nm 20 MHz pulsing laser diode (Picoquant), as controlled by a SepiaII laser driver unit (Picoquant), was attenuated 10 times by a neutral density filter. The light was guided via a D440/514/594 primary dichroic mirror (Chroma) through a water immersed 60x UPlanS-Apo objective (NA 1.2) into the sample. The emission light was guided via a size-adjustable pinhole, set at 120 µm, through the Olympus detection box to the fibre output channel. The optical fibre was coupled to a custom-made detection box (Picoquant) containing PDM avalanche photodiodes (MPD). The light was guided into one of the MPDs where the light was filtered by a 475/45 emission filter (Chroma). The photon arrival times were recorded by a Picohart 300 time-correlated single-photon counting system (Picoquant).

Time-domain FLIM-Data analysis

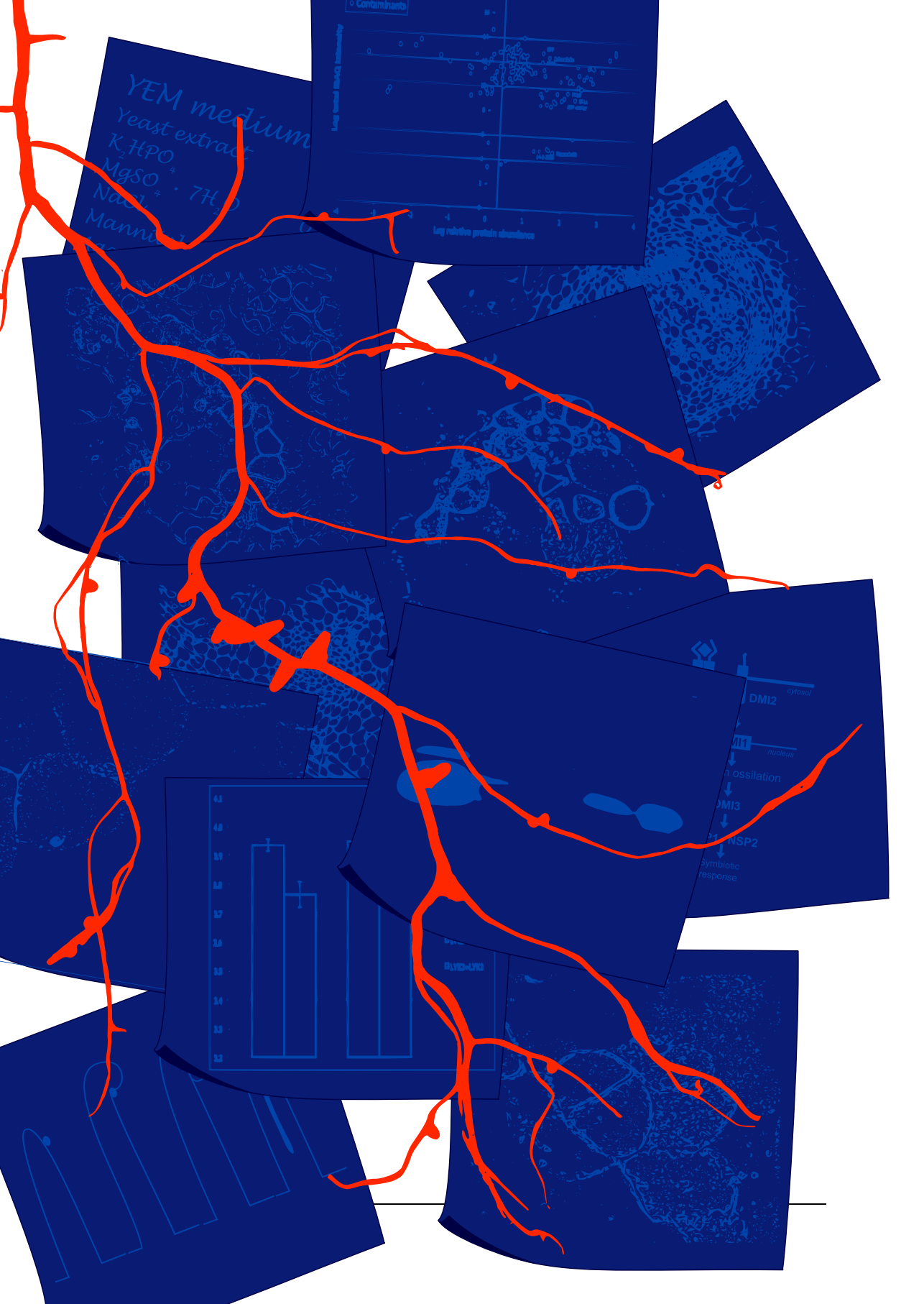
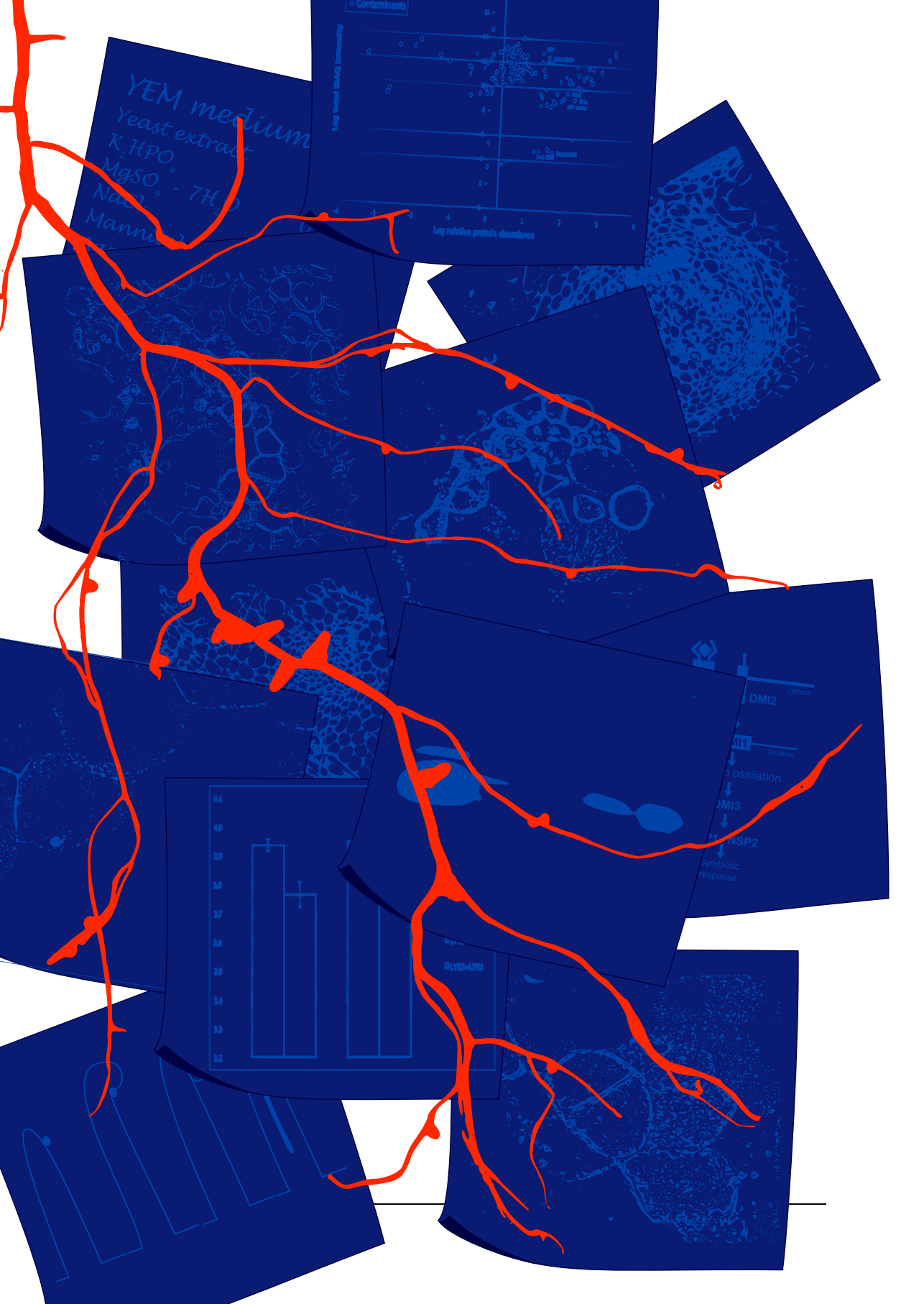
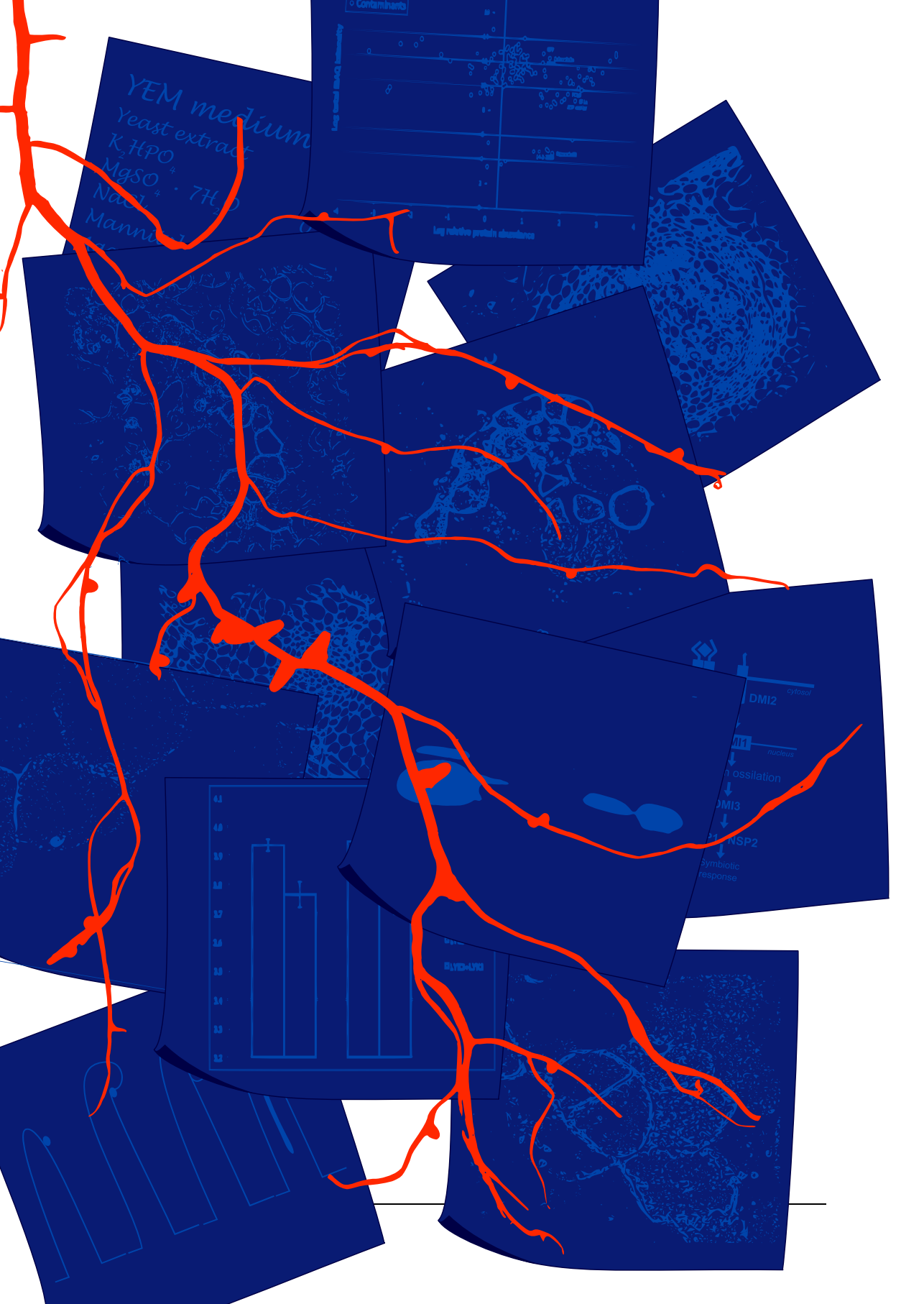
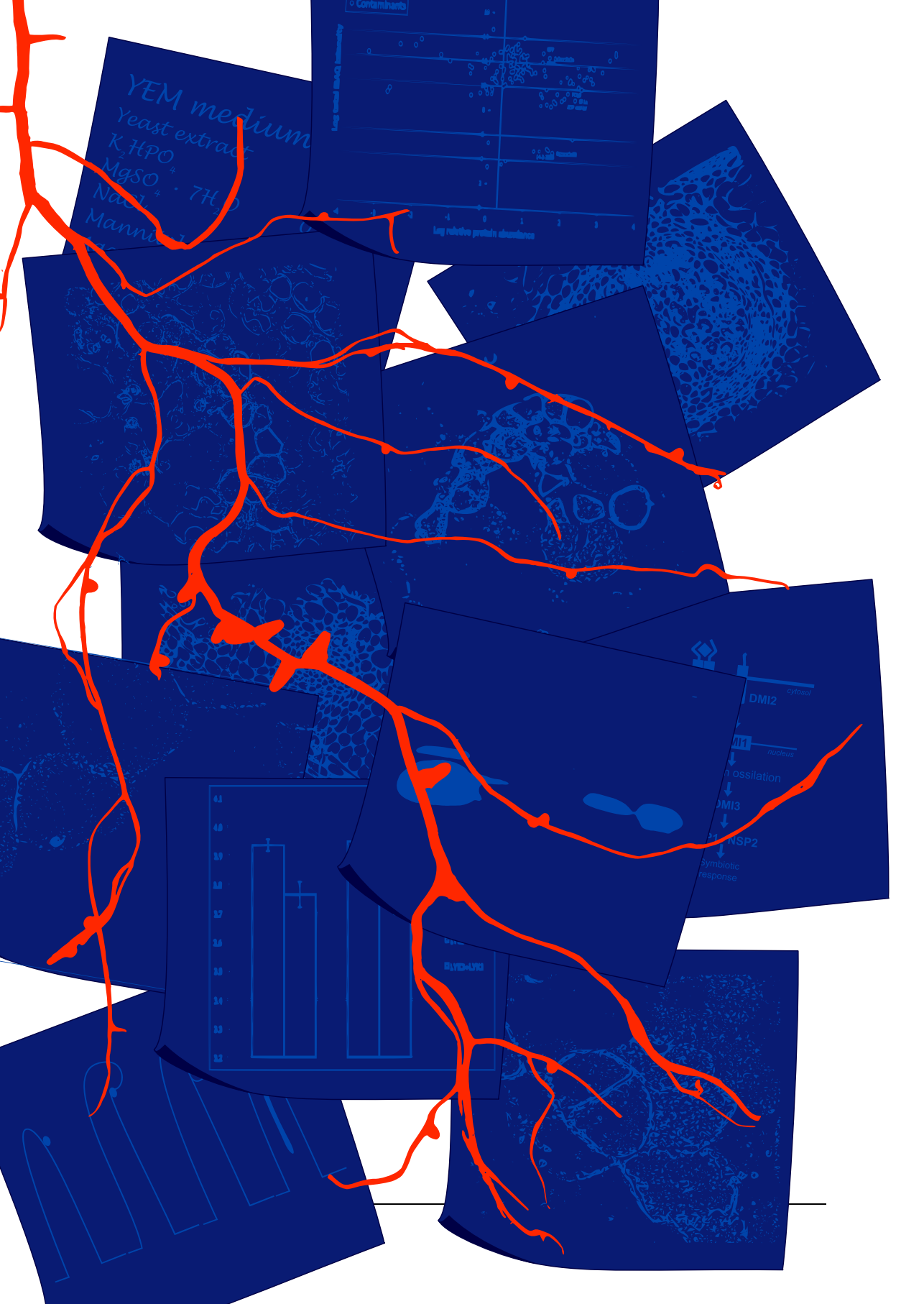
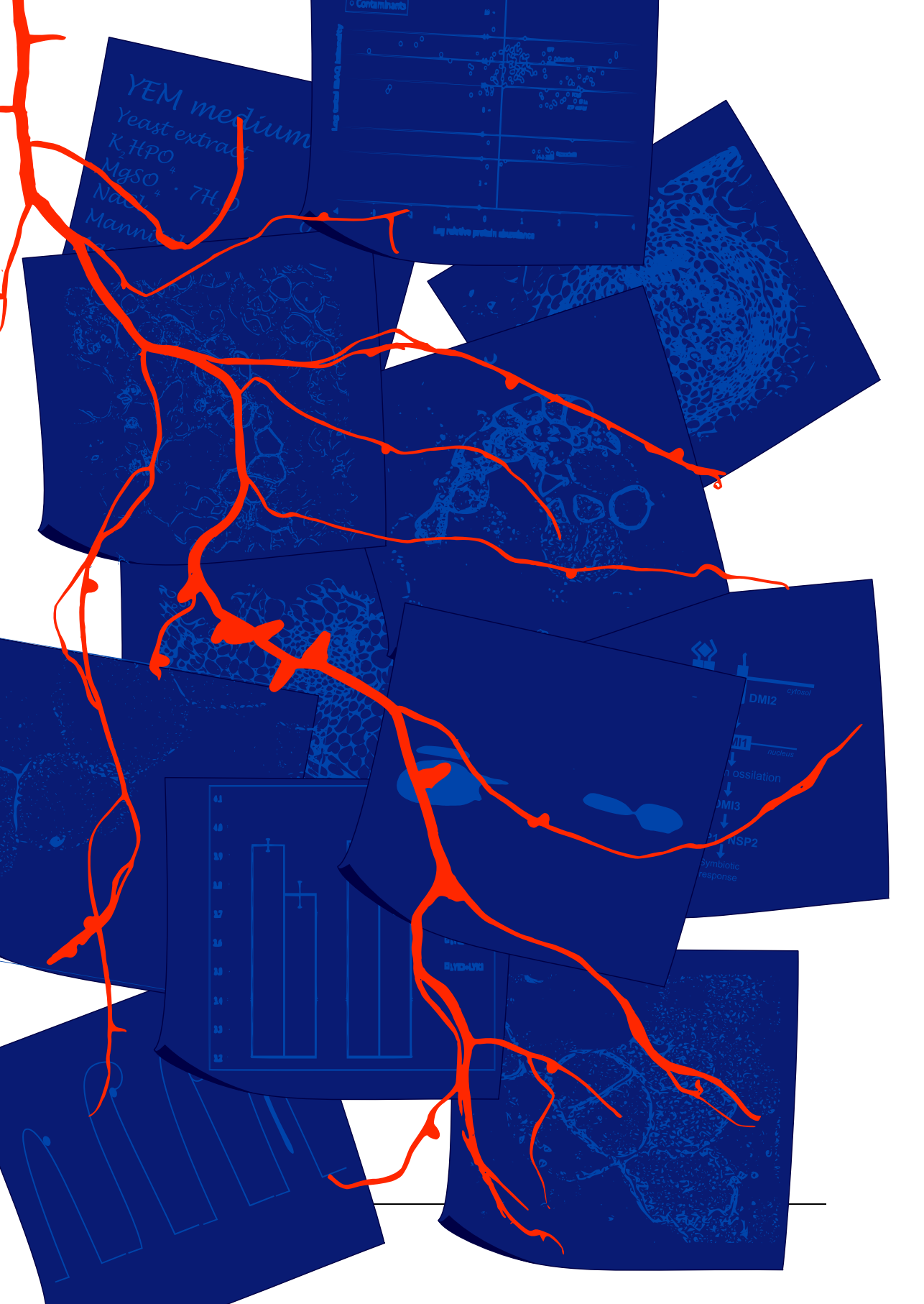
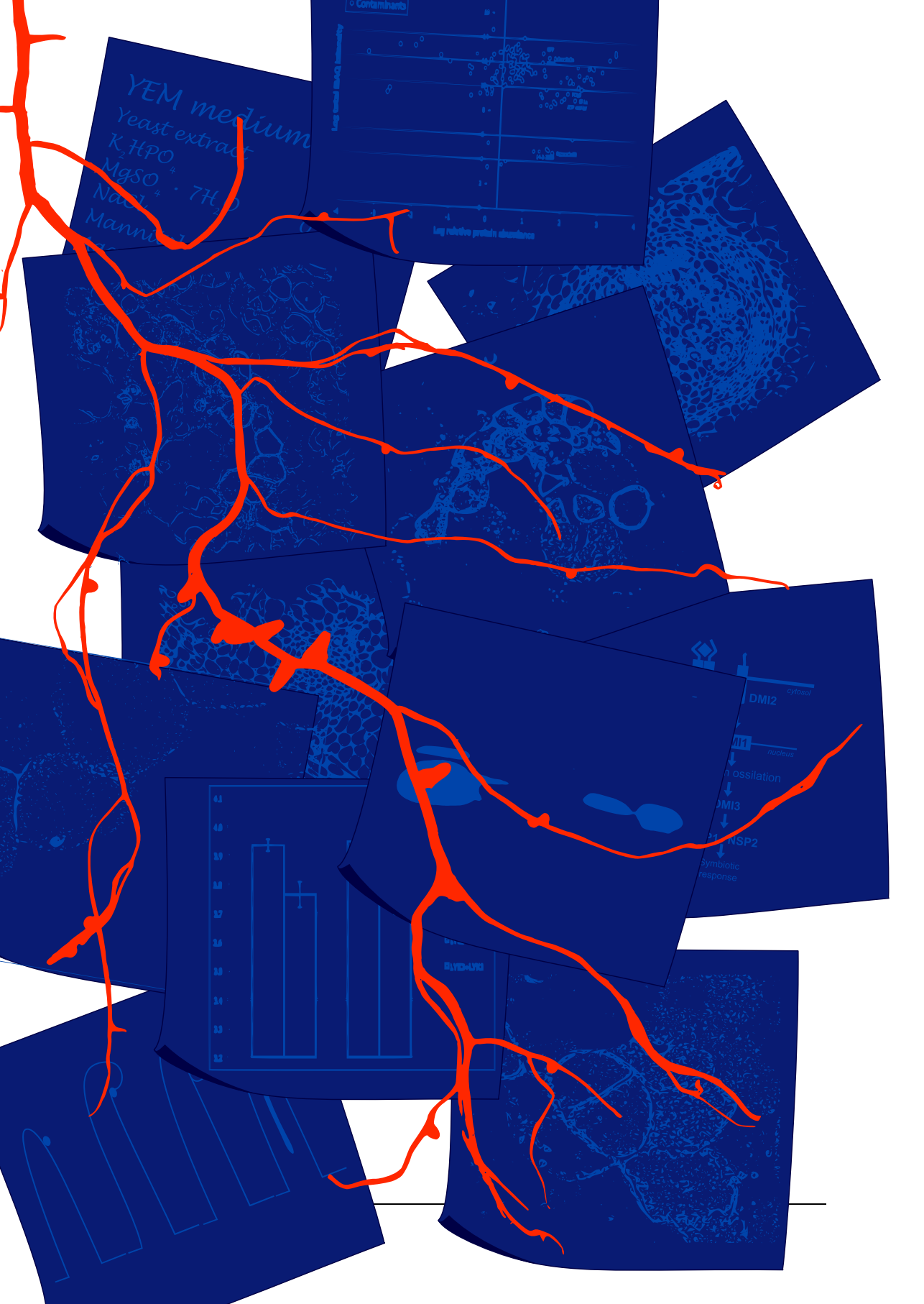
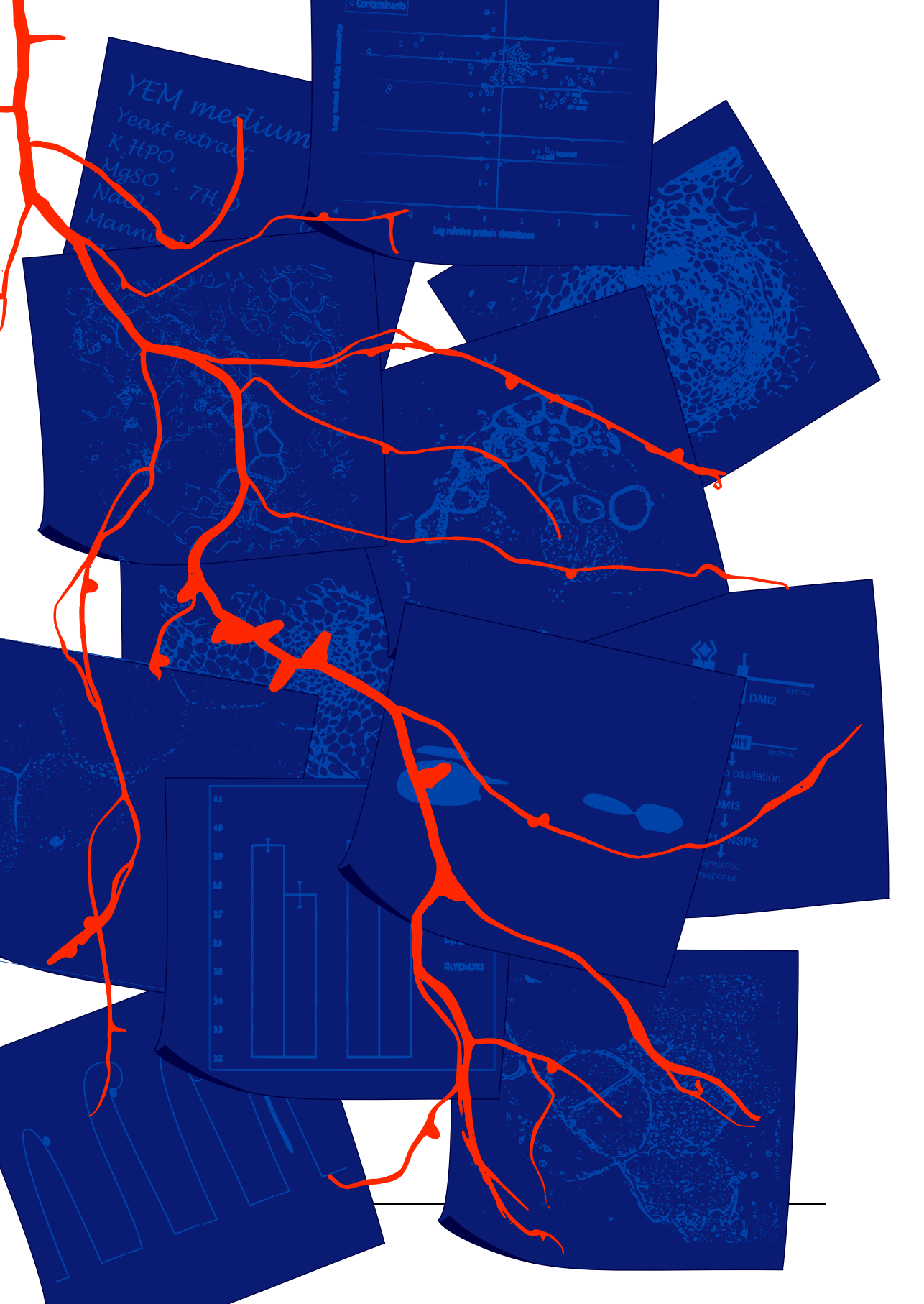
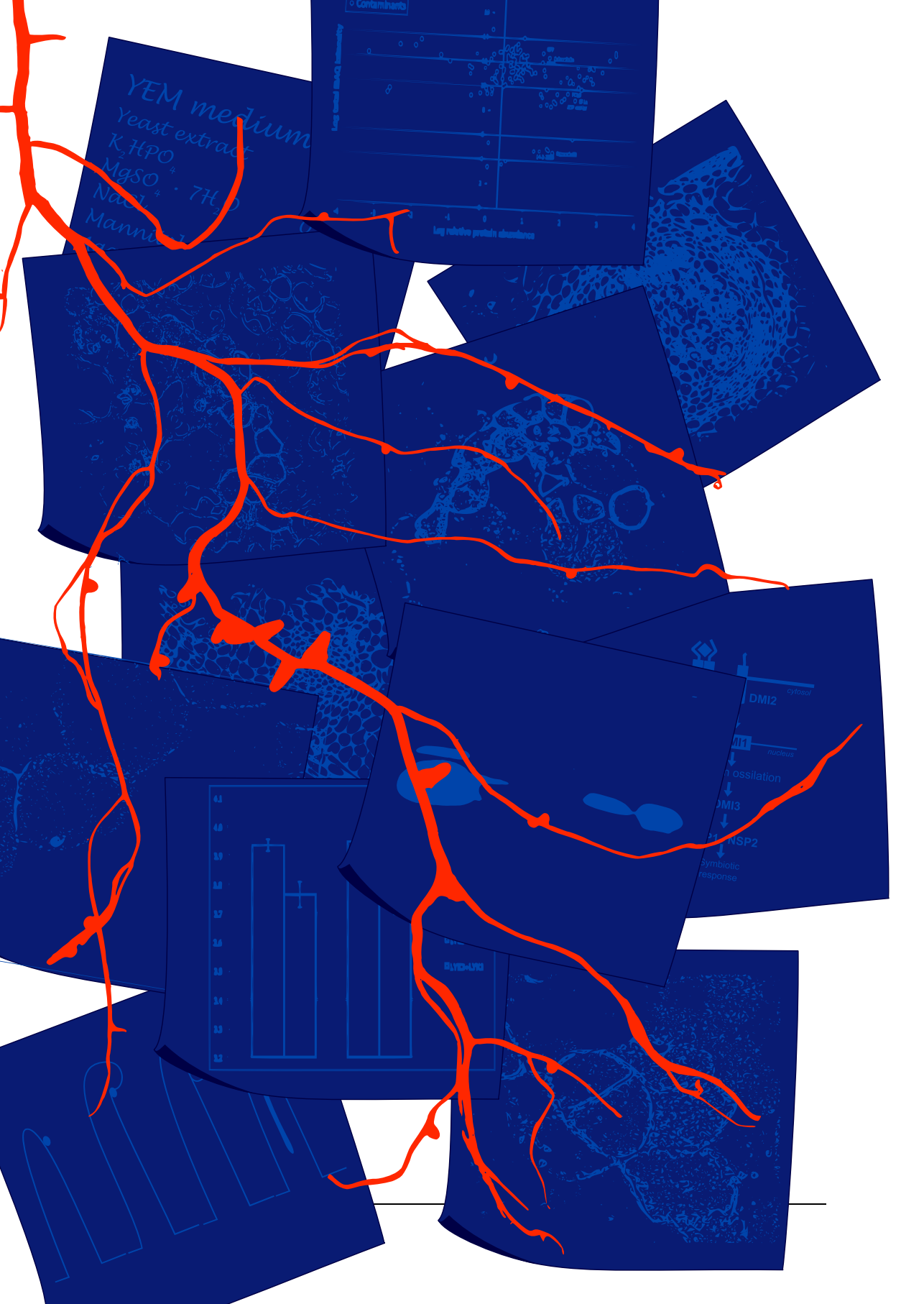
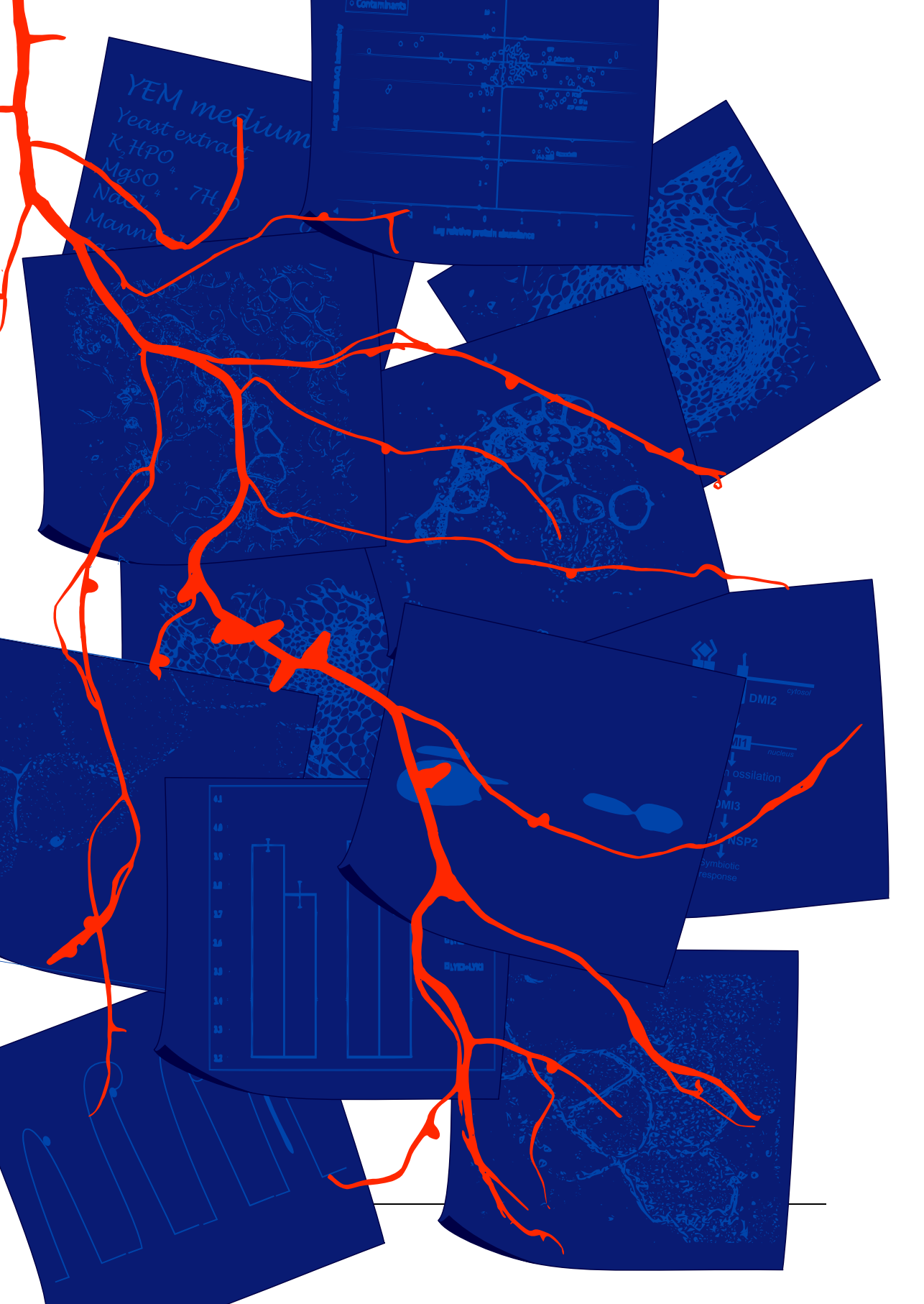
Data was analyzed using n-exponential reconvolution with one or two (for autofluorescence) components in SymPhoTime 64 program. The instrumental response factor (IRF) was calculated from the fitting of the fluorescence decay.

ACKNOWLEDGEMENTS

This work was supported by a Middelgroot investment grant (834.09.003) of the Netherlands Organization for Scientific Research (NWO).

The collage features several scientific elements:

- Root Systems:** A large, prominent image of a plant root system with orange roots and green leaves.
- Microscopic Views:** Multiple electron micrographs showing the cellular structure of plant roots and symbiotic interactions, including root cross-sections and high-magnification views of cell walls and organelles.
- YEM medium:** A handwritten note listing the components of Yeast Extract-Mannitol medium: Yeast extract, K_2HPO_4 , $MgSO_4 \cdot 7H_2O$, NaCl, and Mannitol.
- Scatter Plot:** A scatter plot titled "Log relative protein abundance" showing the relationship between "Log relative protein abundance" (y-axis) and "Log relative protein abundance" (x-axis). It includes a legend for "Contaminants" and "Proteins" and a regression line.
- Bar Graph:** A bar graph showing the relative abundance of proteins in different samples, with the y-axis labeled "Log relative protein abundance" and the x-axis labeled "Log relative protein abundance".
- Diagram:** A schematic diagram of a plant root system showing the interaction between the plant and a microbe. It labels the "cytosol", "DM12", "AT", "DM13", "DM14", and "DM15" regions, and indicates a "symbiotic response".
- Cell Diagram:** A diagram of a cell showing the nucleus, cytoplasm, and various organelles, with labels for "Nucleus", "Cytoplasm", and "Mitochondrion".



Chapter 5.

INTERACTORS OF THE NOD FACTOR RECEPTOR LYK₃

Sjef Moling¹, Kerstin Kaufman^{1,2}, Sjef Boeren³, Erik Limpens¹ and Ton Bisseling^{1,4}

¹Laboratory of Molecular Biology; Wageningen University; Wageningen, The Netherlands

²Institute of Biochemistry and Biology, University of Potsdam, Potsdam, Germany

³Department of Plant Sciences; Laboratory of Biochemistry; Wageningen University; Wageningen, The Netherlands

⁴College of Science; King Saud University; Riyadh, Saudi Arabia

ABSTRACT

The *Medicago truncatula* LysM-domain containing Nod factor receptor kinase LYK3 plays a key role in the rhizobial infection process. We have recently been able to localize GFP-tagged LYK3 exclusively in a highly spatially regulated manner at the nodule apex. Here, we exploit this tagged Nod factor receptor to identify novel interactors of LYK3 by means of co-immunoprecipitation. Therefore, LYK3-GFP was immunoprecipitated from extracts of nodulated roots expressing GFP-tagged LYK3. Subsequent LC-MS/MS analyses identified several putative novel interactors of LYK3. Strikingly, none of the previously described interactors were identified. By studying the co-localization of LYK3 with two of the previously presumed interactors at the plasma membrane, SYMREM1 and FLOT4, we show that these interactions may only occur. For SYMREM1 this interaction may occur only in a very concise time and/or spatial window in the nodule and therefore likely precluded detection in our setup. Several of the novel putative interactors may link Nod factor signaling to vesicle trafficking and organization of the cytoskeleton to control infection.

INTRODUCTION

Legume plants have the unique ability to form a symbiosis with soil bacteria collectively named rhizobia, resulting in the formation of so-called root nodules. The molecular mechanisms underlying this interaction have been studied in the past decades, especially by genetic approaches. This has revealed a signaling cascade that is essential for nodule organogenesis and infection [Catoira *et al.*, 2000; Geurts and Bisseling, 2002; Hocher *et al.*, 2011]. This pathway is activated by two receptor like kinases that are involved in recognition of Nod factors, the lipochito-oligosaccharide signal molecules of rhizobium that induce the nodulation process [Arrighi *et al.*, 2006; Limpens *et al.*, 2003; Radutoiu *et al.*, 2003; Smit *et al.*, 2007]. Receptors often occur in multiprotein complexes containing components to regulate and execute receptor activity and they may even be part of multiple receptor complexes influencing different signaling pathways [Greeff *et al.*, 2012]. Our approach aimed to identify novel interactors of a presumed LYK3 Nod factor receptor complex. Furthermore, we analysed the co-localization of previously identified interactors to determine their spatio-temporal relation with LYK3 in the nodule.

The rhizobium-legume interaction is established in a nitrogen poor environment where the plant secretes among others flavonoids that can induce the rhizobial genes required for Nod factor production and secretion [Hassan and Mathesius, 2012; Schlaman *et al.*, 1998; Sharma and Signer, 1990]. Nod factors are perceived by two receptors called NFP [Arrighi *et al.*, 2006] and LYK3 [Limpens *et al.*, 2003] at the plasma membrane in *Medicago truncatula* (Medicago). An additional LRR-domain containing receptor called SYMRK/DMI2 present at the plasma membrane [Limpens *et al.*, 2005] is required to

generate a secondary signal that is transduced to the nucleus. There it triggers the oscillation of calcium concentration in the nucleus, which in turn activates a calcium and calmodulin dependant kinase called CCaMK/DMI3 [Levy *et al.*, 2004; Mitra *et al.*, 2004]. This leads to transcriptional changes which initiate root nodule formation [Limpens and Bisseling, 2003]. This signal transduction pathway is also functional in the nodule to control rhizobial infection and nodule development [Peiter *et al.*, 2007]. In the nodule the signaling cascade plays an important role in the release of the bacteria from cell-wall bound infection threads that invade nodule cells, leading to the formation of N₂-fixing organelles called symbiosomes [Limpens *et al.*, 2005; Ovchinnikova *et al.*, 2012].

It is known that both Nod factor receptors localize at the plasma membrane and that they have the potential to interact in a heterologous system, although an interaction during the rhizobium interaction has so-far not been reported [Madsen *et al.*, 2011; Pietraszewska-Bogiel *et al.*, 2013]. Such an interaction has also been proposed based on genetic studies [Arrighi *et al.*, 2006; Madsen *et al.*, 2003]. Furthermore, as NFP has an inactive kinase domain lacking the activation loop it is postulated that it requires a co-receptor kinase to transduce a signal [Arrighi *et al.*, 2006; Madsen *et al.*, 2011]. However, in *Medicago* these genetic studies also showed that LYK3 and NFP have distinct functions. In *Medicago* they act either as the entry (LYK3), controlling only rhizobial infection, or as signaling receptor (NFP) controlling all stages of the symbiosis [Arrighi *et al.*, 2006; Limpens *et al.*, 2003; Smit *et al.*, 2007]. Furthermore, also in *Lotus japonicus* only one receptor (NFR1, the ortholog of NFP) is sufficient to induce extracellular alkalinization and both are essential for all other responses [Radutoiu *et al.*, 2003]. These data suggest that LYK3 and NFP might interact, but also have unique functions during nodulation.

More recently several interactors of the Nod factor receptors have been identified mostly based on yeast-two-hybrid screens. These interactors include SYMREM1 [Lefebvre *et al.*, 2010; Toth *et al.*, 2012] and the E3 ubiquitin-ligase PUB1 [Mbengue *et al.*, 2010]. In addition, mainly based on co-localization data, FLOT4 has been postulated as interacting protein [Haney *et al.*, 2011]. Two of these proteins, SYMREM1 and FLOT4, are thought to localize exclusively to detergent-insoluble plasma membrane domains, commonly called lipid rafts. SYMREM1 is a remorin protein that is specifically formed during nodulation. It localizes to infection threads, infection droplets as well as symbiosomes [Lefebvre *et al.*, 2010; Toth *et al.*, 2012]. Remorins do not harbour a transmembrane domain but anchor themselves to the plasma membrane using a C-terminal anchor [Perraki *et al.*, 2012; Toth *et al.*, 2012]. The exact function of remorin proteins is unknown, but they seem to have a function in host invasion and/or act as scaffold proteins that (pre)assemble signaling complexes at the plasma membrane [Jarsch and Ott, 2011]. Knock-down of SYMREM1 as well as a Tnt1 insertion mutant have been reported to form small nodules where release of the bacteria from the infection threads is severely hampered [Lefebvre *et al.*, 2010]. FLOT4 represents a flotillin (or Reggie protein) that is up-regulated upon nodulation. Flotillins, like remorins, exclusively localize to lipid rafts. They are thought to function in clathrin-

independent endocytosis, targeted delivery of cargo and membrane shaping [Hansen and Nichols, 2009; Otto and Nichols, 2011; Stuermer, 2011]. Knock-down of FLOT4 was shown to result in a reduction of nodule number suggesting a function in early stages of infection [Haney and Long, 2010]. Co-localization studies showed that in the absence of Nod factors or bacteria FLOT4 and LYK3 hardly co-localize, but upon stimulation they co-localize in stable membrane domains in root hairs [Haney *et al.*, 2011].

We recently localized the GFP-tagged Nod factor receptors NFP and LYK3 inside nodules of *Medicago* and showed that the receptors accumulate in a narrow zone of ~2 cell layers in the nodule apex, which represents the transition from the meristem to the infection zone. Furthermore, LYK3 appeared to accumulate there in dot-like structures at the plasma membrane, likely representing membrane domains (Chapter 3). In contrast to Haney *et al.* [2011], we (as well as others [Madsen *et al.*, 2011; Mbengue *et al.*, 2010]; Anna Pietraszewska-Bogiel (personal communication) were unable to detect the Nod factor receptors in the roots/ root hairs by fluorescence microscopy. Instead, our results indicate a strict regulation at a post-translational level by which they accumulate only very transiently (Chapter 3).

The ability to localize the GFP-tagged Nod factor receptors in the nodule now offers the opportunity to screen for potential novel interactors through co-immunoprecipitation and co-localization studies. Recently, Riely *et al.* [2013] purified a tagged SYMRK/DMI2 complex from roots and nodules in a comparable manner. Here, we explored the feasibility of these approaches by immunoprecipitating LYK3-GFP and analysing the co-immunoprecipitated proteins by mass spectroscopy to identify potential novel LYK3 interactors. Furthermore, we studied the co-localization of LYK3 with SYMREM1 and FLOT4 in membrane domains inside the nodule.

RESULTS AND DISCUSSION

Co-immuno precipitation

To identify possible interactors of the Nod factor receptor LYK3 we introduced LYK3-GFP into the *Medicago lyk3* knock-out mutant B56 [Smit *et al.*, 2007] by *Agrobacterium rhizogenes* mediated root transformation. LYK3-GFP was expressed either under control of its native promoter or under the control of the Arabidopsis Ubiquitin3 promoter; resulting in two independent biological replicates used for subsequent protein isolation and immunoprecipitation. Total protein extracts were prepared from roots containing nodules ten days after inoculation with *Sinorhizobium meliloti* 2011. Western blot analysis confirmed the expression of the fusion protein, although we also detected some breakdown products (Figure 5.1). As a control we used total protein extract from nodulated non-transgenic *A. rhizogenes* transformed roots. Next, the extracts were used to

immunoprecipitate LYK3-GFP using anti-GFP tagged magnetic beads. Western blot analyses confirmed the presence of the receptor – GFP fusion after immunoprecipitation as well as “free” GFP and break down products (Figure 5.1). The bound proteins were subsequently digested with trypsin and peptides were identified using liquid chromatography followed by MS/MS. Finally, the obtained peptides were queried against the translated Medicago genome (Mt3.5v5) to identify possible interactors of LYK3.

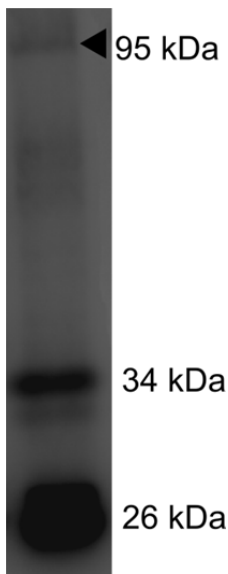


Figure 5.1: western blot analysis of the total protein extract from pLyk3::LYK3-GFP expressing plants after immuno precipitation. HRP-conjugated α -GFP is used to detect the fusion protein (arrow head). Free GFP has an expected size of 26 kDa and LYK3-GFP of 95 kDa.

This resulted in two independent biological replicate data sets representing potential LYK3 interactors; expressing LYK3-GFP from the native promoter (Figure 5.2, Table 5.1) or from the ubiquitin promoter (Figure 5.3, Table 5.2). In both cases we could identify peptides corresponding to LYK3 and GFP within the top most enriched proteins in the sample compared to the control, confirming the precipitation of LYK3-GFP. We noticed that the amount of GFP detected in the samples relative to the control was larger than the amount of LYK3 in the samples. This likely reflects the pull-down of (free) GFP, not conjugated to LYK3, as was observed on the western blot (Figure 5.1). In Chapter 3 we observed that part of the LYK3-GFP fluorescence accumulates in the vacuoles where it is likely degraded. It may be that the (free) GFP moiety is more stable than the LYK3 protein.

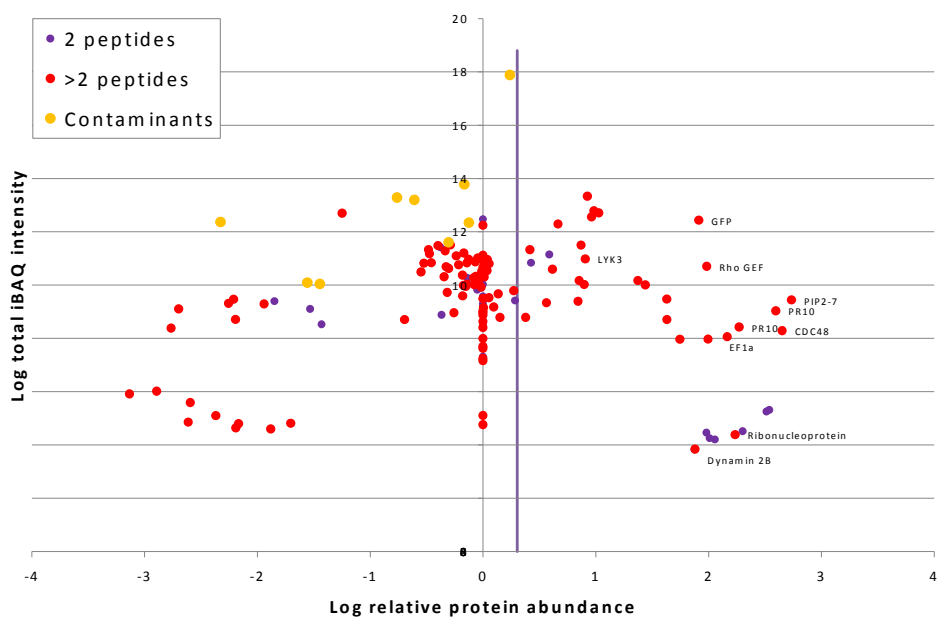


Figure 5.2: possible interactors of LYK3 when expressed from the native promoter plotted as the total intensity as a function of the relative abundance. The vertical (purple) line marks 2-fold enrichment.

Table 5.1: possible interactors of LYK3 when expressed from the native promoter. Proteins showing more then 2-fold enrichment are shown in this table. The Log of the Label free quantification (LFQ) intensity depicts the relative intensity of the protein in either the control or the experimental sample. From the two LFQ intensities the ratio is calculated. The number of peptides used for the identification of the protein are shown. The log of the iBAQ depicts the absolute amount of the protein in either the control or experimental sample.

Protein ID	Protein Description	Log LFQ intensity		Log Ratio	Peptides	Log iBAQ	
		control	pLYK3			control	pLYK3
Medtr4g059390.1	Aquaporin PIP2-7	4.00	6.74	2.74	3	3.89	5.55
Medtr7g101640.1	Cell division cycle protein 48 homolog	4.00	6.65	2.65	5	3.38	4.91
Medtr2g035100.1	Pathogenesis-related protein PR10	4.00	6.60	2.60	4	3.88	5.15
Medtr2g094270.1	Aquaporin PIP2-7	4.00	6.54	2.54	2	0.00	5.31
Medtr3g108280.1	60S acidic ribosomal protein p0	4.00	6.51	2.51	2	0.00	5.25
Medtr5g069050.1	Fructose-bisphosphate aldolase	4.00	6.30	2.30	2	0.00	4.51
Medtr2g035150.1	Pathogenesis-Pathogenesis-related protein PR10	4.00	6.27	2.27	3	3.42	5.00
Medtr4g074800.1	28 kDa ribonucleoprotein, chloroplastic	4.00	6.24	2.24	4	0.00	4.38
Medtr6g021800.1	Elongation factor 1-alpha	4.00	6.17	2.17	3	3.88	4.17
Medtr8g018590.1	Lipoxygenase	4.00	6.06	2.06	2	0.00	4.20
Medtr7g102120.1	S-adenosylmethionine synthetase	4.00	6.01	2.01	2	0.00	4.25
Medtr7g081500.1	Subtilisin-like protease	4.00	6.00	2.00	3	3.76	4.21
Medtr8g087990.1	SH3 domain-containing protein	5.36	7.35	1.98	7	4.98	5.72
Medtr3g099380.1	14-3-3 f-2 protein	4.00	5.98	1.98	2	0.00	4.46
	GFP	6.22	8.13	1.91	11	5.58	6.85
Medtr4g030140.1	Dynamin-2B	4.00	5.88	1.88	5	0.00	3.84
Medtr1g108770.1	ATP synthase subunit beta	4.00	5.87	1.87	2	0.00	3.82
Medtr8g036880.1	ADP,ATP carrier protein 2, mitochondrial	4.00	5.75	1.75	4	3.86	4.10
Medtr7g053120.1	40S ribosomal protein S6	4.00	5.63	1.63	3	4.27	4.43
Medtr6g021670.1	40S ribosomal protein S7-like protein	4.00	5.63	1.63	5	4.81	4.66
Medtr4g015460.1	Beta-glucosidase G1	5.79	7.23	1.44	6	4.41	5.60
Medtr1g011850.1	Histone H2A	5.74	7.11	1.37	4	4.56	5.61

Protein ID	Protein Description	Log LFQ intensity		Log Ratio	Peptides	Log iBAQ	
		control	pLYK3			control	pLYK3
Medtr4g063410.1	Histone H2A	6.98	8.00	1.03	3	6.03	6.68
Medtr4g070240.1	Histone H2B	7.24	8.23	0.98	4	6.09	6.69
Medtr7g114040.1	Histone H2A	6.66	7.62	0.96	4	6.09	6.47
Medtr4g128150.1	Histone H4	7.49	8.42	0.93	8	6.37	6.96
Medtr5g086130.1	LYK3	6.45	7.36	0.91	12	5.17	5.81
AC233572_25.1	Beta-glucan-binding protein 1	6.34	7.24	0.90	8	4.55	5.47
Medtr2g104440.1	Small nuclear ribonucleoprotein E	6.06	6.93	0.87	3	5.36	6.13
Medtr8g088060.1	Ubiquitin	5.94	6.79	0.85	5	4.87	5.30
Medtr5g092010.1	Small nuclear ribonucleoprotein-associated protein B	5.61	6.46	0.84	3	4.49	4.90
Medtr4g097170.1	Histone H3	7.15	7.81	0.67	3	5.81	6.48
Medtr1g018840.1	Cysteine proteinase 3	6.44	7.05	0.62	6	4.96	5.64
Medtr8g092200.1	Small nuclear ribonucleoprotein Sm D3	6.39	6.98	0.59	2	5.44	5.71
Medtr4g103920.1	Glyceraldehyde-3-phosphate dehydrogenase	6.07	6.63	0.56	5	4.22	5.12
Medtr8g105890.1	Small nuclear ribonucleoprotein-like protein	6.22	6.64	0.43	2	5.19	5.64
Medtr1g072370.1	Small nuclear ribonucleoprotein Sm D	6.28	6.69	0.42	3	5.39	5.94
Medtr7g099680.1	Heat shock protein 70	6.03	6.41	0.38	5	4.17	4.61

To aid selecting of potential LYK3 interactors we first considered proteins that show enrichment in both biological replicates. These are summarized in Table 5.3. Among the top enriched proteins we find among others an Elongation Factor 1 α (EF1 α), a Pathogeneses Related protein 10 (PR10), an ADP/ATP carrier protein, a subtilisin like protein, a Dynamin-2B, a Fructose-bisphosphate aldolase, an aquaporin and a 14-3-3 f-2 protein. Because LYK3 has an active kinase domain it is expected to phosphorylate proteins upon Nod factor perception [Limpens *et al.*, 2003; Madsen *et al.*, 2003; Radutoiu *et al.*, 2003] we analysed whether any of the putative interactors shows signs of Nod factor dependent phosphorylation. Therefore, we mined their phosphorylation status using the recently developed Medicago phosphoproteomics database (Rose *et al.*, 2012). This analysis revealed that EF1 α , Dynamin-2B, PR10, fructose-bisphosphate aldolase and 14-3-3 f2 all show (enriched) phosphorylated residues upon Nod factors treatment. Additionally, the Bin/Amphiphysin/Rvs (BAR) and SH3 domain-containing protein (Medtr8g087990.1), which is enriched in the pLYK3: LYK3-GFP immunoprecipitate, is also phosphorylated upon Nod factor treatment.

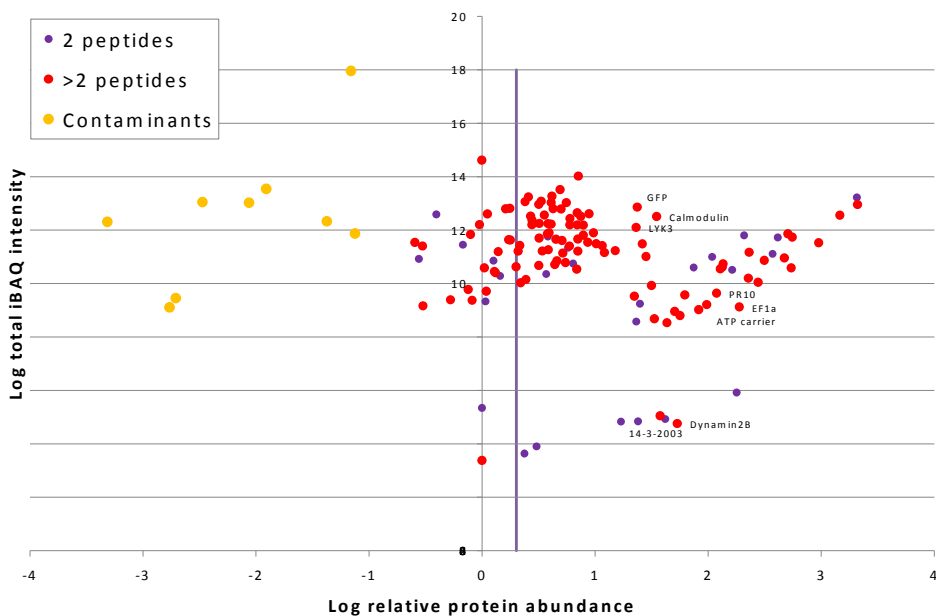


Figure 5.3: possible interactors of LYK3 when expressed from the Ubiquitin promoter plotted as the total intensity as a function of the relative abundance. The vertical (purple) line marks 2-fold enrichment.

Table 5.2: possible interactors of LYK3 when expressed from the Ubiquitin promoter. Proteins showing more than 2-fold enrichment are shown in this table. The Log of the Label free quantification (LFQ) intensity depicts the relative intensity of the protein in either the control or the experimental sample. From the two LFQ intensities the ratio is calculated. The number of peptides used for the identification of the protein are shown. The log of the iBAQ depicts the absolute amount of the protein in either the control or experimental sample.

Protein ID	Protein Description	Log LFQ intensity			Peptides	Log iBAQ	
		control	pLYK3	Log Ratio		control	pLYK3
Medtr2g096570.1	Histone H2A	4.00	7.32	3.32	3	5.73	7.22
Medtr2g082310.1	Histone H3	4.00	7.32	3.32	2	5.94	7.28
Medtr1g081410.1	40S ribosomal protein S24	4.00	7.17	3.17	4	5.42	7.13
Medtr6g021670.1	40S ribosomal protein S7-like protein	4.00	6.98	2.98	5	4.81	6.71
Medtr4g071150.1	Histone H2A	4.00	6.75	2.75	3	5.09	6.65
Medtr5g026750.1	60S ribosomal protein L13	4.00	6.74	2.74	6	4.28	6.31
Medtr2g082510.1	Histone H2A	4.00	6.70	2.70	3	5.25	6.61
Medtr8g091910.1	60S ribosomal protein L6	4.00	6.67	2.67	7	4.74	6.22
Medtr1g075720.1	60S ribosomal protein L14-1	4.00	6.62	2.62	2	5.26	6.46
Medtr2g100410.1	60S ribosomal protein L28-1	4.00	6.57	2.57	2	4.79	6.32
Medtr2g014030.1	40S ribosomal protein S6	4.00	6.50	2.50	3	4.77	6.10
Medtr7g061170.1	40S ribosomal protein S23	4.00	6.44	2.44	3	4.03	6.01
Medtr7g112880.1	60S ribosomal protein L18-3	4.00	6.36	2.36	3	5.10	6.07
Medtr7g053120.1	40S ribosomal protein S6	4.00	6.36	2.36	3	4.27	5.93
Medtr2g086610.1	40S ribosomal protein S25-2	4.00	6.32	2.32	2	5.52	6.29
Medtr6g021800.1	Elongation factor 1-alpha	4.00	6.28	2.28	3	3.88	5.24
Medtr3g108280.1	60S acidic ribosomal protein p0	4.00	6.25	2.25	2	0.00	5.92
Medtr4g059400.1	60S ribosomal protein L12	4.00	6.21	2.21	2	4.55	5.96
Medtr5g033090.1	60S ribosomal protein L27a-3	4.00	6.13	2.13	4	4.76	5.98
Medtr1g088450.1	60S ribosomal protein L22-like	4.00	6.13	2.13	5	4.59	6.03
Medtr2g086500.1	Ribosomal protein L1	4.00	6.11	2.11	10	4.84	5.71
Medtr2g035100.1	Pathogenesis-related protein PR10	4.00	6.08	2.08	4	3.88	5.76
Medtr7g080090.1	60S ribosomal protein L35	4.00	6.04	2.04	2	5.06	5.94
Medtr8g036880.1	ADP,ATP carrier protein 2, mitochondrial	4.00	5.99	1.99	4	3.86	5.34
Medtr7g069950.1	40S ribosomal protein S4	4.00	5.92	1.92	5	3.70	5.32
Medtr5g040570.1	60S ribosomal protein L34	4.00	5.87	1.87	2	4.76	5.84

Protein ID	Protein Description	Log LFQ intensity		Log Ratio	Peptides	Log iBAQ	
		control	pLYK3			control	pLYK3
Medtr7g099960.1	Histone H2B	4.00	5.79	1.79	4	3.99	5.59
Medtr7g081500.1	Subtilisin-like protease	4.00	5.75	1.75	3	3.76	5.04
Medtr4g030140.1	Dynamin-2B	4.00	5.73	1.73	5	0.00	4.76
Medtr2g035150.1	Pathogenesis-related protein PR10	4.00	5.70	1.70	3	3.42	5.53
AC233658_8.1	U3 small nucleolar RNA-associated protein 15 homolog	4.00	5.64	1.64	3	3.65	4.88
Medtr7g102120.1	S-adenosylmethionine synthetase	4.00	5.62	1.62	2	0.00	4.93
Medtr4g074800.1	28 kDa ribonucleoprotein, chloroplastic	4.00	5.58	1.58	4	0.00	5.05
Medtr5g088320.1	Calmodulin	5.88	7.43	1.54	9	5.33	7.18
Medtr5g010260.1	SAR DNA-binding protein-1	4.00	5.52	1.52	7	3.95	4.73
Medtr2g012110.1	60S ribosomal protein L26-1	4.00	5.50	1.50	6	4.52	5.40
AC235668_13.1;I	40S ribosomal protein S3	5.53	6.98	1.45	10	4.62	6.39
Medtr3g093110.1	Ribosomal protein L9	5.66	7.08	1.42	9	4.82	6.66
Medtr7g113160.1	Histone H2A	4.00	5.40	1.40	2	4.00	5.24
Medtr5g069050.1	Fructose-bisphosphate aldolase	4.00	5.38	1.38	2	0.00	4.84
	GFP	6.22	7.59	1.37	11	5.58	7.28
AC235488_13.1	40S ribosomal protein S5	4.00	5.36	1.36	2	3.61	4.97
Medtr5g086130.1	LYK3	6.45	7.81	1.36	12	5.17	6.93
Medtr4g059390.1	Aquaporin PIP2-7	4.00	5.35	1.35	3	3.89	5.64
Medtr3g099380.1	14-3-3 f-2 protein	4.00	5.23	1.23	2	0.00	4.83
Medtr8g012330.1	Ribosomal protein S8	6.13	7.31	1.18	7	4.82	6.41
Medtr8g101980.1	60S ribosomal protein L31	5.57	6.65	1.08	4	4.89	6.27
Medtr8g105110.1	40S ribosomal protein S15-like protein	5.70	6.77	1.06	3	4.81	6.61
Medtr5g006440.1	40S ribosomal protein S3a-like protein	6.03	7.04	1.01	10	4.94	6.56
Medtr4g116410.1	40S ribosomal protein S11	5.97	6.96	0.99	5	5.28	6.62
Medtr3g005430.1	40S ribosomal protein S9	6.45	7.40	0.95	10	5.65	6.95
Medtr5g018940.1	40S ribosomal protein S4	6.13	7.07	0.93	7	5.09	6.45
Medtr2g019670.1	40S ribosomal protein S14	6.12	7.01	0.90	3	5.22	6.59
Medtr4g024270.1	40S ribosomal protein S13	6.22	7.11	0.90	8	5.43	6.76
Medtr1g098170.1	40S ribosomal protein S18	6.35	7.23	0.87	7	5.65	6.86
Medtr4g128150.1	Histone H4	7.49	8.34	0.85	8	6.37	7.65

Protein ID	Protein Description	Log LFQ intensity		Log Ratio	Peptides	Log iBAQ	
		control	pLYK3			control	pLYK3
AC235488_9.1	60S ribosomal protein L21	5.90	6.75	0.85	5	5.26	6.41
Medtr8g088060.1	Ubiquitin	5.94	6.79	0.85	5	4.87	6.34
Medtr3g007700.1	60S ribosomal protein L11	6.46	7.31	0.84	6	5.72	6.92
Medtr7g112770.1	60S ribosomal protein L22-like	6.15	6.99	0.84	6	5.40	6.79
Medtr5g091130.1	60S ribosomal protein L18a	6.00	6.84	0.84	5	4.63	5.91
Medtr2g101900.1	Ribosomal protein L37	5.38	6.19	0.81	2	4.81	5.94
Medtr3g077050.1	60S ribosomal protein L27a-3	6.30	7.07	0.78	4	5.58	6.84
AC140545_25.1;1	60S ribosomal protein L10	6.42	7.20	0.78	6	5.48	6.71
Medtr7g076940.1	60S ribosomal protein L2	6.14	6.91	0.77	7	5.04	6.36
Medtr4g103340.1	60S ribosomal protein L37a	5.64	6.40	0.76	2	5.04	6.30
Medtr4g097170.1	Histone H3	7.15	7.89	0.74	3	5.81	7.22
Medtr1g011850.1	Histone H2A	5.74	6.47	0.74	4	4.56	6.22
Medtr7g099170.1	Ribosome biogenesis protein wdr12	6.11	6.82	0.71	9	5.04	6.10
Medtr5g097200.1	40S ribosomal protein S26	6.08	6.79	0.71	4	5.22	6.39
Medtr1g100960.1	60S ribosomal protein L36	6.52	7.22	0.70	4	5.83	6.95
Medtr4g070240.1	Histone H2B	7.24	7.93	0.69	4	6.09	7.42
Medtr8g105340.1	40S ribosomal protein S2	6.04	6.70	0.66	4	4.67	6.18
Medtr1g023590.1	60S ribosomal protein L13a	6.17	6.83	0.65	4	5.35	6.31
Medtr2g006020.1	Ribosome biogenesis protein bop1	6.19	6.83	0.64	13	4.64	6.07
Medtr7g111590.1	60S ribosomal protein L13	6.85	7.48	0.63	8	5.75	7.06
Medtr4g063410.1	Histone H2A	6.98	7.60	0.62	3	6.03	7.24
Medtr7g069430.1	Ribosome biogenesis protein BRX1 homolog	6.70	7.31	0.61	13	5.59	6.63
Medtr2g038250.1	60S ribosomal protein L7-4	7.04	7.65	0.61	11	6.00	7.04
Medtr1g087910.1	Ribosomal protein L19	6.22	6.82	0.59	4	5.33	6.56
Medtr1g018840.1	Cysteine proteinase 3	6.44	7.02	0.59	6	4.96	6.31
Medtr5g025120.1	60S ribosomal protein L4-1	6.85	7.43	0.58	10	5.57	6.67
Medtr4g120770.1	60S ribosomal protein L14-1	6.06	6.64	0.58	2	5.38	6.38
Medtr8g038170.1	Annexin D4	6.52	7.10	0.58	11	5.34	6.51
Medtr5g075240.1	40S ribosomal protein S16	5.43	6.00	0.57	2	4.60	5.75
Medtr1g098540.1	L3 Ribosomal protein	7.04	7.59	0.55	17	5.71	6.85

Protein ID	Protein Description	Log LFQ intensity		Log Ratio	Peptides	Log iBAQ	
		control	pLYK3			control	pLYK3
Medtr5g028350.1	Unknown Protein	6.21	6.74	0.53	5	5.04	6.17
Medtr2g014220.1	Ribosomal protein L15	7.04	7.56	0.52	7	5.99	7.10
Medtr3g094860.1	60S ribosomal protein L6	6.72	7.23	0.51	7	5.60	6.65
Medtr3g085490.1	60S ribosomal protein L17	6.19	6.69	0.50	5	5.34	6.35
Medtr5g015570.1	60S ribosomal protein L26-1	6.63	7.14	0.50	8	6.05	6.91
Medtr5g081710.1	Maturase	6.19	6.70	0.50	3	4.70	5.97
Medtr8g018590.1	Lipoxygenase	4.00	4.48	0.48	2	0.00	3.90
Medtr4g112780.1	H/ACA ribonucleoprotein complex subunit 2	6.50	6.94	0.44	8	5.69	6.67
Medtr2g035930.1	60S ribosomal protein L27	6.51	6.95	0.44	3	5.56	6.64
Medtr4g063060.1	60S ribosomal protein L23a	6.61	7.04	0.43	6	5.76	6.76
Medtr7g114040.1	Histone H2A	6.66	7.07	0.41	4	6.09	7.15
Medtr4g015460.1	Beta-glucosidase G1	5.79	6.18	0.39	6	4.41	5.75
Medtr1g083460.1	Ribosomal protein L18	6.91	7.29	0.38	4	6.02	7.04
Medtr1g108770.1	ATP synthase subunit beta	4.00	4.37	0.37	2	0.00	3.63
Medtr4g103920.1	Glyceraldehyde-3-phosphate dehydrogenase	6.07	6.41	0.34	5	4.22	5.81
Medtr7g098290.1	60S ribosomal protein L23	6.25	6.59	0.33	3	5.30	6.13
Medtr2g103560.1	Protein MAK16 homolog A	6.37	6.69	0.32	4	5.09	6.12
AC233657_25.1	Ribosome production factor 1	6.17	6.47	0.30	5	4.79	5.83

Several of these components suggest an intriguing, still hypothetical, link between Nod factor perception by LYK3 and reorganization of the cytoskeleton and vesicle trafficking, which play important roles during rhizobial infection. The Elongation Factor 1 alpha (EF1 α), in addition to its role in translation, has been found associated to actin filaments and microtubules and controls the (re)organization of the cytoskeleton [Condeelis, 1995; Durso and Cyr, 1994; Moore *et al.*, 1998; Sasikumar *et al.*, 2012]. It is known that both the actin and microtubule cytoskeleton play important roles during rhizobial infection [Hossain *et al.*, 2012; Miyahara *et al.*, 2010; Timmers *et al.*, 1998; Timmers *et al.*, 1999; Yokota *et al.*, 2009]. Furthermore, in the *lyk3* mutant it was shown that the asymmetric organisation of the microtubule cytoskeleton in root hairs and the re-orientation of the microtubule cytoskeleton to form pre-infection threads, were strongly altered [Catoira *et al.*, 2001]. Therefore it was suggested that LYK3 plays a role in providing positional information for the reorganisation of the microtubular cytoskeleton to control rhizobial infection.

Furthermore, it was recently found that a specific exocytosis pathway is essential for the uptake of the rhizobia by nodule cells [Ivanov *et al.*, 2012]. Both the Dynamin-2B and the BAR-SH3 domain-containing protein would link Nod factor perception to membrane fusion and vesicle trafficking events. Dynamins are ubiquitously expressed GTPases that can act as motor proteins. Furthermore they are involved in the scission of vesicles from the plasma membrane (endocytosis) and the golgi network, as well as their trafficking and fusion to other membranes. They also regulate microtubule and actin cytoskeleton dynamics [Gonzalez-Jamett *et al.*, 2013; Morlot and Roux, 2013]. The BAR-SH3 domain containing protein shows similarity to the Arabidopsis SH3 domain-containing (SH3P) proteins (SH3P1-3), which all contain an N-terminal BAR domain and a C-terminal SH3 domain [Lam *et al.*, 2001]. SH3P1 is involved in the trafficking of clathrin-coated vesicles. It is localized at the plasma membrane and is associated with vesicles of the trans-Golgi network. Yeast complementation studies reveal that SH3P1 has similar functions to the *Saccharomyces cerevisiae* Rvs167p, which is involved in endocytosis and actin cytoskeletal arrangement. The putative interaction and phosphorylation of these proteins by LYK3 may thus control the fusion of vesicles to allow the uptake of the bacteria. Alternatively, these proteins may control the endocytic turn-over of LYK3 at the plasma membrane.

Table 5.3: proteins enriched when expressed from both of the promoters in comparison to the changes in phosphorylation upon NF application according to Rose et al. [2012]. In blue the proteins of which the phosphorylation status is significantly ($p < 0.05$) changed.

Protein ID	Protein description	Log enrichment ratio		Change in phosphorylation status
		Native promoter	Ubiquitin promoter	
Medtr6g021800.1	Elongation factor 1-alpha	2.60	2.28	1.33 (2.73E-3)
Medtr2g035100.1	Pathogenesis-related protein PR10	2.00	2.08	1.24 (1.53E-1)
Medtr8g036880.1	ADP,ATP carrier protein 2, mitochondrial	1.88	1.99	0.85 (4.60E-1)
Medtr7g081500.1	Subtilisin-like protease	2.27	1.75	
Medtr4g030140.1	Dynamin-2B	2.01	1.73	1.18 (2.73E-2)
Medtr2g035150.1	Pathogenesis-related protein PR10	2.24	1.70	1.28 (0.00E0)
Medtr7g102120.1	S-adenosylmethionine synthetase	2.30	1.62	1.09 (3.12E-1)
Medtr4g074800.1	28 kDa ribonucleoprotein, chloroplastic	2.74	1.58	
Medtr5g069050.1	Fructose-bisphosphate aldolase	2.17	1.38	1.18 (2.03E-3)
Medtr4g059390.1	Aquaporin PIP2-7	2.51	1.35	1.11 (2.42E-1)
Medtr3g099380.1	14-3-3 f-2 protein	1.98	1.23	1.19 (5.78E-3)
Medtr4g128150.1	Histone H4	0.93	0.85	
Medtr8g088060.1	Ubiquitin	0.85	0.85	
Medtr4g097170.1	Histone H3	0.67	0.74	
Medtr1g011850.1	Histone H2A	1.37	0.74	
Medtr4g070240.1	Histone H2B	0.98	0.69	
Medtr4g063410.1	Histone H2A	1.03	0.62	
Medtr1g018840.1	Cysteine proteinase 3	0.62	0.59	
Medtr8g018590.1	Lipoxygenase	2.06	0.48	1.17 (1.34E-1)
Medtr7g114040.1	Histone H2A	0.96	0.41	
Medtr4g015460.1	Beta-glucosidase G1	1.44	0.39	1.20 (6.35E-2)
Medtr1g108770.1	ATP synthase subunit beta	1.87	0.37	0.88 (3.24E-1)
Medtr4g103920.1	Glyceraldehyde-3-phosphate dehydrogenase	0.56	0.34	0.72 (8.57E-2)
Medtr8g087990.1	SH3 domain-containing protein	1.98	-0.52	1.09 (3.89E-2)

Proteins from the 14-3-3 family are often involved in signal transduction and two soybean 14-3-3 proteins were found to play a crucial role in nodulation [Radwan *et al.*, 2012]. The 14-3-3 f-2 protein found to interact with LYK3 (Medtr3g099380.1) is not closely related to the proteins found in soybean, but may still be involved in the signal transduction in *Medicago* as it is phosphorylated upon stimulation by Nod factors.

Future work is required to confirm whether the co-immunoprecipitated proteins indeed represent novel LYK3 interactors, using for example yeast-two-hybrid, in vitro pull-down or bi-fluorescence complementation approaches. One of the pitfalls of our approach is that in its current set-up there is a risk of identifying (many) false positives. These could be ubiquitous membrane proteins that, instead of binding to LYK3, are part of small membrane fragments that are co-precipitated during the procedure [Smaczniak *et al.*, 2012]. To improve the reliability of the immunoprecipitation the amount of biological replicates can be increased and a different, unrelated integral membrane protein fused to GFP can be included as a negative control.

Strikingly, we did not detect any peptides corresponding to the published or presumed interactors of LYK3 (NFP, PUB1, SYMREM1 or FLOT4). We hypothesize that the interaction of these proteins with LYK3 only occurs upon Nod factor stimulation, either in the root hairs or the nodule, in line with the co-localization study of LYK3 and FLOT4 in root hairs [Haney *et al.*, 2011]. In support of this hypothesis, we have observed that LYK3 is rapidly removed from the infection thread and plasma membrane in the most distal cell layer of the infection zone (Chapter 3), which is most likely the location of Nod factor perception. In Chapter 4 we showed that LYK3 and NFP do form a heteromer, though the efficiencies were low. Our hypothesis is that only a small portion of the available LYK3 forms a LYK3 – NFP heteromer. Therefore, we could not detect NFP in our immunoprecipitation. To further test the hypothesis of an interaction between LYK3 and SYMREM1 and/or FLOT4 in the nodule, we analysed the co-localization of LYK3 with SYMREM1 and FLOT4 in the nodule apex.

Co-localization with SYMREM1

We co-transformed roots of the *lyk3* mutant B56 [Limpens *et al.*, 2003] with both LYK3-GFP and mCherry-SYMREM1 under control of their native promoters. By using the B56 mutant we were sure that there was no competition of LYK3-GFP with the native receptor. We screened the nodules formed on these plants for fluorescence of both proteins. Figure 5.4 show a typical nodule expressing both proteins. LYK3-GFP accumulates at the transition from meristem to infection zone (Figure 5.4a-c) and appears at the plasma membrane (Figure 5.4d-f). At the plasma membrane LYK3 accumulates in puncta. The labelling of mCherry-SYMREM1 is in line with the data published by Lefebvre *et al.* [2010]; it labels the plasma membrane surrounding the infection threads and the symbiosome membrane. The labelling is not uniform, although clear/distinct puncta could

not be observed. The overlap in localization between LYK3 and SYMREM1 is limited. LYK3 localizes to the plasma membrane in the meristem and the infection zone and localizes in approximately 35% of the cells (Chapter 3) to the infection thread membrane and never to the symbiosome membrane. In these 35% of the cells we did observe co-localization at the infection thread membrane (Figure 5.4d-f). Although interaction at the infection thread membrane may be possible, these results show that this is likely occurring in a narrow temporal window. As a result only a tiny fraction of LYK3 present at the nodule apex will interact with SYMREM1 which may explain why SYMREM1 did not show up in the immunoprecipitation data.

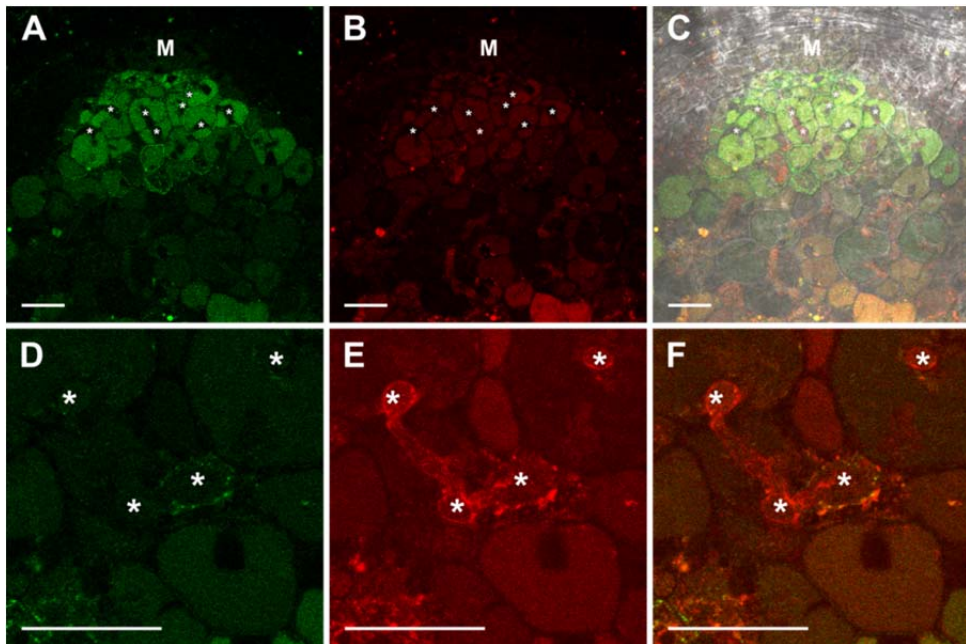


*Figure 5.4: co-localization of LYK3-GFP and mCherry-SYMREM1, both expressed from their native promoter. (A,D) LYK3-GFP (B,E) mCherry-SYMREM1 (C,F) merge. (A-C) An overview of the nodule apex where LYK3 accumulates in two cell layers at the border between meristem and infection zone. SYMREM1 accumulates in the infection zone on the infection threads and on the symbiosome membrane. (D-F) An infection thread where both LYK3 and SYMREM1 accumulate at the membrane. M indicates the position of the meristem, a * marks the infection threads, the bar indicates 25 μ m.*

Co-localization with FLOT4

We also studied the co-localization of LYK3 with FLOT4 as one of the proposed interactors. At that time a Medicago line expressing LYK3-GFP under control of its native promoter in the R108 genetic background became available (Chapter 3). We introduced FLOT4-mCherry under control of the Arabidopsis Ubiquitin3 promoter into this line. From promoter GUS data published by Haney and Long [2010] it is known that FLOT4 is

expressed throughout the infection zone (although at low levels). Although the use of the Ubiquitin3 promoter might have caused an overexpression of FLOT4, we did not observe any phenotypical defects in the nodules ectopically expressing FLOT4. Furthermore, FLOT4-mCherry localized to dot-like structures at the periphery of the cell, similar to the membrane domains reported by Haney *et al.* [2011]. Figure 5.5 shows a typical localization of Ubq:FLOT4-mCherry in the LYK3-GFP stable line. Both fluorescent proteins occur at the cell periphery and in dot/ring-like structures in the cytoplasm, possibly representing endosomes (Figure 5.5). Therefore, an interaction between LYK3 and FLOT4 is possible. Haney *et al.* [2011] showed that co-localization of LYK3 and FLOT4 in the root hairs only occurs upon stimulation by Nod factors, however it remains to be shown whether LYK3 and FLOT4 indeed interact as FLOT4 was not detected in our immunoprecipitation experiment.

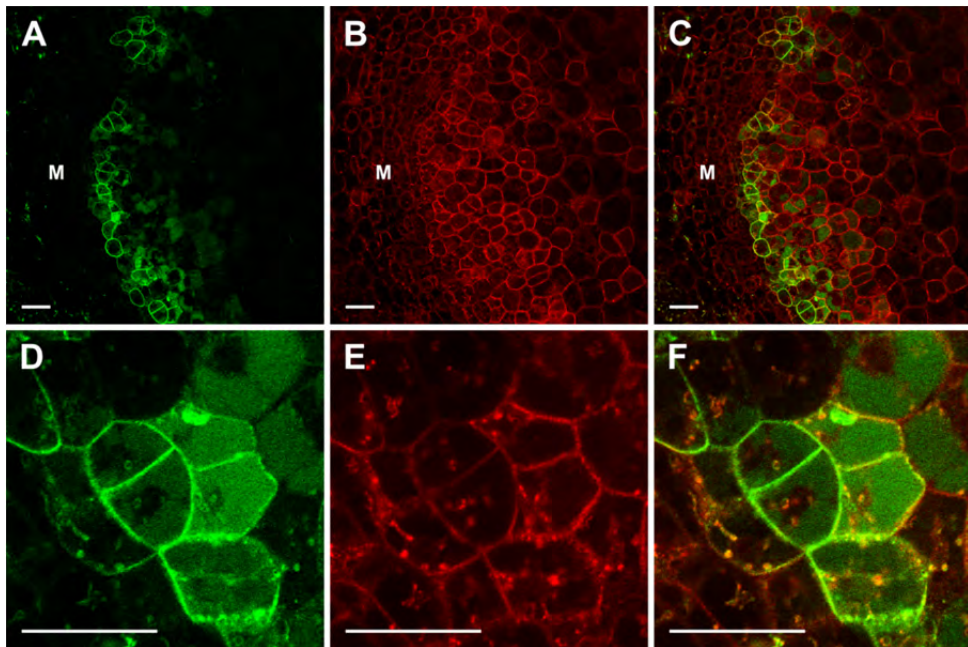


Figure 5.5: co-localization of LYK3-GFP and FLOT4-RFP. (a,d) LYK3-GFP (b,e) FLOT4-RFP (c,f) merge. The M indicates the meristem and the bar indicates 25 μ m.

In conclusion, our data show the potential of identifying novel interacting proteins of the Nod factor receptors through a co-immunoprecipitation approach from *Medicago* nodules, which could give important new insights into the regulation of Nod factor perception and signalling. Such interacting proteins may not be identified by the forward genetics screens

due to possible redundancy or involvement of such proteins in other (basic) cellular functions. Further work is required to verify whether the putative interacting proteins identified here are true LYK3 interactors.

MATERIALS AND METHODS

Constructs, Plant material and transformation

LYK3 was amplified from genomic DNA using Phusion High-Fidelity DNA Polymerase (Finnzymes) using forward primer 3' - CACCACAATATTGTATTGGTGAGATCATATAAGA - 5' and reverse primer 3' - TCTAGTTGACAACAGATTTATGAGAGA - 5'. The obtained sequence was cloned into pENTR™/D-TOPO® (Invitrogen). Next, a GATEWAY® reaction with LR Clonase II plus (Invitrogen) was performed using a pENTRp1p4r containing the Arabidopsis Ubiquitin3 promoter, a pENTRp2rp3 containing mCherry and a 35S terminatior and the pKGW-MGW destination vector to generate the binary construct. SYMREM1 was amplified from genomic DNA using Phusion High-Fidelity DNA Polymerase (Finnzymes) using forward primer 3' - CACCATGGAAGAATCGAAAAACAAACA - 5' (CACC sequence for directional cloning into pENTR™/D-TOPO® is underlined) and reverse primer 3' - CTAAGTGAACCTTAAACCGC - 5'. The obtained fragment was cloned into pENTR™/D-TOPO® (Invitrogen). The SYMREM1 promoter was amplified in the same way using forward primer 3' - AAGCTTAAATTACGTTAGTTTATATAAGGGGTTAAA - 5' (HindIII sequence is underlined) and reverse primer 3' - GGCGCGCCCTCGAGAATGTATTTCTAGGGTTACAGCATTAGA - 5' (AseI sequence is underlined). The obtained fragment was ligated into pJET (Thermo scientific). The promoter was released from the vector using HindIII and AseI and ligated in a pENTR p1p4r containing a MCS and mCherry. Next, a GATEWAY® reaction with LR Clonase II plus (Invitrogen) was performed using a pENTRp2rp3 a 35S terminator and the pKGW-MGW destination vector to generate the binary construct.

FLOT4 was amplified from genomic DNA using Phusion High-Fidelity DNA Polymerase (Finnzymes) using forward primer 3' - CACCATGTACAAGGTAGCAAAAGCATCA - 5' (CACC sequence for directional cloning into pENTR™/D-TOPO® is underlined) and reverse primer 3' - ATTCAAGTTTTTGTCTAGGCAAGA - 5'. The obtained sequence was cloned into pENTR™/D-TOPO® (Invitrogen). Next, a GATEWAY® reaction with LR Clonase II plus (Invitrogen) was performed using a pENTRp1p4r containing the Arabidopsis Ubiquitin3 promoter, a pENTRp2rp3 containing mCherry and a 35S terminatior and the pKGW-MGW destination vector to generate the binary construct.

Plants were transformed by *Agrobacterium rhizogenes*-mediated hairy root transformation according to [Limpens *et al.*, 2004]. The transgenic plants were inoculated with *S.meliloti* 2011.

Protein isolation and Co-Immuno precipitation

The *Medicago truncatula lyk3* mutant B56 was transformed with a binary vector containing pLYK3:LYK3-GFP or pUBQ3:LYK3-GFP. Ten days after inoculation with *S. meliloti* 2011 transgenic roots were harvested based on complementation of the mutant phenotype. The roots containing nodules were frozen in liquid nitrogen for co-immuno precipitation.

LYK3 and potential associated proteins were immuno precipitated according to [Smaczniak *et al.*, 2012]. About 1 gram of root containing nodule tissue was ground in liquid nitrogen and resuspended in 3ml of lysis buffer (150 mM NaCl, 1% Triton® X-100, 50 mM Tris-HCl (pH8.0)) on ice. To isolate the proteins the suspension was sonicated three times for 10 seconds. To obtain clear supernatant the suspension was centrifugated three times at maximum speed at 4°C. The cleared supernatant was supplemented with 50µl anti-GFP magnetic microbeads (µMACS™ GFP Isolation Kit, Milteny Biotec, Germany) and incubated for 1 hour at 4°C on a rotary disc. A µMACS™ column was prepared with lysis buffer, the sample was loaded and washed 5 times with lysis buffer and 2 times with 20mM Tris-HCl (pH 7.5). Finally, the IP-samples were eluted in 50 µl 8M urea. The samples were digested with trypsin according to Smaczniak *et al.* [2012]. In short samples were diluted in ammonium bicarbonate, disulfide bounds were reduced with DTT and free thiol groups were alkylated with Iodoacetamide. Peptides were then digested using 15 µl of 0.1 µg/µl sequence grade trypsin over night at room temperature and subsequently desalted.

Western blot

Proteins were separated on a 10% SDS-PAGE gel and subsequently blotted on a nitrocellulose membrane. After blocking in PBS + 0.3% Tween®-20+ 3% BSA the membrane was incubate with αGFP-HRP (Milteny Biotec, Germany) 1:5000 in PBS + 0.3% Tween®-20 + 1% BSA for 1h at room temperature. The membrane was washed 3 times for 20 minutes in PBS+ 0.3% Tween®-20 + 1% BSA and briefly with PBS. The membrane was developed using the Immun-Star™ WesternC™ Chemiluminescence Kit (Bio-Rad, USA) and imaged on a ChemiDoc MP system (Bio-Rad, USA).

Protein complex identification

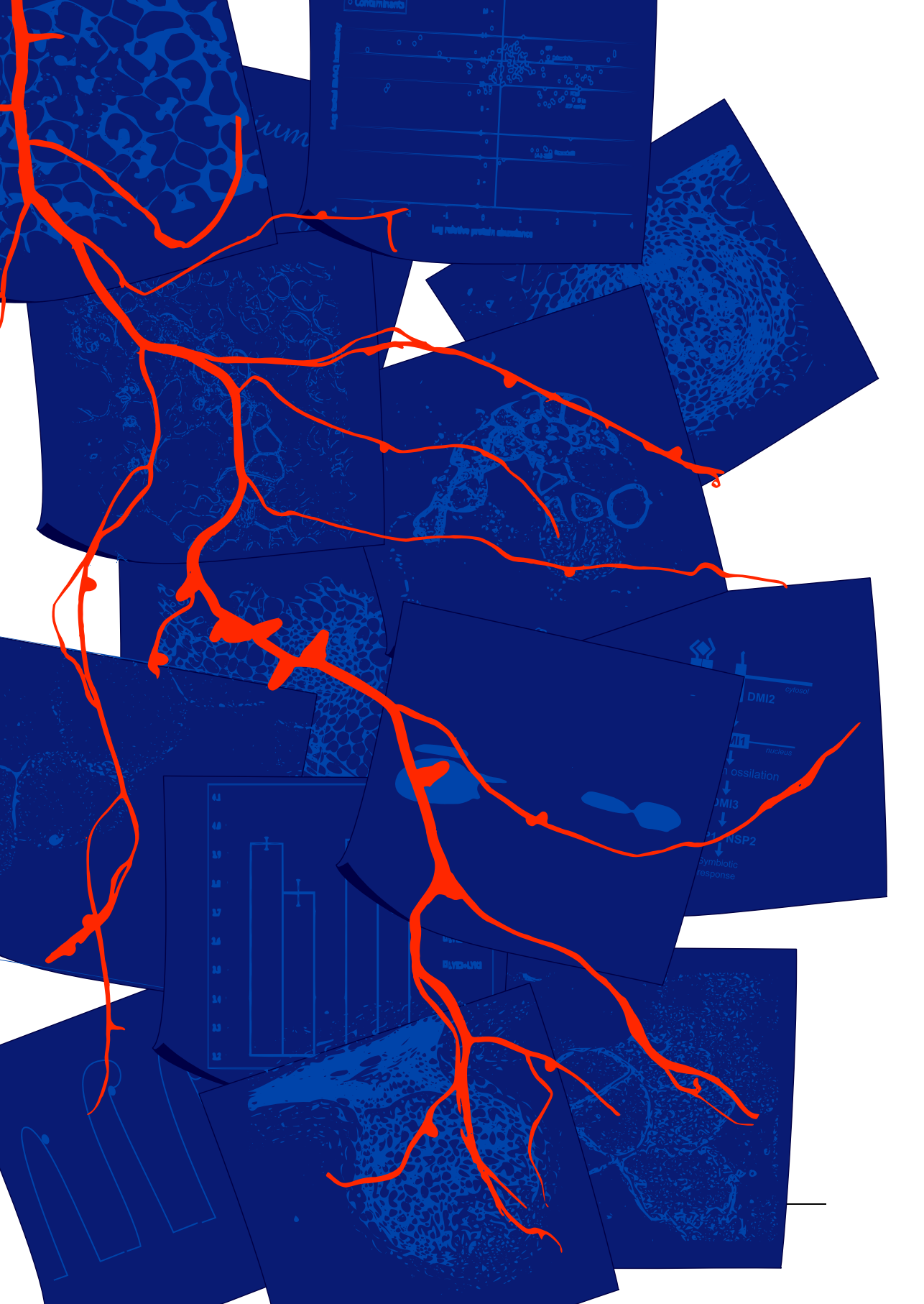
The peptides isolated were identified according to Smaczniak *et al.* [2012]. The samples were measures in a LC-MS/MS setup and identified using label-free protein quantification with MaxQuant against a six frame translation of the *M.truncatula* genomen (Mt3.5v5) [Young *et al.*, 2011].

Fluorescent microscopy.

Nodules from transgenic plants were selected and hand sections were made using double-razor blades and mounted on microscope slides in 0.9% NaCl and further analyzed on a Zeiss LSM 510 confocal laser scanning microscope (Carl-Zeiss Axiovert [Oberkochen, Germany] 100 M equipped with a LSM510, an argon laser with a 488-nm laser line, a helium-neon laser with a 543- nm laser line); 488 nm (GFP) and 543 nm (mRFP); GFP emission was selectively detected using a 505- to 530-nm band-pass filter; mCherry emission was detected using a 560- to 615-nm band-pass or 560-nm long-pass filter.

ACKNOWLEDGEMENTS

We like to thank Thomas Ott for providing us with the SYMREM1 promoter sequence.



Chapter 6.

LASER CAPTURE MICRODISSECTION TO STUDY SPATIAL DIFFERENCES IN GENE EXPRESSION OF THE NOD FACTOR SIGNALING CASCADE

Erik Limpens¹, Sjeff Moling¹, Guido Hooiveld², Patrícia Pereira³, Ton Bisseling^{1,4},
Jörg Becker³, Helge Küster⁵

¹ *Laboratory of Molecular Biology, Wageningen University, Wageningen, The Netherlands*

² *Division of Human Nutrition, Wageningen University, Wageningen, The Netherlands*

³ *Plant Genomics, Instituto Gulbenkian de Ciência, Oeiras, Portugal*

⁴ *College of Science; King Saud University; Riyadh, Saudi Arabia*

⁵ *Institut für Pflanzengenetik, Leibniz Universität, Hannover, Germany*

Published in *PLoS One*, 2013; 8(5): e64377 in a modified form

ABSTRACT

Legumes have the unique ability to host nitrogen-fixing *Rhizobium* bacteria as symbiosomes inside root nodule cells. To get insight into this key process, which forms the heart of the endosymbiosis, we isolated specific cells/tissues at different stages of symbiosome formation from nodules of the model legume *Medicago truncatula* using laser-capture microdissection. Next, we determined their associated expression profiles using Affymetrix *Medicago* GeneChips. Cells were collected from the nodule infection zone divided into a distal (where symbiosome formation and division occur) and proximal region (where symbiosomes are mainly differentiating), as well as infected cells from the fixation zone containing mature nitrogen fixing symbiosomes. As non-infected cells/tissue we included nodule meristem cells and uninfected cells from the fixation zone. Here, we present a comprehensive gene expression map of an indeterminate *Medicago* nodule and selected genes that show specific(enriched) expression in the different cells or tissues. Validation of the obtained expression profiles, by comparison to published gene expression profiles and experimental verification, indicates that the data can be used as digital “in situ”. This digital “in situ” offers a genome-wide insight into genes specifically associated with subsequent stages of symbiosome and nodule cell development, and can serve to guide future functional studies. Our data further highlight an important yet underestimated role for uninfected cells in nodule functioning.

INTRODUCTION

Legume plants have the unique ability to host nitrogen-fixing bacteria, collectively called rhizobia, in a newly formed organ, the so-called root nodule. Inside specialized cells of the nodule, the rhizobium bacteria are accommodated as novel organelle-like structures called symbiosomes [Roth and Stacey, 1989]. Symbiosomes fix atmospheric nitrogen into ammonium which is transferred to the plant in return for carbohydrates [Oldroyd *et al.*, 2011]. This symbiosis is one of the most important sources of biologically fixed nitrogen and allows legumes to grow in nitrogen poor soil conditions, without the need of chemical fertilizer. To better understand this ecologically and agriculturally important interaction a key goal is the identification of the transcriptome changes that are associated with the different stages of the interaction and to link gene expression to the corresponding developmental processes. One of the key processes that occurs in the nodule, and is at the heart of the symbiosis, is the accommodation and development of the bacteria into nitrogen-fixing symbiosomes. Here, we aim to characterize the transcriptome of specific cells/tissues inside the nodule at different stages of symbiosome formation in the model legume *Medicago truncatula* (*Medicago*). The developmentally structured organization of *Medicago* nodules makes them an ideal system to study the different stages of nodule and symbiosome development.

Nodule development is triggered by rhizobial lipochito-oligosaccharide signal molecules, called Nod factors that activate a signaling cascade which triggers transcriptional responses that control both nodule organogenesis as well as rhizobial infection and symbiosome formation [Kouchi *et al.*, 2010]. Rhizobia enter the root and developing nodule through tubular structures called infection threads. Typically, these infection threads originate in root hairs that curl around attached bacteria after which they traverse the cortex to deliver the bacteria to the developing primordium [Emons and Mulder, 2000]. When the infection threads reach the cells of the nodule primordium, the bacteria are released from the cell wall bound infection threads and are taken up into the cells through an endocytosis-like process by which they become surrounded by a specialized plant membrane and organelle-like symbiosomes are formed [Jones *et al.*, 2007]. After the infection threads invade the nodule primordium, an apical meristem is established that continues to add cells to the developing nodule [Timmers *et al.*, 1998]. In *Medicago*, this meristem stays active by which an elongated nodule is formed with a highly ordered organization where infection thread formation followed by symbiosome formation and subsequent development occur along a developmental gradient [Vasse *et al.*, 1990];

Zone I of the nodule consists of the apical nodule meristem, consisting of uninfected dividing cells. In Zone II, the infection zone, plant and bacterial cell differentiation occur and this zone can be further divided into a distal and proximal region [Vasse *et al.*, 1990]. In the distal infection zone, ~4 cell layers just below the meristem, infection threads invade the cells coming from the meristem. Here so-called unwalled infection droplets extrude from the cell wall bound infection threads from where the bacteria are individually pinched off into the cytoplasm by which they become surrounded by the plant-derived symbiosome membrane [Brewin, 2004; Limpens *et al.*, 2009]. Next, the bacteria (now called bacteroids) divide and start filling the cells. In *Medicago*, bacteroid and symbiosome membrane division are strictly coupled by which symbiosomes remain single bacteria-containing compartments. In the proximal ~4 cell layers of the infection zone, the bacterioids lose their ability to divide and start elongating. This terminal differentiation process has been correlated with endoreduplication and cell enlargement occurring in both the host cell as well as the bacteria and involves a family of nodule-specific cysteine-rich NCR peptides [Mergaert *et al.*, 2006; Van de Velde *et al.*, 2010]. In this way the individual symbiosomes become >10x bigger and almost completely fill the host cells. In Zone III, the fixation zone, the bacteria are fully differentiated into their nitrogen fixing form and nitrogen fixation takes place, which is facilitated by the micro-aerobic conditions in the infected nodules cells and correlates with the induction of bacterial nitrogen fixation genes [Ott *et al.*, 2005; Soupene *et al.*, 1995]. Some cells originating from the meristem never become infected by the bacteria and these can be clearly seen as relatively small uninfected cells in between the large infected cells. These uninfected cells are thought to play an essential role in metabolite transport to and from the infected cells [White *et al.*, 2007]. Eventually, as the nodule ages (~3-4 weeks post-inoculation), the symbiosis starts to break down and senescence of both symbiosomes and host cells occurs in Zone IV (senescent zone) [Van de

Velde *et al.*, 2006]. The different zones mentioned above, except for the meristem, are surrounded at the periphery by the nodule parenchyma (nodule inner cortex), vascular bundles and the nodule endodermis. Further, the entire nodule is surrounded by an outer cortex [Vasse *et al.*, 1990].

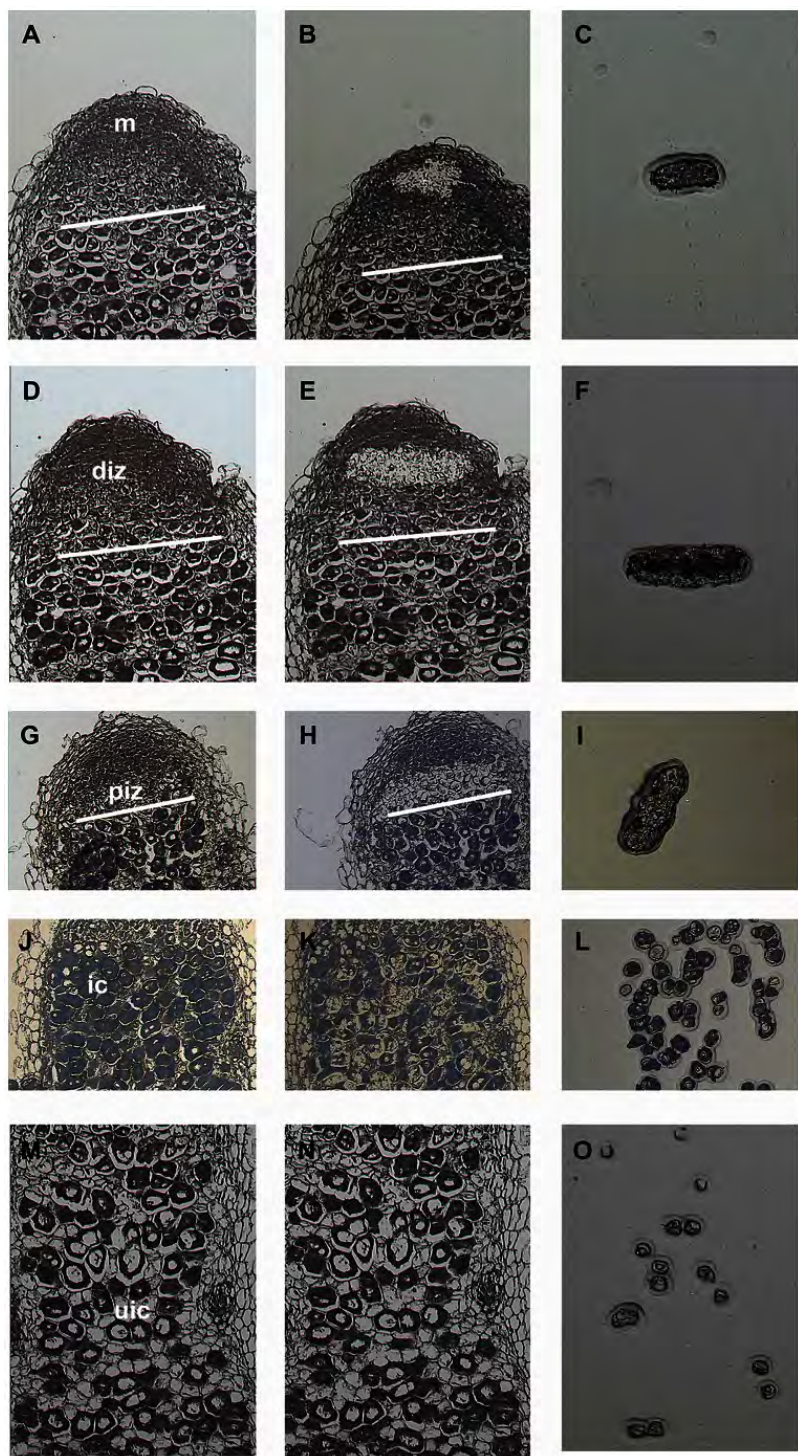
In the past years, various expression profiling strategies have been used during both early and late stages of nodulation to identify the genes that are associated with different stages of the interaction [Benedito *et al.*, 2008; Czaja *et al.*, 2012; El Yahyaoui *et al.*, 2004; Gamas *et al.*, 1996; Godiard *et al.*, 2007; Hogslund *et al.*, 2009; Kuster *et al.*, 2004; Lohar *et al.*, 2006; Manthey *et al.*, 2004; Mitra and Long, 2004]. Such studies either focused on identifying transcriptome changes within hours of treatment with symbiotic signals, with *Rhizobium* inoculation, or compared whole nodules at different time points after inoculation. To establish a link between gene expression and processes in the nodule, such as meristem formation, symbiosome formation, differentiation or maintenance, two recent studies combined transcriptome analyses of wild-type *Medicago* nodules with that of nodules impaired in their development due to bacterial and plant mutations [Maunoury *et al.*, 2010; Moreau *et al.*, 2011]. This revealed several expression profiles that correlated with distinct developmental programs in the nodule. However, this approach does not clearly distinguish between different cell types and the use of plant and bacterial mutants has the inherent risk that genes are affected that are not normally expressed at corresponding developmental stages in wild-type nodules. Furthermore, genes that are differentially expressed in a specific cell type or at a specific stage might not be detected in whole nodule samples due to dilution effects by other more abundant cells.

Here, we used laser-capture microdissection (LCM) to isolate specific nodule cells at different stages of symbiosome development. To this end, we collected cells from the infection zone, divided into a distal region (where symbiosome formation and division occur) and a proximal region (where symbiosomes are mainly differentiating), as well as infected cells from the fixation zone containing mature nitrogen fixing symbiosomes. To include uninfected reference/control tissues, we also collected cells from the meristem as well as uninfected cells from the fixation zone. The captured cells/tissues were used to determine their associated expression profiles using Affymetrix *Medicago* GeneChips [Benedito *et al.*, 2008]. The resulting digital “*in situ*” offers a valuable data set to identify novel genes controlling nodule development and to unravel the unique ability of legumes to host the bacteria as nitrogen fixing organelles, which forms the heart of the *Rhizobium*-legume symbiosis, at a molecular level.

RESULTS AND DISCUSSION

Laser capture microdissection of Medicago nodules

To isolate distinct nodule cells at different stages of symbiosome development we used LCM, which allows the rapid and specific isolation of cells/tissues based on conventional histological identification [Schnable *et al.*, 2004]. To preserve as best as possible the zonation and histological detail, three week old nodules were fixed with Farmer's fixative and embedded in paraffin (according to Kerk *et al.* [2003]). Three week old Medicago nodules typically contain an active meristem at the apex, a well-defined infection zone and an active fixation zone. The quality of the RNA in the paraffin embedded tissues was checked before and after fixation and sectioning. Approximately 300 ng high quality total RNA could be isolated from a single paraffin embedded nodule (data not shown). Subsequently, 8 micrometer thick median longitudinal sections were used to isolate cells from the meristem, 4 cell layers of the distal infection zone (DIZ), 4 cell layers from the proximal infection zone (PIZ), infected (IC), and uninfected (UIC) cells from the fixation zone (Figure 6.1a–o). Only those sections were used that showed a well-defined zonation and where histological preservation was sufficient to allow the identification of the different cell types. However, as the exact borders between the meristematic cells and the cells of the distal infection zone and between the distal and proximal infection zones are difficult to distinguish precisely by light microscopy, it is possible that some overlap exists between these laser-captured tissues. The same holds for the uninfected cells, which are relatively small, highly vacuolated and have irregular shapes in between the large infected cells. For each tissue/cell-type 3 biological replicates (e.g. different nodules) each consisting of 50 cells pooled from 8 consecutive sections were collected and used for RNA isolation.



Cell-type specific expression profiling of Medicago root nodules

To determine the transcriptome of the isolated cell/tissue types we used the Affymetrix Medicago GeneChips, which contains 50900 Medicago probe sets representing the majority of genes in this species [Benedito *et al.*, 2008]. The RNA isolated from the LCM cells was amplified using a two-step RNA amplification protocol to obtain sufficient material for hybridization experiments (see methods).

Analyses of the expression levels of control genes (i.e. GAPDH), divided into 3'- and 5'-regions, showed that there is a bias towards the 3'-end of transcripts (data not shown). This can be due to the two-step T7 amplification protocol and/or due to degradation of RNA in the LCM samples. Each gene on the Medicago GeneChip is represented by 11 probes. To account for this 3'-bias we reanalyzed the data using only the five most 3' located probe sets instead of all 11 probe sets. Expression data are available at the Gene Expression Omnibus (GEO accession GSE43354). Although most probe sets on the Medicago array are designed in the 3' part of transcripts, the observed 3'-bias may affect the reliable detection of genes for which the probe sets on the array are located in more 5' regions.

To identify genes specifically correlated with the developmental processes in the different cell/tissue types we first selected genes that show enriched expression, at least 2-fold higher ($q < 0.01$), compared to (the average of) all other LCM samples in: 1) the meristem (M), 2) the distal infection zone (DIZ), 3) the proximal infection zone (PIZ), 4) the complete infection zone (DIZ and PIZ), 5) infected cells (IC) of the fixation zone, and 6) uninfected cells (UIC). From this analysis, we next selected those genes that show at least a 2 fold higher enrichment factor in an individual/specific cell-type compared to any of the other cell types. These genes will be referred to as “cell-type enriched” genes and are summarized in Table 6.1. In total 4999 genes show at least 2-fold enriched expression in a specific nodule tissue/cell type.

← Figure 6.1: Laser capture microdissection of nodule cells. Panels represent 8 μ M thick longitudinal sections of 3-week old Medicago nodules before capture (a,d,g,j,m), after capture (b,e,h,k,n) and captured/isolated cells (c,f,i,l,o). Cells/tissues were isolated from the meristem (m; a-c), distal infection zone (diz; d-f), proximal infection zone (piz; g-i), infected cells zone (ic; j-l) and uninfected cells (uic; m-o) from the fixation zone.

Table 6.1: Number of genes showing cell/tissue specific or enriched expression.

Meristem	Distal infection zone	Proximal infection zone	Total infection zone	Infected cells	Uninfected cells
895	53	70	299	1909	2072
Total: 4999 genes					

Validation of cell-type specific expression in Medicago root nodules

To validate the “specificity” of the obtained digital expression profiles and to establish to what extent the array data can be used as digital “in situ” we first compared the LCM microarray data to published expression profiles from promoter-reporter analyses or in situ hybridizations (summarized in Table 6.2). Additionally, we analyzed the expression profile of several selected genes in the nodule (Table 6.2).

Meristem vs infection zone: First, we compared the meristem to the infection zone and surrounding cortex. The absence of MtN13 (Mtr.33137.1.S1_at; Mtr.37852.1.S1_at) gene expression from the “meristem-specific/enriched” data set, which is known to be highly expressed specifically in the nodule cortex [Gamas et al., 1998], indicates that the meristem LCM sample is not significantly contaminated with nodule cortex cells (although some contamination can be observed in case of probeset Mtr.37852.1.S1_at). In addition, several genes that are reported to be specifically/most highly expressed in the infection zone were examined. These include for example MtN1, MtN6, MtAnn1, DNF1/DAS12, MtRR4, MtN9/MtMMPL1 and MtEFD [Combiér et al., 2007; Gamas et al., 1998; Journet et al., 2001; Mathis et al., 1999; Niebel Fde et al., 1998; Vernie et al., 2008; Wang et al., 2010]. All these genes show infection zone specific/enriched expression in the LCM samples (Table 6.2), validating the results of the LCM analysis. As an additional example, we verified the infection zone-specific expression of the early nodulin MtENOD12 (Mtr.8924.1.S1_at) by in situ hybridization. This showed that MtENOD12 is indeed most highly expressed throughout the infection zone of the nodule and not (or hardly) in the nodule meristem (Figure 6.2a,b).

To our knowledge, there are currently no genes described in literature that are specifically/exclusively expressed in the nodule meristem of Medicago. At the switch from meristem to infection zone, the meristem-derived cells still enter the cell cycle, but instead of dividing they undergo several rounds of endoreduplication [Cebolla *et al.*, 1999; Foucher and Kondorosi, 2000]. Therefore, we looked whether genes associated with G2/M transition/cytokinesis are specifically enriched in the meristem data set. Indeed, the cytokinesis-specific t-SNARE/syntaxin *Knolle* (Mtr.41560.1.S1_at) and several cyclin and

cyclin-dependent kinase genes that are required for G2/M transition (B-type cyclins: Mtr.31360.1.S1_at, Mtr.31859.1.S1_at; cyclin-dependent kinases (CDK2): Mtr.50839.1.S1_at, Mtr.43543.1.S1_at) show “meristem specific/enriched” expression [Foucher and Kondorosi, 2000; Fung and Poon, 2005; Lauber *et al.*, 1997]. Among the genes that appear nodule “meristem specific/enriched” is also the *WUSCHEL-RELATED HOMEODOMAIN* gene (*MtWOX5*; Mtr.33304.1.S1_at), which is thought to also control stem cell activity in the root meristem. Recently, it has been shown by promoter-GUS analyses that *MtWOX5* is indeed expressed in the nodule meristematic region, most specifically at the tips of the vascular bundles [Osipova *et al.*, 2012]. These cells may be related to meristem-organizing quiescent center cells, although the exact organization of the nodule meristem and stem cell niche is not known.

The Nod factor receptor LYK3 (Mtr.142.1.S1_s_at) also shows meristem enriched expression in the LCM data. Previous *in situ* hybridizations have shown that *LYK3* is expressed in the proximal site of the nodule meristem at the border with the infection zone, where it may control the invasion of the meristematic cells by infection threads [Limpens *et al.*, 2005]. To further confirm the predictive value of the “meristem specific/enriched” data set, the putative promoter region of a ROP GTPase, (Mtr.35940.1.S1_at, Mtr.15539.1.S1_at), was isolated and its expression determined by promoter-GUS analysis. This confirmed the “meristem”-specific expression of this gene in Medicago nodules (Figure 6.2c,d). These data indicate that the meristematic region as captured can be clearly distinguished from the infection zone.

Distal vs proximal infection zone: The infection zone can be further divided into a distal and proximal zone based on the developmental status of the symbiosomes in this part of the nodule. In the distal part (~4 cell layers just below the meristem), after infection threads have invaded the meristem-derived cells, symbiosomes are formed (bacteria are released from the infection threads) and symbiosomes divide. In the proximal ~4 cell layers symbiosomes have stopped dividing and are terminally differentiating by which they become much bigger and fill the growing nodule cells. To identify genes potentially associated with these different stages, we selected infection zone specific/enriched genes that are >2x more enriched in the distal infection zone compared to the proximal infection zone or vice-versa. Two genes have been shown to be most highly expressed in the distal infection zone. These are the early nodulin *ENOD11* (Mtr.13473.1.S1_at) and annexin *MtANN1* (Mtr.14183.1.S1_at) [Journet *et al.*, 2001; Niebel Fde *et al.*, 1998]. Both genes show distal infection zone specific/enriched expression in the LCM array data, confirming the specificity of the captured cells. Among the genes that show a “proximal infection zone specific/enriched” expression is the nodule-specific *IRE* gene (Mtr.15644.1.S1_s_at). This AGC-like kinase has been shown to be most highly expressed in the proximal part of nodule via promoter-GUS analyses [Pislariu and Dickstein, 2007b]. Additional genes that have been reported to be expressed most highly in the proximal infection zone and which show enrichment in the proximal infection zone LCM data, include the phytocyanin-like

ENOD20 (Mtr.17106.1.S1_at) [Vernoud *et al.*, 1999] and glycine-rich protein-encoding genes (*GRPs*; Mtr.858.1.S1_s_at, Mtr.49309.1.S1_at) [Kevei *et al.*, 2002]. These data validate the specificity of the LCM data to distinguish distal from proximal cells in the infection zone of the nodule.

Infected vs uninfected cells: The fixation zone consists of two cell types; infected and uninfected cells. To validate the specificity of the infected versus uninfected LCM data we looked for genes that are reported to be specifically expressed in either cell type. However, although uninfected cells play an essential role in metabolite transport in functional nodules, to our knowledge currently no uninfected-cell specific markers have been described. One of the genes that show an uninfected cell “specific” expression from the LCM data is the *MtENOD8.2* (Mtr.8511.1.S1_at) gene. *ENOD8.2*, like its close homolog *ENOD8.1*, belongs to the GDSL family of lipase and esterase proteins [Dickstein *et al.*, 2002]. To verify the uninfected cell specific expression the putative promoter-region of *MtENOD8.2* was fused to β -glucuronidase (GUS) and its expression pattern analyzed in nodules. This analysis confirmed the uninfected cell “specific expression” of *MtENOD8.2* (Figure 6.2e,f). Additionally, *ENOD8.2* was found to be expressed in the nodule parenchyma. Therefore, the uninfected cell specific/enriched data set presented here offers a first insight into this essential nodule cell type.

Table 6.2: Selection of genes with known expression profiles used for validation. Per nodule region is the Enrichment Factor (EF) compared to the average of all other LCM samples, p-value and q-value shown.

Gene Reference	Medicago GeneChip ID	A Mean	Meristem			Distal infection zone			Proximal infection zone			Infection zone			Infected cell			Uninfected cell		
			EF	p	q	EF	p	q	EF	p	q	EF	p	q	EF	p	q	EF	p	q
Meristem																				
MtWOX5	Mtr.33304.1.S1_at	3.44	42.87	0	0	1.28	0.65	0.88	0.47	0.16	0.75	0.71	0.43	0.68	0.21	0.01	0.05	0.19	0.01	0.07
MtHAP2, [Combier <i>et al.</i> , 2006]	Mtr.43750.1.S1_at	12.32	1.1	0.74	0.69	2.74	0	0.28	2.06	0.02	0.53	3.17	0	0.02	0.26	0	0	0.61	0.1	0.31
MtLYK3, [Limpens <i>et al.</i> , 2005]	Mtr.142.1.S1_s_at	3.88	23.41	0	0	9.52	0	0.13	0.34	0.04	0.61	2.21	0.07	0.39	0.11	0	0.01	0.12	0	0.01
MtROP2, this study, Figure 6.2	Mtr.35940.1.S1_at	2.23	35.44	0	0.01	1.59	0.54	0.86	0.39	0.22	0.78	0.73	0.61	0.75	0.12	0.01	0.05	0.39	0.22	0.43
Infection Zone																				
MtN1	Mtr.37500.1.S1_at	8.68	0.4	0.36	0.57	20.66	0.01	0.4	25.73	0	0.34	65.62	0	0.01	0.05	0.01	0.04	0.1	0.03	0.19
MtN6	Mtr.43850.1.S1_at	9.21	6.1	0	0.02	29.22	0	0	17.25	0	0.01	63.33	0	0	0.02	0	0	0.02	0	0
DNF1	Mtr.43876.1.S1_at	12.35	0.42	0	0	1.52	0.01	0.42	2.05	0	0.06	2.13	0	0	1.25	0.13	0.25	0.61	0	0.04
MtN9/MtMMPL1	Mtr.43552.1.S1_at	6.96	0.36	0.09	0.36	6.4	0.01	0.37	15.64	0	0.09	21.55	0	0	2.59	0.11	0.24	0.01	0	0
MtEFD	Mtr.41581.1.S1_at	9.14	0.11	0	0.02	4.94	0.01	0.39	5.64	0	0.33	9.19	0	0.01	1.57	0.38	0.44	0.21	0.01	0.08
MtENOD12	Mtr.8924.1.S1_at	7.82	1.4	0.62	0.66	17.5	0	0.19	12.15	0	0.28	35.63	0	0	0.14	0.01	0.06	0.02	0	0
Distal Infection Zone																				
MtENOD11	Mtr.13473.1.S1_at	7.95	26.21	0	0.02	59.65	0	0.04	1.99	0.34	0.81	24.15	0	0.01	0.02	0	0	0.02	0	0
MtERN1	Mtr.7556.1.S1_at	7.08	20.65	0	0	52.07	0	0	6.42	0	0.17	48.16	0	0	0.01	0	0	0.01	0	0
MtERN2	Mtr.43947.1.S1_at	3.23	1.15	0.68	0.68	5.09	0	0.09	0.68	0.25	0.79	2.28	0.01	0.15	0.35	0.01	0.04	0.71	0.32	0.49
MtAnn1	Mtr.14183.1.S1_at	7.25	0.15	0.06	0.3	4.51	0.13	0.73	1.35	0.75	0.88	3.34	0.13	0.49	1.65	0.6	0.53	0.66	0.67	0.62
Proximal Infection Zone																				
MtIRE	Mtr.15644.1.S1_s at	5.12	0.13	0	0.05	3.34	0.05	0.63	7.22	0	0.31	8.35	0	0.03	2.27	0.16	0.29	0.15	0	0.05

Gene Reference	Medicago GeneChip ID	A Mean	Meristem			Distal infection zone			Proximal infection zone			Infection zone			Infected cell			Uninfected cell		
			EF	p	q	EF	p	q	EF	p	q	EF	p	q	EF	p	q	EF	p	q
MtENOD20	Mtr.17106.1.S1_at	7.03	0.08	0	0.01	11.26	0	0.13	26.86	0	0.02	45.06	0	0	0.74	0.57	0.52	0.06	0	0
MtGRPs, <i>M. sativa</i>	Mtr.858.1.S1_s_at	3.72	0.37	0.03	0.23	1.61	0.28	0.8	10.72	0	0.05	6.68	0	0.01	0.54	0.17	0.29	0.29	0.01	0.1
MtGRPs, <i>M. sativa</i>	Mtr.49309.1.S1_at	4.05	0.21	0.03	0.21	1.13	0.85	0.9	19.17	0	0.11	7.77	0	0.06	1.86	0.35	0.42	0.12	0	0.06
Infected Cells																				
Leghemoglobins	Mtr.38572.1.S1_at	9.23	0.33	0	0.02	0.73	0.25	0.79	0.76	0.3	0.81	0.68	0.08	0.43	3.73	0	0	1.46	0.16	0.38
Leghemoglobins	Mtr.40138.1.S1_at	6.98	0.25	0.05	0.29	0.42	0.2	0.77	0.62	0.47	0.83	0.41	0.11	0.47	5.93	0.02	0.07	2.59	0.17	0.39
Leghemoglobins	Mtr.43465.1.S1_at	9.76	0.31	0	0.03	0.63	0.12	0.73	0.67	0.17	0.75	0.56	0.02	0.26	5.46	0	0	1.4	0.25	0.45
Leghemoglobins	Mtr.47990.1.S1_at	7.49	0.16	0	0.01	1.05	0.89	0.9	0.48	0.07	0.66	0.63	0.15	0.52	5.71	0	0.01	2.19	0.05	0.24
Leghemoglobins	Mtr.5077.1.S1_at	2.73	1.4	0.22	0.49	0.45	0.01	0.42	0.45	0.01	0.42	0.34	0	0.02	2.83	0	0.01	1.27	0.38	0.51
Leghemoglobins	Mtr.51231.1.S1_x_at	12.41	0.35	0	0.04	0.85	0.56	0.86	0.78	0.38	0.82	0.76	0.24	0.58	3.54	0	0.01	1.23	0.46	0.55
Nodulin-26	Mtr.2246.1.S1_at	8.05	0.04	0	0.05	1.5	0.64	0.88	1.55	0.62	0.86	1.76	0.43	0.69	49.08	0	0.01	0.21	0.09	0.3
Nodulin-25	Mtr.41813.1.S1_at	6.08	0.17	0.12	0.4	0.36	0.35	0.82	0.64	0.69	0.87	0.38	0.28	0.61	43.45	0	0.02	0.58	0.62	0.6
MtNCR001	Mtr.10380.1.S1_at	8.57	0.55	0.05	0.28	0.63	0.12	0.73	0.58	0.07	0.67	0.51	0.01	0.18	3.96	0	0	1.26	0.42	0.53
MtNCR0035	Mtr.10684.1.S1_at	12.07	0.34	0	0.06	0.5	0.04	0.6	1.1	0.75	0.88	0.67	0.13	0.49	3.56	0	0.01	1.47	0.22	0.43
MtCaML2	Mtr.40731.1.S1_at	11.19	0.38	0.01	0.12	0.58	0.11	0.72	0.56	0.09	0.7	0.47	0.01	0.19	5.23	0	0	1.58	0.18	0.4
MtCaML3	Mtr.37968.1.S1_at	7.36	0.18	0.02	0.19	0.3	0.09	0.69	0.28	0.07	0.67	0.19	0.01	0.15	15.87	0	0.01	4.27	0.05	0.23
MtCaML6	Mtr.43719.1.S1_at	7.39	0.09	0	0.01	0.41	0.09	0.7	0.38	0.07	0.66	0.29	0.01	0.15	30.96	0	0	2.34	0.1	0.32
MtIPD3	Mtr.3453.1.S1_s_at	4.96	0.2	0.02	0.17	0.4	0.15	0.75	0.28	0.05	0.63	0.23	0.01	0.17	19.26	0	0	2.32	0.18	0.4
Uninfected Cells																				
Asparagine synthetases, <i>M. sativa</i>	Mtr.8498.1.S1_at	11.95	0.67	0.62	0.66	0.42	0.29	0.8	0.2	0.06	0.65	0.19	0.02	0.26	2.57	0.25	0.36	6.86	0.03	0.18
Asparagine synthetases, <i>M. sativa</i>	Mtr.8499.1.S1_at	8.1	0.34	0.22	0.48	0.27	0.14	0.74	0.18	0.06	0.65	0.13	0.01	0.17	1.75	0.51	0.5	33.86	0	0.02

Gene Reference	Medicago GeneChip ID	A Mean	Meristem			Distal infection zone			Proximal infection zone			Infection zone			Infected cell			Uninfected cell		
			EF	p	q	EF	p	q	EF	p	q	EF	p	q	EF	p	q	EF	p	q
Asparagine synthetases, <i>M. sativa</i>	Mtr.32211.1.S1_at	3.5	0.25	0.03	0.21	0.44	0.17	0.76	0.26	0.03	0.58	0.24	0.01	0.15	3.57	0.04	0.13	9.77	0	0.02
Asparagine synthetases, <i>M. sativa</i>	Mtr.7084.1.S1_at	4.52	0.57	0.35	0.56	0.67	0.49	0.85	0.56	0.33	0.81	0.52	0.18	0.54	0.73	0.59	0.53	6.44	0.01	0.07
MtbHLH1	Mtr.10993.1.S1_at	7.33	2.09	0.22	0.49	0.76	0.64	0.87	0.69	0.54	0.85	0.65	0.38	0.66	0.1	0	0.01	9.18	0	0.03
MtENOD8.2, This study	Mtr.8511.1.S1_at	4.39	0.25	0.02	0.16	0.77	0.61	0.87	0.17	0	0.33	0.26	0.01	0.13	0.24	0.01	0.07	123.34	0	0

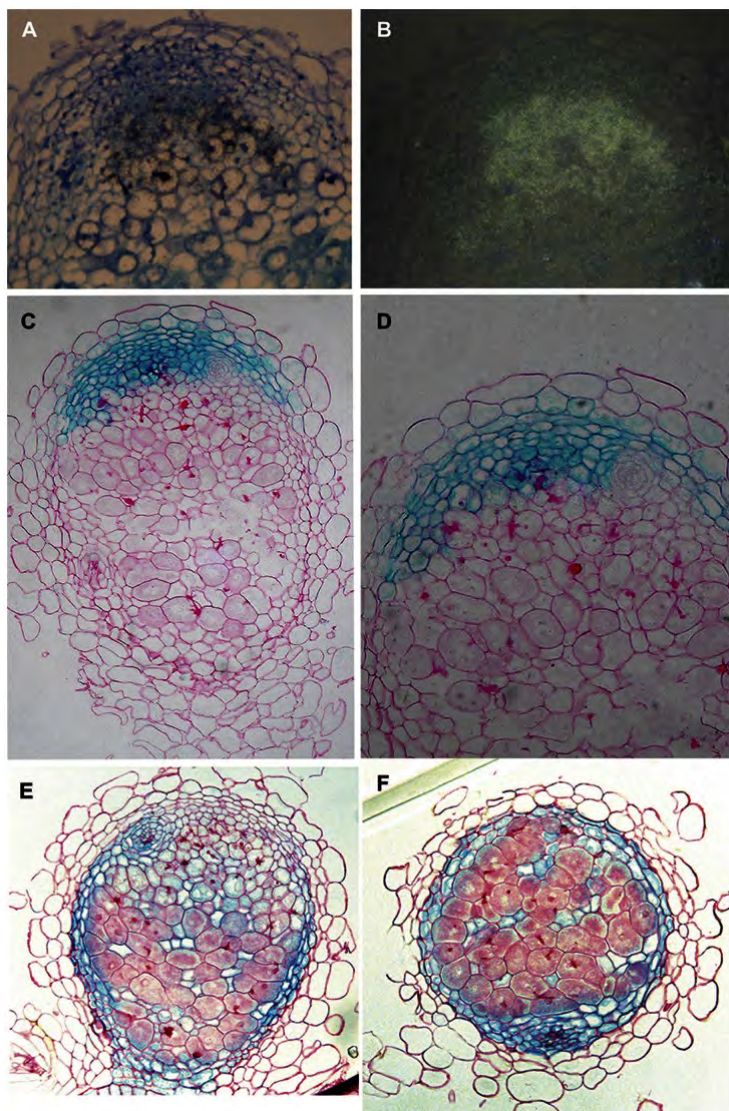


Figure 6.2 LCM data validation. (a,b) In situ localization of MtENOD12 (antisense probe) in the infection zone of longitudinal sections of 14-day-old Medicago nodules, representing brightfield (a; signal appears as black dots) and epipolarization images (b). (c,d) Promoter-GUS analysis of Medicago ROP GTPase (Mtr.35940.1.S1_at, Mtr.15539.1.S1_at), showing β -glucuronidase (GUS) activity in the nodule meristem. (e,f) Promoter-GUS analysis of MtENOD8.2, showing β -glucuronidase activity in the non-infected cells of the nodule as well as in the nodule parenchyma.

In contrast to uninfected cells, several genes have been reported that show specific/highly enriched expression in the infected cells of the fixation zone. These include: Leghemoglobin genes [Ott et al., 2005], aquaporin Nodulin-26 [Fortin et al., 1987], Nodulin-25 [Mergaert et al., 2003], sulfate transporter SST1 [Krusell et al., 2005], NCRs including for example NCR001/NCR035 [Mergaert et al., 2003; Van de Velde et al., 2010], and Calmodulin-like/CaML genes [Liu et al., 2006]. All these genes indeed show specific/enriched expression in the LCM infected cells from the fixation zone (Table 6.2) confirming the specificity of the LCM data.

Cell/Tissue-specific Characteristics of Gene Expression in Medicago Root Nodules

Next, we examined the nodule cell/tissue-specific transcriptomes for characteristics that may be linked to the specific processes that occur in these cell types, with a special focus on symbiosome development and function.

“Meristem enriched”

The nodule meristem was captured to serve as one of the uninfected reference/control tissues for the infected nodule cell types. However, in addition, the meristem enriched transcriptome gives first insight into molecular players that controls its organization.

Among the genes that appear nodule “meristem enriched” are many genes that are associated with meristematic/ dividing cells. These include the WUSCHEL-RELATED HOMEBOX5 gene (MtWOX5; Mtr.33304.1.S1_at), SCARECROW (MtSCR; Mtr.39371.1.S1_at) and BABY BOOM gene (MtBBM; Mtr.21627.1.S1_at) which are known to control stem cell activity in the root meristem [Galinha *et al.*, 2007; Peret *et al.*, 2009]. This supports the hypothesis that nodule formation recruits a program involved in lateral root formation [Couzigou *et al.*, 2012; Ferguson and Reid, 2005]. Furthermore, the array data indicate an important role for auxin signaling in the control and maintenance of a functional nodule meristem. Several auxin signaling related genes show a “meristem specific” expression in the nodule. These include for example: AUX/IAA’s (Mtr.43054.1.S1_at, Mtr.38407.1.S1_at, Mtr.43345.1.S1_at, Mtr.10432.1.S1_at, Mtr.48811.1.S1_at, Mtr.13714.1.S1_at, Mtr.41219.1.S1_at, Mtr.33279.1.S1_at), ARF’s (Mtr.26217.1.S1_at, Mtr.35827.1.S1_at, Mtr.11167.1.S1_at, Mtr.39377.1.S1_at, Mtr.24462.1.S1_at, Mtr.44217.1.S1_at), TIR1-like F-box (Mtr.37555.1.S1_at), PIN auxin efflux carriers (Mtr.45124.1.S1_at, Mtr.38716.1.S1_at) and auxin responsive genes such as GH3-like (Mtr.6663.1.S1_at, Mtr.40094.1.S1_at, Mtr.41237.1.S1_at) and SAUR-like genes (Mtr.20120.1.S1_at, Mtr.19927.1.S1_x_at). The importance of auxin in the nodule meristem was also suggested from the activation of auxin responsive promoters in the nodule meristem [Grunewald *et al.*, 2009]. Furthermore, auxin signaling has been linked to the control of nodule numbers in the process of autoregulation. One of the genes that is

highly expressed in the nodule meristem is the *Medicago* ortholog (Mtr.43054.1.S1_at) of IAA14/SLR (SOLITAIRY ROOT), which has been shown to control lateral root formation [Fukaki *et al.*, 2002; Vanneste *et al.*, 2005]. In *Arabidopsis*, a stabilizing mutation in IAA14 blocks lateral root formation by inhibiting the auxin response factors ARF7 and ARF19 [Fukaki *et al.*, 2002; Okushima *et al.*, 2005]. Interestingly, several mutants, such as the pea *cochleata* and *Medicago* *noot* mutant, have been identified where the nodule meristem switches to a root meristem and roots emerge from the nodules [Brewin, 2004; Ferguson and Reid, 2005]. Therefore, the upregulation of IAA14 expression in the nodule meristem may play a role in inhibiting the switch to a lateral root meristem. However, given the number of auxin-related signaling genes, auxin signaling in the nodule meristem is likely to be a complex process involving various feedback loops.

“Infection zone enriched”

The infection zone data set may contain numerous candidate genes that control the formation and development of symbiosomes. The nodule-specific signal peptidase subunit MtDNF1/DAS12, the putative metallo-peptidase MtMMPL1 and the AP2/ERF transcription factor MtEFD have indeed been shown to control infection and symbiosome development in this part of the nodule. MtEFD has been shown to be able to induce the expression of the A-type cytokinin response regulator MtRR4, which is thought to negatively regulate cytokinin signaling [Vernie *et al.*, 2008]. MtRR4 (Mtr.9656.1.S1_at) indeed shows specific expression in the infection zone, with highest expression in the proximal part (see transcriptional regulators below). Therefore, downregulation of cytokinin signaling in the infection zone may be required for proper differentiation of symbiosome and nodule cells.

Terminal symbiosome differentiation is triggered by nodule-specific cysteine-rich peptides (NCRs) that resemble antimicrobial peptides. These NCRs contain a N-terminal signal peptide, which is processed by a nodule specific signal peptidase complex containing DNF1 that is active in the infection zone of the nodule, by which these peptides are targeted to the symbiosomes via a secretory pathway [Van de Velde *et al.*, 2010; Wang *et al.*, 2010]. Most NCR peptides are specifically induced in the infected cells of the infection zone, as also determined by in situ hybridization or promoter-GUS analysis [Mergaert *et al.*, 2003; Van de Velde *et al.*, 2010]. However, several NCR encoding genes (Mtr.35829.1.S1_at, Mtr.29559.1.S1_at, Mtr.37119.1.S1_at) are specifically enriched in the infection zone, of which most tend to be higher expressed in the proximal part of the infection zone where terminal differentiation is observed (see also “proximal enriched” below). These NCRs may be key candidates that initiate the bacterial differentiation process.

“Distal infection zone enriched”

To identify “distal infection zone enriched” genes we selected infection zone enriched genes that are >2x enriched in the distal infection zone compared to the proximal infection zone. Among these genes are ENOD11 (Mtr.13473.1.S1_at), ERN1 (Mtr.7556.1.S1_at), ERN2 (Mtr.43947.1.S1_at) and MtN2 (Mtr.3197.1.S1_at) [Andriankaja *et al.*, 2007; Gamas

et al., 1996; Journet *et al.*, 2001; Liu *et al.*, 2006]. It has been shown that the AP2/ERF transcription factors ERN1 and ERN2 function in the Nod factor signaling pathway and bind to a conserved motif GCAGGCC (NF-box) in the promoter region of ENOD11 where they act as transcriptional activators [Liu *et al.*, 2006]. MtERN1 has been shown to be required for infection thread initiation and maintenance of infection thread growth in the epidermis [Middleton *et al.*, 2007]. Therefore, it can be hypothesized that ERN1 similarly controls infection events in the distal infection zone of the nodule through the activation of specific genes. It is known that the rhizobial nod genes involved in Nod factor production are still expressed by rhizobia inside infection threads in the distal infection zone of the nodule [Schlaman *et al.*, 1991; Sharma and Signer, 1990], where also the Nod factor receptors are expressed [Limpens *et al.*, 2005] and that they are switched off as soon as the bacteria are released into the cells [Marie *et al.*, 1994]. This suggests that Nod factor (NF) perception and signaling occur in these cells. To investigate whether this is also reflected in the LCM expression data, we compared the induction of genes 24 hours after NF treatment in the root (reported by Czaja *et al.* [2012]) with the genes specifically enriched in the apical part of nodule. This showed that ~20% (10 genes) of the “distal infection zone specific” genes are also induced 24 hours after NF treatment in plantlet roots, whereas only 1,5% (13) of the meristem specific genes or 4% (3) proximal infection zone specific genes are induced by Nod factor treatment there. This supports the hypothesis that NF signaling occurs at the transition from the meristem to the distal infection zone. However, overall, <10% of the 283 NF-induced genes show specific expression in the apical part of the nodule, which suggests that many of the 24 h NF-induced genes are specifically induced in root tissues.

An interesting gene that shows “specific” expression in the distal infection zone is the Medicago ortholog (Mtr.26489.1.S1_at) of a recently identified pectate lyase (LjNPL) in *Lotus japonicus*. LjNPL was shown to control infection thread formation revealing that the plant actively contributes to plant cell wall degradation to facilitate rhizobial infection [Xie *et al.*, 2012]. Therefore, MtNPL may also be involved in infection thread formation in the nodule and/or the formation of unwallled infection droplets to allow symbiosome formation. The putative MtNPL promoter region does not contain a conserved NF-box, indicating that different/additional transcription factors control the induction of this gene, such as the putative transcription factor NIN which was shown to bind to the LjNPL promoter [Xie *et al.*, 2012].

Another component that is implicated in rhizobial infection is the ARP2/3 complex which controls actin polymerization. Mutations in the SCAR/WAVE complex, involved in the activation of the ARP2/3 complex, block infection by rhizobia [Miyahara *et al.*, 2010]. Among the distal infection zone enriched genes is a subunit of the ARP2/3 complex (Mtr.37170.1.S1_at). Interestingly, an ortholog of this subunit was recently shown in *Lotus* to control rhizobial infection [Hossain *et al.*, 2012]. Therefore, control of the actin

cytoskeleton likely also plays a key role in the nodule to control infection thread formation and possibly symbiosome formation [Davidson and Newcomb, 2001].

One of the most specifically expressed genes in the distal infection zone encodes a putative protease inhibitor, Mtr.35511.1.S1_at. This gene is also highly induced in arbuscular mycorrhizal (AM) roots, specifically in cells containing arbuscules [Gaude *et al.*, 2012]. It has recently become clear that rhizobia recruited the signaling pathway, including lipochitooligosaccharide signal molecules and receptor, from the ancient AM symbiosis to establish an intracellular symbiotic interface [Maillet *et al.*, 2011; Pislariu and Dickstein, 2007a]. Therefore, it is tempting to speculate that this protease inhibitor is involved in the intracellular accommodation of both symbionts. However, despite the shared signaling pathway there is overall only a limited overlap in genes that show enriched expression in mycorrhized roots and symbiosome containing nodule cells.

“Proximal infection zone enriched”

Among the genes that show a “proximal infection zone enriched” expression is the nodule-specific AGC kinase gene IRE (Mtr.15644.1.S1_s_at) [Pislariu and Dickstein, 2007b]. AGC kinases are key regulators of cell growth and MtIRE could potentially play an important role in symbiosome and/or nodule cell enlargement, possibly through the regulation of vesicle trafficking or cytoskeletal organization [Pislariu and Dickstein, 2007a].

Another striking (distal and) proximal infection zone specific gene is a close homolog of the CLAVATA1-related AtBAM3 receptor-like kinase (Mtr.4752.1.S1_at). In Arabidopsis BAM kinases regulate meristem function at shoot and flower meristems through complex interactions with CLAVATA signaling [Deyoung and Clark, 2008]. CLE peptides have been identified as ligands for such receptor-like kinases and another CLAVATA1 homolog, in Medicago called SUNN, has been shown to control nodule number in the process of autoregulation of nodule numbers [Mortier *et al.*, 2010]. It is therefore tempting to speculate that MtBAM3 plays a role in the perception of CLE peptides (such as the recently identified MtCLE12 and MtCLE13) in the nodule to control the balance between cell proliferation and differentiation.

As mentioned above, terminal symbiosome differentiation is triggered by nodule-specific NCR peptides [Van de Velde *et al.*, 2010]. Several NCR peptides appear most highly induced in the proximal part of the infection zone coinciding with the induction of symbiosome differentiation. These include: Mtr.4538.1.S1_at, Mtr.48527.1.S1_at and Mtr.10836.1.S1_at. Most of these NCR genes, including the infection zone-enriched NCRs Mtr.35829.1.S1_at, Mtr.29559.1.S1_at, Mtr.37119.1.S1_at, already show enriched expression in the distal infection zone. Therefore, these NCR's may be key NCR peptides to initiate symbiosome differentiation.

Several genes involved in cytokinin signaling show highest expression in the proximal infection zone. These include a histidine phosphotransfer encoding gene (Mtr.11120.1.S1_at), two cytokinin-specific phosphoribohydrolase LOGs (Mtr.39530.1.S1_at, Mtr.50458.1.S1_at) which activate cytokinins [Kurakawa *et al.*, 2007], as well as two A-type RR genes (Mtr.9656.1.S1_at (MtRR4), Mtr.17273.1.S1_s_at) and a cytokinin oxidase (Mtr.14413.1.S1_at) that negatively regulate cytokinin signaling. Therefore, we speculate that cytokinin signaling is tightly regulated in the (proximal) infection zone of the nodule to control the proper differentiation of nodule cells and symbiosomes.

Differential expression of the Nod factor signaling genes inside the nodule

Nod factor perception and signaling has mostly been studied in the root epidermis. Our cell- and tissue-specific transcriptome analysis support the notion that NF perception also plays an important role inside the nodule. Especially at the border of the meristem and the distal infection zone, where the Nod factor receptors NFP and LYK3 are also mostly present [Arrighi *et al.*, 2006; Limpens *et al.*, 2003; Smit *et al.*, 2007] (Table 6.3). This is also the area where rhizobium bacteria are still producing Nod factors inside the infection threads [Marie *et al.*, 1994; Schlaman *et al.*, 1991]. Nod factor perception at the epidermis is known to activate a signaling cascade that triggers transcriptional responses in the nucleus. This signaling cascade is also required to establish an arbuscular mycorrhizal symbiosis and is therefore called the common symbiotic (sym) pathway [Gough and Cullimore, 2011; Oldroyd, 2013].

The core components of this Nod factor signaling cascade have been identified by genetics approaches, especially in the model legumes Lotus and Medicago [Jones *et al.*, 2007]. In brief, after perception by the Nod factor receptors, the LRR-type receptor SymRK present at the plasma membrane [Limpens *et al.*, 2005] is required to generate a secondary signal that triggers calcium oscillations in the nucleus [Oldroyd and Downie, 2004; Oldroyd *et al.*, 2011]. This calcium spiking response additionally requires the presence of a putative cation channel DMI1 at the nuclear envelope [Ane *et al.*, 2004] as well as components of a nuclear pore complex [Kanamori *et al.*, 2006; Saito *et al.*, 2007]. This calcium spiking is interpreted by the calcium and calmodulin-dependant kinase CCaMK/DMI3 [Levy *et al.*, 2004; Mitra *et al.*, 2004]. DMI3 interacts with Cyclops/IPD3 [Limpens *et al.*, 2011; Messinese *et al.*, 2007], which may act a transcription factor. Nod factor induced transcriptional responses additionally require the transcription factors NSP1 and NSP2 and NIN [Kalo *et al.*, 2005; Marsh *et al.*, 2007; Smit *et al.*, 2005].

As the Nod factor receptors, NFP and LYK3, appear to be enriched at the transition from the meristem to the distal infection zone (Table 6.3), it might be expected that expression of

the common sym pathway components is also enriched in this part of nodule. Alternatively, in case the common sym pathway is activated by other signals and controls additional signaling events, the expression domains may differ. To examine this we determined the expression domains of the common sym pathway components using our LCM array data (Table 6.3).

Previous *in situ* hybridization studies have shown that DMI2 and DMI3 are most highly expressed in the apical part of the nodule coinciding with the expression domain of LYK3 [Limpens *et al.*, 2005]. Indeed DMI2 and DMI3 have been implicated in controlling the release of the bacteria from the infection threads which occurs in this part of the nodule [Capoen *et al.*, 2005; Limpens *et al.*, 2005] [Godfroy *et al.*, 2006]. However, the laser capture data suggest a role for DMI2 and DMI3 also at later stages of nodule/symbiosome development. In fact, we observe a only slight (non-significant) enrichment of DMI2 and DMI3 in the meristem and (distal) infection zone (Table 6.3). On explanation for the discrepancy with the *in situ* hybridization data could be that the probes on the Gene Chip do not reliably detect these genes in the laser captured samples. However, a role for DMI2 at later stages of symbiosome development is supported by the phenotype of the *SYM41* mutant, which represents a weak DMI2/SYM19 allele in pea resulting in reduced expression levels [Ovchinnikova, 2012]. In pea *sym41* nodules release from the infection threads still occurs but the symbiosomes fail to differentiate. This suggests a role for DMI2 in symbiosome differentiation [Morzhina *et al.*, 2000; Ovchinnikova, 2012]. Furthermore, a translational fusion of DMI3 to GFP under the control of its native promoter showed that the expression domain of DMI3 in the nodule is much broader than that of the Nod factor receptors, extending towards the fixation zone [Smit *et al.*, 2005].

Even more striking, the cation channel DMI1 appears most specifically enriched in the infected cells of the fixation zone (Table 6.3). This relatively late expression domain is supported by the data from [Moreau *et al.*, 2011] but is somewhat different from *in situ* hybridization and promoter-GUS analyses, which indicate strongest expression throughout the entire infection zone [Limpens *et al.*, 2005; Riely *et al.*, 2007]. Although, these differences may be caused by the probes in the micro array that are used to this gene, our data as well as the *in situ* and promoter-GUS studies indicate that DMI1 is more broadly expressed than the Nod factor receptors, DMI2 and DMI3 inside the nodule. This suggests an additional, so far unknown, role for DMI1 at late stages of nodule/symbiosome development.

The same holds for the interacting protein of DMI3, IPD3. IPD3 appears most enriched in the entire infection zone and especially in the infected cells of the fixation zone, which is supported by promoter-GUS analysis (Table 6.3), [Messinese *et al.*, 2007; Ovchinnikova *et al.*, 2012]). As the expression domain of IPD3 appears to be even broader than that of DMI3, it suggests that IPD3 has an additional function. Mutant analysis show that in the earlier stages IPD3 is required for release of the bacteria from the infection threads, but may also control symbiosome differentiation [Benaben *et al.*, 1995; Horvath *et al.*, 2011;

Ovchinnikova *et al.*, 2012]. Due to these early blocks roles for IPD3 at later stages have so far not been revealed.

The transcription factors NSP1 and NSP2 do not show enrichment in any of the cells/tissues examined and appear to be expressed at a relatively low level. This is similar to their expression profile in roots, where expression of NSP1/2 is also not induced upon Nod factor application [Kalo *et al.*, 2005; Smit *et al.*, 2005]. Complementation studies using a non-legume *NSP1* gene from *Nicotiana benthamiana* have also suggested a role for NSP1 in symbiosome development or maintenance inside the nodule.

In contrast to NSP1 and NSP2, the putative transcription factor NIN, which is induced upon Nod factor application in the root, is expressed broadly throughout the infection zone, with strongest enrichment in the proximal infection zone (Table 6.3), in agreement with *in situ* hybridizations in pea [Borisov *et al.*, 2003]. This also suggests an important role for NIN at later stages of nodule/symbiosome development.

Table 6.3: Differential expression of the known Nod Factor signaling genes as enrichment factor (EF) of the transcript compared to the mean of all samples. Significant ($p < 0.01$, $q < 0.1$) enrichment is shown in blue.

Gene	Medicago GeneChip ID	A Mean	Meristem			Distal infection zone			Proximal infection zone			Infected cell			Uninfected cell			Published expression	Reference
			EF	p	q	EF	p	q	EF	p	q	EF	p	q	EF	p	q		
NFP	Mtr.15789.1.S1_at	3.788	8.179	0.004	0.071	7.799	0.004	0.348	0.631	0.463	0.834	0.152	0.007	0.045	0.163	0.009	0.094	Infection zone	[Arrighi <i>et al.</i> , 2006]
LYK3	Mtr.142.1.S1_s_at	3.8845	23.411	0.000	0.003	9.522	0.000	0.132	0.344	0.044	0.615	0.111	0.000	0.006	0.117	0.000	0.013	Infection zone	[Limpens <i>et al.</i> , 2005]
DMI2	Mtr.51192.1.S1_at	8.1981	1.322	0.448	0.603	1.186	0.640	0.875	0.693	0.322	0.809	0.877	0.720	0.576	1.049	0.895	0.683	Infection zone	[Limpens <i>et al.</i> , 2005]
DMI1	Mtr.124.1.S1_s_at	2.3641	0.415	0.164	0.443	0.542	0.326	0.813	0.424	0.174	0.754	9.767	0.002	0.017	1.075	0.907	0.686	Infection zone	[Limpens <i>et al.</i> , 2005; Riely <i>et al.</i> , 2007]
DMI3	Mtr.8930.1.S1_at	9.444	1.424	0.327	0.549	1.555	0.225	0.785	1.372	0.379	0.818	0.806	0.546	0.512	0.408	0.021	0.153	Infection zone	[Limpens <i>et al.</i> , 2005]
IPD3	Mtr.42174.1.S1_at	12.2548	0.313	0.000	0.011	1.219	0.406	0.831	1.013	0.955	0.896	2.298	0.003	0.023	1.124	0.620	0.605	Infection/ fixation zone	[Ovchinnikova <i>et al.</i> , 2012]
NSP1	Mtr.6956.1.S1_at	1.4359	1.103	0.430	0.595	0.847	0.191	0.771	1.270	0.068	0.663	0.932	0.568	0.521	0.904	0.421	0.530		
NSP2	Mtr.44789.1.S1_at	4.3405	1.318	0.443	0.601	1.609	0.195	0.773	1.039	0.914	0.892	1.391	0.362	0.427	0.326	0.006	0.070		
NIN	Mtr.28094.1.S1_at	11.9669	0.394	0.001	0.039	1.57	0.076	0.676	2.240	0.004	0.336	1.193	0.466	0.478	0.604	0.050	0.235	Meristem/ infection zone	[Borisov <i>et al.</i> , 2003]
SYMREM1	Mtr.13003.1.S1_at	11.6771	0.093	0.000	0.000	2.347	0.002	0.273	2.972	0.000	0.104	1.978	0.010	0.054	0.780	0.299	0.477	Infection/ fixation zone	[Lefebvre <i>et al.</i> , 2010]
FLOT4	Mtr.11786.1.S1_at	2.1321	0.857	0.464	0.609	1.193	0.404	0.830	1.009	0.966	0.897	1.167	0.465	0.478	0.831	0.381	0.514	Infection zone	[Haney and Long, 2010]

The same holds for the Nod factor induced remorin gene, *SYMREM1*. *SYMREM1* has been identified as an interacting protein of the receptors LYK3, NFP and DMI2, and has been postulated to play a role in establishing a signaling complex to control the release of the bacteria from the infection threads [Lefebvre *et al.*, 2010]. However, the expression domain of *SYMREM1* in the nodule is much broader than that of the receptors covering the infection zone and the infected cells of the fixation zone. Therefore, it is likely that *SYMREM* plays additional roles in symbiosome development in the infection or fixation zone.

Taken together these analyses show that there is little co-enrichment of the Nod factor signaling pathway components and the Nod factor receptors in the meristem and distal infection zone. This might suggest that (parts of) the Nod factor signaling pathway can be activated via other receptors or signal molecules in the nodule to control later stages of nodule development. However, they are all expressed in the region where the two Nod factor receptor genes are active. So in this region they can be involved in Nod factor signaling.

Additional Nod factor receptors in the nodule

It has been hypothesized that Nod factors might be perceived by multiple (complexes) of LysM domain containing receptors and that different receptor complexes may be active in different cell types [Arrighi *et al.*, 2006; Gough, 2003; Madsen *et al.*, 2011]. Medicago contains multiple LysM domain containing proteins some of which are expressed in nodules, raising the possibility that these members may play additional roles in Nod factor perception in the nodule [Arrighi *et al.*, 2006; Zhang *et al.*, 2007]. Therefore, we made a survey of all LysM domain containing proteins on the Medicago Gene Chip and analyzed which LysM domain containing proteins are enriched in the different nodule tissues. These data are summarized in Table 6.4. With the exception of LYR3 and LYK6 all previously reported LysM-domain containing receptor-like proteins [Arrighi *et al.*, 2006] where represent on the Medicago gene chip.

Several LysM-domain containing proteins are enriched in the meristematic region, coinciding with the expression of NFP and LYK3 there. These include the type-II LysM domain containing receptor kinase LYR4 as well as the potentially GPI-anchored proteins LYM1 and LYM2 [Arrighi *et al.*, 2006; Fliegmann *et al.*, 2011]. LYR4 is found enriched in the uninfected cells together with LYM2. Therefore, these may play a role in the formation and development of the uninfected cells. LYM homologs in rice and Arabidopsis have been implicated in chitin signaling and peptidoglycan signaling as part of a receptor complex with LysM domain containing receptor kinases [Buist *et al.*, 2008; Shimizu *et al.*, 2010; Willmann *et al.*, 2011]. The strong enrichment of these proteins especially in the meristematic region, may suggest that they play an important, currently unknown role in Nod factor perception as part of receptor complexes.

In the distal infection, co-inciding with NFP and LYK3 expression, the receptor kinase LYK10 appears to be specifically induced. This makes LYK10 an intriguing candidate to play a role in the signaling events that control the uptake of the bacteria into the nodules cells. LYK10 might act redundantly to form additional complexes with NFP and/or LYK3 in these cells.

Table 6.4: Differential expression of *LysM* genes as enrichment factor (EF) of the transcript compared to the mean of all samples. Significant ($p < 0.01$, $q < 0.1$) enrichment is shown in blue.

Gene	Annotation	Medicago GeneChip ID	A	Mean	Meristem			Distal infection zone			Proximal infection zone			Infected cell enrichment			Uninfected cell enrichment		
					EF	p	q	EF	p	q	EF	p	q	EF	p	q	EF	p	q
AC235671_2	LYM2	Mtr.12383.1.S1_at	6.9018	26.410	0.000	0.018	0.298	0.112	0.722	0.764	0.712	0.871	0.036	0.000	0.005	4.625	0.049	0.234	
Medtr5g086310.1	LYK3	Mtr.142.1.S1_s_at	3.8845	23.411	0.000	0.003	9.522	0.000	0.132	0.344	0.044	0.615	0.111	0.000	0.006	0.117	0.000	0.013	
Medtr5g019040.1	NFP	Mtr.15789.1.S1_at	3.788	8.179	0.004	0.071	7.799	0.004	0.348	0.631	0.463	0.834	0.152	0.007	0.045	0.163	0.009	0.094	
CR936328_37.4 / Medtr5g085790.1	LYR4	Mtr.36136.1.S1_at	5.1135	7.195	0.003	0.066	0.193	0.010	0.461	0.573	0.340	0.813	0.206	0.013	0.066	6.107	0.006	0.069	
Medtr3g072410.1	LYM1	Mtr.9585.1.S1_at	5.8634	3.925	0.006	0.096	1.647	0.264	0.800	1.932	0.146	0.732	0.451	0.084	0.198	0.178	0.001	0.022	
Medtr5g033490.1	LYK10	Mtr.25148.1.S1_at	4.1953	1.880	0.235	0.496	4.537	0.010	0.452	1.012	0.982	0.898	0.384	0.080	0.194	0.302	0.033	0.192	
Medtr5g086120.1	LYK4	Mtr.25025.1.S1_s_at	1.5279	1.685	0.003	0.060	1.107	0.497	0.851	0.942	0.687	0.867	0.739	0.055	0.155	0.771	0.094	0.310	
Medtr5g086090.1	LYK4	Mtr.51452.1.S1_x_at	2.8357	1.581	0.149	0.428	1.775	0.076	0.676	1.100	0.757	0.876	0.512	0.042	0.132	0.633	0.150	0.371	
MTR_5g086080	LYK5	Mtr.25028.1.S1_at	1.3791	1.395	0.020	0.182	1.110	0.426	0.836	0.948	0.680	0.867	0.801	0.104	0.225	0.850	0.224	0.429	
Medtr5g086040.1	LYK6	Mtr.15754.1.S1_s_at	3.7379	1.318	0.528	0.632	0.926	0.860	0.899	0.604	0.256	0.787	1.007	0.988	0.649	1.348	0.495	0.560	
Medtr5g086110.1	LYR12	Mtr.15758.1.S1_at	2.0784	1.238	0.225	0.489	1.666	0.008	0.427	0.736	0.090	0.691	0.955	0.787	0.597	0.690	0.043	0.221	
Medtr5g086040.1	LYK6	Mtr.15753.1.S1_s_at	2.3897	1.203	0.335	0.553	1.144	0.479	0.846	0.843	0.372	0.817	0.786	0.213	0.330	1.097	0.627	0.607	
AC157350_6.4	LYR11	Mtr.7967.1.S1_at	1.9142	1.196	0.271	0.519	0.892	0.478	0.846	1.106	0.530	0.845	0.791	0.155	0.279	1.071	0.667	0.620	
Medtr5g086040.3	LYK6	Mtr.33379.1.S1_s_at	1.4867	1.164	0.344	0.559	1.020	0.898	0.904	0.873	0.395	0.821	1.258	0.159	0.283	0.767	0.107	0.328	
Medtr3g080050.1	LYK9	Mtr.14019.1.S1_at	1.7878	1.158	0.316	0.544	1.582	0.005	0.376	0.951	0.729	0.874	0.863	0.315	0.400	0.665	0.011	0.103	
Medtr5g086xxx	LYK2	Mtr.100.1.S1_at	2.2976	1.127	0.590	0.654	0.906	0.656	0.877	1.243	0.333	0.811	1.181	0.457	0.474	0.667	0.082	0.295	
Medtr5g085790.1	LYR4	Mtr.13318.1.S1_at	2.0098	1.109	0.511	0.626	1.012	0.937	0.908	0.839	0.268	0.794	1.059	0.712	0.574	1.003	0.985	0.703	
contig_52036_1	LYK8	Mtr.45170.1.S1_at	1.5541	1.097	0.549	0.640	1.059	0.708	0.883	1.032	0.840	0.885	0.919	0.587	0.528	0.907	0.528	0.572	
Medtr8g078300.1	LYR1	Mtr.19870.1.S1_at	2.0283	1.093	0.610	0.659	1.201	0.302	0.806	0.957	0.800	0.881	1.230	0.245	0.353	0.647	0.022	0.158	
Medtr5g086030.1	LYK7	Mtr.51429.1.S1_s_at	1.6691	0.996	0.973	0.748	1.217	0.141	0.744	0.845	0.205	0.768	1.119	0.390	0.442	0.872	0.298	0.476	

[illegible]

Two novel LysM domain containing receptor kinases, here named LYR5 and LYR7 appear to be enriched in the infected cells of the fixation zone. As the bacteria inside in the infected cells are no longer producing Nod factors it is unlikely that these receptor kinases play a role in Nod factor signaling [Marie *et al.*, 1994]. However, a potential role in perceiving Nod factors from the apoplast cannot be ruled out. Alternatively, they could play a role in the perception of rhizobial peptidoglycan molecules or currently unknown molecules perceived by LysM domains.

Finally, several LysM domain containing proteins appear to be (specifically) enriched in the uninfected cells. Besides the earlier mentioned LYM2 and LYR4, these include LYK7, an F-box protein containing LysM domains (Mtr.41479.1.S1_at) and two previously unreported LYR-type proteins (lacking active kinase domains); here named LYR9 (Mtr.26304.1.S1_at) and LYR11 (Mtr.9195.1.A1_at)(Table 6.4). These proteins could be involved in the perception of bacteria in the apoplast to control the development of the uninfected cells.

From this analysis it is clear that the perception of Nod factors and Nod factor-like molecules in the nodule might be much more complex than previously anticipated. More work is need to unravel the interplay of this intriguing family of proteins.

CONCLUSION

Here we present a comprehensive gene expression map of an indeterminate Medicago nodule, covering the nodule meristem, (distal and proximal) infection zone as well as infected and uninfected cells from the fixation zone. Our LCM array data fit very well with published gene expression profiles and several cell/tissue specific genes were experimentally verified, indicating that the data may be used as digital “in situ”. Many nodule-specific processes that are essential for a successful nitrogen fixing symbiosis, such as symbiosome formation, differentiation and maintenance, nodule meristem development, nodule cell differentiation (infected vs uninfected cells), and metabolite transport processes in the nodule are still far from understood. Therefore, the cell- and tissue-specific data sets presented here offer a valuable resource for further functional studies.

ACKNOWLEDGEMENTS

This work was supported by the Niels Stensen Foundation (g) and the Dutch Organization for Scientific Research (NWO grant N° 3184319448). Helge Küster and Jörg D. Becker acknowledge support from the Fundação para a Ciência e a Tecnologia project PTDC/AGR–GPL/70592/2006.

MATERIAL AND METHODS

Plant growth and infection

Medicago truncatula accession Jemalong A17 was used. Nodulation was done according to Limpens *et al.* [2004] using 2 ml a suspension (OD₆₀₀ 0.1) of *Sinorhizobium meliloti* strain Sm2011 per plant in (agra)perlite saturated with nitrate-free Fåhræus medium. Three weeks after inoculation nodules were harvested for LCM. *Agrobacterium rhizogenes* mediated root transformation were performed as described by Limpens *et al.* [2004], using *A. rhizogenes* strain MSU440.

Laser capture microdissection

Three week-old nodules were fixed in Farmer's fixative (3:1 ethanol:acetic acid), after 30 min. vacuum, at 4 °C overnight. Fixed nodules were further dehydrated through an ethanol series: 75%, 85%, 100% (4x) for 15 min. each at room temperature (RT). At the first 100% ethanol step eosin B was added to facilitate the recognition of the nodule meristem during the sectioning steps. Nodules were subsequently infiltrated with xylene: ethanol 1:3, 1:1, 3:1 and finally 100% xylene (3x); 30 min at RT each. Next, the nodules were infiltrated with liquid filtered paraffin (Paraplast) at 60 °C for 2 days including 4 changes of paraffin. After solidification, 8 µm sections were cut on a RJ2035 microtome (Leica Microsystems, Rijswijk, The Netherlands). Only those consecutive sections that contained a well developed nodule meristem (based on eosin B staining observed using a binocular) were subsequently deparaffinized using 100% xylene 2x 5 min. each, air dried and immediately used for laser capture using a PixCell II LCM system (Arcturus). For each biological replicate, 8 consecutive sections containing ~50 cells/section were collected and used for RNA isolation. Sections that showed a distorted nodule ontology were discarded. Three biological replicates were collected per cell/tissue-type.

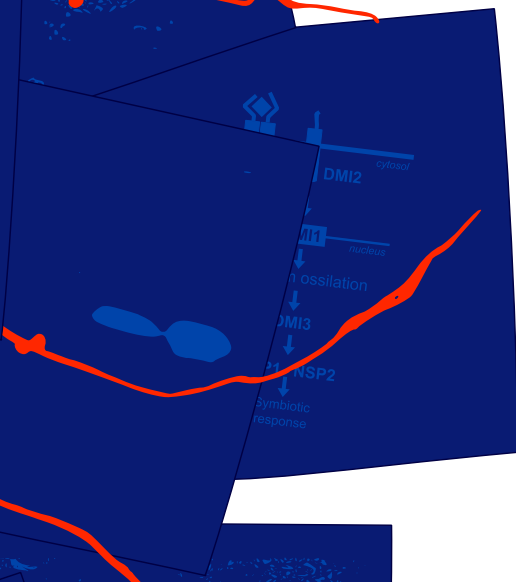
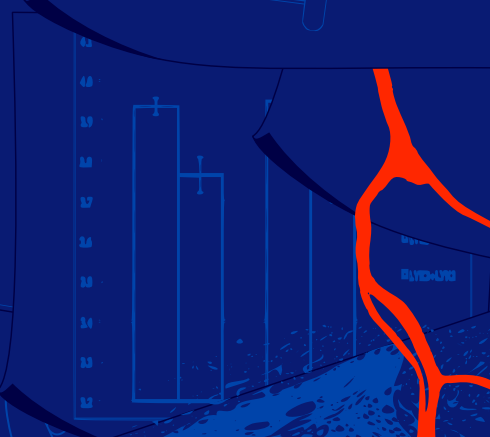
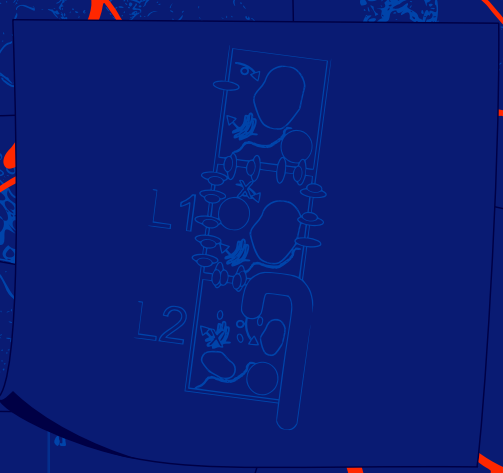
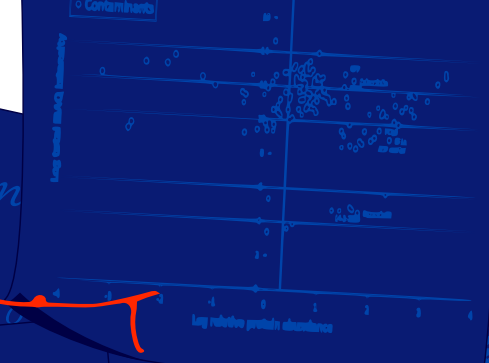
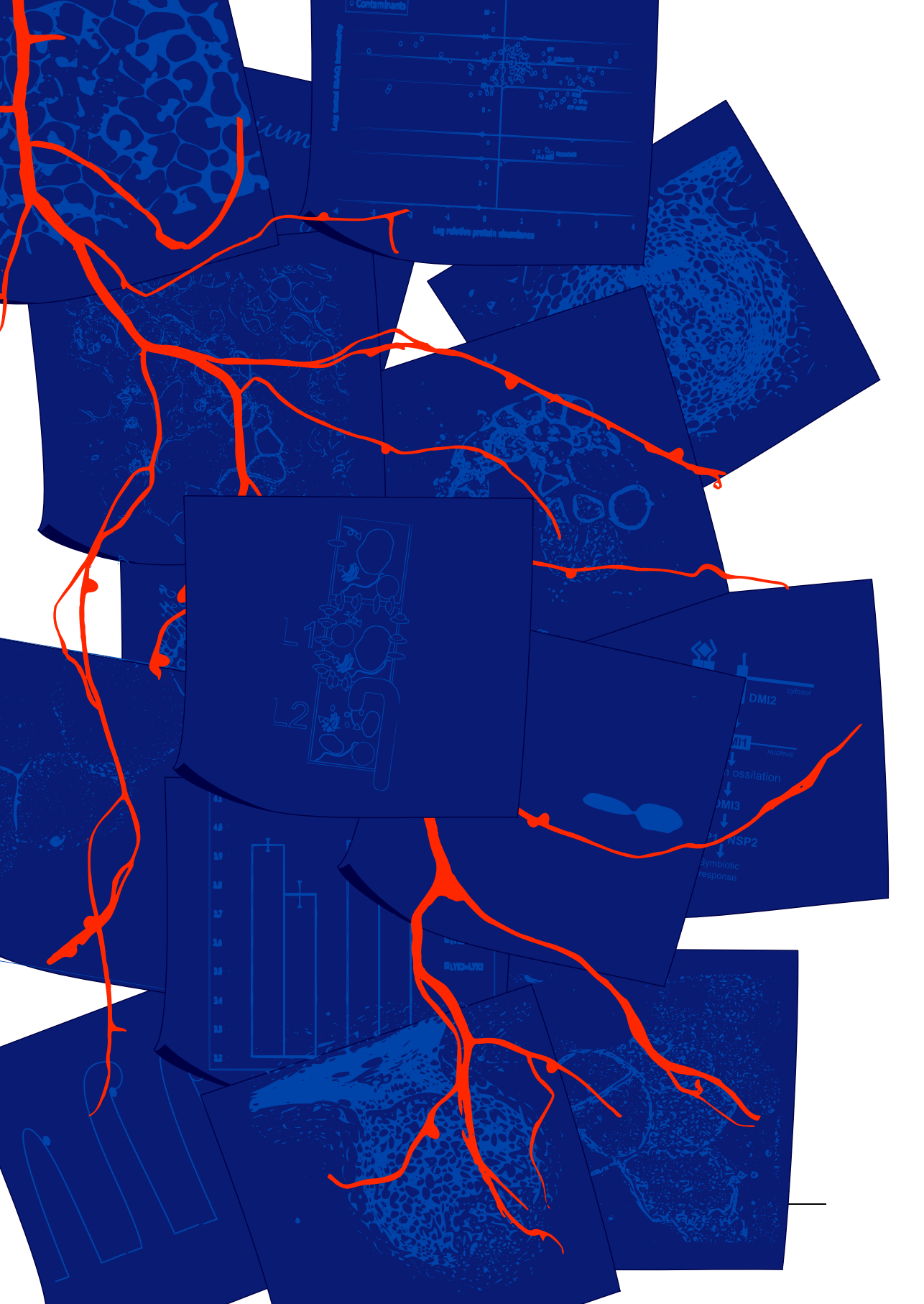
RNA extraction and GeneChip hybridizations

The Qiagen RNeasy Micro kit was used for RNA isolation according to manufacturer's instructions, with one modification: 50 ng poly-Inosine was added to 350 µl RLT buffer as carrier RNA. On-column DNase treatment was performed according to the manufacturer's recommendation. Amount and quality of the RNA isolated from the LCM samples was too low to be accurately determined using an Agilent 2100 Bioanalyzer due to the added poly-I. Quality of the RNA was verified after paraffin embedding and sectioning using agarose gel electrophoresis and using a ND-1000 spectrophotometer (NanoDrop Technologies).

RNA was processed for use on Affymetrix (Santa Clara, CA, USA) *Medicago* GeneChips. Samples were amplified according to the first amplification cycle of the Affymetrix Two-

cycle Target Labeling kit user manual. Briefly, total RNA containing spiked-in poly-A+ RNA controls was used in a reverse transcription reaction (Two-cycle Target Labeling kit; Affymetrix, Santa Clara, CA, USA) to generate first-strand cDNA. After second-strand synthesis, double-stranded cDNA was used in a 16 h in vitro transcription (IVT) reaction to generate aRNA (Two-cycle Target Labeling kit). The generated aRNA samples were then processed according to the Affymetrix GeneChip 3' IVT Express kit user manual. Briefly, 100 ng of aRNA was used in a reverse transcription reaction (GeneChip 3' IVT Express Kit; Affymetrix, Santa Clara, CA, USA) to generate first-strand cDNA. Double-stranded cDNA obtained by second-strand synthesis was then used in a 16 h IVT reaction to generate aRNA (GeneChip 3' IVT Express Kit). Size distribution of in vitro transcribed aRNA and fragmented aRNA, respectively, was assessed via an Agilent 2100 Bioanalyzer (Agilent, Böblingen, Germany), using an RNA 6000 Nano Assay. 30 µg to 40 µg of fragmented aRNA was added to a 250-µl hybridization cocktail containing hybridization controls. 200 µl of the mixture was hybridized on GeneChips for 16 h at 45°C. Standard post-hybridization wash and double-stain protocols (FS450_0001; GeneChip HWS kit; Affymetrix, Santa Clara, CA, USA) were used on an Affymetrix GeneChip Fluidics Station 450. GeneChips were scanned on an Affymetrix GeneChip scanner 3000 7G.

Packages from the Bioconductor project [Gentleman *et al.*, 2004] were used to analyse the array data according to Storey and Tibshirani [2003]. Only the 5 most 3'located probe sets on the GeneChip were used to account for observed 3'bias. To identify genes enriched in a particular LCM sample, genes were first selected that show enriched expression, at least 2-fold higher ($p < 0.01$, $q < 0.1$), compared to the average of all other LCM samples. An intensity-based moderated T-statistic (IBMT)[Sartor *et al.*, 2006] was used to calculate p-values and q-values corrected for multiple testing [van de Wiel *et al.*, 1990]. The obtained (relative) expression values were further analyzed using Microsoft Office Excel 2007 software. Genes that showed ≥ 2 x more enrichment compared to all other samples were selected as “cell-type specific/enriched” genes. Expression data were further compared to expression data obtained from the Medicago Gene Expression Atlas (<http://mtgea.noble.org/v2/> [Benedito *et al.*, 2008]) and data (24h NF treatment) published by Czaja *et al.* [2012]. MapMan software (version 3.5.1) (<http://mapman.gabipd.org/web/guest/mapman>) was used to analyze gene profiles using the Mt_AFFY_Mt3.1_0510 mapping.



Chapter 7. GENERAL DISCUSSION

Nod factor perception at the root hair interface plays an essential role to trigger symbiotic responses leading to the formation of a root nodule and infection by rhizobium bacteria [D'Haeze and Holsters, 2002; Geurts and Bisseling, 2002; van Brussel *et al.*, 1992]. In addition to this essential role in initiating the symbiosis in the epidermis, it has become clear that Nod factor perception also plays key roles at later stages of nodule development and infection. This thesis reports the latest findings on Nod factor perception in the nodule of the model legume *Medicago truncatula* (Medicago). In Medicago Nod factors are perceived by at least two LysM-domain receptor kinases, named NFP and LYK3 [Arrighi *et al.*, 2006; Limpens *et al.*, 2003; Smit *et al.*, 2007]. In this final chapter the results that were obtained on the accumulation, internalization and function of NFP and LYK3 inside the nodule will be discussed and placed in the light of previously published data. We summarize our data in a model to explain the observed accumulation in a narrow zone at the apex of the nodule (Chapter 3). In this zone bacteria are released and the bacteria infect the nodules cells. The release in these cells is different from the release in the nodule primordium. This chapter discusses the apparent differences with respect to intracellular accommodation of the rhizobia and the stringency on Nod factor perception. Finally, the role of lipid domains (lipid rafts) in the rhizobium – legume symbiosis will be discussed.

ACCUMULATION OF THE NOD FACTOR RECEPTORS IN NODULES

In Chapter 3 we showed that NFP and LYK3 accumulate at the nodule apex. There, the receptors accumulate in a narrow zone of two cell layers (L1 and L2), which mark the border between meristem and infection zone. There are two aspects that need discussion: the accumulation per se and the accumulation in a narrow zone. Previous studies already indicated that Nod factor receptors are expressed at the nodule apex, as shown by *in situ* hybridizations [Limpens *et al.*, 2005]. Further, also other, downstream components of the Nod factor signaling cascade are expressed in nodules, especially in the (distal) infection zone. Several components were shown to be required for the release of rhizobia from the infection threads to allow their uptake and resulting symbiosome formation [Capoen *et al.*, 2005; Ovchinnikova *et al.*, 2012; Yano *et al.*, 2008]. Our data show that there is a very stringent control on the accumulation of the Nod factor receptors, which acts at a post-translational level, to control this process.

The ability to visualize the Nod factor receptors at the nodule apex is in sharp contrast to the data on LYK3 accumulation reported by Haney *et al.* [2011] who were the first to report

the localization and accumulation of a Nod factor receptor in a legume. They could not visualise LYK3 in Medicago nodules. In contrast to our data, Haney *et al.* [2011] showed (a) the dynamic localization of LYK3 in root hairs of Medicago. LYK3 localizes in highly mobile puncta in the plasma membrane of root hairs prior to contact with rhizobia. Furthermore, they show (b) that upon stimulation by rhizobia (but not Nod factors) LYK3 is no longer dynamic, but increasingly co-localizes in puncta with the flotillin FLOT4, a presumed marker for lipid rafts. Further, (c) at four days after inoculation LYK3 could still be detected along the length of the infection thread membrane inside the root hairs.

Haney *et al.* [2011] are the first to show the localization and accumulation of a Nod factor receptor in a legume. From the phenotype of the receptor mutants it is known that they have a crucial function in root hairs. Despite numerous attempts we (as well as others) were not able to reproduce these data on the localization of LYK3 in root hairs. Possibly the receptor accumulate in the root hairs at very low levels (near background levels), which impaired their visualization through fluorescence/confocal microscopy. However, also using the more sensitive spinning disk confocal microscopy we could not visualize LYK3-GFP in the roots hairs. There is genetic evidence which suggests that very low levels of LYK3 are sufficient, and possibly essential, to trigger symbiotic responses. Studies on *lyk3* mutants show that LYK3 is first essential for root hair deformation and infection thread initiation, but not for the earlier steps [Catoira *et al.*, 2001; Limpens *et al.*, 2003]. As LYK3 is not needed prior root hair deformation, one could suggest that LYK3 is also not present before root hair deformation. Furthermore, studies on a weak allele of *LYK3* show that a reduction of 90% of the *LYK3* transcript was still sufficient to trigger LYK3-dependent responses [Smit *et al.*, 2007]. Assuming that this reduction also results in a reduction in the amount of receptor protein that accumulates in root hairs, this suggests that the amount of receptor needed (and present?) in root hairs is low. Low steady state levels of LYK3 and NFP might even be required as there are indications that over-accumulation of these receptors can trigger defence responses [Lefebvre *et al.*, 2012; Pietraszewska-Bogiel *et al.*, 2013]. Therefore, there appears to be active mechanisms present in legume roots to keep the Nod factor receptors at low levels, similar to the situation inside nodules, as discussed further below. Though LYK3 should be present in root hairs, the low levels make it hard to study it there. This may also be the reason why we and others were not able to repeat the localization studies in root hairs.

Two remarkable conclusions of Haney *et al.* [2011] are that the change in dynamic behaviour of LYK3 only occurs after inoculation with rhizobia but not in response to Nod factors and that it persists in infection threads that have already passed the epidermal cell. The conclusion that Nod factors alone are not enough to change the behaviour of LYK3 is remarkable, as it suggests that ligands other than Nod factors control the behaviour of LYK3. However, I hypothesize that the method that Haney and co-workers used is not perfectly suited to study these changes in dynamic behaviour. They studied the dynamics of the LYK3 receptor 24 hours after incubation with rhizobia, Nod factors or buffer treatment.

After incubation they measured LYK3 dynamics in the tip of root hairs. Studies by Goedhart *et al.* [2000] have shown that Nod factors added to root hairs do not accumulate in the new outgrowth (tip) of root hairs. Instead, the Nod factors rapidly accumulate in the cell wall of more mature part of the root hairs. Therefore, the amount of Nod factor available at the new outgrowths may be too low to affect LYK3 behaviour in this part of the root hair. Rhizobia on the other hand continuously produce Nod factors and thus can stimulate the receptor in the outgrowth (tip) of root hairs.

The reported changes in the dynamics of LYK3 and co-localization with FLOT4 upon stimulation are intriguing. The perception of the Nod factors could allow the receptors to stop moving around and to form local signaling complexes. In addition, it was observed that LYK3 stimulation increased the formation of intracellular LYK3-marked vesicles. It is currently not clear whether these vesicles represent exo- or endocytotic transport of the receptor. However, flotillins have been implicated in endocytotic events [Hansen and Nichols, 2009; Stuermer, 2011]. Therefore, it would be interesting to determine whether localization to FLOT4 domains is a causal event for the induced formation of these vesicles. We know that FLOT4 is required for proper infection thread formation [Haney and Long, 2010]. This suggests that endocytosis of the receptor is important for the induction of infection thread initiation. Endocytosis of receptors is one of the major regulators of signaling [Goh and Sorkin, 2013; Irani and Russinova, 2009]. When the receptor is no longer present at the plasma membrane, perception of the ligand is no longer possible. Therefore endocytosis can regulate signaling.

The reported persistent accumulation of LYK3 in the infection thread four days after inoculation with rhizobia [Haney *et al.*, 2011] is also remarkable in the light of our data. At that time the infection thread passed many cells and in the cell where LYK3 accumulation is observed (epidermis) the infection thread passed some time ago and is no longer growing [Rae *et al.*, 1992]. We show that the receptors are rapidly removed from the infection thread as soon as it enters a cell. Also from a biological point of view it's unlikely that the plant needs to perceive Nod factors along the entire infection thread. On the other hand, the controls do not show fluorescence at the infection thread [Haney *et al.*, 2011].

Based on the behaviour of LYK3 in the nodule (Chapter 3) we hypothesize that in root hairs the receptors accumulate at very low levels before stimulation with Nod factors or bacteria. Upon stimulation accumulation would increase and upon infection thread initiation accumulation should go down again. This in contrast with the data of [Haney *et al.*, 2011] where accumulation of the receptor does not increase upon Nod factor perception and does not decrease after perception. Preliminary data on the accumulation of LYK3-GFP in nodule primordia indicates that LYK3 indeed accumulates prior to infection thread penetration (Figure 7.1). The down-regulation of receptor levels at the place where Nod factor concentrations are highest, could be important to prevent the activation of defence responses [Lefebvre *et al.*, 2012; Pietraszewska-Bogiel *et al.*, 2013]. This defence responses may be a result of the evolution of the Nod factor receptors. LysM domains recognise

peptidoclycans, which are often pathogen associated molecules [Wan *et al.*, 2008; Zhang *et al.*, 2007]. Domain swaps between the Nod factor receptors and the chitin receptor CERK1 show that the intracellular parts of the Nod factor receptors still stimulate the defence pathways [Wang *et al.*, 2014].

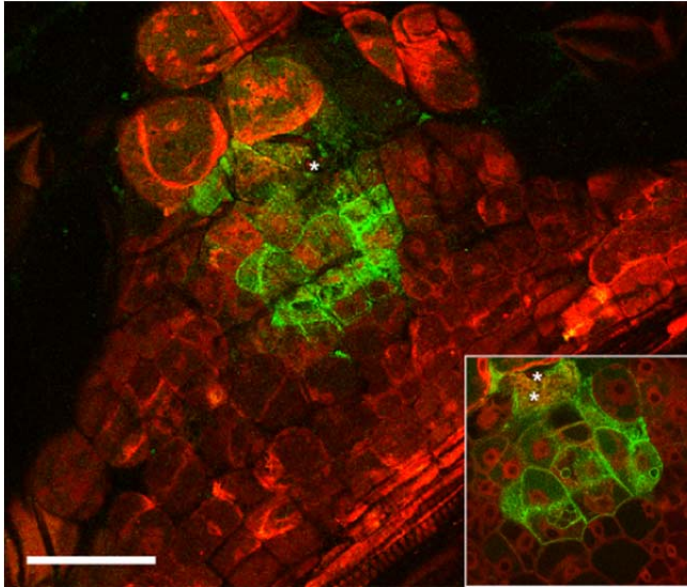


Figure 7.1: accumulation of LYK3-GFP in primordia seven days after inoculation with *Rhizobia*. The infection thread is marked with an astrix (*). Bar indicates 50 μ m.

THE FUNCTION OF NOD FACTOR PERCEPTION IN NODULES

Our data show that Nod factor perception inside the nodule plays a key role in the control of release of the bacteria from infection threads (Chapter 3). It was already known that other components of the symbiotic signaling cascade are essential for release [Limpens *et al.*, 2005; Ovchinnikova *et al.*, 2012]. Therefore, it seems logical that perception of Nod factors is required to activate the downstream components to allow uptake of the bacteria. Release of the rhizobia from the infection threads and subsequent uptake into the host cell is a process that the plant needs to control. Here the bacteria become internalized and the plant has to perform an additional check to make sure that the right bacteria enter. Furthermore, the plant likely needs to restrict the release of rhizobia. In fact, only a few bacteria are locally released from the cell wall bound infection threads at the unwallled infection droplets. After release, these bacteria proliferate and populate the infected nodule cells. After this initial release, unwallled infection droplets are no longer formed. My hypothesis is that all rhizobia in a single cell need to be at the same developmental stage. Having bacteroids at different stages is not beneficial as they will have different requirements on the host. The rapid down-regulation of the Nod factor receptors may be a

mechanism to restrict the release process. This would fit with the observed hypertrophied infection droplets when LYK3 was overexpressed (Chapter 3).

It has been suggested that Nod factors [D'Haeze *et al.*, 1998] or Nod factor receptors [Madsen *et al.*, 2010] are not needed for bacterial release. Contrary to that, our data suggest that Nod factor perception by the Nod factor receptors is needed for bacterial release. The receptors are present in the layer where release takes place, the bacteria produce Nod factors [Marie *et al.*, 1994] and a knock down of one of the receptors causes abnormal release. In the experiments of D'Haeze *et al.* [1998] nodules are co-inoculated with and bacteria with altered surface polysaccharides and bacteria not producing Nod factors. Only the latter were able to infect the nodule cells. I hypothesize that the bacteria that do produce Nod factors activate release. Either the Nod factors diffuse from the Nod factor producing bacteria to the Nod factor receptors or bacteria with altered surface polysaccharides did acquire the Nod factors in their cell wall. Their experiments do show that next to Nod factors the surface polysaccharides are important for bacterial release. The experiments of Madsen *et al.* [2010] crossed an always active CCamK with a Nod factor double mutant. In these plants normal nodules are formed in the absence of the receptors. I suggest that the always active CCamK is sufficient to activate the Nod factor signaling cascade and thus allow release.

RECEPTOR COMPLEX FORMATION

NFP and LYK3 both localize to a narrow zone of two cells that forms the border between meristem and infection zone in the nodule. We showed for the first time, in the biological context of the rhizobium – legume symbiosis, that the two receptors form a heteromer (Chapter 4). We also identified several novel putative interactors of LYK3 (0). Interesting NFP, which we showed in Chapter 4 to interact with LYK3, was not found in this screen. Most likely, only a small portion of the LYK3-GFP forms a heteromer with NFP. Our FRET-FLIM studies show that the FRET efficiency is low for the LYK3-NFP heteromer (4.4%). This low efficiency could be due to a limited fraction of LYK3 that forms heteromers with NFP. Instead, our experiments show that LYK3 forms homomers with a slightly higher FRET efficiency (5%). About the biological role of LYK3 homomers we can only speculate. These homomers could compete with NFP for interaction. In this case the ability of LYK3 to form homomers limits the formation of LYK3-NFP heteromers and thus control downstream signaling from the heteromer. Another hypothesis is that the formation of the LYK3 homomer has a distinct function and signals a specific process. From the *lyk3* and *nfp* mutant studies we know that the two receptors differently affect downstream responses [Amor *et al.*, 2003; Arrighi *et al.*, 2006; Limpens *et al.*, 2003]. Also our results on the knock-down of the individual receptors in the nodule we indicate differential effects of LYK3 and NFP. When NFP is knocked down release is blocked, where knock down of LYK3 causes the formation of large unwallled droplets indicating slow release. The formation of the LYK3 homomer could be involved in the signaling/

functions that are not shared with NFP. As NFP has a non-functional kinase domain, it is likely that additional receptor kinases interact with NFP to control LYK3-independent responses, although kinase independent signaling roles cannot be excluded. Therefore, it would be interesting to see whether other receptor kinases can interact with NFP to allow signaling. Such a receptor kinase would either be redundant, as it was not found in genetic screens, or it is essential for plant development. Possible candidates could include other LysM domain receptor kinases [Arrighi *et al.*, 2006]. In Chapter 6 we show that there are, at least based on differential expression in the nodule, candidates that could interact with NFP. These include the type-II LysM domain containing receptor kinase LYR4 as well as the potentially GPI-anchored proteins LYM1 and LYM2 [Arrighi *et al.*, 2006; Fliegmann *et al.*, 2011].

The FRET-FLIM studies show a limited interaction between LYK3 and NFP, which could explain the absence of NFP in the LYK3-GFP co-immunoprecipitation. We hypothesize that only a small portion of the available LYK3 protein forms a heteromer and the rest of the LYK3 is in the process of degradation. Strikingly, we did not detect any of the reported LYK3 interactors in immunoprecipitates of LYK3. We could not detect PUB1 [Mbengue *et al.*, 2010] or SYMREM1 [Lefebvre *et al.*, 2010]. Most likely these interactions occur during a short period of time or in a distinct location or cell type. The interactions of LYK3 with PUB1 and SYMREM1 were observed in heterologous systems. The proteins were expressed in non-legumes or yeast and under control of strong constitutively active promoters. This questions the biological relevance of these interactions. The used screening methods do prove that the proteins have the potential to interact with each other. They cannot show co-localization of the proteins. Both proteins need to be expressed in the same cell and need to accumulate in the same subcellular location to allow interaction.

With our immunoprecipitation approach (0) we identified several new putative interactors of LYK3 that link Nod factor signaling with vesicle traffic (Dynamin-2B, BAR-SH3 domain-containing protein) and the cytoskeleton (EF1 α). The phosphorylation status of these proteins changes quickly upon Nod factor application [Rose *et al.*, 2012], suggesting that they are a direct target of the receptors. For the formation of symbiosomes an enormous amount of membrane is needed. Each single bacterium is surrounded by a plant derived membrane, and the cells of the fixation zone are completely filled with bacteria. Therefore, it is quite logical that symbiosis modulates vesicle traffic [Roth and Stacey, 1989]. Furthermore, traffic from and to the symbiosomes is needed for the exchange of nutrients. Also vesicle traffic is often associated with the uptake of biotic agents [Barocchi *et al.*, 2005]. Recently it was recently found that a specific exocytosis pathway is essential for the uptake of the rhizobia by nodule cells [Ivanov *et al.*, 2012]. It is known that both the actin and microtubule cytoskeleton play important roles during rhizobial infection [Timmers, 2008]. The plant cytoskeleton is involved in many processes including root hair deformation, infection thread development, cell differentiation, pre-infection structures and primordium and meristem formation [Timmers, 2008]. Therefore, it is not so strange that

the Nod factor receptors are associated with modulators of the cytoskeleton. Furthermore, in the *lyk3* mutant it was shown that the asymmetric organisation of the microtubule cytoskeleton in root hairs and the re-orientation of the microtubule cytoskeleton to form pre-infection threads, were strongly altered [Catoira *et al.*, 2001]. As both vesicle traffic and the cytoskeleton are core cellular processes, it's not so strange that the putative intractors we found were not discovered in the genetic screens. Alterations in these processes compromises plant development as such.

One of the drawbacks of the immunoprecipitation is that the samples can be enriched with ubiquitous membrane proteins. Small membrane fractions may be attached to the isolated receptor and these membrane fractions can contain proteins that do not interact with the receptor (false positive). To overcome this problem the experiment could be repeated in triplicates to remove these false positives by statistics. Furthermore, the candidates found with this method need to be tested with an additional method to prove that they do interact in the biological system. Also their co-localization in the biological context needs to be proven as the proteins need to be present at the same location at the same time in order to form a complex. One of the tools to show co-expression is the “digital *in situ*” we presented in 0.

NOD FACTOR PERCEPTION AND THE NOD FACTOR SIGNALING CASCADE

Next to the physical interaction between LYK3 and other proteins we determined the expression of Nod factor signaling components in the different zones of nodules (0). These data provided us with a “digital *in situ*” experiment of genes known to be involved in Nod factor signaling. As the encoded proteins are considered to be part of one signaling cascade it would be expected that they show a similar expression profile. Given this expectation it is thus rather remarkable that for instance DMI1 is strongly enriched in infected cells where Nod factor perception does not take place and not in the meristem/ infection zone [Riely *et al.*, 2007]. Also the expression domain of IPD3 (the interactor of DMI3) and DMI3 is different. This suggests that IPD3 and DMI3 also function separate from each other, next to their function in Nod factor perception.

A similar approach was used by Roux *et al.* [2014] where they combined laser capture microdissection combined with RNA sequencing. Most of their findings are in line with the differential expression we present in Chapter 6 (Table 7.1). In line with our data they found an enrichment of LYK3 and NFP in the meristem/ infection zone. Furthermore, they found NSP1 and NSP2 and to a lesser extend DMI2 and DMI3 to be enriched in the meristem/ infection zone. These enrichments were not significant in our analysis. Also in line with our data they found an enrichment of DMI1, IPD3 and PUB1 in the infected cells of the nodule and an enrichment of SYMREM1 in the proximal infection zone. They also speculate on the role of additional LysM domain containing proteins in the nodule to activate the Nod

factor signaling cascade. Although the two genes they suggest as a candidate in the infection/ fixation zone (LYR2 and LYR4) show no significant enrichment in any of the nodule zones. Because Roux *et al.* [2014] performed an RNA sequencing experiment they were also able to study the differential expression of the rhizobial genome. Remarkable, they show that the Nod-genes are still actively transcribed in the fixation zone. This is in contrast to the data of Marie *et al.* [1994] that show that Nod factors are no longer produced after infection. Perhaps intercellular bacteria which still produce Nod factors contributed to the RNA sample of Roux *et al.* [2014] or bacteria do produce Nod factors which are perceived by unknown LysM domain containing proteins.

Table 7.1: Comparison of the found differential expression patterns in the nodule to the data of Roux *et al.* [2014].

Gene	Enrichment according to our data	Enrichment according to Roux <i>et al.</i> [2014]
NFP	Mersitem/ distal infection zone	Mersitem/ distal infection zone
LYK3	Mersitem/ distal infection zone	Mersitem/ distal infection zone
DMI2	Ubiquitous	Ubiquitous
DMI1	Infected cells	Infected cells
DMI3	Ubiquitous	Ubiquitous
IPD3	Fixation zone	Fixation zone
NSP1	Ubiquitous	Meristem
NSP2	Ubiquitous	Meristem/ distal infection zone
NIN	Proximal infection zone	Proximal infection zone
SYMREM1	Proximal infection zone/ infected cells	Infection zone/ fixation zone
FLOT4	Ubiquitous	Ubiquitous

It was suggested by Hayashi *et al.* [2013] that the upstream component (receptors) of Nod factor signaling are not needed for the activation of the signaling cascade in de cortex and nodule. They expressed the receptors under control of an epidermis specific promoter in the mutant background which restored nodulation. This indicates that the promoter they used is sufficient to express the receptors in the appropriate cells. When we used the tomato Extensin1 promoter [Mirabella *et al.*, 2004] in a similar approach. We observed that this promoter is also active in the nodule apex, and especially in the transition from meristem to

infection zone (Figure 7.2). Whether the promoter used by Hayashi *et al.* [2013] is also active in the nodule is unknown. The very specific accumulation of the Nod factor receptors at the border between meristem and infection and the nodule specific knockdown suggests that the receptors do have a function in the nodule. Perhaps, the determinate nature of Lotus nodules has an alternative requirement for Nod factor perception than the indeterminate nodule of Medicago.

Another experiment that conflicts with the need for the Nod factor receptors to perceive Nod factors in the nodule is the work of Okazaki *et al.* [2013]. They showed that in soybean the rhizobium *Bradyrhizobium elkanii* uses the type III secretion system to activate the Nod factor signaling cascade independent of Nod factors and the Nod factor receptors. The hypothesis is that *B. elkanii* injects yet unknown components that activate the Nod factor signaling cascade. It's known that for instance exogenous cytokinin can induce early nodulins and that gain of function mutants in CCamK or the cytokinin receptor induce spontaneous nodules. Although it is interesting to see Nod factor independent activation of the symbiotic signaling cascade, it may be a specific feature of *B. elkanii* as the common symbiont for soy, *B. japonicum*, does not harbour this feature.

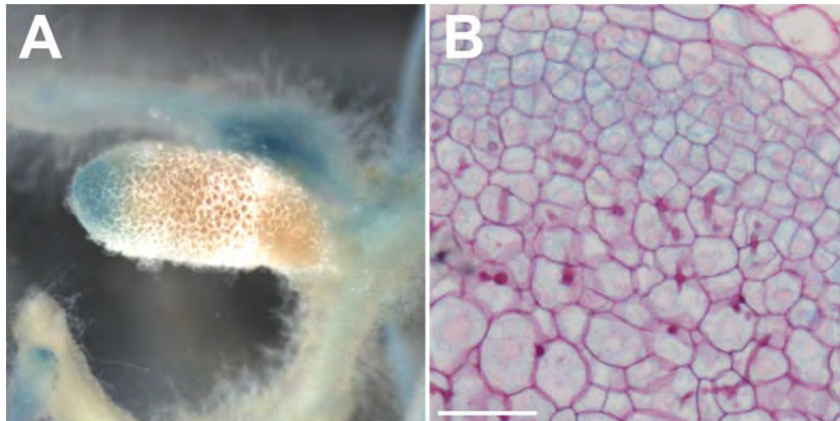


Figure 7.2: Activity of the *LeExtensin1* promoter in nodules formed on *pLeEXT1::GUS* transformed roots. (A) whole mount image of a nodule showing promoter activity in the nodule apex. (B) Longitudinal section through a nodules showing promoter activity in the nodule meristem and infection zone. Bar indicates 50 μ m.

A MODEL FOR NFP AND LYK3 ACCUMULATION

We show that both NFP and LYK3 are expressed in nodules and that they accumulate at the plasma membrane for a short time. We observed the proteins in an narrow zone of about two cell layers wide that form the border between meristem and infection zone. This accumulation in a narrow zone seems to be biological important as ectopic expression causes nodules in which for example premature senescence is induced.

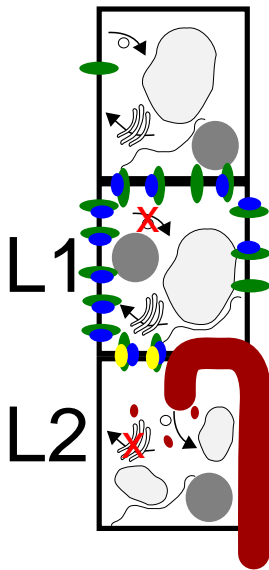


Figure 7.3: A model for Nod factor accumulation in layers L1 and L2 of Medicago nodules. Prior to L1 the receptors (green/ blue) are produced, but continuously degraded resulting in an extremely low concentration at the plasma membrane. In layer L1 the receptors can perceive the bacterial Nod factor. Nod factor perception initially results in the formation of a receptor complex (green/ blue/ yellow) which accumulates at the plasma membrane. When the receptor complex has reached a threshold level it triggers release of symbiosomes (red) from infection threads and activates a negative feedback by which the complex is rapidly internalized and targeted for degradation.

The accumulation of the Nod factor receptors is only in part regulated at the transcription level as the respective promoters are active in a markedly broader zone including the entire meristem (Chapter 3). Therefore, we propose a post-translational mechanism that can explain how the receptors accumulate in such a narrow region (Figure 7.3). The receptor genes are broadly expressed in the nodule meristem. The receptors are initially targeted to the plasma membrane via the exocytotic pathway, from which they are rapidly removed for degradation in the vacuole. This in analogy to the recycling of e.g. the Arabidopsis auxin efflux carrier PIN1. Although PIN1 is not degraded upon endocytosis. PIN1 is continuously removed from the plasma membrane to create the subcellular accumulation that is needed for its biological function [Geldner *et al.*, 2001]. For PIN2 this recycling does not occur, but it was shown that breakdown of this protein in the vacuoles occurs dependent on environmental signals [Kleine-Vehn *et al.*, 2008; Sun *et al.*, 2011]. Also AtCERK1/BRI1,

SRK and AtCRINCLY4 are continuously removed from the plasma membrane for recycling (AtCERK1/BRI1) or degradation (SRK and AtCRINCLY4) [Gifford *et al.*, 2005; Ivanov and Gaude, 2009; Russinova *et al.*, 2004; Shah *et al.*, 2002]. For NFP we know that in the meristem the receptor is targeted to the vacuoles, indicating that the receptor indeed is targeted for degradation in the meristem. Because of this mechanism the accumulation of the receptors in the plasma membrane is below the detection limit of fluorescent microscopy, although I propose that some receptor is present in the plasma membrane of cells younger than layer L1. A similar mechanism might be active in the epidermis to keep the Nod factor receptors at very low levels.

In layer L1 and L2 the receptors perceive Nod factors produced by rhizobia that are present in the apoplast and in infection threads that are starting to be formed. I hypothesize that perception of the rhizobial Nod factor activates a mechanism by which the receptors accumulate at the plasma membrane. One option is that perception of the Nod factor itself causes the receptors to dimerize. We know from our studies that such a dimer is formed (Chapter 4). From work on the chitin receptor AtCERK1 we know that perception of chitin, which has a structure very similar to Nod factors, triggers dimerization of AtCERK1 [Liu *et al.*, 2012]. Although, for chitin only an octamer has the ability to dimerize the receptor. The shorter Nod factor may not have the same property. This dimerization of AtCERK1 furthermore is essential for the activation of downstream targets [Liu *et al.*, 2012]. The dimerization of a receptor on itself may slow down the removal of the receptors [Gregar *et al.*, 2004]. Endocytosis of the larger complex is slower than endocytosis of the single proteins. This results in a higher accumulation of the receptors at the plasma membrane. Ofcourse, other mechanisms, like complex formation with other components, can also result in a higher accumulation of the receptors. However, I hypothesize that the process that causes a higher accumulation is set off by Nod factor perception followed by heteromerization/homomerization of the Nod factor receptors.

In layer L2, the situation changes. Because of the accumulation of the receptors, signaling increases above a second threshold. The high level of Nod factor perception subsequently triggers the endocytic degradation of the receptors. Activation of the Nod factor signaling cascade in this case also leads to the activation of a negative feedback loop. This is a general mechanism for down regulation of signaling genes upon perception of the ligand. This was shown for instance for Auxin [Abel *et al.*, 1995; Benjamins and Scheres, 2008; Niklas and Kutschera, 2012] and the flagellin receptor AtFLS2 [Beck *et al.*, 2012; Robatzek *et al.*, 2006].

I hypothesize that such a negative feedback also occurs during Nod factor signaling. Such a mechanism limits signaling for example to prevent the induction of defence responses and to limit the formation of unwallled infection droplets. Such post-translational mechanism, depending on the endocytic turnover of the receptors, could result in the accumulation of the receptors that we described in Chapter 3 and Chapter 4.

A recent study by Antolin-Llovera *et al.* [2014] shows that also SYMRK (the lotus homologue of DMI2) forms a complex with the Nod factor receptor NFR5 (homologue of NFP). The formation of this complex occurs only in the absence of symbiotic stimulation. When no stimulation is present the extracellular malectin-like domain is cleaved off. The remaining receptors after release of the domain forms a complex with NFR5 and is most likely degraded [Antolin-Llovera *et al.*, 2014]. These data indicate that SYMRK may be the regulator of receptor accumulation in the plasma membrane of L1 and L2 and that this is symbiont dependant.

NOD FACTOR SIGNALING IN PRIMORDIA VS INFECTION ZONE

We showed in this thesis that Nod factor signaling inside the nodule is important for release of the bacteria from the infection threads and thus intracellular infection of the nodule cells. However, there appears to be a difference in the Nod factor dependent control of rhizobial uptake in the nodule primordium cells and nodule meristem derived cells. Our detailed analyses of nodule formation (Chapter 2) resulted in a nodule fate map. This fate map shows that release of bacteria from the infection threads occurs in two stages: in the primordium and in cells derived from the nodule meristem. There seems to be a more stringent control on the release of rhizobia from the infection threads in the meristem derived cells. At the same time, infection thread formation appears to be most stringently controlled in the root epidermis [Hayashi *et al.*, 2013; Smit *et al.*, 2007]. The best evidence for a more stringent demand on Nod factor signaling in meristem-derived cells comes from the pea *sym41* mutant [Ovchinnikova, 2012]. This splicing mutant of the DIM2/SymRK homologue has ~90% reduced transcript levels. Nodules are formed on *sym41* indicating that the reduced transcript levels do not interfere with early events in the epidermis and the primordium. However, in the nodules formed no infection occurs in cells derived from the meristem indicating a more stringent demand for Nod factor signaling in these cells. Several other mutants indicate a difference between nodule primordium and meristem derived cells with respect to the ability to form symbiosomes. For instance, nodules in which SYMREM1 is knocked down via RNAi show eight perfectly infected cell layers at the base of the nodule [Lefebvre *et al.*, 2010], whereas release in cells derived from the meristem is impaired. It would be interesting to find an explanation for the differential requirement of Nod factor perception and signaling.

NOD FACTOR SIGNALING AND LIPID RAFTS

Lipid rafts are small domains that exist in membranes and have a different lipid and protein composition compared to the rest of the membrane [Simons and Ikonen, 1997]. These domains are thought to be involved in many cellular processes as they create a unique environment, a liquid ordered phase, for membrane proteins embedded in these domain [Bhat and Panstruga, 2005; Rietveld and Simons, 1998]. Especially signaling components

like receptor kinases localize in such domains [Bhat and Panstruga, 2005]. In contrast to the enthusiasm of several research groups, the lipid raft concept is received with scepticism by others [Munro, 2003]. However, sceptics argue mainly about the definition of a raft instead of the occurrence of distinct signaling domains in the membrane in biological systems [Bhat and Panstruga, 2005; Munro, 2003]. We observed that LYK3 accumulates in puncta in the plasma membrane in cells of the nodule. LYK3 has been suggested to interact with SYMREM1 and was reported to co-localized with FLOT4 in puncta upon stimulation by rhizobia in *Medicago* root hairs [Haney *et al.*, 2011; Lefebvre *et al.*, 2010]. For both FLOT4 and SYMREM1 the exact biological function is not known, but both preferably localize to lipid rafts. The occurrence of these domains and the non-uniform distribution of components in the plasma membrane is an intriguing phenomenon. The biological importance of these domains is not yet fully understood. In animal membranes lipid rafts are most studied. Lipid rafts are regions of 5-50 nm rich in cholesterol, glycolipids and sphingolipids [Simons and Ikonen, 1997]. It is suggested that plants also contain such a membrane organization [Bhat and Panstruga, 2005; Jarsch and Ott, 2011; Lefebvre *et al.*, 2007; Urbanus and Ott, 2012].

Also in the *Medicago* – rhizobium symbiosis it has been suggested that lipid domains have an important function [Lefebvre *et al.*, 2007; Urbanus and Ott, 2012]. The observed localization of LYK3 in puncta at the plasma membrane suggest they may be part of a raft. This would be supported by the reported interaction with the lipid raft marker SYMREM1 [Lefebvre *et al.*, 2010]. Our co-localization data show that such an interaction could indeed occur in nodules at the infection thread membrane, although it seems to be limited in time and space. LYK3 does localize to the infection thread membrane where SYMREM1 accumulates. The accumulation of LYK3 on the infection thread was observed in 35% of the cells that do accumulate LYK3. On the other hand, the localization of LYK3 in puncta at the plasma membrane does not appear to depend on SYMREM1. Whether there are different membrane domains/lipid rafts in plant cells and how many is currently not known. However, the observed differential localization of FLOT4 and SYMREM1 suggest that these presumed lipid raft markers do not label the same domains (0). Interestingly, many bacteria make use of lipid rafts for their interaction and internalization into a host cell in animal systems [Lafont and van der Goot, 2005]. Furthermore, lipid rafts were shown to occur at the sites where pathogenic fungi penetrate plant cells [Bhat *et al.*, 2005]. In analogy, our data suggest that the membrane surrounding the site of bacterial release (ie. at the unwallled infection droplet) is different from that of the rest of the membrane. Here, LYK3 only accumulates in 35% of the cells where accumulation of LYK3 was observed. Furthermore, only at the site of bacterial release accumulation of SYMREM1 was observed when expressed from its endogenous promoter [Lefebvre *et al.*, 2010]. Such a specialized membrane domain could attract specific components to the site of bacterial release and redirect vesicle traffic specific to this site [Surma *et al.*, 2012]. This exocytotic pathway is needed for bacterial release [Ivanov *et al.*, 2012] and my hypothesis is that lipid rafts direct these exocytotic vesicles to the site of release.

REFERENCES

- Abel S., Nguyen M. D. and Theologis A. 1995. The PS-IAA4/5-like family of early auxin-inducible mRNAs in *Arabidopsis thaliana*. *J Mol Biol.* 251(4): 533-549
- Amor B. B., Shaw S. L., Oldroyd G. E., Maillet F., Penmetsa R. V., Cook D., Long S. R., Denarie J. and Gough C. 2003. The NFP locus of *Medicago truncatula* controls an early step of Nod factor signal transduction upstream of a rapid calcium flux and root hair deformation. *Plant J.* 34(4): 495-506
- Andriankaja A., Boisson-Dernier A., Frances L., Sauviac L., Jauneau A., Barker D. G. and de Carvalho-Niebel F. 2007. AP2-ERF Transcription Factors Mediate Nod Factor Dependent Mt ENOD11 Activation in Root Hairs via a Novel cis-Regulatory Motif. *Plant Cell.*
- Ane J. M., Kiss G. B., Riely B. K., Penmetsa R. V., Oldroyd G. E., Ayax C., Levy J., Debelle F., Baek J. M., Kalo P., *et al.* 2004. *Medicago truncatula* DMI1 required for bacterial and fungal symbioses in legumes. *Science.* 303(5662): 1364-1367
- Antolin-Llovera M., Ried M. K. and Parniske M. 2014. Cleavage of the SYMBIOSIS RECEPTOR-LIKE KINASE Ectodomain Promotes Complex Formation with Nod Factor Receptor 5. *Curr Biol.* 24(4): 422-427
- Ardourel M., Demont N., Debelle F., Maillet F., de Billy F., Prome J. C., Denarie J. and Truchet G. 1994. Rhizobium meliloti lipooligosaccharide nodulation factors: different structural requirements for bacterial entry into target root hair cells and induction of plant symbiotic developmental responses. *Plant Cell.* 6(10): 1357-1374
- Arrighi J. F., Barre A., Ben Amor B., Bersoult A., Soriano L. C., Mirabella R., de Carvalho-Niebel F., Journet E. P., Gherardi M., Huguet T., *et al.* 2006. The *Medicago truncatula* lysin motif-receptor-like kinase gene family includes NFP and new nodule-expressed genes. *Plant Physiol.* 142(1): 265-279
- Barocchi M. A., Masignani V. and Rappuoli R. 2005. Opinion: Cell entry machines: a common theme in nature? *Nat Rev Microbiol.* 3(4): 349-358
- Beck M., Zhou J., Faulkner C., MacLean D. and Robatzek S. 2012. Spatio-temporal cellular dynamics of the *Arabidopsis* flagellin receptor reveal activation status-dependent endosomal sorting. *Plant Cell.* 24(10): 4205-4219
- Becker W. 2012. Fluorescence lifetime imaging--techniques and applications. *J Microsc.* 247(2): 119-136
- Benaben V., Duc G., Lefebvre V. and Huguet T. 1995. TE7, An Inefficient Symbiotic Mutant of *Medicago truncatula* Gaertn. cv Jemalong. *Plant Physiol.* 107(1): 53-62
- Benedito V. A., Torres-Jerez I., Murray J. D., Andriankaja A., Allen S., Kakar K., Wandrey M., Verdier J., Zuber H., Ott T., *et al.* 2008. A gene expression atlas of the model legume *Medicago truncatula*. *Plant J.* 55(3): 504-513
- Benjamins R. and Scheres B. 2008. Auxin: the looping star in plant development. *Annu Rev Plant Biol.* 59(443-465
- Berg R. H., Langenstein B. and Silvester W. B. 1999. Development in the *Datisca-Coriaria* nodule type. *Canadian Journal of Botany-Revue Canadienne De Botanique.* 77(9): 1334-1350
- Bhat R. A., Miklis M., Schmelzer E., Schulze-Lefert P. and Panstruga R. 2005. Recruitment and interaction dynamics of plant penetration resistance components in a plasma membrane microdomain. *Proc Natl Acad Sci U S A.* 102(8): 3135-3140
- Bhat R. A. and Panstruga R. 2005. Lipid rafts in plants. *Planta.* 223(1): 5-19
- Bisseling T., Been C., Klugkist J., Kammen A. and Nadler K. 1983. Nodule-specific host proteins in effective and ineffective root nodules of *Pisum sativum*. *Embo J.* 2(6): 961-966

- Bleckmann A., Weidtkamp-Peters S., Seidel C. A. and Simon R.** 2010. Stem cell signaling in Arabidopsis requires CRN to localize CLV2 to the plasma membrane. *Plant Physiol.* 152(1): 166-176
- Bond L.** 1948. Origin and developmental morphology of root nodules of *Pisum sativum*. *Botanical Gazette.* 109(411-434).
- Borisov A. Y., Madsen L. H., Tsyganov V. E., Umehara Y., Voroshilova V. A., Batagov A. O., Sandal N., Mortensen A., Schauser L., Ellis N., et al.** 2003. The Sym35 gene required for root nodule development in pea is an ortholog of Nin from *Lotus japonicus*. *Plant Physiol.* 131(3): 1009-1017
- Brewin N. J.** 1991. Development of the Legume Root Nodule. *Annual Review of Cell Biology.* 7(1): 191-226
- Brewin N. J.** 2004. Plant Cell Wall Remodelling in the Rhizobium–Legume Symbiosis. *Critical Reviews in Plant Sciences.* 23(4): 293-316
- Broghammer A., Krusell L., Blaise M., Sauer J., Sullivan J. T., Maolanon N., Vinther M., Lorentzen A., Madsen E. B., Jensen K. J., et al.** 2012. Legume receptors perceive the rhizobial lipochitin oligosaccharide signal molecules by direct binding. *Proc Natl Acad Sci U S A.* 109(34): 13859-13864
- Buist G., Steen A., Kok J. and Kuipers O. P.** 2008. LysM, a widely distributed protein motif for binding to (peptidoglycans. *Mol Microbiol.* 68(4): 838-847
- Burssens S., Himanen K., van de Cotte B., Beeckman T., Van Montagu M., Inze D. and Verbruggen N.** 2000. Expression of cell cycle regulatory genes and morphological alterations in response to salt stress in *Arabidopsis thaliana*. *Planta.* 211(5): 632-640
- Capoen W., Goormachtig S., De Rycke R., Schroevers K. and Holsters M.** 2005. SrSymRK, a plant receptor essential for symbiosome formation. *Proc Natl Acad Sci U S A.* 102(29): 10369-10374
- Catoira R., Galera C., de Billy F., Penmetsa R. V., Journet E. P., Maillet F., Rosenberg C., Cook D., Gough C. and Denarie J.** 2000. Four genes of *Medicago truncatula* controlling components of a nod factor transduction pathway. *Plant Cell.* 12(9): 1647-1666
- Catoira R., Timmers A. C., Maillet F., Galera C., Penmetsa R. V., Cook D., Denarie J. and Gough C.** 2001. The HCL gene of *Medicago truncatula* controls Rhizobium-induced root hair curling. *Development.* 128(9): 1507-1518
- Cebolla A., Vinardell J. M., Kiss E., Olah B., Roudier F., Kondorosi A. and Kondorosi E.** 1999. The mitotic inhibitor ccs52 is required for endoreduplication and ploidy-dependent cell enlargement in plants. *Embo J.* 18(16): 4476-4484
- Chabaud M., de Carvalho-Niebel F. and Barker D. G.** 2003. Efficient transformation of *Medicago truncatula* cv. Jemalong using the hypervirulent *Agrobacterium tumefaciens* strain AGL1. *Plant Cell Rep.* 22(1): 46-51
- Chen C., Gao M., Liu J. and Zhu H.** 2007. Fungal symbiosis in rice requires an ortholog of a legume common symbiosis gene encoding a Ca²⁺/calmodulin-dependent protein kinase. *Plant Physiol.* 145(4): 1619-1628
- Combier J. P., Frugier F., de Billy F., Boualem A., El-Yahyaoui F., Moreau S., Vernie T., Ott T., Gamas P., Crespi M., et al.** 2006. MtHAP2-1 is a key transcriptional regulator of symbiotic nodule development regulated by microRNA169 in *Medicago truncatula*. *Genes Dev.* 20(22): 3084-3088
- Combier J. P., Vernie T., de Billy F., El Yahyaoui F., Mathis R. and Gamas P.** 2007. The MtMMP1 early nodulin is a novel member of the matrix metalloendoproteinase family with a role in *Medicago truncatula* infection by *Sinorhizobium meliloti*. *Plant Physiol.* 144(2): 703-716
- Condeelis J.** 1995. Elongation factor 1 alpha, translation and the cytoskeleton. *Trends Biochem Sci.* 20(5): 169-170
- Couzigou J. M., Zhukov V., Mondy S., Abu el Heba G., Cosson V., Ellis T. H., Ambrose M., Wen J., Tadege M., Tikhonovich I., et al.** 2012. NODULE ROOT and COCHLEATA maintain nodule development and are legume orthologs of Arabidopsis BLADE-ON-PETIOLE genes. *Plant Cell.* 24(11): 4498-4510

- Czaja L. F., Hogekamp C., Lamm P., Maillet F., Martinez E. A., Samain E., Denarie J., Kuster H. and Hohnjec N.** 2012. Transcriptional responses toward diffusible signals from symbiotic microbes reveal MtNFP- and MtDMI3-dependent reprogramming of host gene expression by arbuscular mycorrhizal fungal lipochitooligosaccharides. *Plant Physiol.* 159(4): 1671-1685
- D'Haeze W., Gao M., De Rycke R., Van Montagu M., Engler G. and Holsters M.** 1998. Roles for Azorhizobial Nod Factors and Surface Polysaccharides in Intercellular Invasion and Nodule Penetration, Respectively. *Molecular Plant-Microbe Interactions.* 11(10): 999-1008
- D'Haeze W. and Holsters M.** 2002. Nod factor structures, responses, and perception during initiation of nodule development. *Glycobiology.* 12(6): 79R-105R
- Davidson A. L. and Newcomb W.** 2001. Changes in actin microfilament arrays in developing pea root nodule cells. *Canadian Journal of Botany.* 79(7): 767-776
- Defaria S. M., Lewis G. P., Sprent J. I. and Sutherland J. M.** 1989. Occurrence of Nodulation in the Leguminosae. *New Phytologist.* 111(4): 607-619
- Deguchi Y., Banba M., Shimoda Y., Chechetka S. A., Suzuri R., Okusako Y., Ooki Y., Toyokura K., Suzuki A., Uchiumi T., *et al.*** 2007. Transcriptome profiling of *Lotus japonicus* roots during arbuscular mycorrhiza development and comparison with that of nodulation. *DNA Res.* 14(3): 117-133
- Deinum E. E., Geurts R., Bisseling T. and Mulder B. M.** 2012. Modeling a cortical auxin maximum for nodulation: different signatures of potential strategies. *Front Plant Sci.* 3(96)
- Dello Ioio R., Linhares F. S. and Sabatini S.** 2008. Emerging role of cytokinin as a regulator of cellular differentiation. *Curr Opin Plant Biol.* 11(1): 23-27
- Deyoung B. J. and Clark S. E.** 2008. BAM receptors regulate stem cell specification and organ development through complex interactions with CLAVATA signaling. *Genetics.* 180(2): 895-904
- Di Laurenzio L., Wysocka-Diller J., Malamy J. E., Pysh L., Helariutta Y., Freshour G., Hahn M. G., Feldmann K. A. and Benfey P. N.** 1996. The SCARECROW Gene Regulates an Asymmetric Cell Division That Is Essential for Generating the Radial Organization of the Arabidopsis Root. *Cell.* 86(3): 423-433
- Dickstein R., Hu X., Yang J., Ba L., Coque L., Kim D., Cook D. R. and Yeung A. T.** 2002. Differential expression of tandemly duplicated *Enod8* genes in *Medicago*. *Plant Science.* 163(2): 333-343
- Downie J. A.** 2007. Plant science. Infectious heresy. *Science.* 316(5829): 1296-1297
- Doyle J. J.** 2011. Phylogenetic perspectives on the origins of nodulation. *Mol Plant Microbe Interact.* 24(11): 1289-1295
- Dudley M. E., Jacobs T. W. and Long S. R.** 1987. Microscopic studies of cell divisions induced in alfalfa roots by *Rhizobium meliloti*. *Planta.* 171(3): 289-301
- Durso N. A. and Cyr R. J.** 1994. A calmodulin-sensitive interaction between microtubules and a higher plant homolog of elongation factor-1 alpha. *Plant Cell.* 6(6): 893-905
- El Yahyaoui F., Kuster H., Ben Amor B., Hohnjec N., Puhler A., Becker A., Gouzy J., Vernie T., Gough C., Niebel A., *et al.*** 2004. Expression profiling in *Medicago truncatula* identifies more than 750 genes differentially expressed during nodulation, including many potential regulators of the symbiotic program. *Plant Physiol.* 136(2): 3159-3176
- Emons A. M. and Mulder B. M.** 2000. How the deposition of cellulose microfibrils builds cell wall architecture. *Trends Plant Sci.* 5(1): 35-40
- Esseling J. J., Lhuissier F. G. and Emons A. M.** 2003. Nod factor-induced root hair curling: continuous polar growth towards the point of nod factor application. *Plant Physiol.* 132(4): 1982-1988
- Fehér D. and Bokor R.** 1926. Untersuchungen fiber die bakterielle Wurzelsymbiose einiger Leguminosenhölzer. *Planta.* 2(4-5): 406-413
- Ferguson B. J. and Reid J. B.** 2005. Cochleata: getting to the root of legume nodules. *Plant Cell Physiol.* 46(9): 1583-1589
- Ferguson B. J., Indrasumunar A., Hayashi S., Lin M. H., Lin Y. H., Reid D. E. and Gresshoff P. M.** 2010. Molecular analysis of legume nodule development and autoregulation. *J Integr Plant Biol.* 52(1): 61-76

- Fliegmann J., Uhlenbroich S., Shinya T., Martinez Y., Lefebvre B., Shibuya N. and Bono J. J.** 2011. Biochemical and phylogenetic analysis of CEBiP-like LysM domain-containing extracellular proteins in higher plants. *Plant Physiol Biochem.* 49(7): 709-720
- Fortin M. G., Morrison N. A. and Verma D. P.** 1987. Nodulin-26, a peribacteroid membrane nodulin is expressed independently of the development of the peribacteroid compartment. *Nucleic Acids Res.* 15(2): 813-824
- Foucher F. and Kondorosi E.** 2000. Cell cycle regulation in the course of nodule organogenesis in *Medicago*. *Plant Mol Biol.* 43(5-6): 773-786
- Fukaki H., Tameda S., Masuda H. and Tasaka M.** 2002. Lateral root formation is blocked by a gain-of-function mutation in the SOLITARY-ROOT/IAA14 gene of *Arabidopsis*. *Plant J.* 29(2): 153-168
- Fung T. K. and Poon R. Y.** 2005. A roller coaster ride with the mitotic cyclins. *Semin Cell Dev Biol.* 16(3): 335-342
- Galinha C., Hofhuis H., Luijten M., Willemsen V., Blilou I., Heidstra R. and Scheres B.** 2007. PLETHORA proteins as dose-dependent master regulators of *Arabidopsis* root development. *Nature.* 449(7165): 1053-1057
- Gamas P., Niebel Fde C., Lescure N. and Cullimore J.** 1996. Use of a subtractive hybridization approach to identify new *Medicago truncatula* genes induced during root nodule development. *Mol Plant Microbe Interact.* 9(4): 233-242
- Gamas P., de Billy F. and Truchet G.** 1998. Symbiosis-specific expression of two *Medicago truncatula* nodulin genes, MtN1 and MtN13, encoding products homologous to plant defense proteins. *Mol Plant Microbe Interact.* 11(5): 393-403
- Gamborg O. L., Murashige T., Thorpe T. A. and Vasil I. K.** 1976. Plant tissue culture media. *In Vitro.* 12(7): 473-478
- Gaude N., Bortfeld S., Duensing N., Lohse M. and Krajinski F.** 2012. Arbuscule-containing and non-colonized cortical cells of mycorrhizal roots undergo extensive and specific reprogramming during arbuscular mycorrhizal development. *Plant J.* 69(3): 510-528
- Geldner N., Friml J., Stierhof Y. D., Jurgens G. and Palme K.** 2001. Auxin transport inhibitors block PIN1 cycling and vesicle trafficking. *Nature.* 413(6854): 425-428
- Genre A., Chabaud M., Timmers T., Bonfante P. and Barker D. G.** 2005. Arbuscular mycorrhizal fungi elicit a novel intracellular apparatus in *Medicago truncatula* root epidermal cells before infection. *Plant Cell.* 17(12): 3489-3499
- Genre A., Chabaud M., Balzergue C., Puech-Pages V., Novero M., Rey T., Fournier J., Rochange S., Becard G., Bonfante P., *et al.*** 2013. Short-chain chitin oligomers from arbuscular mycorrhizal fungi trigger nuclear Ca²⁺ spiking in *Medicago truncatula* roots and their production is enhanced by strigolactone. *New Phytol.* 198(1): 190-202
- Gentleman R. C., Carey V. J., Bates D. M., Bolstad B., Dettling M., Dudoit S., Ellis B., Gautier L., Ge Y., Gentry J., *et al.*** 2004. Bioconductor: open software development for computational biology and bioinformatics. *Genome Biol.* 5(10): R80
- Geurts R. and Bisseling T.** 2002. Rhizobium nod factor perception and signalling. *Plant Cell.* 14 Suppl(S239-249)
- Geurts R., Lillo A. and Bisseling T.** 2012. Exploiting an ancient signalling machinery to enjoy a nitrogen fixing symbiosis. *Curr Opin Plant Biol.* 15(4): 438-443
- Gherbi H., Markmann K., Svistoonoff S., Estevan J., Autran D., Giczey G., Auguy F., Peret B., Laplace L., Franche C., *et al.*** 2008. SymRK defines a common genetic basis for plant root endosymbioses with arbuscular mycorrhiza fungi, rhizobia, and Frankiabacteria. *Proc Natl Acad Sci U S A.* 105(12): 4928-4932
- Gifford M. L., Robertson F. C., Soares D. C. and Ingram G. C.** 2005. ARABIDOPSIS CRINKLY4 function, internalization, and turnover are dependent on the extracellular crinkly repeat domain. *Plant Cell.* 17(4): 1154-1166
- Godfroy O., Debelles F., Timmers T. and Rosenberg C.** 2006. A rice calcium- and calmodulin-dependent protein kinase restores nodulation to a legume mutant. *Mol Plant Microbe Interact.* 19(5): 495-501

- Godiard L., Niebel A., Micheli F., Gouzy J., Ott T. and Gamas P.** 2007. Identification of new potential regulators of the *Medicago truncatula*-*Sinorhizobium meliloti* symbiosis using a large-scale suppression subtractive hybridization approach. *Mol Plant Microbe Interact.* 20(3): 321-332
- Goedhart J., Hink M. A., Visser A. J., Bisseling T. and Gadella T. W., Jr.** 2000. In vivo fluorescence correlation microscopy (FCM) reveals accumulation and immobilization of Nod factors in root hair cell walls. *Plant J.* 21(1): 109-119
- Goedhart J., von Stetten D., Noirclerc-Savoye M., Lelimousin M., Joosen L., Hink M. A., van Weeren L., Gadella T. W., Jr. and Royant A.** 2012. Structure-guided evolution of cyan fluorescent proteins towards a quantum yield of 93%. *Nat Commun.* 3(751)
- Goh L. K. and Sorkin A.** 2013. Endocytosis of receptor tyrosine kinases. *Cold Spring Harb Perspect Biol.* 5(5): a017459
- Gonzalez-Jamett A. M., Momboisse F., Haro-Acuna V., Bevilacqua J. A., Caviedes P. and Cardenas A. M.** 2013. Dynamin-2 Function and Dysfunction Along the Secretory Pathway. *Front Endocrinol (Lausanne).* 4(126)
- Gonzalez-Sama A., de la Pena T. C., Kevei Z., Mergaert P., Lucas M. M., de Felipe M. R., Kondorosi E. and Pueyo J. J.** 2006. Nuclear DNA endoreduplication and expression of the mitotic inhibitor Ccs52 associated to determinate and lupinoid nodule organogenesis. *Mol Plant Microbe Interact.* 19(2): 173-180
- Gough C.** 2003. Rhizobium symbiosis: insight into Nod factor receptors. *Curr Biol.* 13(24): R973-975
- Gough C. and Cullimore J.** 2011. Lipo-chitoooligosaccharide signaling in endosymbiotic plant-microbe interactions. *Mol Plant Microbe Interact.* 24(8): 867-878
- Greeff C., Roux M., Mundy J. and Petersen M.** 2012. Receptor-like kinase complexes in plant innate immunity. *Front Plant Sci.* 3(209)
- Gregan B., Jurgensen J., Papsdorf G., Furkert J., Schaefer M., Beyermann M., Rosenthal W. and Oksche A.** 2004. Ligand-dependent differences in the internalization of endothelin A and endothelin B receptor heterodimers. *J Biol Chem.* 279(26): 27679-27687
- Grunewald W., van Noorden G., Van Isterdael G., Beeckman T., Gheysen G. and Mathesius U.** 2009. Manipulation of auxin transport in plant roots during Rhizobium symbiosis and nematode parasitism. *Plant Cell.* 21(9): 2553-2562
- Guan D., Stacey N., Liu C., Wen J., Mysore K. S., Torres-Jerez I., Vernie T., Tadege M., Zhou C., Wang Z. Y., *et al.*** 2013. Rhizobial infection is associated with the development of peripheral vasculature in nodules of *Medicago truncatula*. *Plant Physiol.* 162(1): 107-115
- Guo Y., Han L., Hymes M., Denver R. and Clark S. E.** 2010. CLAVATA2 forms a distinct CLE-binding receptor complex regulating Arabidopsis stem cell specification. *Plant J.* 63(6): 889-900
- Hadri A.-Z., Spaik H. P., Bisseling T. and Brewin N. J.** 1998. Diversity of root nodulation and rhizobial infection process. The Rhizobiaceae: Molecular Biology of Model Plant-Associated Bacteria. 347-360
- Haney C. H. and Long S. R.** 2010. Plant flotillins are required for infection by nitrogen-fixing bacteria. *Proc Natl Acad Sci U S A.* 107(1): 478-483
- Haney C. H., Riely B. K., Tricoli D. M., Cook D. R., Ehrhardt D. W. and Long S. R.** 2011. Symbiotic Rhizobia Bacteria Trigger a Change in Localization and Dynamics of the *Medicago truncatula* Receptor Kinase LYK3. *Plant Cell.* 23(7): 2774-2787
- Hansen C. G. and Nichols B. J.** 2009. Molecular mechanisms of clathrin-independent endocytosis. *J Cell Sci.* 122(Pt 11): 1713-1721
- Hassan S. and Mathesius U.** 2012. The role of flavonoids in root-rhizosphere signalling: opportunities and challenges for improving plant-microbe interactions. *J Exp Bot.* 63(9): 3429-3444
- Hata S., Kobae Y. and Banba M.** 2010. Interactions between plants and arbuscular mycorrhizal fungi. *Int Rev Cell Mol Biol.* 281(1-48)
- Hayashi T., Shimoda Y., Sato S., Tabata S., Imaizumi-Anraku H. and Hayashi M.** 2013. Rhizobial infection does not require cortical expression of upstream common symbiosis genes responsible for the induction of Ca spiking. *Plant J.*

- Heldin C. H.** 1995. Dimerization of cell surface receptors in signal transduction. *Cell*. 80(2): 213-223
- Herrbach V., Remblière C., Gough C. and Bensmihen S.** 2014. Lateral root formation and patterning in *Medicago truncatula*. *Journal of Plant Physiology*. 171(3–4): 301-310
- Hink M. A., Shah K., Russinova E., de Vries S. C. and Visser A. J.** 2008. Fluorescence fluctuation analysis of *Arabidopsis thaliana* somatic embryogenesis receptor-like kinase and brassinosteroid insensitive 1 receptor oligomerization. *Biophys J*. 94(3): 1052-1062
- Hirsch A. M.** 1992. Developmental Biology of Legume Nodulation. *New Phytologist*. 122(2): 211-237
- Hocher V., Alloisio N., Bogusz D. and Normand P.** 2011. Early signaling in actinorhizal symbioses. *Plant Signal Behav.* 6(9): 1377-1379
- Hogslund N., Radutoiu S., Krusell L., Voroshilova V., Hannah M. A., Goffard N., Sanchez D. H., Lippold F., Ott T., Sato S., *et al.*** 2009. Dissection of symbiosis and organ development by integrated transcriptome analysis of *lotus japonicus* mutant and wild-type plants. *PLoS One*. 4(8): e6556
- Horvath B., Yeun L. H., Domonkos A., Halasz G., Gobbato E., Ayaydin F., Miro K., Hirsch S., Sun J., Tadege M., *et al.*** 2011. *Medicago truncatula* IPD3 is a member of the common symbiotic signaling pathway required for rhizobial and mycorrhizal symbioses. *Mol Plant Microbe Interact*. 24(11): 1345-1358
- Hossain M. S., Liao J., James E. K., Sato S., Tabata S., Jurkiewicz A., Madsen L. H., Stougaard J., Ross L. and Szczyglowski K.** 2012. *Lotus japonicus* ARPC1 is required for rhizobial infection. *Plant Physiol*. 160(2): 917-928
- Howard R. J., Ferrari M. A., Roach D. H. and Money N. P.** 1991. Penetration of hard substrates by a fungus employing enormous turgor pressures. *Proceedings of the National Academy of Sciences*. 88(24): 11281-11284
- Irani N. G. and Russinova E.** 2009. Receptor endocytosis and signaling in plants. *Curr Opin Plant Biol*. 12(6): 653-659
- Ishikawa-Ankerhold H. C., Ankerhold R. and Drummen G. P.** 2012. Advanced fluorescence microscopy techniques--FRAP, FLIP, FLAP, FRET and FLIM. *Molecules*. 17(4): 4047-4132
- Ivanov R. and Gaude T.** 2009. Endocytosis and endosomal regulation of the S-receptor kinase during the self-incompatibility response in *Brassica oleracea*. *Plant Cell*. 21(7): 2107-2117
- Ivanov S., Fedorova E. and Bisseling T.** 2010. Intracellular plant microbe associations: secretory pathways and the formation of perimicrobial compartments. *Curr Opin Plant Biol*. 13(4): 372-377
- Ivanov S., Fedorova E. E., Limpens E., De Mita S., Genre A., Bonfante P. and Bisseling T.** 2012. Rhizobium-legume symbiosis shares an exocytotic pathway required for arbuscule formation. *Proc Natl Acad Sci U S A*. 109(21): 8316-8321
- Jaillais Y., Belkhadir Y., Balsemao-Pires E., Dangl J. L. and Chory J.** 2011. Extracellular leucine-rich repeats as a platform for receptor/coreceptor complex formation. *Proc Natl Acad Sci U S A*. 108(20): 8503-8507
- Jarsch I. K. and Ott T.** 2011. Perspectives on remorin proteins, membrane rafts, and their role during plant-microbe interactions. *Mol Plant Microbe Interact*. 24(1): 7-12
- Jefferson R. A., Kavanagh T. A. and Bevan M. W.** 1987. GUS fusions: beta-glucuronidase as a sensitive and versatile gene fusion marker in higher plants. *Embo J*. 6(13): 3901-3907
- Jeong Y. J., Shang Y., Kim B. H., Kim S. Y., Song J. H., Lee J. S., Lee M. M., Li J. and Nam K. H.** 2010. BAK7 displays unequal genetic redundancy with BAK1 in brassinosteroid signaling and early senescence in *Arabidopsis*. *Mol Cells*. 29(3): 259-266
- Jones K. M., Kobayashi H., Davies B. W., Taga M. E. and Walker G. C.** 2007. How rhizobial symbionts invade plants: the Sinorhizobium-Medicago model. *Nat Rev Microbiol*. 5(8): 619-633
- Journet E. P., El-Gachtouli N., Vernoud V., de Billy F., Pichon M., Dedieu A., Arnould C., Morandi D., Barker D. G. and Gianinazzi-Pearson V.** 2001. *Medicago truncatula* ENOD11: a novel RPRP-encoding early nodulin gene expressed during mycorrhization in arbuscule-containing cells. *Mol Plant Microbe Interact*. 14(6): 737-748

Kalo P., Gleason C., Edwards A., Marsh J., Mitra R. M., Hirsch S., Jakab J., Sims S., Long S. R., Rogers J., *et al.* 2005. Nodulation signaling in legumes requires NSP2, a member of the GRAS family of transcriptional regulators. *Science*. 308(5729): 1786-1789

Kanamori N., Madsen L. H., Radutoiu S., Frantescu M., Quistgaard E. M., Miwa H., Downie J. A., James E. K., Felle H. H., Haaning L. L., *et al.* 2006. A nucleoporin is required for induction of Ca²⁺ spiking in legume nodule development and essential for rhizobial and fungal symbiosis. *Proc Natl Acad Sci U S A*. 103(2): 359-364

Karimi M., Inze D. and Depicker A. 2002. GATEWAY vectors for Agrobacterium-mediated plant transformation. *Trends Plant Sci*. 7(5): 193-195

Karlova R., Boeren S., Russinova E., Aker J., Vervoort J. and de Vries S. 2006. The Arabidopsis SOMATIC EMBRYOGENESIS RECEPTOR-LIKE KINASE1 protein complex includes BRASSINOSTEROID-INSENSITIVE1. *Plant Cell*. 18(3): 626-638

Kerk N. M., Ceserani T., Tausta S. L., Sussex I. M. and Nelson T. M. 2003. Laser capture microdissection of cells from plant tissues. *Plant Physiol*. 132(1): 27-35

Kevei Z., Vinardell J. M., Kiss G. B., Kondorosi A. and Kondorosi E. 2002. Glycine-rich proteins encoded by a nodule-specific gene family are implicated in different stages of symbiotic nodule development in *Medicago* spp. *Mol Plant Microbe Interact*. 15(9): 922-931

Kiss E., Olah B., Kalo P., Morales M., Heckmann A. B., Borbala A., Lozsa A., Kontar K., Middleton P., Downie J. A., *et al.* 2009. LIN, a novel type of U-box/WD40 protein, controls early infection by rhizobia in legumes. *Plant Physiol*. 151(3): 1239-1249

Kleine-Vehn J., Leitner J., Zwiewka M., Sauer M., Abas L., Luschign C. and Friml J. 2008. Differential degradation of PIN2 auxin efflux carrier by retromer-dependent vacuolar targeting. *Proc Natl Acad Sci U S A*. 105(46): 17812-17817

Kouchi H., Imaizumi-Anraku H., Hayashi M., Hakoyama T., Nakagawa T., Umehara Y., Suganuma N. and Kawaguchi M. 2010. How many peas in a pod? Legume genes responsible for mutualistic symbioses underground. *Plant Cell Physiol*. 51(9): 1381-1397

Kremers G. J., Goedhart J., van Munster E. B. and Gadella T. W., Jr. 2006. Cyan and yellow super fluorescent proteins with improved brightness, protein folding, and FRET Forster radius. *Biochemistry*. 45(21): 6570-6580

Krusell L., Krause K., Ott T., Desbrosses G., Kramer U., Sato S., Nakamura Y., Tabata S., James E. K., Sandal N., *et al.* 2005. The sulfate transporter SST1 is crucial for symbiotic nitrogen fixation in *Lotus japonicus* root nodules. *Plant Cell*. 17(5): 1625-1636

Kuppusamy K. T., Endre G., Prabhu R., Penmetsa R. V., Veereshlingam H., Cook D. R., Dickstein R. and Vandenbosch K. A. 2004. LIN, a *Medicago truncatula* gene required for nodule differentiation and persistence of rhizobial infections. *Plant Physiol*. 136(3): 3682-3691

Kurakawa T., Ueda N., Maekawa M., Kobayashi K., Kojima M., Nagato Y., Sakakibara H. and Kyoizuka J. 2007. Direct control of shoot meristem activity by a cytokinin-activating enzyme. *Nature*. 445(7128): 652-655

Kuster H., Hohnjec N., Krajinski F., El Y. F., Manthey K., Gouzy J., Dondrup M., Meyer F., Kalinowski J., Brechenmacher L., *et al.* 2004. Construction and validation of cDNA-based Mt6k-RIT macro- and microarrays to explore root endosymbioses in the model legume *Medicago truncatula*. *J Biotechnol*. 108(2): 95-113

Lafont F. and van der Goot F. G. 2005. Oiling the key hole. *Mol Microbiol*. 56(3): 575-577

Lam B. C., Sage T. L., Bianchi F. and Blumwald E. 2001. Role of SH3 domain-containing proteins in clathrin-mediated vesicle trafficking in Arabidopsis. *Plant Cell*. 13(11): 2499-2512

Lancelle S. A. and Torrey J. G. 1985. Early Development of Rhizobium-Induced Root-Nodules of *Parasponia-Rigida*. 2. Nodule Morphogenesis and Symbiotic Development. *Canadian Journal of Botany-Revue Canadienne De Botanique*. 63(1): 25-35

Laporte P., Lepage A., Fournier J., Catrice O., Moreau S., Jardinaud M. F., Mun J. H., Larrainzar E., Cook D. R., Gamas P., *et al.* 2014. The CCAAT box-binding transcription factor NF-YA1 controls rhizobial infection. *J Exp Bot*. 65(2): 481-494

- Laskowski M., Grieneisen V. A., Hofhuis H., Hove C. A., Hogeweg P., Maree A. F. and Scheres B. 2008. Root system architecture from coupling cell shape to auxin transport. *PLoS Biol.* 6(12): e307
- Lauber M. H., Waizenegger I., Steinmann T., Schwarz H., Mayer U., Hwang I., Lukowitz W. and Jurgens G. 1997. The Arabidopsis KNOLLE protein is a cytokinesis-specific syntaxin. *J Cell Biol.* 139(6): 1485-1493
- Lefebvre B., Furt F., Hartmann M. A., Michaelson L. V., Carde J. P., Sargueil-Boiron F., Rossignol M., Napier J. A., Cullimore J., Bessoule J. J., *et al.* 2007. Characterization of lipid rafts from *Medicago truncatula* root plasma membranes: a proteomic study reveals the presence of a raft-associated redox system. *Plant Physiol.* 144(1): 402-418
- Lefebvre B., Timmers T., Mbengue M., Moreau S., Herve C., Toth K., Bittencourt-Silvestre J., Klaus D., Deslandes L., Godiard L., *et al.* 2010. A remorin protein interacts with symbiotic receptors and regulates bacterial infection. *Proc Natl Acad Sci U S A.* 107(5): 2343-2348
- Lefebvre B., Klaus-Heisen D., Pietraszewska-Bogiel A., Herve C., Camut S., Auriac M. C., Gascioli V., Nurisso A., Gadella T. W. and Cullimore J. 2012. Role of N-glycosylation sites and CXC motifs in trafficking of *medicago truncatula* Nod factor perception protein to plasma membrane. *J Biol Chem.* 287(14): 10812-10823
- Legocki R. P. and Verma D. P. 1980. Identification of "nodule-specific" host proteins (nodoulin) involved in the development of rhizobium-legume symbiosis. *Cell.* 20(1): 153-163
- Lerouge P., Roche P., Faucher C., Maillet F., Truchet G., Prome J. C. and Denarie J. 1990. Symbiotic host-specificity of *Rhizobium meliloti* is determined by a sulphated and acylated glucosamine oligosaccharide signal. *Nature.* 344(6268): 781-784
- Levy J., Bres C., Geurts R., Chalhoub B., Kulikova O., Duc G., Journet E. P., Ane J. M., Lauber E., Bisseling T., *et al.* 2004. A putative Ca²⁺ and calmodulin-dependent protein kinase required for bacterial and fungal symbioses. *Science.* 303(5662): 1361-1364
- Libbenga K. R. and Harkes P. A. A. 1973. Initial Proliferation of Cortical Cells in Formation of Root Nodules in *Pisum-Sativum* L. *Planta.* 114(1): 17-28
- Limpens E. and Bisseling T. 2003. Signaling in symbiosis. *Curr Opin Plant Biol.* 6(4): 343-350
- Limpens E., Franken C., Smit P., Willemsse J., Bisseling T. and Geurts R. 2003. LysM domain receptor kinases regulating rhizobial Nod factor-induced infection. *Science.* 302(5645): 630-633
- Limpens E., Ramos J., Franken C., Raz V., Compaan B., Franssen H., Bisseling T. and Geurts R. 2004. RNA interference in *Agrobacterium rhizogenes*-transformed roots of *Arabidopsis* and *Medicago truncatula*. *J Exp Bot.* 55(399): 983-992
- Limpens E., Mirabella R., Fedorova E., Franken C., Franssen H., Bisseling T. and Geurts R. 2005. Formation of organelle-like N₂-fixing symbiosomes in legume root nodules is controlled by DMI2. *Proc Natl Acad Sci U S A.* 102(29): 10375-10380
- Limpens E., Ivanov S., van Esse W., Voets G., Fedorova E. and Bisseling T. 2009. *Medicago* N₂-fixing symbiosomes acquire the endocytic identity marker Rab7 but delay the acquisition of vacuolar identity. *Plant Cell.* 21(9): 2811-2828
- Limpens E., Ovchinnikova E., Journet E. P., Chabaud M., Cosson V., Ratet P., Duc G., Fedorova E., Liu W., Op den Camp R., *et al.* 2011. IPD3 controls the formation of nitrogen-fixing symbiosomes in pea and *Medicago*. *Mol Plant Microbe Interact.* 24(11): 1333-1344
- Limpens E., Moling S., Hooiveld G., Pereira P. A., Bisseling T., Becker J. D. and Kuster H. 2013. cell- and tissue-specific transcriptome analyses of *Medicago truncatula* root nodules. *PLoS One.* 8(5): e64377
- Liu J., Miller S. S., Graham M., Bucciarelli B., Catalano C. M., Sherrier D. J., Samac D. A., Ivashuta S., Fedorova M., Matsumoto P., *et al.* 2006. Recruitment of novel calcium-binding proteins for root nodule symbiosis in *Medicago truncatula*. *Plant Physiol.* 141(1): 167-177
- Liu T., Liu Z., Song C., Hu Y., Han Z., She J., Fan F., Wang J., Jin C., Chang J., *et al.* 2012. Chitin-induced dimerization activates a plant immune receptor. *Science.* 336(6085): 1160-1164

- Liu W., Kohlen W., Lillo A., Op den Camp R., Ivanov S., Hartog M., Limpens E., Jamil M., Smaczniak C., Kaufmann K., *et al.* 2011. Strigolactone biosynthesis in *Medicago truncatula* and rice requires the symbiotic GRAS-type transcription factors NSP1 and NSP2. *Plant Cell*. 23(10): 3853-3865
- Lohar D. P., Sharopova N., Endre G., Penuela S., Samac D., Town C., Silverstein K. A. and VandenBosch K. A. 2006. Transcript analysis of early nodulation events in *Medicago truncatula*. *Plant Physiol*. 140(1): 221-234
- Luyten E. and Vanderleyden J. 2000. Survey of genes identified in *Sinorhizobium meliloti* spp., necessary for the development of an efficient symbiosis. *European Journal of Soil Biology*. 36(1): 1-26
- Madsen E. B., Madsen L. H., Radutoiu S., Olbryt M., Rakwalska M., Szczyglowski K., Sato S., Kaneko T., Tabata S., Sandal N., *et al.* 2003. A receptor kinase gene of the LysM type is involved in legume perception of rhizobial signals. *Nature*. 425(6958): 637-640
- Madsen E. B., Antolín-Llovera M., Grossmann C., Ye J., Vieweg S., Broghammer A., Krusell L., Radutoiu S., Jensen O. N., Stougaard J., *et al.* 2011. Autophosphorylation is essential for the in vivo function of the *Lotus japonicus* Nod factor receptor 1 and receptor-mediated signalling in cooperation with Nod factor receptor 5. *The Plant Journal*. 65(3): 404-417
- Madsen L. H., Tirichine L., Jurkiewicz A., Sullivan J. T., Heckmann A. B., Bek A. S., Ronson C. W., James E. K. and Stougaard J. 2010. The molecular network governing nodule organogenesis and infection in the model legume *Lotus japonicus*. *Nat Commun*. 1(1): 1-12
- Maillet F., Poinso V., Andre O., Puech-Pages V., Haouy A., Gueunier M., Cromer L., Giraudet D., Formey D., Niebel A., *et al.* 2011. Fungal lipochitooligosaccharide symbiotic signals in arbuscular mycorrhiza. *Nature*. 469(7328): 58-63
- Manthey K., Krajinski F., Hohnjec N., Firnhaber C., Puhler A., Perlick A. M. and Kuster H. 2004. Transcriptome profiling in root nodules and arbuscular mycorrhiza identifies a collection of novel genes induced during *Medicago truncatula* root endosymbioses. *Mol Plant Microbe Interact*. 17(10): 1063-1077
- Marhavý P., Bielach A., Abas L., Abuzeineh A., Duclercq J., Tanaka H., Pařezová M., Petrášek J., Friml J., Kleine-Vehn J., *et al.* 2011. Cytokinin Modulates Endocytic Trafficking of PIN1 Auxin Efflux Carrier to Control Plant Organogenesis. *Dev Cell*. 21(4): 796-804
- Marie C., Plaskitt K. A. and Downie J. A. 1994. Abnormal Bacteroid Development in Nodules Induced by a Glucosamine Synthase Mutant of *Rhizobium ieguminosarum*. *Mol Plant Microbe Interact*. 7(4): 482-487
- Markmann K., Giczey G. and Parniske M. 2008. Functional adaptation of a plant receptor-kinase paved the way for the evolution of intracellular root symbioses with bacteria. *PLoS Biol*. 6(3): e68
- Marsh J. F., Rakocevic A., Mitra R. M., Brocard L., Sun J., Eschstruth A., Long S. R., Schultze M., Ratet P. and Oldroyd G. E. 2007. *Medicago truncatula* NIN is essential for rhizobial-independent nodule organogenesis induced by autoactive calcium/calmodulin-dependent protein kinase. *Plant Physiol*. 144(1): 324-335
- Mathis R., Grosjean C., de Billy F., Huguet T. and Gamas P. 1999. The early nodulin gene MtN6 is a novel marker for events preceding infection of *Medicago truncatula* roots by *Sinorhizobium meliloti*. *Mol Plant Microbe Interact*. 12(6): 544-555
- Maunoury N., Redondo-Nieto M., Bourcy M., Van de Velde W., Alunni B., Laporte P., Durand P., Agier N., Marisa L., Vaubert D., *et al.* 2010. Differentiation of symbiotic cells and endosymbionts in *Medicago truncatula* nodulation are coupled to two transcriptome-switches. *PLoS One*. 5(3): e9519
- Mbengue M., Camut S., de Carvalho-Niebel F., Deslandes L., Froidure S., Klaus-Heisen D., Moreau S., Rivas S., Timmers T., Herve C., *et al.* 2010. The *Medicago truncatula* E3 Ubiquitin Ligase PUB1 Interacts with the LYK3 Symbiotic Receptor and Negatively Regulates Infection and Nodulation. *Plant Cell*. 22(10): 3474-3488
- Mellersh D. and Parniske M. 2006. Common symbiosis genes of *Lotus japonicus* are not required for intracellular accommodation of the rust fungus *Uromyces loti*. *New Phytol*. 170(4): 641-644

Mergaert P., Nikovics K., Kelemen Z., Maunoury N., Vaubert D., Kondorosi A. and Kondorosi E. 2003. A novel family in *Medicago truncatula* consisting of more than 300 nodule-specific genes coding for small, secreted polypeptides with conserved cysteine motifs. *Plant Physiol.* 132(1): 161-173

Mergaert P., Uchiumi T., Alunni B., Evanno G., Cheron A., Catrice O., Mausset A. E., Barloy-Hubler F., Galibert F., Kondorosi A., *et al.* 2006. Eukaryotic control on bacterial cell cycle and differentiation in the *Rhizobium-legume* symbiosis. *Proc Natl Acad Sci U S A.* 103(13): 5230-5235

Messinese E., Mun J. H., Yeun L. H., Jayaraman D., Rouge P., Barre A., Loughon G., Schornack S., Bono J. J., Cook D. R., *et al.* 2007. A novel nuclear protein interacts with the symbiotic DMI3 calcium- and calmodulin-dependent protein kinase of *Medicago truncatula*. *Mol Plant Microbe Interact.* 20(8): 912-921

Middleton A. M., King J. R., Bennett M. J. and Owen M. R. 2010. Mathematical Modelling of the Aux/IAA Negative Feedback Loop. 72(6): 1383-1407

Middleton P. H., Jakab J., Penmetsa R. V., Starker C. G., Doll J., Kalo P., Prabhu R., Marsh J. F., Mitra R. M., Kereszt A., *et al.* 2007. An ERF transcription factor in *Medicago truncatula* that is essential for Nod factor signal transduction. *Plant Cell.* 19(4): 1221-1234

Mirabella R., Franken C., van der Krogt G. N., Bisseling T. and Geurts R. 2004. Use of the fluorescent timer DsRED-E5 as reporter to monitor dynamics of gene activity in plants. *Plant Physiol.* 135(4): 1879-1887

Mitra R. M., Gleason C. A., Edwards A., Hadfield J., Downie J. A., Oldroyd G. E. and Long S. R. 2004. A Ca²⁺/calmodulin-dependent protein kinase required for symbiotic nodule development: Gene identification by transcript-based cloning. *Proc Natl Acad Sci U S A.* 101(13): 4701-4705

Mitra R. M. and Long S. R. 2004. Plant and bacterial symbiotic mutants define three transcriptionally distinct stages in the development of the *Medicago truncatula*/Sinorhizobium meliloti symbiosis. *Plant Physiol.* 134(2): 595-604

Miyahara A., Richens J., Starker C., Morieri G., Smith L., Long S., Downie J. A. and Oldroyd G. E. 2010. Conservation in function of a SCAR/WAVE component during infection thread and root hair growth in *Medicago truncatula*. *Mol Plant Microbe Interact.* 23(12): 1553-1562

Moore R. C., Durso N. A. and Cyr R. J. 1998. Elongation factor-1 α stabilizes microtubules in a calcium/calmodulin-dependent manner. *Cell Motil Cytoskeleton.* 41(2): 168-180

Moreau S., Verdenaud M., Ott T., Letort S., de Billy F., Niebel A., Gouzy J., de Carvalho-Niebel F. and Gamas P. 2011. Transcription reprogramming during root nodule development in *Medicago truncatula*. *PLoS One.* 6(1): e16463

Morlot S. and Roux A. 2013. Mechanics of dynamin-mediated membrane fission. *Annu Rev Biophys.* 42(629-649)

Mortier V., Den Herder G., Whitford R., Van de Velde W., Rombauts S., D'Haeseleer K., Holsters M. and Goormachtig S. 2010. CLE peptides control *Medicago truncatula* nodulation locally and systemically. *Plant Physiol.* 153(1): 222-237

Morzhina E. V., Tsyganov V. E., Borisov A. Y., Lebsky V. K. and Tikhonovich I. A. 2000. Four developmental stages identified by genetic dissection of pea (*Pisum sativum* L.) root nodule morphogenesis. *Plant Sci.* 155(1): 75-83

Munro S. 2003. Lipid rafts: elusive or illusive? *Cell.* 115(4): 377-388

Murray J. D. 2011. Invasion by invitation: rhizobial infection in legumes. *Mol Plant Microbe Interact.* 24(6): 631-639

Nakagawa T., Kaku H., Shimoda Y., Sugiyama A., Shimamura M., Takanashi K., Yazaki K., Aoki T., Shibuya N. and Kouchi H. 2011. From defense to symbiosis: limited alterations in the kinase domain of LysM receptor-like kinases are crucial for evolution of legume-Rhizobium symbiosis. *Plant J.* 65(2): 169-180

Nap J. P. and Bisseling T. 1990. Developmental biology of a plant-prokaryote symbiosis: the legume root nodule. *Science.* 250(4983): 948-954

- Niebel Fde C., Lescure N., Cullimore J. V. and Gamas P.** 1998. The *Medicago truncatula* MtAnn1 gene encoding an annexin is induced by Nod factors and during the symbiotic interaction with *Rhizobium meliloti*. *Mol Plant Microbe Interact.* 11(6): 504-513
- Niklas K. J. and Kutschera U.** 2012. Plant development, auxin, and the subsystem incompleteness theorem. *Front Plant Sci.* 3(37)
- Nutman P. S.** 1948. Physiological Studies on Nodule Formation .1. The Relation between Nodulation and Lateral Root Formation in Red Clover. *Annals of Botany.* 12(46): 81-96
- Okazaki S., Kaneko T., Sato S. and Saeki K.** 2013. Hijacking of leguminous nodulation signaling by the rhizobial type III secretion system. *Proc Natl Acad Sci U S A.* 110(42): 17131-17136
- Okushima Y., Overvoorde P. J., Arima K., Alonso J. M., Chan A., Chang C., Ecker J. R., Hughes B., Lui A., Nguyen D., *et al.*** 2005. Functional genomic analysis of the AUXIN RESPONSE FACTOR gene family members in *Arabidopsis thaliana*: unique and overlapping functions of ARF7 and ARF19. *Plant Cell.* 17(2): 444-463
- Oldroyd G. E. and Downie J. A.** 2004. Calcium, kinases and nodulation signalling in legumes. *Nat Rev Mol Cell Biol.* 5(7): 566-576
- Oldroyd G. E., Murray J. D., Poole P. S. and Downie J. A.** 2011. The Rules of Engagement in the Legume-Rhizobial Symbiosis. *Annu Rev Genet.* 45(119-144)
- Oldroyd G. E.** 2013. Speak, friend, and enter: signalling systems that promote beneficial symbiotic associations in plants. *Nat Rev Microbiol.* 11(4): 252-263
- Op den Camp R., Streng A., De Mita S., Cao Q., Polone E., Liu W., Ammiraju J. S., Kudrna D., Wing R., Untergasser A., *et al.*** 2011. LysM-type mycorrhizal receptor recruited for rhizobium symbiosis in nonlegume *Parasponia*. *Science.* 331(6019): 909-912
- Osipova M. A., Mortier V., Demchenko K. N., Tsyganov V. E., Tikhonovich I. A., Lutova L. A., Dolgikh E. A. and Goormachtig S.** 2012. Wuschel-related homeobox5 gene expression and interaction of CLE peptides with components of the systemic control add two pieces to the puzzle of autoregulation of nodulation. *Plant Physiol.* 158(3): 1329-1341
- Ott T., van Dongen J. T., Gunther C., Krusell L., Desbrosses G., Vigeolas H., Bock V., Czechowski T., Geigenberger P. and Udvardi M. K.** 2005. Symbiotic leghemoglobins are crucial for nitrogen fixation in legume root nodules but not for general plant growth and development. *Curr Biol.* 15(6): 531-535
- Otto G. P. and Nichols B. J.** 2011. The roles of flotillin microdomains--endocytosis and beyond. *J Cell Sci.* 124(Pt 23): 3933-3940
- Ovchinnikova E.** 2012. Genetic analysis of symbiosome formation. (PhD thesis)
- Ovchinnikova E., Journet E. P., Chabaud M., Cosson V., Ratet P., Duc G., Fedorova E., Liu W., den Camp R. O., Zhukov V., *et al.*** 2012. IPD3 controls the formation of nitrogen-fixing symbiosomes in pea and *Medicago* Spp. *Mol Plant Microbe Interact.* 24(11): 1333-1344
- Parniske M.** 2000. Intracellular accommodation of microbes by plants: a common developmental program for symbiosis and disease? *Curr Opin Plant Biol.* 3(4): 320-328
- Pawlowski K. and Demchenko K. N.** 2012. The diversity of actinorhizal symbiosis. *Protoplasma.* 249(4): 967-979
- Peiter E., Sun J., Heckmann A. B., Venkateshwaran M., Riely B. K., Otegui M. S., Edwards A., Freshour G., Hahn M. G., Cook D. R., *et al.*** 2007. The *Medicago truncatula* DMI1 protein modulates cytosolic calcium signaling. *Plant Physiol.* 145(1): 192-203
- Penmetsta R. V. and Cook D. R.** 1997. A Legume Ethylene-Insensitive Mutant Hyperinfected by Its Rhizobial Symbiont. *Science.* 275(5299): 527-530
- Peret B., De Rybel B., Casimiro I., Benkova E., Swarup R., Laplace L., Beeckman T. and Bennett M. J.** 2009. *Arabidopsis* lateral root development: an emerging story. *Trends Plant Sci.* 14(7): 399-408
- Perraki A., Cacas J. L., Crowet J. M., Lins L., Castroviejo M., German-Retana S., Mongrand S. and Raffaele S.** 2012. Plasma membrane localization of *Solanum tuberosum* remorin from group 1, homolog 3 is mediated by conformational changes in a novel C-terminal anchor and required for the restriction of potato virus X movement]. *Plant Physiol.* 160(2): 624-637

- Pichon M., Journet E. P., Dedieu A., de Billy F., Truchet G. and Barker D. G. 1992. Rhizobium meliloti elicits transient expression of the early nodulin gene ENOD12 in the differentiating root epidermis of transgenic alfalfa. *Plant Cell*. 4(10): 1199-1211
- Pietraszewska-Bogiel A. and Gadella T. W. 2011. FRET microscopy: from principle to routine technology in cell biology. *J Microsc*. 241(2): 111-118
- Pietraszewska-Bogiel A. 2013. Insights into Nod factor signaling mediated by Medicago truncatula LysM receptor-like kinases, MtNFP and MtLYK3. (PhD thesis)
- Pietraszewska-Bogiel A., Lefebvre B., Koini M. A., Klaus-Heisen D., Takken F. L., Geurts R., Cullimore J. V. and Gadella T. W. 2013. Interaction of Medicago truncatula Lysin Motif Receptor-Like Kinases, NFP and LYK3, Produced in Nicotiana benthamiana Induces Defence-Like Responses. *PLoS One*. 8(6): e65055
- Pietraszewska-Bogiel A., van't Veer I., Crosby K. C., Goedhart J., Hink M. A. and Gadella T. W. submitted. Oligomerization of Medicago truncatula receptor-like kinases, NFP and LYK3, as reported with Förster Resonance Energy Transfer-Fluorescence Lifetime Imaging Microscopy.
- Pislariu C. I. and Dickstein R. 2007a. The AGC Kinase MtIRE: A Link to Phospholipid Signaling During Nodulation? *Plant Signal Behav*. 2(4): 314-316
- Pislariu C. I. and Dickstein R. 2007b. An IRE-like AGC kinase gene, MtIRE, has unique expression in the invasion zone of developing root nodules in Medicago truncatula. *Plant Physiol*. 144(2): 682-694
- Radutoiu S., Madsen L. H., Madsen E. B., Felle H. H., Umehara Y., Gronlund M., Sato S., Nakamura Y., Tabata S., Sandal N., *et al*. 2003. Plant recognition of symbiotic bacteria requires two LysM receptor-like kinases. *Nature*. 425(6958): 585-592
- Radwan O., Wu X., Govindarajulu M., Libault M., Neece D. J., Oh M. H., Berg R. H., Stacey G., Taylor C. G., Huber S. C., *et al*. 2012. 14-3-3 proteins SGF14c and SGF14l play critical roles during soybean nodulation. *Plant Physiol*. 160(4): 2125-2136
- Rae A. L., Bonfante-Fasolo P. and Brewin N. J. 1992. Structure and growth of infection threads in the legume symbiosis with Rhizobium leguminosarum. *The Plant Journal*. 2(3): 385-395
- Riely B. K., Lounnon G., Ane J. M. and Cook D. R. 2007. The symbiotic ion channel homolog DMI1 is localized in the nuclear membrane of Medicago truncatula roots. *Plant J*. 49(2): 208-216
- Riely B. K., Larrainzar E., Haney C. H., Mun J. H., Gil-Quintana E., Gonzalez E. M., Yu H. J., Tricoli D., Ehrhardt D. W., Long S. R., *et al*. 2013. Development of tools for the biochemical characterization of the symbiotic receptor-like kinase DMI2. *Mol Plant Microbe Interact*. 26(2): 216-226
- Rietveld A. and Simons K. 1998. The differential miscibility of lipids as the basis for the formation of functional membrane rafts. *Biochim Biophys Acta*. 1376(3): 467-479
- Rival P., de Billy F., Bono J. J., Gough C., Rosenberg C. and Bensmihen S. 2012. Epidermal and cortical roles of NFP and DMI3 in coordinating early steps of nodulation in Medicago truncatula. *Development*. 139(18): 3383-3391
- Robatzek S., Chinchilla D. and Boller T. 2006. Ligand-induced endocytosis of the pattern recognition receptor FLS2 in Arabidopsis. *Genes Dev*. 20(5): 537-542
- Roppolo D., De Rybel B., Tendon V. D., Pfister A., Alassimone J., Vermeer J. E. M., Yamazaki M., Stierhof Y.-D., Beeckman T. and Geldner N. 2011. A novel protein family mediates Casparian strip formation in the endodermis. 473(7347): 380-383
- Rose C. M., Venkateshwaran M., Volkening J. D., Grimsrud P. A., Maeda J., Bailey D. J., Park K., Howes-Podoll M., den Os D., Yeun L. H., *et al*. 2012. Rapid phosphoproteomic and transcriptomic changes in the rhizobia-legume symbiosis. *Mol Cell Proteomics*. 11(9): 724-744
- Roth L. E. and Stacey G. 1989. Bacterium release into host cells of nitrogen-fixing soybean nodules: the symbiosome membrane comes from three sources. *Eur J Cell Biol*. 49(1): 13-23
- Roux B., Rodde N., Jardinaud M. F., Timmers T., Sauviac L., Cottret L., Carrere S., Sallet E., Courcelle E., Moreau S., *et al*. 2014. An integrated analysis of plant and bacterial gene expression in symbiotic root nodules using laser-capture microdissection coupled to RNA sequencing. *Plant J*. 77(6): 817-837

- Roux M., Schwessinger B., Albrecht C., Chinchilla D., Jones A., Holton N., Malinovsky F. G., Tor M., de Vries S. and Zipfel C. 2011. The Arabidopsis leucine-rich repeat receptor-like kinases BAK1/SERK3 and BKK1/SERK4 are required for innate immunity to hemibiotrophic and biotrophic pathogens. *Plant Cell*. 23(6): 2440-2455
- Russinova E., Borst J. W., Kwaaitaal M., Cano-Delgado A., Yin Y., Chory J. and de Vries S. C. 2004. Heterodimerization and endocytosis of Arabidopsis brassinosteroid receptors BRI1 and AtSERK3 (BAK1). *Plant Cell*. 16(12): 3216-3229
- Saito K., Yoshikawa M., Yano K., Miwa H., Uchida H., Asamizu E., Sato S., Tabata S., Imaizumi-Anraku H., Umehara Y., *et al.* 2007. NUCLEOPORIN85 is required for calcium spiking, fungal and bacterial symbioses, and seed production in *Lotus japonicus*. *Plant Cell*. 19(2): 610-624
- Sartor M. A., Tomlinson C. R., Wesselkamper S. C., Sivaganesan S., Leikauf G. D. and Medvedovic M. 2006. Intensity-based hierarchical Bayes method improves testing for differentially expressed genes in microarray experiments. *BMC Bioinformatics*. 7(538)
- Sasikumar A. N., Perez W. B. and Kinzy T. G. 2012. The many roles of the eukaryotic elongation factor 1 complex. *Wiley Interdiscip Rev RNA*. 3(4): 543-555
- Schlaman H. R., Horvath B., Vijgenboom E., Okker R. J. and Lugtenberg B. J. 1991. Suppression of nodulation gene expression in bacteroids of *Rhizobium leguminosarum* biovar viciae. *J Bacteriol*. 173(14): 4277-4287
- Schlaman H. R. M., Phillips D. A. and Kondorosi E. 1998. Genetic Organization and Transcriptional Regulation of Rhizobial Nodulation Genes. *The Rhizobiaceae* 361-386
- Schnable P. S., Hochholdinger F. and Nakazono M. 2004. Global expression profiling applied to plant development. *Curr Opin Plant Biol*. 7(1): 50-56
- Schulze B., Mentzel T., Jehle A. K., Mueller K., Beeler S., Boller T., Felix G. and Chinchilla D. 2010. Rapid heteromerization and phosphorylation of ligand-activated plant transmembrane receptors and their associated kinase BAK1. *J Biol Chem*. 285(13): 9444-9451
- Schwessinger B., Roux M., Kadota Y., Ntoukakis V., Sklenar J., Jones A. and Zipfel C. 2011. Phosphorylation-dependent differential regulation of plant growth, cell death, and innate immunity by the regulatory receptor-like kinase BAK1. *PLoS Genet*. 7(4): e1002046
- Shah K., Russinova E., Gadella T. W., Jr., Willemse J. and De Vries S. C. 2002. The Arabidopsis kinase-associated protein phosphatase controls internalization of the somatic embryogenesis receptor kinase 1. *Genes Dev*. 16(13): 1707-1720
- Sharma S. B. and Signer E. R. 1990. Temporal and spatial regulation of the symbiotic genes of *Rhizobium meliloti* in planta revealed by transposon Tn5-gusA. *Genes Dev*. 4(3): 344-356
- Shimizu T., Nakano T., Takamizawa D., Desaki Y., Ishii-Minami N., Nishizawa Y., Minami E., Okada K., Yamane H., Kaku H., *et al.* 2010. Two LysM receptor molecules, CEBiP and OsCERK1, cooperatively regulate chitin elicitor signaling in rice. *Plant J*. 64(2): 204-214
- Simons K. and Ikonen E. 1997. Functional rafts in cell membranes. *Nature*. 387(6633): 569-572
- Singh S., Katzer K., Lambert J., Cerri M. and Parniske M. 2014. CYCLOPS, a DNA-binding transcriptional activator, orchestrates symbiotic root nodule development. *Cell Host Microbe*. 15(2): 139-152
- Smaczniak C., Li N., Boeren S., America T., van Dongen W., Goerdal S. S., de Vries S., Angenent G. C. and Kaufmann K. 2012. Proteomics-based identification of low-abundance signaling and regulatory protein complexes in native plant tissues. *Nat Protoc*. 7(12): 2144-2158
- Smit P., Raedts J., Portyanko V., Debelle F., Gough C., Bisseling T. and Geurts R. 2005. NSP1 of the GRAS protein family is essential for rhizobial Nod factor-induced transcription. *Science*. 308(5729): 1789-1791
- Smit P., Limpens E., Geurts R., Fedorova E., Dolgikh E., Gough C. and Bisseling T. 2007. Medicago LYK3, an entry receptor in rhizobial nodulation factor signaling. *Plant Physiol*. 145(1): 183-191
- Soupe E., Foussard M., Boistard P., Truchet G. and Batut J. 1995. Oxygen as a key developmental regulator of *Rhizobium meliloti* N₂-fixation gene expression within the alfalfa root nodule. *Proc Natl Acad Sci U S A*. 92(9): 3759-3763

- Spaink H. P., Sheeley D. M., van Brussel A. A., Glushka J., York W. S., Tak T., Geiger O., Kennedy E. P., Reinhold V. N. and Lugtenberg B. J.** 1991. A novel highly unsaturated fatty acid moiety of lipo-oligosaccharide signals determines host specificity of *Rhizobium*. *Nature*. 354(6349): 125-130
- Stewart W. D. P.** 1966. Nitrogen Fixation in Plants.
- Storey J. D. and Tibshirani R.** 2003. Statistical significance for genomewide studies. *Proc Natl Acad Sci U S A*. 100(16): 9440-9445
- Streng A., op den Camp R., Bisseling T. and Geurts R.** 2011. Evolutionary origin of rhizobium Nod factor signaling. *Plant Signal Behav.* 6(10): 1510-1514
- Stuermer C. A.** 2011. Reggie/flotillin and the targeted delivery of cargo. *J Neurochem*. 116(5): 708-713
- Sugimoto K., Gordon S. P. and Meyerowitz E. M.** 2011. Regeneration in plants and animals: dedifferentiation, transdifferentiation, or just differentiation? *Trends Cell Biol.* 21(4): 212-218
- Sun J., Chen Q., Qi L., Jiang H., Li S., Xu Y., Liu F., Zhou W., Pan J., Li X., *et al.*** 2011. Jasmonate modulates endocytosis and plasma membrane accumulation of the *Arabidopsis* PIN2 protein. *New Phytol.* 191(2): 360-375
- Sun W., Cao Y., Jansen Labby K., Bittel P., Boller T. and Bent A. F.** 2012. Probing the *Arabidopsis* flagellin receptor: FLS2-FLS2 association and the contributions of specific domains to signaling function. *Plant Cell*. 24(3): 1096-1113
- Sun Y., Wallrabe H., Booker C. F., Day R. N. and Periasamy A.** 2010. Three-color spectral FRET microscopy localizes three interacting proteins in living cells. *Biophys J*. 99(4): 1274-1283
- Surma M. A., Klose C. and Simons K.** 2012. Lipid-dependent protein sorting at the trans-Golgi network. *Biochim Biophys Acta*. 1821(8): 1059-1067
- Timmers A. C., Auriac M. C., de Billy F. and Truchet G.** 1998. Nod factor internalization and microtubular cytoskeleton changes occur concomitantly during nodule differentiation in alfalfa. *Development*. 125(3): 339-349
- Timmers A. C., Auriac M. C. and Truchet G.** 1999. Refined analysis of early symbiotic steps of the *Rhizobium-Medicago* interaction in relationship with microtubular cytoskeleton rearrangements. *Development*. 126(16): 3617-3628
- Timmers A. C.** 2008. The role of the plant cytoskeleton in the interaction between legumes and rhizobia. *J Microsc.* 231(2): 247-256
- Tirichine L., Imaizumi-Anraku H., Yoshida S., Murakami Y., Madsen L. H., Miwa H., Nakagawa T., Sandal N., Albrechtsen A. S., Kawaguchi M., *et al.*** 2006. Deregulation of a Ca²⁺/calmodulin-dependent kinase leads to spontaneous nodule development. *Nature*. 441(7097): 1153-1156
- Toth K., Stratil T. F., Madsen E. B., Ye J., Popp C., Antolin-Llovera M., Grossmann C., Jensen O. N., Schussler A., Parniske M., *et al.*** 2012. Functional Domain Analysis of the Remorin Protein LjSYMREM1 in *Lotus japonicus*. *PLoS One*. 7(1): e30817
- Truchet G., Roche P., Lerouge P., Vasse J., Camut S., Debilly F., Prome J. C. and Denarie J.** 1991. Sulfated lipo-oligosaccharide signals of *Rhizobium-meliloti* elicit root nodule organogenesis in Alfalfa. *Nature*. 351(6328): 670-673
- Urbanus S. L. and Ott T.** 2012. Plasticity of plasma membrane compartmentalization during plant immune responses. *Front Plant Sci*. 3(181)
- Valentin G., Verheggen C., Piolot T., Neel H., Coppey-Moisand M. and Bertrand E.** 2005. Photoconversion of YFP into a CFP-like species during acceptor photobleaching FRET experiments. *Nat Methods*. 2(11): 801
- van Brussel A. A., Bakhuizen R., van Spronsen P. C., Spaink H. P., Tak T., Lugtenberg B. J. and Kijne J. W.** 1992. Induction of pre-infection thread structures in the leguminous host plant by mitogenic lipo-oligosaccharides of *Rhizobium*. *Science*. 257(5066): 70-72
- Van de Velde W., Guerra J. C., De Keyser A., De Rycke R., Rombauts S., Maunoury N., Mergaert P., Kondorosi E., Holsters M. and Goormachtig S.** 2006. Aging in legume symbiosis. A molecular view on nodule senescence in *Medicago truncatula*. *Plant Physiol*. 141(2): 711-720

Van de Velde W., Zehirov G., Szatmari A., Debreczeny M., Ishihara H., Kevei Z., Farkas A., Mikulass K., Nagy A., Tiricz H., *et al.* 2010. Plant peptides govern terminal differentiation of bacteria in symbiosis. *Science*. 327(5969): 1122-1126

van de Wiel C., Scheres B., Franssen H., van Lierop M. J., van Lammeren A., van Kammen A. and Bisseling T. 1990. The early nodulin transcript ENOD2 is located in the nodule parenchyma (inner cortex) of pea and soybean root nodules. *Embo J.* 9(1): 1-7

Vanneste S., De Rybel B., Beemster G. T., Ljung K., De Smet I., Van Isterdael G., Naudts M., Iida R., Gruissem W., Tasaka M., *et al.* 2005. Cell cycle progression in the pericycle is not sufficient for SOLITARY ROOT/IAA14-mediated lateral root initiation in *Arabidopsis thaliana*. *Plant Cell*. 17(11): 3035-3050

Vasse J., de Billy F., Camut S. and Truchet G. 1990. Correlation between ultrastructural differentiation of bacteroids and nitrogen fixation in alfalfa nodules. *J Bacteriol.* 172(8): 4295-4306

Vermeer J. E. M., von Wangenheim D., Barberon M., Lee Y., Stelzer E. H. K., Maizel A. and Geldner N. 2014. A Spatial Accommodation by Neighboring Cells Is Required for Organ Initiation in *Arabidopsis*. *Science*. 343(6167): 178-183

Vernie T., Moreau S., de Billy F., Plet J., Combier J. P., Rogers C., Oldroyd G., Frugier F., Niebel A. and Gamas P. 2008. EFD Is an ERF transcription factor involved in the control of nodule number and differentiation in *Medicago truncatula*. *Plant Cell*. 20(10): 2696-2713

Vernoud V., Journet E.-P. and Barker D. G. 1999. MtENOD20, a Nod Factor-Inducible Molecular Marker for Root Cortical Cell Activation. *Molecular Plant-Microbe Interactions*. 12(7): 604-614

Vinardell J. M., Fedorova E., Cebolla A., Kevei Z., Horvath G., Kelemen Z., Tarayre S., Roudier F., Mergaert P., Kondorosi A., *et al.* 2003. Endoreduplication mediated by the anaphase-promoting complex activator CCS52A is required for symbiotic cell differentiation in *Medicago truncatula* nodules. *Plant Cell*. 15(9): 2093-2105

Vogel S. S., Thaler C. and Koushik S. V. 2006. Fanciful FRET. *Sci STKE*. 2006(331): re2

Wais R. J., Galera C., Oldroyd G., Catoira R., Penmetsa R. V., Cook D., Gough C., Denarie J. and Long S. R. 2000. Genetic analysis of calcium spiking responses in nodulation mutants of *Medicago truncatula*. *Proc Natl Acad Sci U S A*. 97(24): 13407-13412

Wall L. G. 2000. The Actinorhizal Symbiosis. *J Plant Growth Regul.* 19(2): 167-182

Wan J., Zhang X. C., Neece D., Ramonell K. M., Clough S., Kim S. Y., Stacey M. G. and Stacey G. 2008. A LysM receptor-like kinase plays a critical role in chitin signaling and fungal resistance in *Arabidopsis*. *Plant Cell*. 20(2): 471-481

Wang D., Griffiths J., Starker C., Fedorova E., Limpens E., Ivanov S., Bisseling T. and Long S. 2010. A nodule-specific protein secretory pathway required for nitrogen-fixing symbiosis. *Science*. 327(5969): 1126-1129

Wang W., Xie Z. P. and Staehelin C. 2014. Functional analysis of chimeric LysM domain receptors mediating Nod factor-induced defense signaling in *Arabidopsis thaliana* and chitin-induced nodulation signaling in *Lotus japonicus*. *Plant J.*

Wang X., Li X., Meisenhelder J., Hunter T., Yoshida S., Asami T. and Chory J. 2005. Autoregulation and homodimerization are involved in the activation of the plant steroid receptor BRI1. *Dev Cell*. 8(6): 855-865

Wang X., Kota U., He K., Blackburn K., Li J., Goshe M. B., Huber S. C. and Clouse S. D. 2008. Sequential transphosphorylation of the BRI1/BAK1 receptor kinase complex impacts early events in brassinosteroid signaling. *Dev Cell*. 15(2): 220-235

Webster G., Poulton P. R., Cocking E. C. and Davey M. R. 1995. The Nodulation of Micro-Propagated Plants of *Parasponia-Andersonii* by Tropical Legume Rhizobia. *J Exp Bot.* 46(290): 1131-1137

White J., Prell J., James E. K. and Poole P. 2007. Nutrient sharing between symbionts. *Plant Physiol.* 144(2): 604-614

Willmann R., Lajunen H. M., Erbs G., Newman M. A., Kolb D., Tsuda K., Katagiri F., Fliegmann J., Bono J. J., Cullimore J. V., *et al.* 2011. *Arabidopsis* lysin-motif proteins LYM1

LYM3 CERK1 mediate bacterial peptidoglycan sensing and immunity to bacterial infection. *Proc Natl Acad Sci U S A.* 108(49): 19824-19829

Xie F., Murray J. D., Kim J., Heckmann A. B., Edwards A., Oldroyd G. E. and Downie J. A. 2012. Legume pectate lyase required for root infection by rhizobia. *Proc Natl Acad Sci U S A.* 109(2): 633-638

Yang W. C., de Blank C., Meskiene I., Hirt H., Bakker J., van Kammen A., Franssen H. and Bisseling T. 1994. Rhizobium nod factors reactivate the cell cycle during infection and nodule primordium formation, but the cycle is only completed in primordium formation. *Plant Cell.* 6(10): 1415-1426

Yano K., Yoshida S., Muller J., Singh S., Banba M., Vickers K., Markmann K., White C., Schuller B., Sato S., *et al.* 2008. CYCLOPS, a mediator of symbiotic intracellular accommodation. *Proc Natl Acad Sci U S A.* 105(51): 20540-20545

Yokota K., Fukai E., Madsen L. H., Jurkiewicz A., Rueda P., Radutoiu S., Held M., Hossain M. S., Szczyglowski K., Morieri G., *et al.* 2009. Rearrangement of actin cytoskeleton mediates invasion of *Lotus japonicus* roots by *Mesorhizobium loti*. *Plant Cell.* 21(1): 267-284

Young N. D., Debelle F., Oldroyd G. E. D., Geurts R., Cannon S. B., Udvardi M. K., Benedito V. A., Mayer K. F. X., Gouzy J., Schoof H., *et al.* 2011. The *Medicago* genome provides insight into the evolution of rhizobial symbioses. *Nature.* 480(7378): 520-524

Zhang X. C., Wu X., Findley S., Wan J., Libault M., Nguyen H. T., Cannon S. B. and Stacey G. 2007. Molecular evolution of lysin motif-type receptor-like kinases in plants. *Plant Physiol.* 144(2): 623-636

SUMMARY

Legumes are unique in that they are able to establish a mutual symbiotic interaction with nitrogen fixing soil bacteria generally referred to as rhizobia. This interaction starts off in the root epidermis where the bacterial signal molecule, the Nod factor, is perceived by the plant (Nod factor signaling). This recognition sets in motion a series of responses leading to the formation of a root nodule. This organ is specifically created to host the bacteria in an intracellular manner. The rhizobia develop into a mature, nitrogen fixing state in these infected cells. The rhizobia are surrounded by a host membrane and this forms a cell wall free symbiotic interface, that allows the exchange of nutrients between the symbionts. The comparison of the mechanism controlling symbiotic interface formation in rhizobium symbiosis and the much more common symbiosis with arbuscular mycorrhizal (AM) fungi strongly suggest that rhizobia co-opted parts of the AM symbiosis. The signalling as well as cellular processes controlling symbiotic interface formation in the ancient AM symbiosis have been recruited by the rhizobium nodule symbiosis. In this thesis I present the results of my research on the role of and mechanisms controlling Nod factor signalling on symbiotic interface formation in nodules of the model legume *Medicago truncatula* (Medicago).

To study the role of Nod factor signaling in the formation of a symbiotic interface it was essential to define a fate map for Medicago root nodules. The formation of a nodule starts, after Nod factor perception in the epidermis, with divisions in the cortex, pericycle and endodermis. Divisions in the cortex start from the inner most layer and spread outwards. When cortical layer 4 (C4) and C5 have already divided a few times, mitotic activity is induced in C3 and ultimately C2 divides. After the first periclinal divisions have been induced in C3, cells derived from C4 and C5 stop dividing and form about 8 cell layers. C3 continues to divide and ultimately forms the nodule meristem. The infection thread that developed in the root hairs has to penetrate the primordium before the first periclinal divisions occur in C3. The cells derived from C4 and C5 are then infected by bacteria from the infection thread in the primordium. After the establishment of a meristem this meristem adds new cells to the nodule, which are gradually infected when they leave the meristem and enter the infection zone. The fate map shows that formation of the symbiotic interface occurs in two ways: first in cells of the primordium and later in the infection zone in daughter cells derived from the meristem.

For the infection of daughter cells derived from the meristem the Nod factor receptors (NFP and LYK3 in Medicago) are needed, most likely to perceive the Nod factor. When we knocked down one of the receptors in a nodule specific manner release of bacteria is hampered (NFP) or massive unwallled droplets were observed (LYK3) indicating most likely slow release. This shows that the receptors are needed for the formation of the

symbiotic interface in the nodule. In line with this function in the infection zone we found the receptors to accumulate in the nodule apex. The receptors accumulate in a narrow zone of two cell layers that is the border between the meristem and the infection zone. The receptors accumulate to a zone markedly narrower than the zone where the promoters are active. In this narrow zone the receptors accumulate at the cell periphery, most likely the plasma membrane. Outside this layer we observed accumulation of the receptors in the vacuoles suggesting degradation. In cells with LYK3 at the plasma membrane LYK3 occurs only in 35% of the cells at the membrane surrounding infection threads. The removal of LYK3 from the plasma membrane appears to be first completed at the membrane surrounding the infection thread. As the receptors are expressed in a broader zone, post-transcriptional mechanisms limit their accumulation at the plasma membrane. Ectopic expression experiments show that broader expression, and most likely accumulation, could induce defence responses (NFP) and reduces infection (LYK3). Therefore the accumulation of the receptors needs to be limited and the receptors are only allowed to accumulate in a narrow zone where Nod factor perception could take place.

As both receptors accumulate in the same cell layers we tested whether they form heteromeric complexes. It was already proposed at their discovery that NFP and LYK3 should form a complex based on their phenotype and the lack of an active kinase domain in NFP. Also most receptors form complexes to modulate their (kinase) activity. We show that a heteromeric complex is also formed in the proper biological context in nodules. The cell death responses that are induced when the receptors are co-expressed in heterologous systems are avoided in *Medicago* nodules. Also homomeric complexes containing LYK3 were observed in nodules. This homomeric complex is formed either as an addition to the heteromeric complex with NFP or the complex with NFP contains multiple LYK3 molecules.

As receptors often function in larger complexes we performed immunoprecipitation coupled with mass spectrometry to detect possible interactors of LYK3. With this we detected several protein interactors of LYK3 including a EF1 α , Dynamin-2B, PR10, fructose-bisphosphate aldolase and 14-3-3 f2 protein. Some of these proteins have a function in the regulation of vesicle transport and the cytoskeleton. Remarkable, other known or putative interactors of LYK3 (NFP, PUB1, SYMREM1 and FLOT4) were not detected. To test why we could not find these interactors we performed co-localization experiments. These experiments show that the interaction with SYMREM1 and the putative interaction with FLOT4 could take place as both proteins co-localize with LYK3. SYMREM1 accumulates at the membrane surrounding the infection threads and at the symbiosomes. As LYK3 also, although transient, accumulates at the membrane surrounding the infection threads, LYK3 and SYREM1 co-localize there. This shows that these interactors could form a complex with LYK3, although the complex is most likely very transient. This transient nature makes the complexes difficult to detect.

Because co-localization is a prerequisite for two proteins to interact we studied the expression of the *Medicago* genome. We used laser capture micro-dissection experiment to isolate RNA from different zones of the nodules and measured the differential expression of the *Medicago* genome. This experiment provides us with a digital *in situ* experiment for *Medicago* nodules. The data show that the genes from the Nod factor signaling cascade do not show the same expression pattern. The Nod factor receptor mRNAs of NFP and LYK3 are enriched in the meristem and distal infection zone. This is in line with our localization studies where the receptors accumulate at the border between meristem and infection zone. Most genes from the Nod factor signaling cascade show no differential expression at all (expressed equal in the entire nodule), where *in situ* or promoter GUS studies show enrichment of all these genes in the meristem/ infection zone. Further, some show remarkable behaviour. DMI1 and IPD3, for instance, are enriched in infected cells. These data could point to a new function for these proteins which is not related to the known signaling cascade. Also a survey on the differential expression of other LysM domain containing proteins show that there are more candidates that may have an important role in Nod factor perception. These LysM domain containing proteins are also enriched in the meristem and/or infection zone and could thus function as a co-receptor for NFP or LYK3.

Nod factor perception is the key step in the progress of the rhizobium – legume symbiosis. Not only in the early steps in the root epidermis, but also in the nodule. Because of the developmental gradient in the indeterminate *Medicago* nodule this nodule is a perfect biological system to study the cell biology of the symbiosis. The differential expression analysis and the nodule fate map are important tools for these studies.

SAMENVATTING

Vlinderbloemige planten kunnen een unieke symbiotische interactie aangaan met vrij levende stikstofbindende bodembacteriën die rhizobia worden genoemd. Deze interactie begint in de epidermis van de wortel waar het signaalmolecuul van de bacteriën, de Nod-factor, wordt herkend door de plant. Deze herkenning wordt Nod-factorsignalering genoemd en zorgt voor de activering van een breed scala aan reacties die uiteindelijk leiden tot de vorming van een wortelknol. Deze knol is een nieuw orgaan dat speciaal voor de bacteriën wordt gemaakt. De bacteriën worden opgenomen in de cellen van de plant in zogenaamde symbiosomen en binden daar de stikstof uit de lucht. De bacteriën zijn in de cel omgeven door een membraan afkomstig van de plant. Over dit membraan, een zogenaamd celwandvrijgrensvlak, vindt de uitwisseling van voedingsstoffen plaats tussen de bacteriën (stikstof) en de plant (suikers). De vorming van dit grensvlak lijkt heel erg op wat we zien in een veel gangbaardere symbiose: die tussen planten en arbusculaire mycorrhiza (AM) schimmels. Zowel de signaleringsmechanismen als de cellulaire processen die de symbiose controleren zijn overeenkomstig. Omdat de AM-symbiose veel ouder is en voorkomt bij de meeste planten denken wij dat vlinderbloemige planten deze mechanismen van de AM-symbiose hebben ontleend om zo de symbiose met rhizobia mogelijk te maken. In dit proefschrift presenteer ik mijn onderzoek naar de rol van Nod-factorsignalering en de mechanismen die deze signalering controleren op de vorming van het symbiotisch grensvlak in knollen van *Medicago truncatula*.

Om de rol van Nod-factorsignalering op de vorming van het symbiotisch grensvlak te bestuderen was het essentieel om te weten hoe een knol gevormd wordt. Hiertoe hebben we in kaart gebracht welke bijdrage de verschillende cellen van de wortel hieraan leveren. Na de herkenning van de Nod-factoren in de epidermis start de vorming van een knol met delingen in de pericykel, endodermis en cortex. De delingen in de cortex starten in de binnenste cellagen en verspreiden zich naar de buitenkant van de wortel. Zodra de 4^e corticale cellaag (C4) en C5 een paar keer gedeeld hebben worden ook in C3 en uiteindelijk in C2 celdeling geïnduceerd. Nadat C3 de eerste keer parallel deelt stopt de celdeling in C4 en C5. Op dat moment zijn er ongeveer 8 cellagen ontstaan uit C4 en C5. Delingen in C3 gaan door en uit deze laag wordt uiteindelijk het knolmeristeem (stamcellen) gevormd dat zorgt voor de verdere groei van de knol. De infectiedraad die in de wortelharen is ontstaan en naar het knolprimordium (C4 en C5) toegroeit moet het primordium bereiken voordat C3 deelt. Lukt dit niet, dan kan de infectiedraad deze laag niet meer passeren en stopt de groei en ontwikkeling van de knol. Na het bereiken van het primordium worden de bacteriën uit de infectiedraad opgenomen in de cellen van het primordium (infectie). Zodra het meristeem is gevormd voegt dit meristeem nieuwe cellen toe aan de knol. Deze cellen worden geleidelijk geïnfecteerd als ze het meristeem verlaten en de infectiezone ingaan.

Het in kaart brengen van de bijdrage van de verschillende cellen aan de vorming van een knol laat zien dat cellen van de knol op twee manier geïnfecteerd worden. Eerst vindt er infectie plaats in de cellen in het primordium en later in de dochtercellen van het meristeem in de infectiezone.

Voor het infecteren van de dochtercellen van het meristeem zijn twee Nod-factorreceptoren nodig. In *Medicago* heten deze LYK3 en NFP. Hoogstwaarschijnlijk zijn deze receptoren nodig om de Nod-factor waar te nemen, maar dat is nooit aangetoond. Als we deze receptoren specifiek in de knol uitschakelen zien we dat de infectie van knolcellen geblokkeerd is (als we NFP uitschakelen) of dat er enorme infectiestructuren worden gevormd doordat de infectie traag plaats vindt (als we LYK3 uitschakelen). Dit experiment laat zien dat de Nod-factorreceptoren nodig zijn voor de vorming van een celwandvrijgrensvlak in de knol. In overeenstemming met deze functie zagen we dat de receptoren accumuleren in de top van de knol. Ze accumuleren in een zeer smalle zone van twee cellagen die de grens vormen tussen het meristeem en de infectiezone, precies waar we ze verwachten als ze betrokken zijn bij infectie. Deze zone waar de receptoren accumuleren is veel smaller dan de zone waar de receptoren tot expressie worden gebracht. In de smalle zone tussen meristeem en infectiezone zien we de receptoren aan de rand van de cel, waarschijnlijk in het plasmamembraan. Buiten deze zone zien we de receptoren ook accumuleren, maar dan in de vacuolen waar ze waarschijnlijk afgebroken worden. Als we LYK3 zien accumuleren in het plasmamembraan dan zien we slechts in 35% van de cellen dat LYK3 ook accumuleert op het membraan rond de infectiedraad. Het lijkt erop dat de receptoren van het plasmamembraan verwijderd worden en dat dit proces het eerst voltooid is rond de infectiedraad. Omdat de receptoren in een breed gebied tot expressie komen, maar slechts in een smal gebied accumuleren moeten er post-transcriptionele mechanismen zijn die hun accumulatie beperken. Om te zien waarom het belangrijk is dat de receptoren in een smalle zone accumuleren hebben we de receptoren in de hele knol hoog tot expressie gebracht. Daarmee laten we waarschijnlijk ook meer receptor accumuleren. Als we dat doen zien we dat de plant een afweerreactie vertoont (bij NFP) en dat infectie niet meer zo goed optreedt (bij LYK3). Dat is de reden dat de accumulatie van de receptoren beperkt moet worden tot een smalle zone waar ook Nod-factorherkenning op kan treden.

Omdat beide receptoren accumuleren in dezelfde cellen hebben we ook onderzocht of er een receptorcomplex wordt gevormd. Al bij de ontdekking van de receptoren werd er gesuggereerd dat er een complex tussen LYK3 en NFP gevormd zou moeten worden. Dit werd gesuggereerd omdat NFP geen kinaseactiviteit heeft en de fenotypes van de *lyk3* mutant en de *nfp* mutant vergelijkbaar zijn. Daarnaast is vorming van een complex iets dat we zien bij heel veel receptoren. Receptoren vormen deze complexen om hun (kinase) activiteit te reguleren. Onze experimenten laten zien dat LYK3 en NFP inderdaad een complex vormen en dat ze dit doen in de juiste biologische omgeving van een knol. Wanneer de Nod-factorreceptoren in andere planten tot expressie worden gebracht treedt er celdood op, een reactie die wij niet zagen in de knol. Naast het complex met NFP vormt

LYK3 ook een complex met zichzelf. Dit complex kan bestaan naast het complex met NFP, of het kan zijn dat er een complex wordt gevormd tussen NFP en meerdere LYK3 moleculen.

Omdat receptoren vaak voorkomen in hele grote complexen hebben we ook gekeken naar welke andere eiwitten in een complex met LYK3 voorkomen. Om dat te doen hebben we eiwitten geïsoleerd en LYK3 afgevangen met een antilichaam. De eiwitten die een complex vormen met LYK3 hebben we geïdentificeerd met massaspectrometrie. De eiwitten die we hiermee konden detecteren zijn onder andere een groeifactor (EF1 α), dynamine-2B, PR10, fructose-bisfosfaat aldolase en een 14-3-3 f2 eiwit. Een aantal van deze eiwitten hebben een functie in het reguleren van het cytoskelet en transport in de cel met behulp van blaasjes (vesikels). Opvallend is dat de eiwitten waarvan bekend is of aangenomen wordt dat ze een complex vormen met LYK3 (NFP, PUB1, SYMREM1 en FLOT4) niet door ons gevonden zijn. Om te onderzoeken waarom deze niet zijn gevonden hebben we gekeken of deze eiwitten wel op dezelfde plek accumuleren als LYK3. Onze experimenten laten zien dat een interactie met SYMREM1 en FLOT4 mogelijk zijn omdat beide accumuleren op dezelfde plek als LYK3. SYMREM1 accumuleert in het membraan rond de infectiedraden en op het symbiosoommembraan. Omdat LYK3, hoewel slechts beperkt, ook accumuleert in het membraan rond de infectiedraad is een interactie op die plek mogelijk. Deze experimenten laten zien dat de bekende interactors van LYK3 een complex kunnen vormen, al is dit vaak zeer beperkt in relatie tot de hoeveelheid LYK3. Dat is waarschijnlijk ook de reden dat we ze niet hebben geïdentificeerd met massaspectrometrie.

Omdat een van de voorwaarden voor twee eiwitten om een complex te vormen is dat ze accumuleren in dezelfde cel hebben we de expressie van het *Medicago* genoom in de knol bestudeerd. Om dat te doen hebben we met een laser cellen uit de verschillende zones van de knol gehaald en vervolgens RNA geïsoleerd uit deze cellen. Dit experiment laat opmerkelijk genoeg zien dat de genen betrokken bij Nod-factrorsignalering niet op dezelfde wijze tot expressie komen in de knol. Het mRNA van LYK3 en NFP is verrijkt in het meristeem en in de infectiezone. Dit zijn dezelfde gebieden als waar we ook het LYK3 en NFP eiwit zagen accumuleren. De meeste andere genen betrokken bij Nod-factrorsignalering komen in de hele knol gelijk tot expressie. Dit is in tegenstelling met *in situ* of promoter-GUS experimenten die laten zien dat ze vooral tot expressie komen in het meristeem of de infectiezone. Daarnaast zien we voor een aantal genen een bijzonder expressiepatroon. Bijvoorbeeld bij DMI1 en IPD3, welke vooral tot expressie komen in de geïnfecteerde cellen. Deze expressie wijst mogelijk op een nieuwe functie voor deze eiwitten die niets te maken heeft met de tot nu toe bekende Nod-factrorsignaleringsroute. Daarnaast laat een analyse van de expressie van eiwitten met een LysM-domein zien dat een aantal hiervan mogelijk een rol hebben in Nod-factorherkenning. Deze eiwitten komen namelijk ook tot expressie in het meristeem en/ of de infectiezone waarmee ze mogelijk een co-receptor kunnen zijn voor NFP of LYK3.

Nod-factorherkenning is de eerste en belangrijkste stap in de voortgang van de symbiose tussen vlinderbloemige planten en rhizobiumbacteriën. Niet alleen in de initiële stappen in de wortelepidermis hebben ze deze functie, maar ook in de knol. Doordat alle stappen van de knolontwikkeling tegelijk in een enkele Medicagoknol zichtbaar zijn vormt deze knol een perfect biologisch systeem voor het bestuderen van de celbiologie van de rhizobiumsymbiose. Onze analyses van de genexpressie in de knol en de bijdrage van de verschillende cellen aan het ontstaan van de knol zijn daarbij belangrijke hulpmiddelen.

ACKNOWLEDGEMENTS

A PhD is an amazing experience where you experience both highs and lows. At times you'll feel like you're on top of the world. Sometimes you feel you're on your own finishing your thesis and have no clue where you're going. After almost seven years many people contributed to the end result you read/ will read/ should have read. Some contributed to the science, some contributed to my personal moral. All these contributions were essential for the completion. Thank you all for what you did!

For the science part I like to thank Ton for having me in the lab and for stimulating me to write a project proposal for NWO. Although I did not get the grant, it was a very useful experience and the perfect start for my PhD. And even though this thesis is somewhat different from the proposal we wrote it was an excellent basis. Thank you also for always stimulating my love for molecular and cell biology. Things could have gone faster if you'd ask me, but we finally managed to complete the thesis. My thanks go also to Erik, for the day to day supervision, and to people I collaborated with: Anna Pietraszewska, Sjeff Boeren, Thomas Ott and Kerstin Kaufmann. I had a great time at the lab, so I also have to thank all the staff, PhD's and students that I met. I'm not going to name all of them, but I do like to mention Henk, Marijke, Elena and the Toolbox students. This because they were not only involved in the science part, but also important for the social part of working together.

Next to the science, and maybe even more important, my thanks go to everyone who was there for me when I needed them. In the good times and the times I was not so sure how to finish this. Knowing that you're not alone in this is a great comfort. First of all my special thanks go to Erika because she was not only there to celebrate but also to hear my complaints and frustration. *Dank je wel schat*. I also like to thank my parents, in-laws and Bianca for their never ending support. I'm sure I never made it without you. I'm grateful that I made it to the end and received everything I needed.

CURRICULUM VITAE

Sjef Moling was born on May the 24th, 1981 and grew up in the town of Munstergeleen in the province of Limburg in the south of the Netherlands. After his high school he started his scientific education as a biotechnology student at Wageningen University, Wageningen, the Netherlands in the year 2000. He specialised himself in cellular and molecular biology and worked for his thesis in the laboratory of Virology and the laboratory of Molecular Biology on plant – microbe interactions. In the laboratory of Virology he could exploit his passion for microscopy. Under supervision of dr. Ribeiro and dr. Van Lent he studied the formation of TSWV particles with both confocal and electron microscopy. In the laboratory of Molecular Biology he came into first contact with the rhizobium – legume symbiosis. Under the supervision of prof. Bisseling and dr. Limpens he studied small G-proteins (ROPs) during this symbiosis. After an internship at Durham University, Durham, United Kingdom with prof. Hussey and dr. Deeks on signaling to the actin cytoskeleton he completed his scientific education with a *cum laude* degree in 2007. During the last part of his education he already wrote the proposal for his PhD project for the NWO Top Talent program. Wageningen University selected him as one of their representatives for this program. Though, NWO did not grant his proposal he started his PhD project with prof. Bisseling and dr. Limpens in September 2007. During this PhD research he focussed on Nod factor perception inside nodule of the model legume *Medicago truncatula* with this thesis as a result.

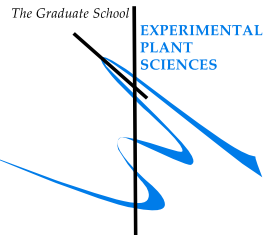
PUBLICATIONS

Moling S. and Bisseling T. In press. Evolution of Rhizobium nodulation; from nodule specific genes (nodulins) to recruitment of common processes. In Bruijn, F. de (Ed.), Biological Nitrogen Fixation

Limpens E., Moling S., Hooiveld, G., Pereira, P. A., Bisseling, T., Becker, J. D. and Kuster H. 2013. Cell- and tissue-specific transcriptome analyses of Medicago truncatula root nodules. PLoS One 8(5): e64377.

Ribeiro D., Jung M., Moling S., Borst J.W., Goldbach R. and Kormelink R. 2013. The Cytosolic Nucleoprotein of the Plant-Infecting Bunyavirus Tomato Spotted Wilt Recruits Endoplasmic Reticulum-Resident Proteins to Endoplasmic Reticulum Export Sites. The Plant Cell Online. 25(9): 3602-3614.

Education Statement of the Graduate School Experimental Plant Sciences



Issued to: **Sjef Moling**
 Date: **25 August 2014**
 Group: **Laboratory of Molecular Biology, Wageningen University & Research Centre**

1) Start-up phase	<u>date</u>
► First presentation of your project Lipid rafts and symbiosis: A greasy story of domains in plant-microbe interaction	Dec 19, 2007
► Writing or rewriting a project proposal A greasy story of domains in plant-microbe interaction	Dec 19, 2007
► Writing a review or book chapter Evolution of Rhizobium nodulation; from nodule specific genes (nodulins) to recruitment of common processes in Biological Nitrogen Fixation Book	Jul 02, 2013
► MSc courses	
► Laboratory use of isotopes	

Subtotal Start-up Phase **13.5 credits***

2) Scientific Exposure	<u>date</u>
► EPS PhD student days EPS PhD student day, Utrecht University	Jun 01, 2010
EPS PhD student day, Wageningen University	May 20, 2011
► EPS theme symposia EPS theme 1 'Developmental Biology of Plants', Wageningen University	Oct 11, 2007
EPS theme 1 'Developmental Biology of Plants', Wageningen University	Jan 28, 2010
EPS theme 1 'Developmental Biology of Plants', Leiden University	Jan 20, 2011
EPS theme 1 'Developmental Biology of Plants', Wageningen University	Jan 19, 2012
EPS theme 1 'Developmental Biology of Plants', Leiden University	Jan 17, 2013
► NWO Lunteren days and other National Platforms ALW meeting 'Experimental Plant Sciences', Lunteren	Apr 07-08, 2008
ALW meeting 'Experimental Plant Sciences', Lunteren	Apr 06-07, 2009
ALW meeting 'Experimental Plant Sciences', Lunteren	Apr 19-20, 2010
ALW meeting 'Experimental Plant Sciences', Lunteren	Apr 04-05, 2011
ALW meeting 'Experimental Plant Sciences', Lunteren	Apr 02-03, 2012
ALW meeting 'Experimental Plant Sciences', Lunteren	Apr 22, 2013
► Seminars (series), workshops and symposia Capita selecta Physics and physical chemistry of cellular processes (Frans Leermakers and Fred Wouters)	Nov 02, 2007
Invited seminar Koen Visscher: Single molecule experiments unravel how mechanical forces control gene expression during transcription and translation	Dec 21, 2007
Flying Seminar Richard Vierstra	Apr 14, 2008
Invited seminar Jean Philippe Combier: Post translational regulation of MtHAP2.1 during nodule development	Apr 15, 2008
Flying Seminar Simon Gilroy: How do plants feel?	May 19, 2008
Invited seminar Niko Geldner: The Arabidopsis root endodermis as a model for epithelial polarity in plants	May 29, 2008

Flying Seminar Zhenbiao Yang: Coordination of cell polarity formation in plant tissues by hormone and ROP GTPase signaling	Jun 23, 2008
Symposium "Microspectroscopy in Biology"	Sep 24, 2008
Invited seminar Pamela Hines: Science from an editors view; Science organization, tips about being an author and a referee, programs at AAAS, alternative careers etc	Nov 06, 2008
Art meets Science	Oct 16, 2009
Invited seminar Valerie Williamson: Connecting genetics and genomics of pathogenicity and behavior in root-knot nematodes	Oct 23, 2009
Symposium Photosynthesis: from femto to Peta and from nano to Global	Nov 05, 2009
Invited seminar Matteo Brilli - From Bioinformatics to systems biology: building a mathematical model integrating metabolism and gene regulation.	Apr 29, 2010
Invited seminar Toby Kiers: Evolution of Cooperation in Rhizosphere Mutualisms	Jun 17, 2010
Invited seminar Heribert Hirt: Engineering Protein Kinase Signall Transduction to Regulate Stress Responses in Plants	Sep 08, 2010
Invited seminar Naoto Sibuya: Chitin Perception and Signalling in Rice and Arabidopsis	Sep 09, 2010
Invited seminar David Baulcombe: Mobile RNA silencing in plants	Sep 27, 2010
Invited seminar Peter Cook: Transcription factories as organizers of the genome: the role of fixed polymerases	Oct 27, 2010
EPS Cellular Signaling Symposium	Nov 04, 2010
Invited seminar Sasan Ali Niaei Fard: Genetic variation in the molecular network regulating stoma at different humid levels	Jun 17, 2011
Invited seminar Emma Granqvist: Calcium Signaling in plant - microbe interactions	Sep 06, 2011
Invited seminar Liedewij Laan: How adaptable is the establishment of cell morphology	Jan 06, 2012
Workshop new developments in plant endomembrane biology	Jun 15, 2012
Invited seminar Joop Vermeer: Endodermal cell responses are essential for lateral root initiation and outgrowth	Aug 31, 2012
Invited seminar David Baulcombe: Plant versus Virus	Oct 10, 2012
Invited seminar Karin Busch: Exploration of mitochondrial membrane microcompartments	Nov 07, 2012
Invited seminar Saïd Amrar: Plant research in the Sahara	Nov 28, 2012
Invited seminar Johannes Hohlbein: Single-molecule Biophysics: The fluorescence-based toolkit	May 03, 2013
Workshop Advanced Light Microscopy facilities at Wageningen UR	Jun 13, 2013
Invited seminar Eric Kramer: Auxin and plasmodesmata; measuring fluxes in the root	Jul 02, 2013
► Seminar plus	
Seminar plus - Simon Gilroy	May 19, 2008
► International symposia and congresses	
European Nitrogen Fixation Conference, Ghent, Belgium	Aug 30-Sep 03, 2008
EMBO meeting 2009	Aug 29-Sep 01, 2009
Botanical Microscopy 2011	Apr 17-21, 2011
► Presentations	
ALW Meeting Experimental Plant Sciences 2012	Apr 03, 2012
Seminar for the Ott group in Munich	Oct 09, 2012
► IAB interview	
Meeting with a member of the International Advisory Board	Dec 02, 2009
► Excursions	

Subtotal Scientific Exposure

16.4 credits*

3) In-Depth Studies	<u>date</u>
▶ EPS courses or other PhD courses	
An introduction to Electron Microscopy	Jun 21-25, 2010
Advanced course Guide to Scientific Artwork	May 09-10, 2011
▶ Journal club	
Participation in a literature discussion group	2007-2011
▶ Individual research training	

*Subtotal In-Depth Studies 5.1 credits**

4) Personal development	<u>date</u>
▶ Skill training courses	
PhD Competence Assessment	Apr 22, 2008
EPS Expectations Career Day	Nov 19, 2010
Techniques for Writing and Presenting a Scientific Paper	Feb 15-18, 2011
BCFCareerevent	May 26, 2011
Scientific Writing	Sep 20-Nov 15, 2011
▶ Organisation of PhD students day, course or conference	
▶ Membership of Board, Committee or PhD council	

*Subtotal Personal Development 3.1 credits**

TOTAL NUMBER OF CREDIT POINTS*	38.8
Herewith the Graduate School declares that the PhD candidate has complied with the educational requirements set by the Educational Committee of EPS which comprises of a minimum total of 30 ECTS credits	
* A credit represents a normative study load of 28 hours of study.	

Lay-out: Sjef Moling
Cover: Sticky notes with lab data as the basis for everything that's about
perception in the rhizobium - Medicago symbiosis
Printed by: GVO drukkers & vormgevers B.V. | Ponsen & Looijen